# Dynamics of Oceans:
# Pt 3: Small-Scales and Climate

Professor Baylor Fox-Kemper

Brown University
Dept. of Earth, Environmental, and Planetary Sciences
(Formerly U. Colorado Atmospheres and Oceans)
Supported by NASA (NNX09AF38G), NSF (0934737, 1245944, 2220280), ONR (N00014-17-1-2963), NOAA (NA19OAR4310366), Gulf of Mexico Research Initiative, Schmidt Futures

Boulder School for Condensed Matter and Materials Physics
July 18, 2022

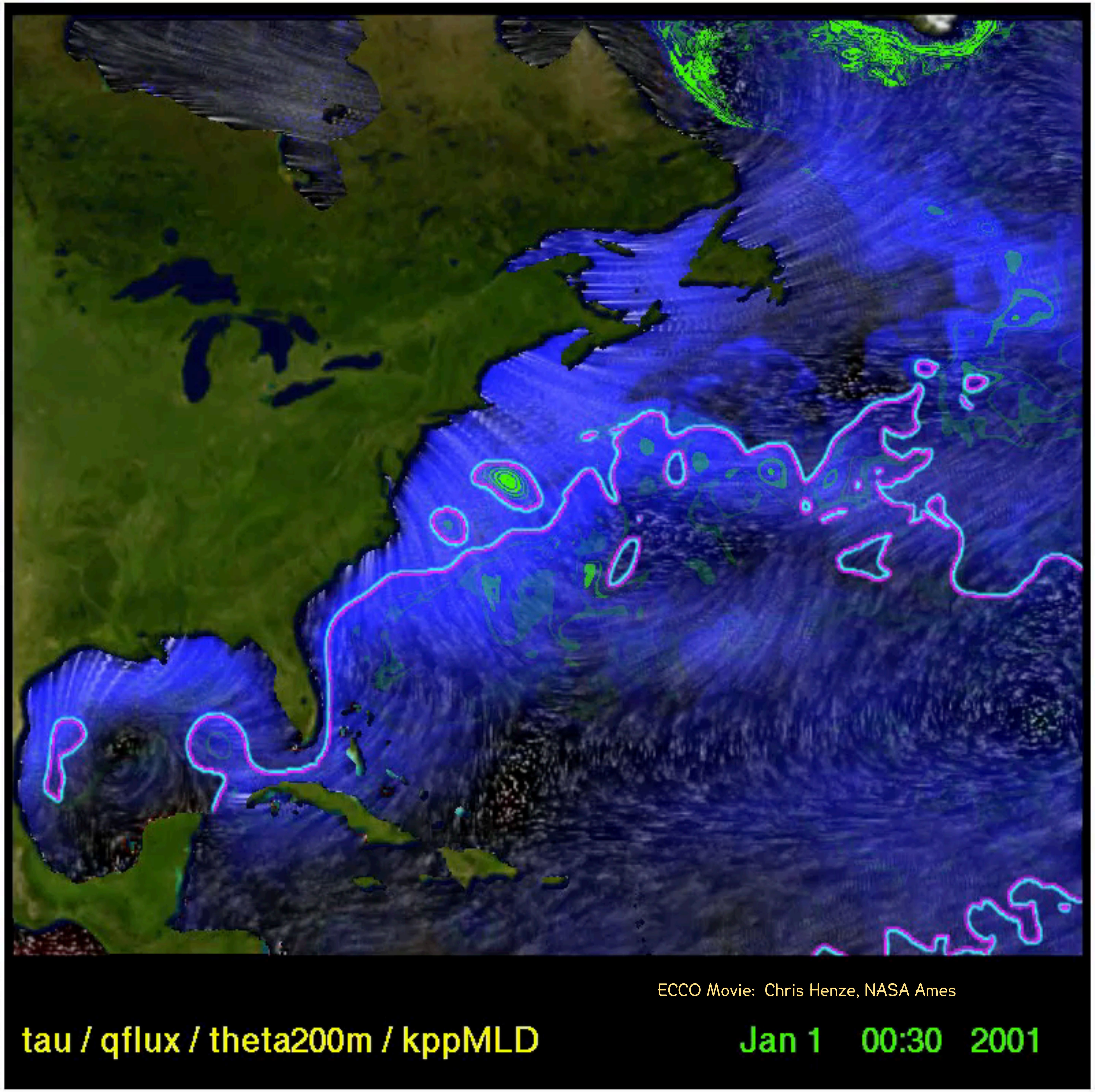


Weather,
Atmosphere
Fast

Ocean,
Climate
Slow

3.4m of ocean water has same heat capacity as the WHOLE atmosphere

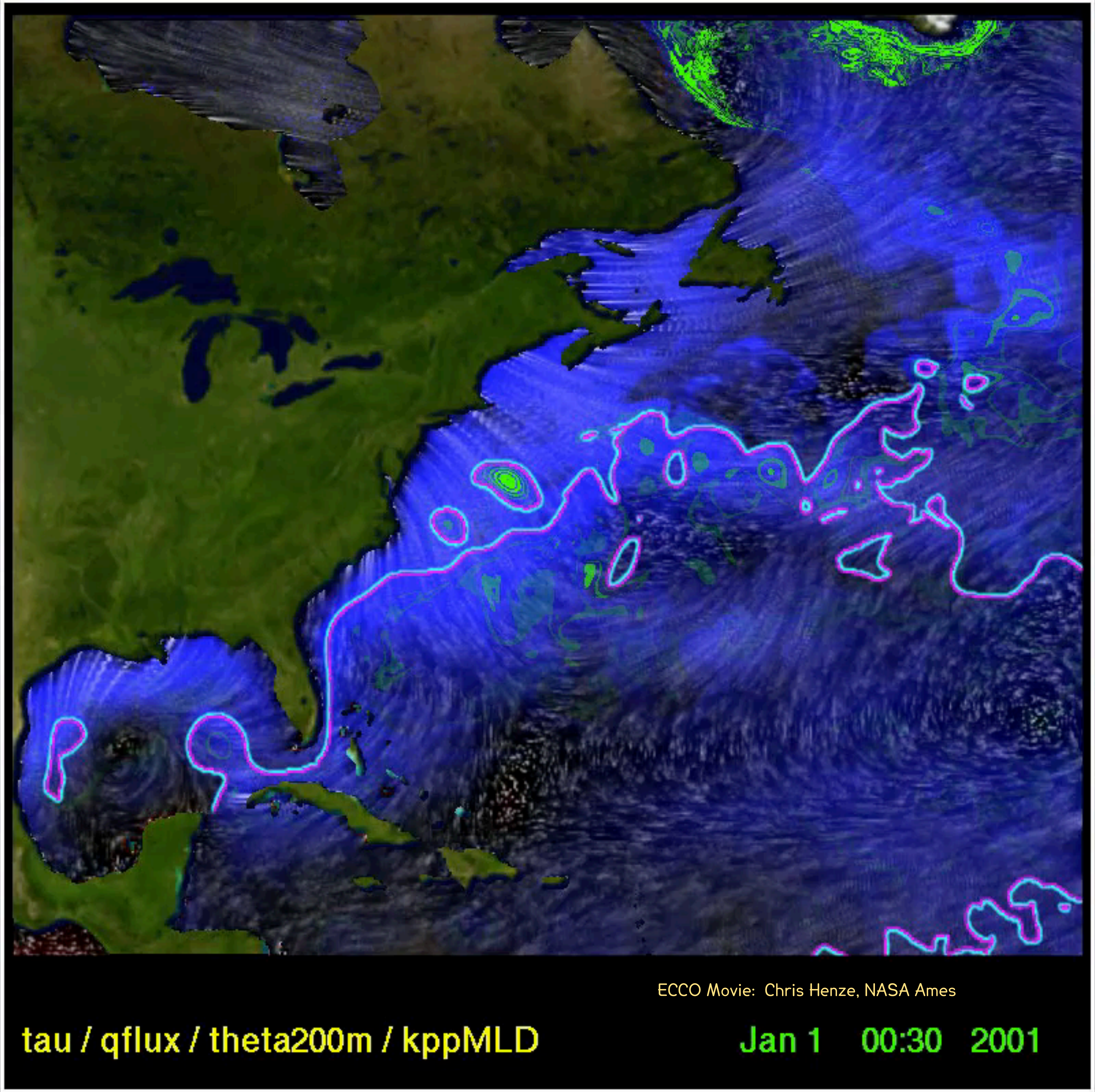


Weather,
Atmosphere
Fast

Ocean,
Climate
Slow

3.4m of ocean water has same heat capacity as the WHOLE atmosphere

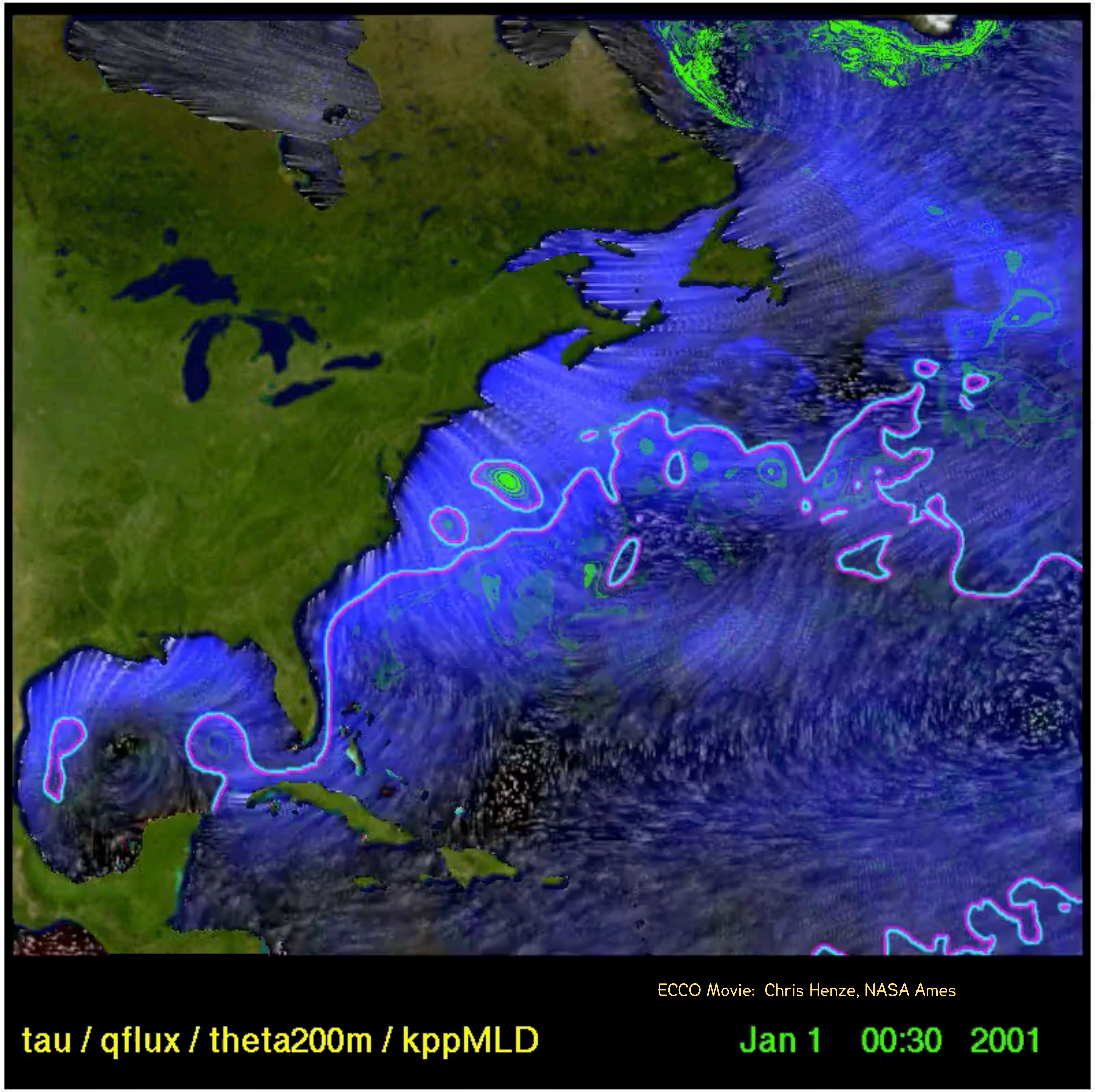


Weather,
Atmosphere
Fast

Ocean, Climate
Slow

3.4m of ocean water has same heat capacity as the WHOLE atmosphere

The essence of the Hasselmann 2021 Nobel in Physics!

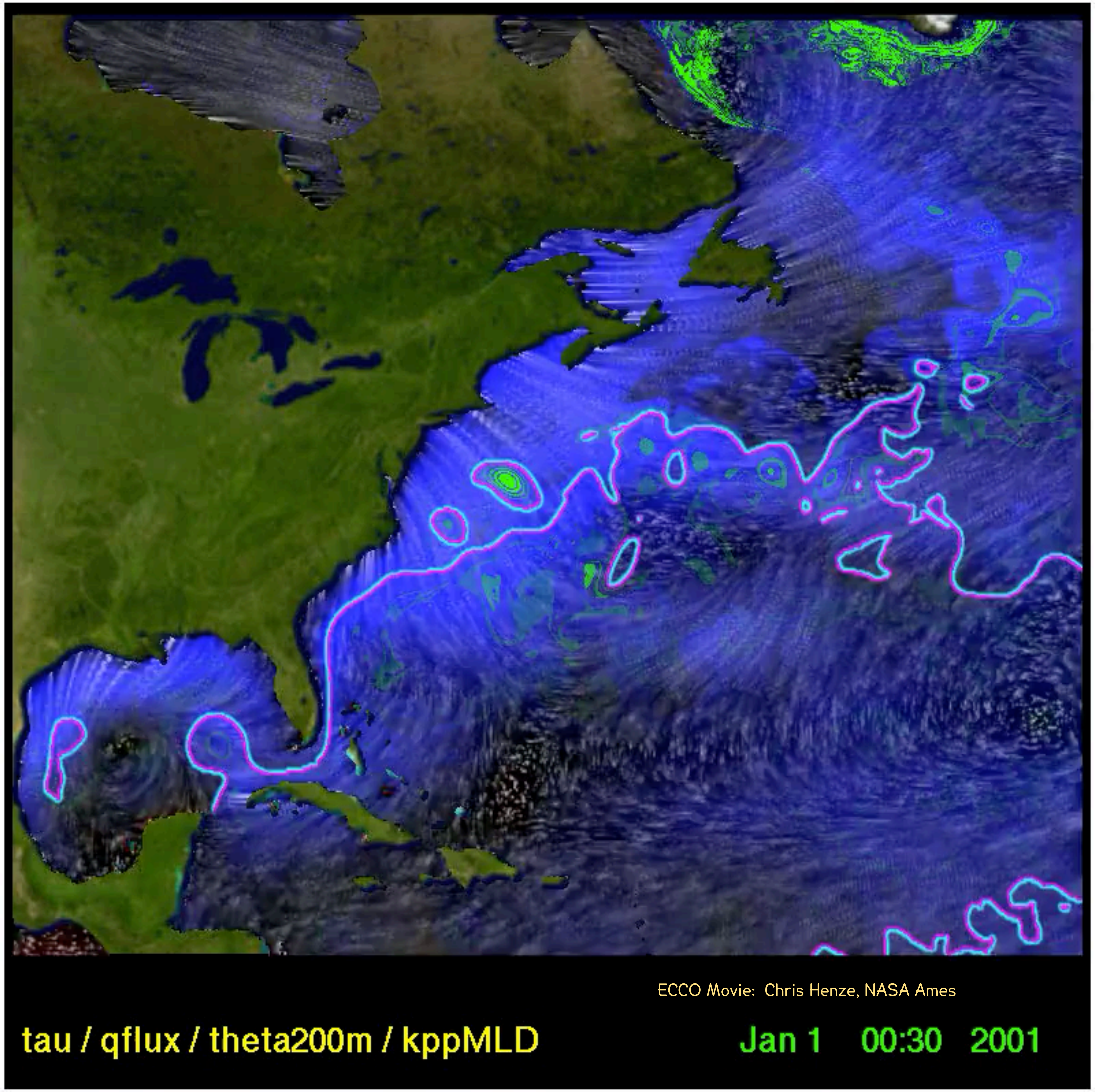


Weather,
Atmosphere
Fast

Ocean, Climate
Slow

3.4m of ocean water has same heat capacity as the WHOLE atmosphere

The essence of the Hasselmann 2021 Nobel in Physics!

# For Today: Small-scales affect Climate

- Key Ocean Climate Questions
- Large Eddy Simulation Closures
  - Smagorinsky, Leith, QG Leith
- Effects on Global Kinetic Energy
- Submesoscale affects Mixed Layer
- Wave-Driven Turbulence affects Mixed Layer
- Regional Mixed Layer Depth affects Climate Sensitivity

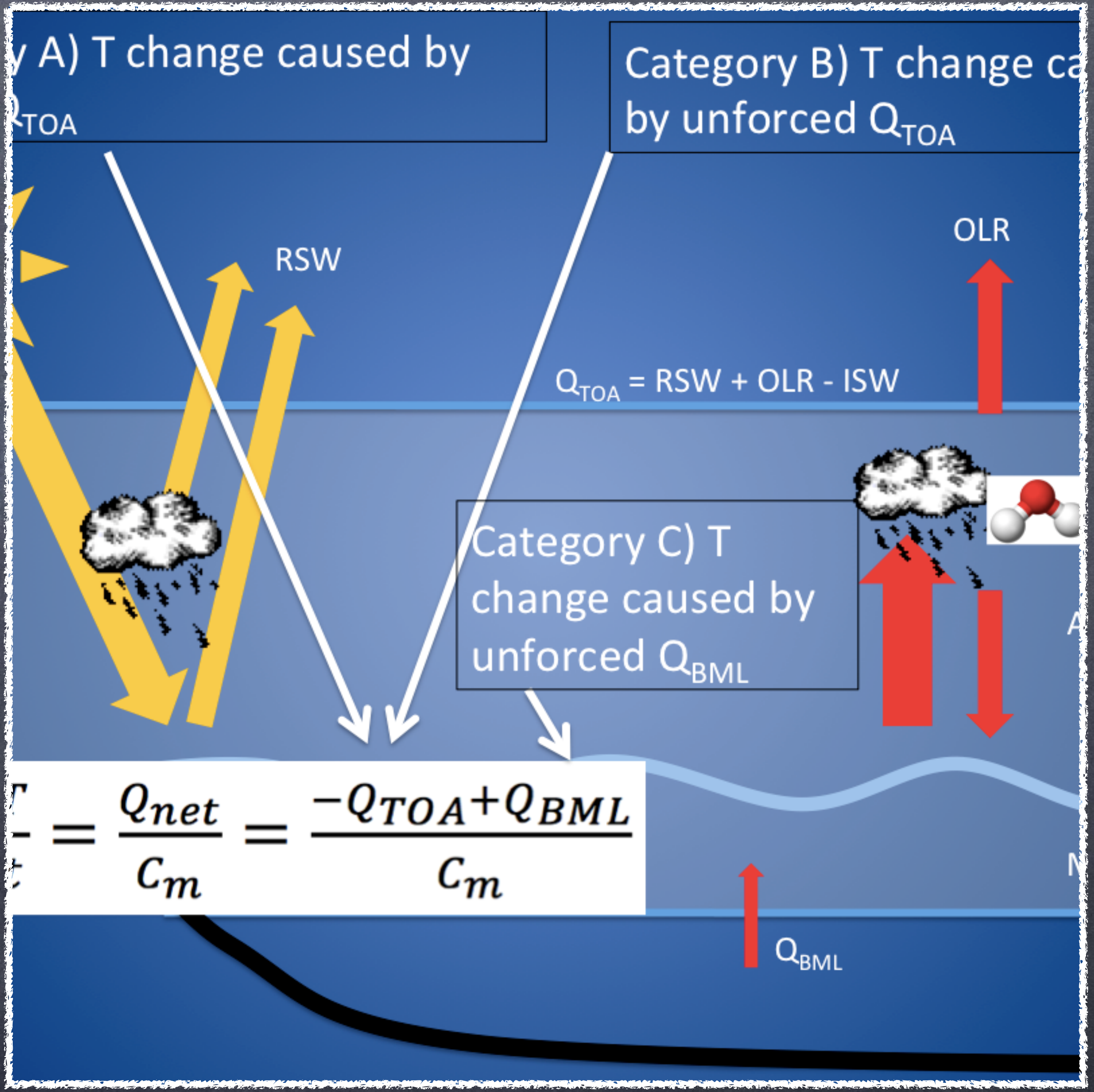

# Key Ocean Climate Questions

- Sea Level Rise
- Ocean Anthropogenic Heat Uptake
  - Earth's Energy Balance
- Ocean Anthropogenic Carbon Uptake
  - Earth's Carbon Balance
  - Ocean Acidification
- Will Currents & Stratification Change?
  - Affects the above & ecosystems...

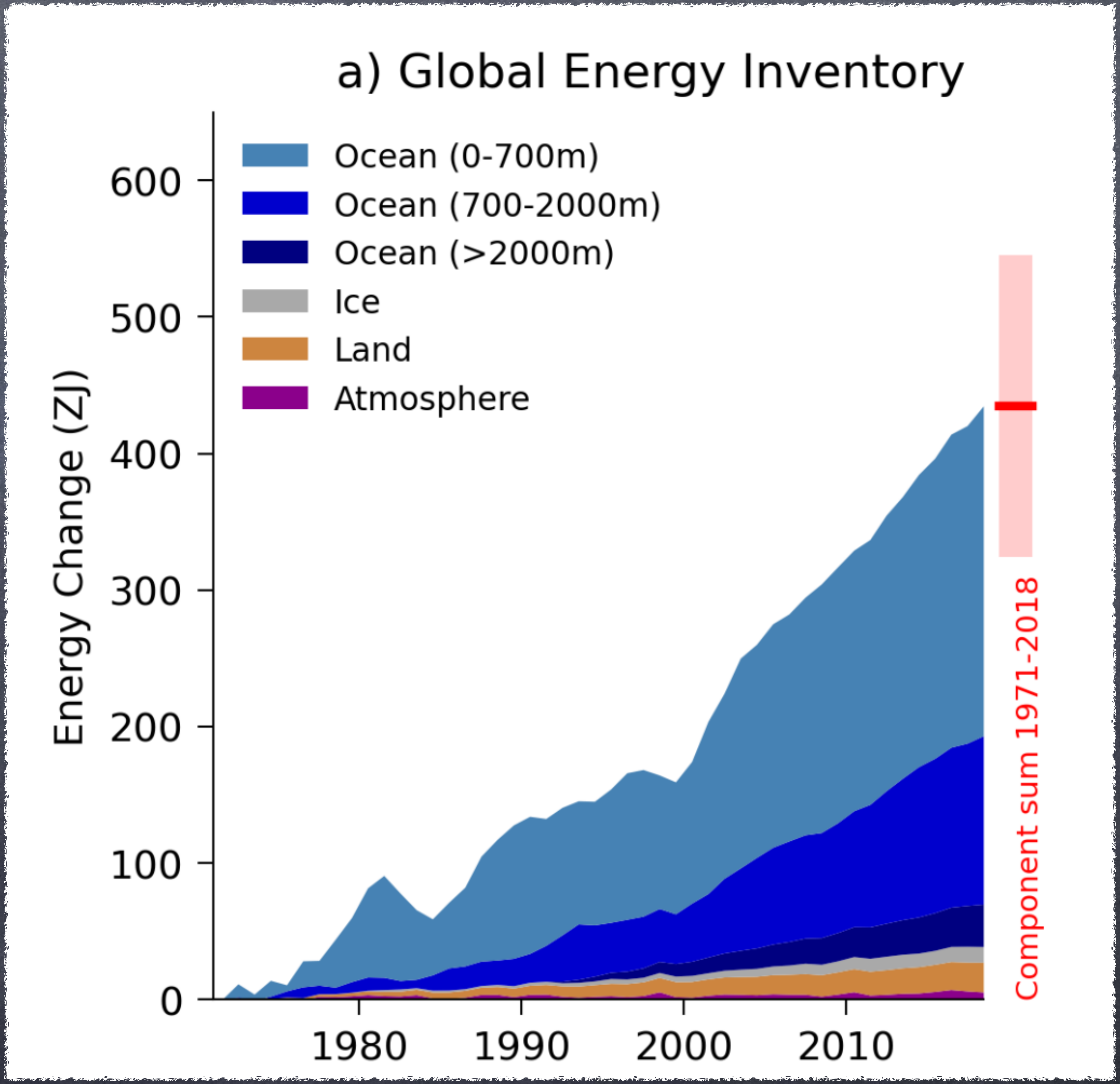

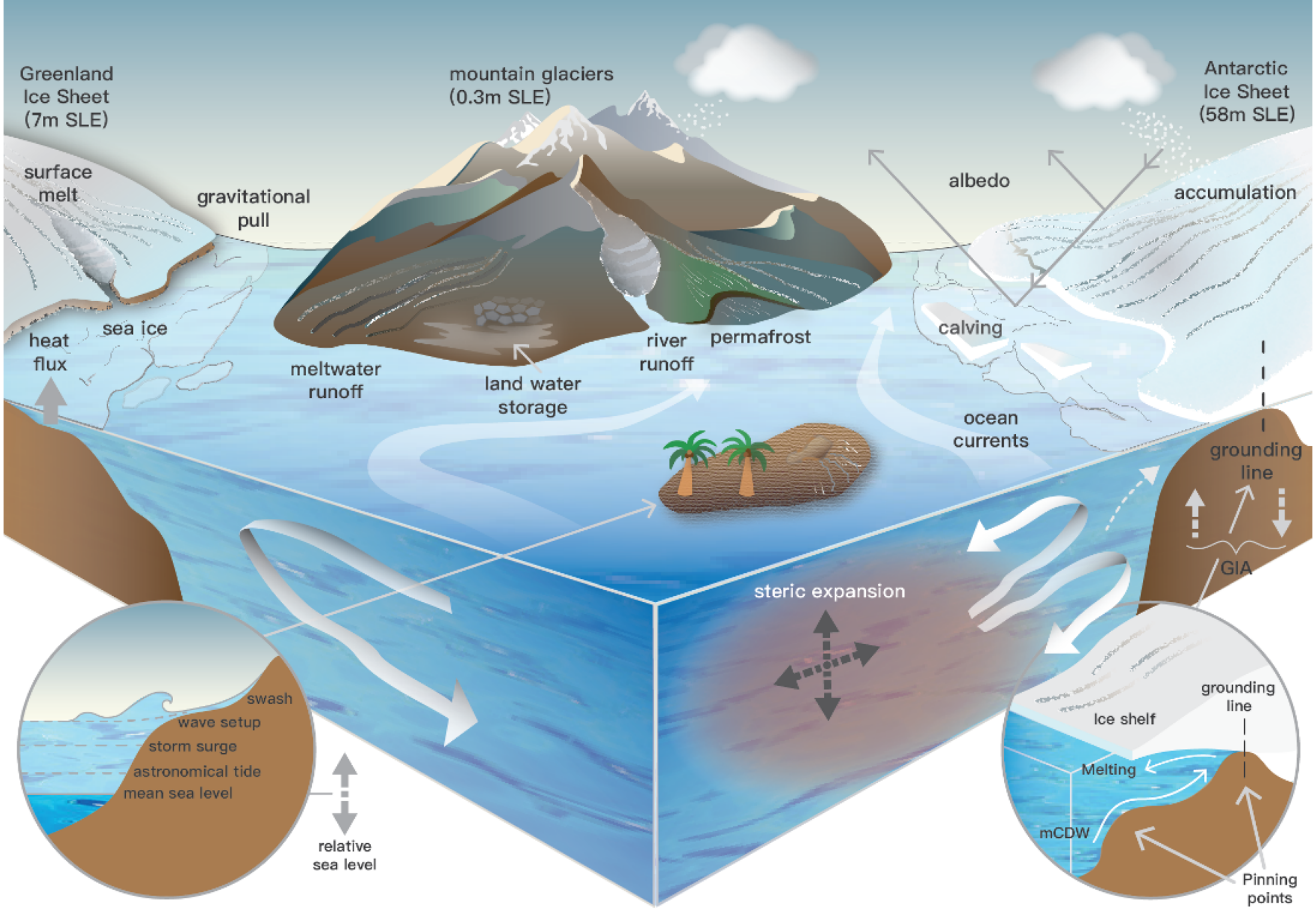


(a)

climate change

# our IPCC chapter emphasizes

# PROCESSES contributing to sea level rise

**Components of ocean, cryosphere and sea level assessed in this chapter.** (a) Schematic of processes (mCDW=modified Circumpolar Deep Water, GIA=Glacial Isostatic Adjustment). White arrows indicate ocean circulation. Pinning points indicate where the grounding line is most stable and ice sheet retreat will slow.

# Heating of the climate system has caused global mean sea level rise through ice loss on land and thermal expansion from ocean warming (high confidence)

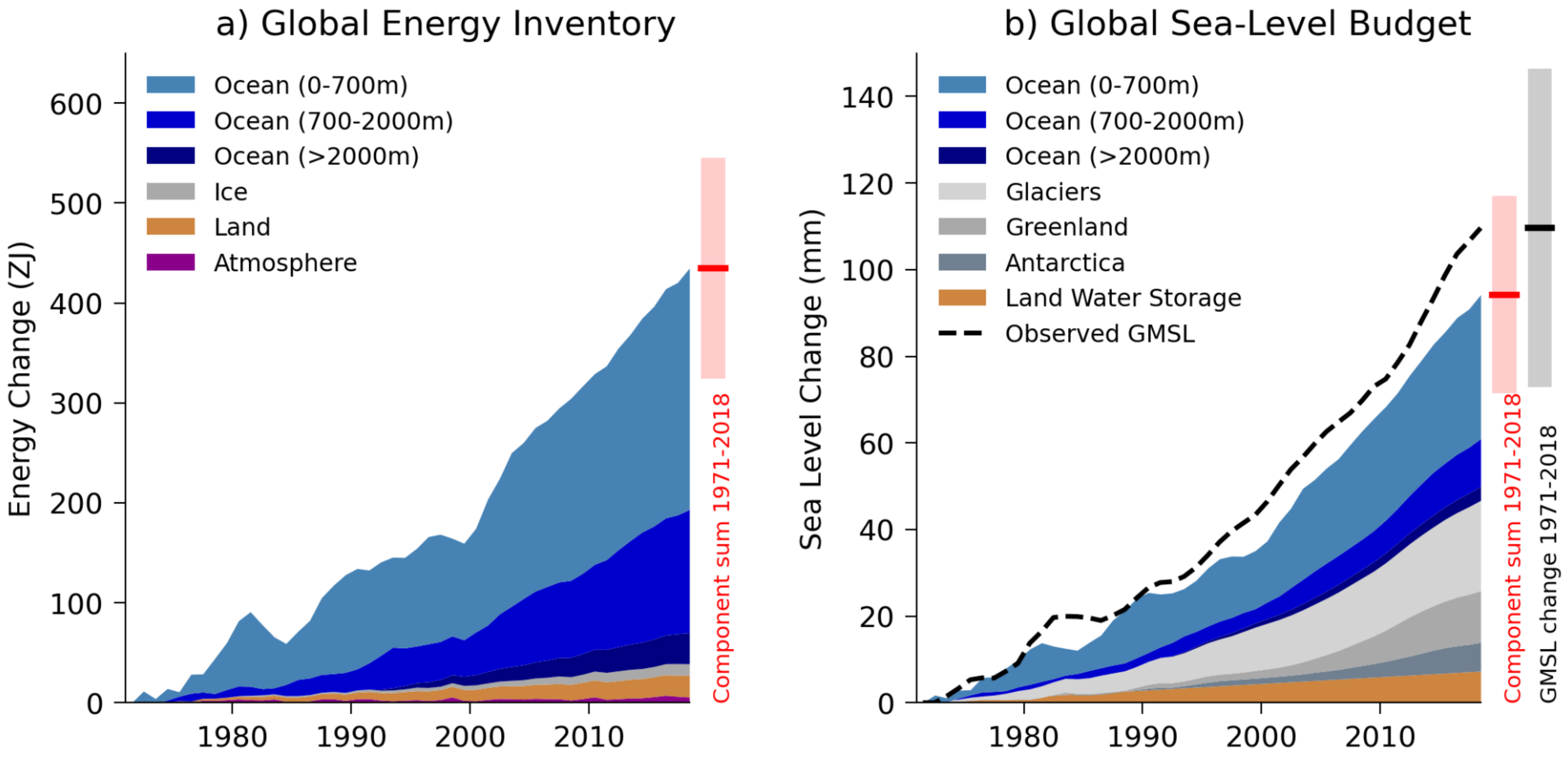

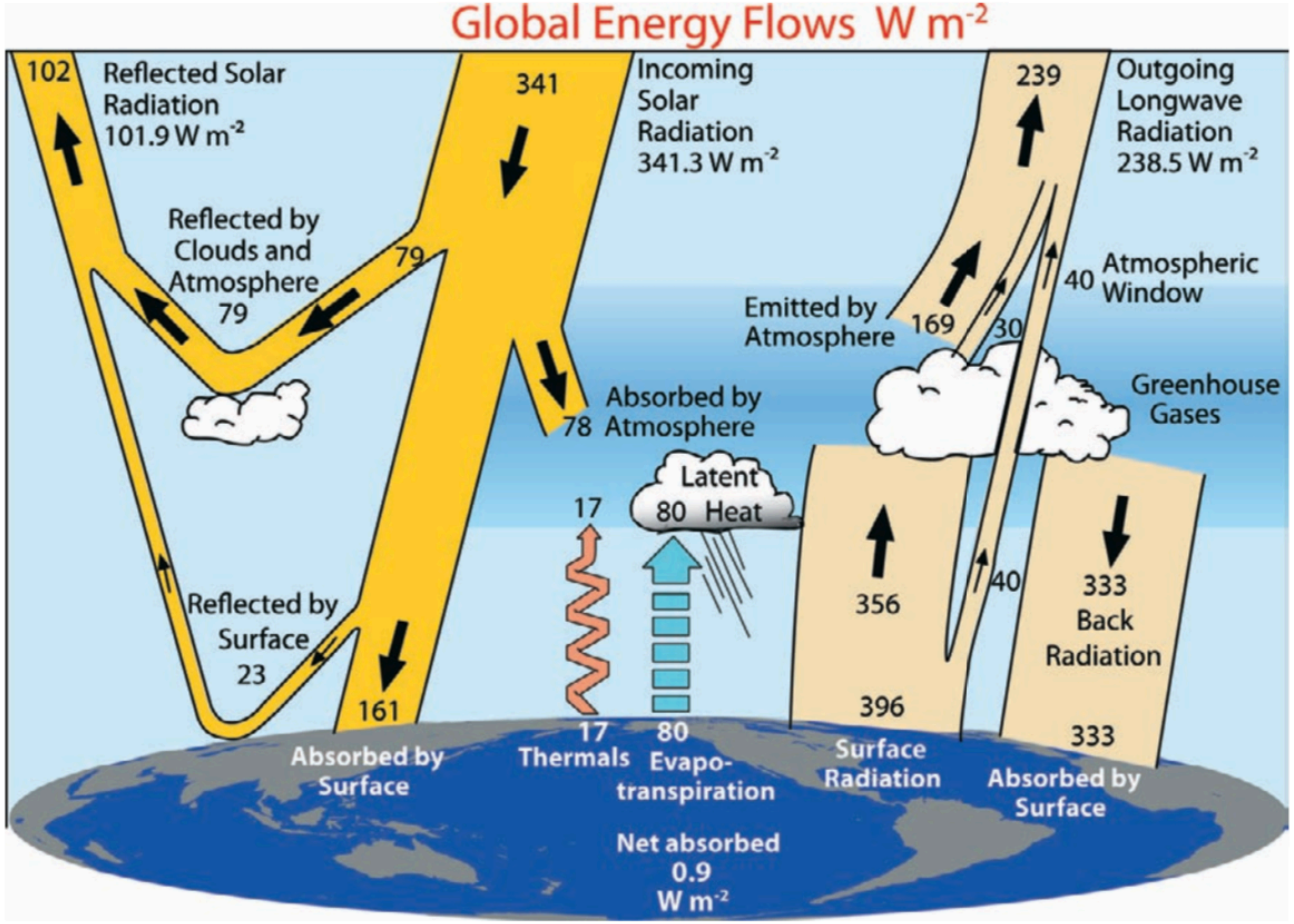


**FIG. 1.** The global annual mean Earth's energy budget for the Mar 2000 to May 2004 period (W $m^{-2}$). The broad arrows indicate the schematic flow of energy in proportion to their importance.

Image: Trenberth et al. 2009

Top of Atmosphere Imbalance!!

341.3-101.9-238.5=0.9

This equals net absorbed

Simple: Planetary Energy Balance

$$c\frac{dT}{dt} = R_{\text{incoming}}(T) - R_{\text{outgoing}}(T)$$

# GMST: Surface Energy Budget=Ocean Heat Content Budget

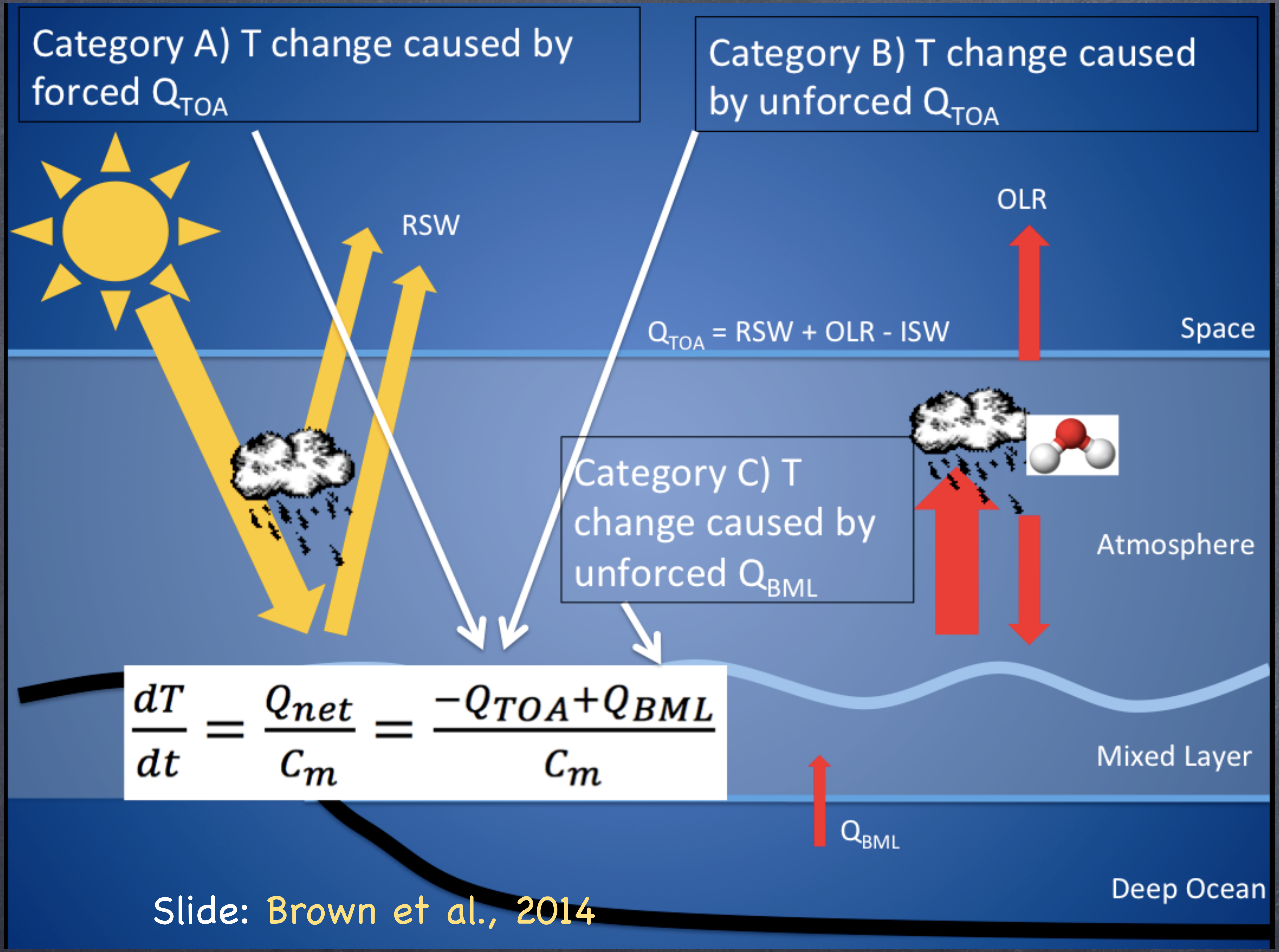


Top of Atmosphere Imbalance!!

341.3-101.9-238.5=0.9

This equals net absorbed

- 3.4m of ocean has heat capacity of whole atmosphere
- Ocean Mixed Layer is about 100m deep.

Video: ZEKE HAUSFATHER, Carbon Brief, 2017
www.carbonbrief.org/analysis-how-well-have-climate-models-projected-global-warming

Evaluating the Performance of Past Climate Model Projections
Z. Hausfather, H.F. Drake,T. Abbott, G.A. Schmidt, 2019
https://doi.org/10.1029/2019GL085378

Video: ZEKE HAUSFATHER, Carbon Brief, 2017
www.carbonbrief.org/analysis-how-well-have-climate-models-projected-global-warming

Evaluating the Performance of Past Climate Model Projections

Z. Hausfather, H.F. Drake,T. Abbott, G.A. Schmidt, 2019

https://doi.org/10.1029/2019GL085378

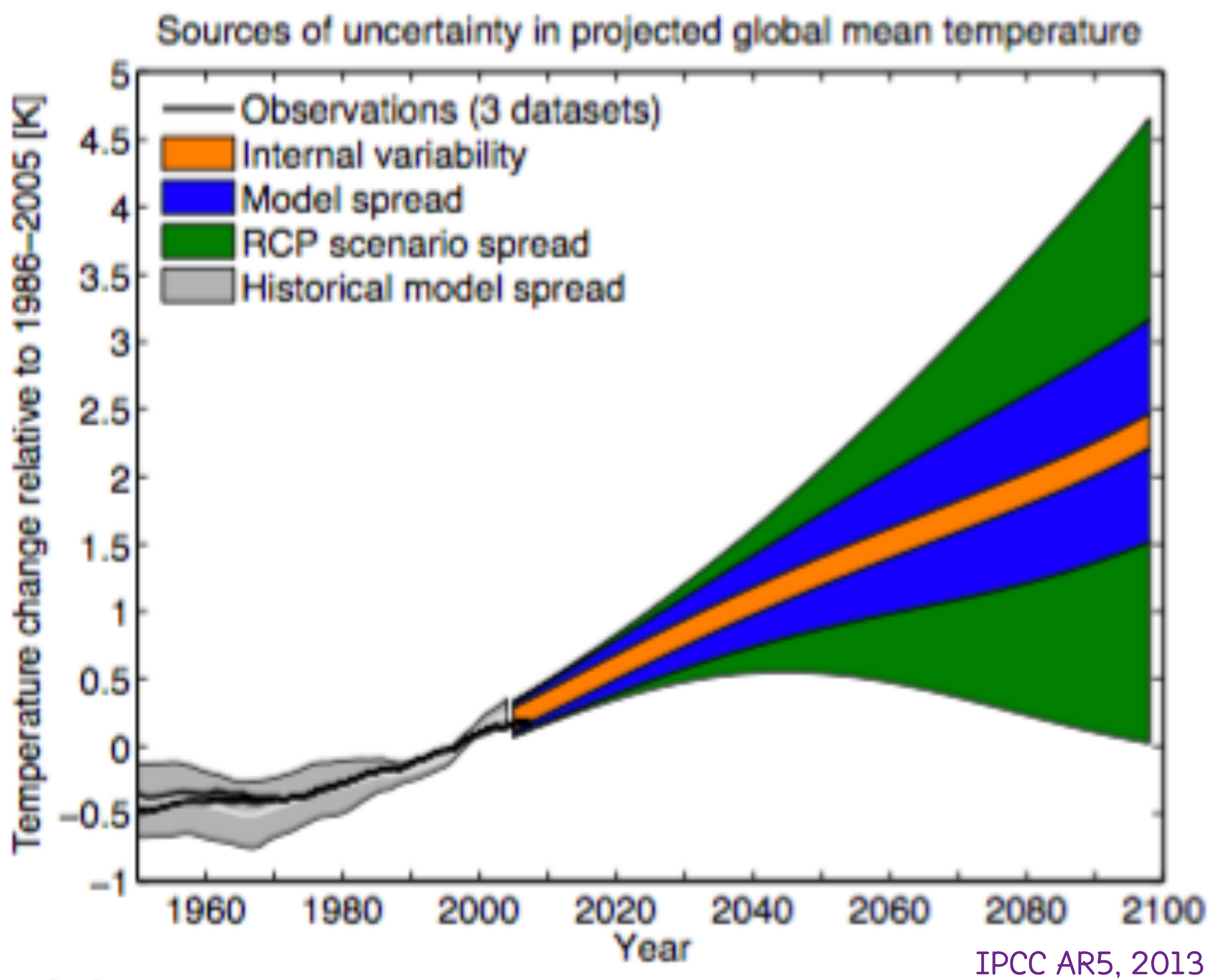


IPCC AR5, 2013

Indeed, Hausfather et al. 2019 show that the early climate projections often went wrong because they assumed the wrong human emissions profile, not the wrong climate response.

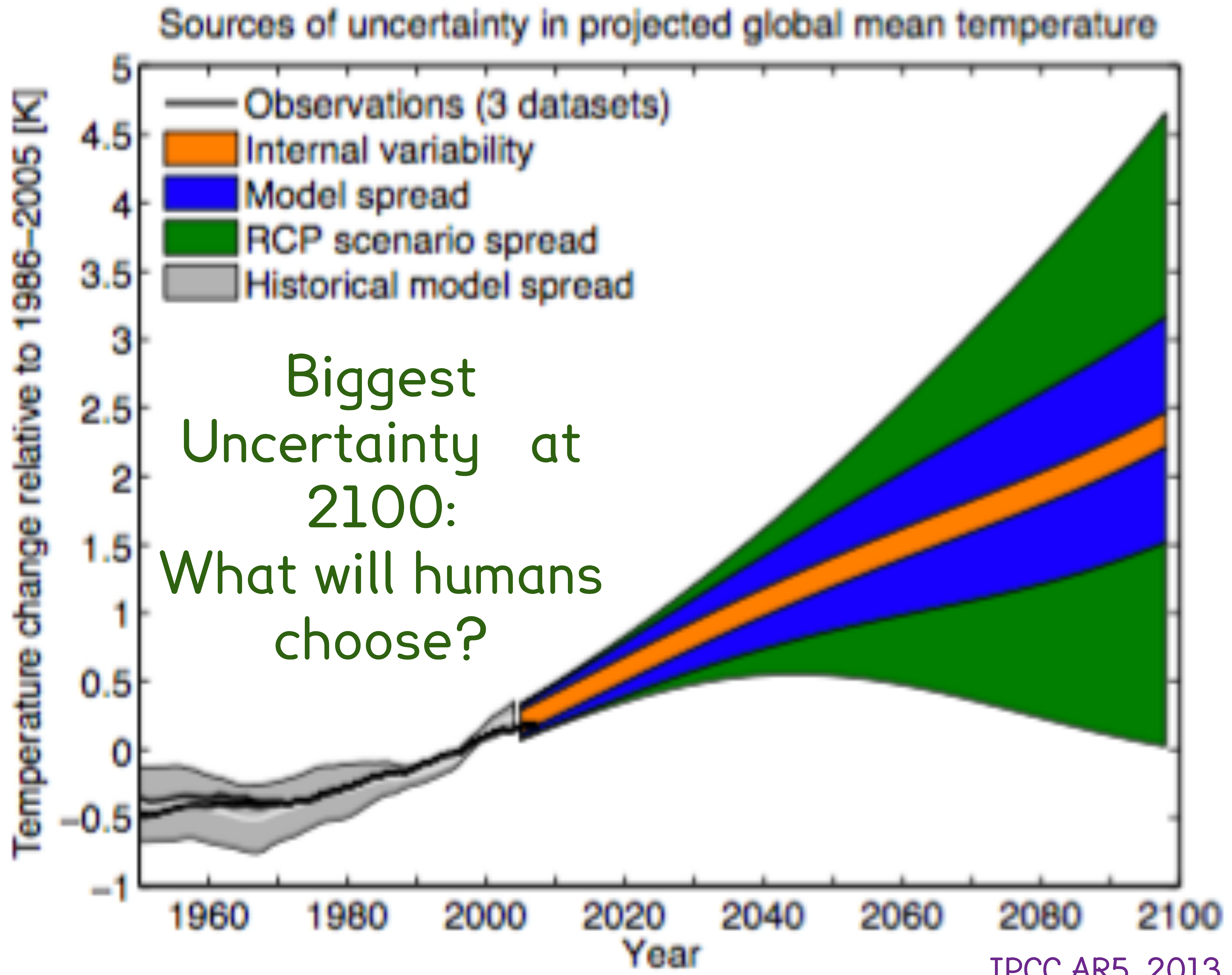


IPCC AR5, 2013

Indeed, Hausfather et al. 2019 show that the early climate projections often went wrong because they assumed the wrong human emissions profile, not the wrong climate response.

# Handling the partially-resolved mesoscale...

- In effect, the mesoscale in (highest-resolution) climate models is a Large Eddy Simulation for these modes.
- What kind of LES closure will work?

# The Character of the Mesoscale

100 km

(Capet et al., 2008)

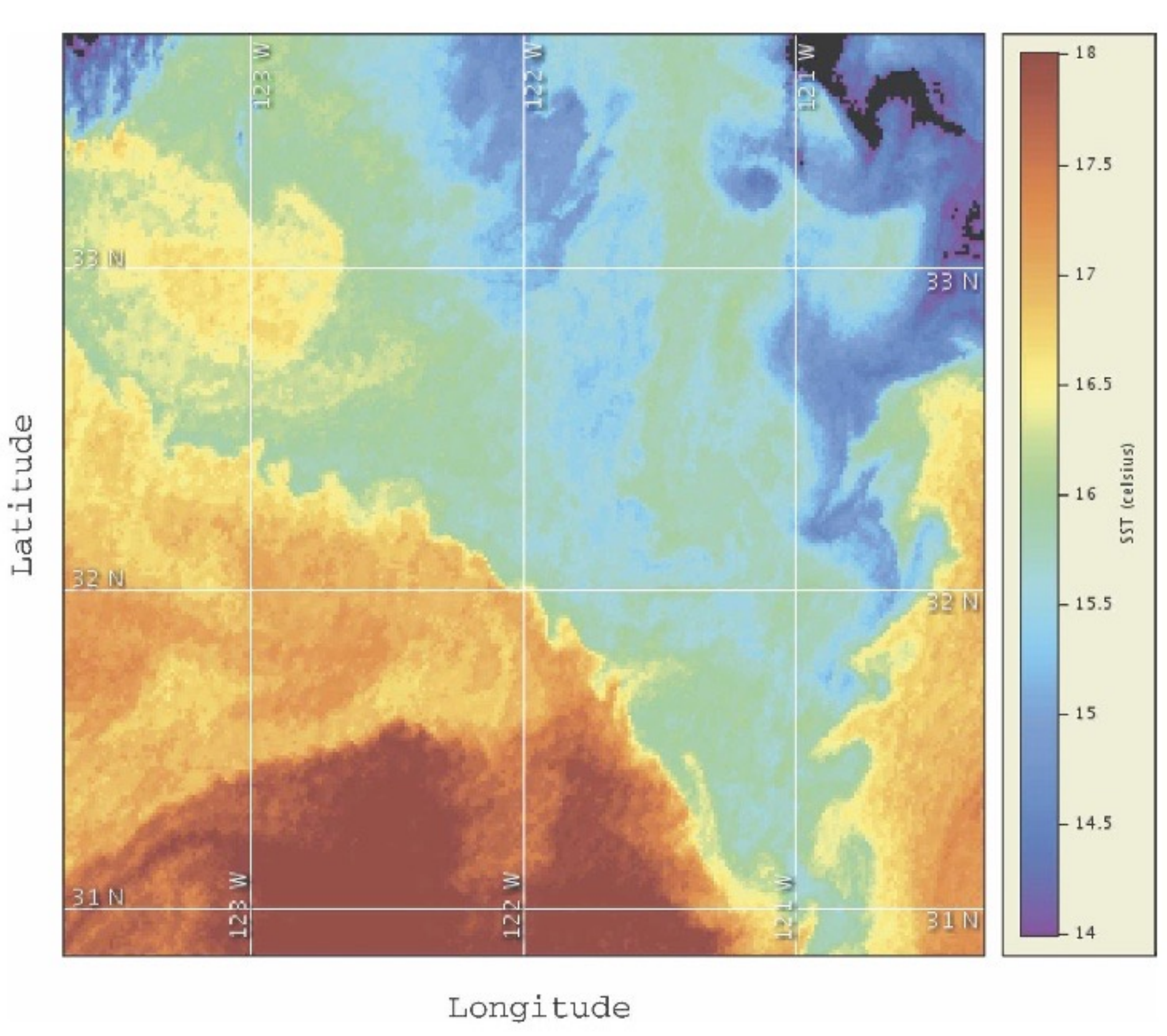


FIG. 16. Sea surface temperature measured at 1832 UTC 3 Jun 2006 off Point Conception in the California Current from CoastWatch (http://coastwatch.pfeg.noaa.gov). The fronts between recently upwelled water (i.e., 15°–16°C) and offshore water (≥17°C) show submesoscale instabilities with wavelengths around 30 km (right front) or 15 km (left front). Images for 1 day earlier and 4 days later show persistence of the instability events.

- Boundary Currents
- Eddies
- Ro=O(0.1)
- Ri=O(1000)
- Full Depth
- Eddies strain to produce Fronts
- 100km, months

(NASA GSFC Gallery)

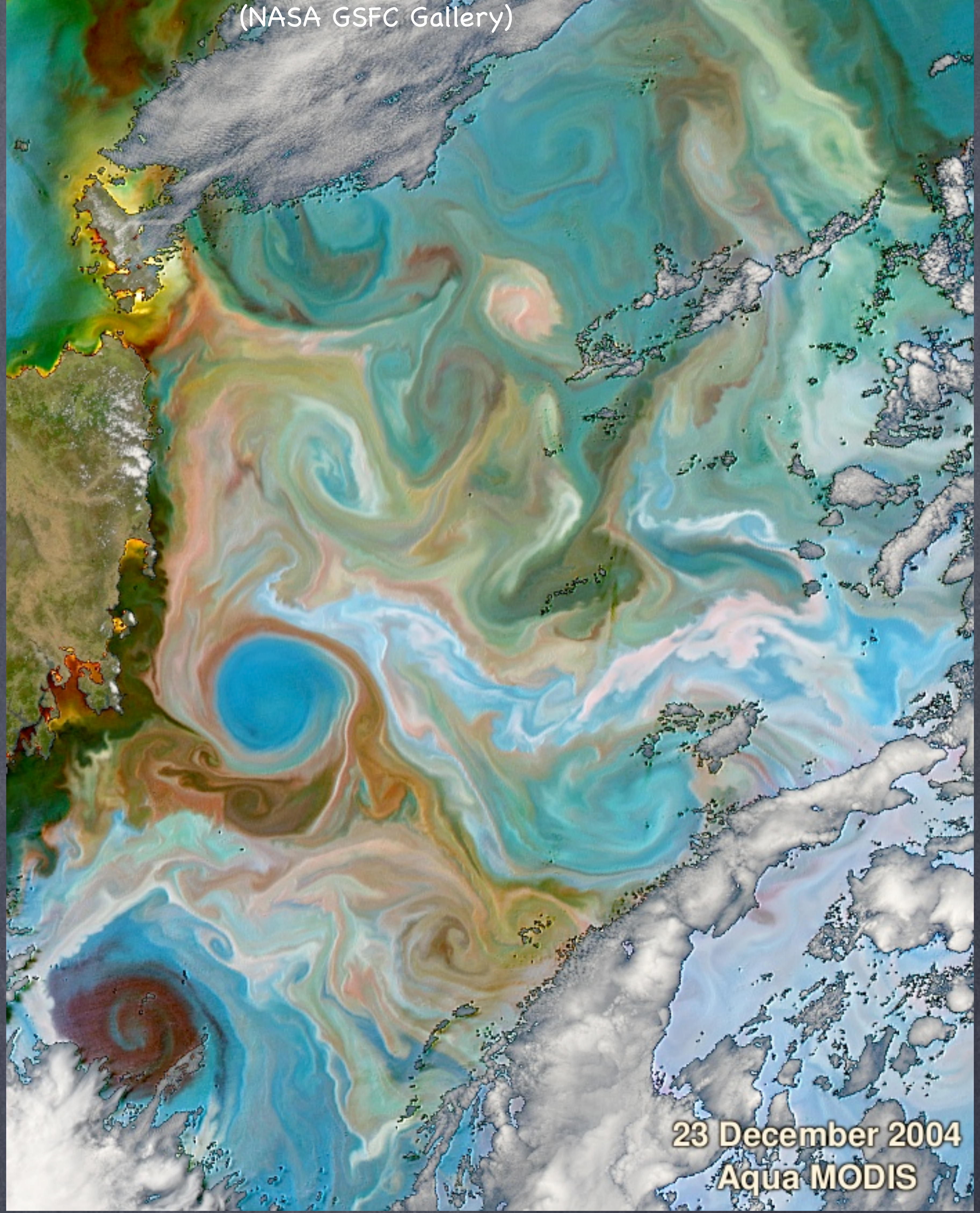


Eddy processes mainly baroclinic & barotropic instability. Parameterizations of baroclinic instability (GM, Visbeck...).

# The Character of the Mesoscale

100 km

(NASA GSFC Gallery)

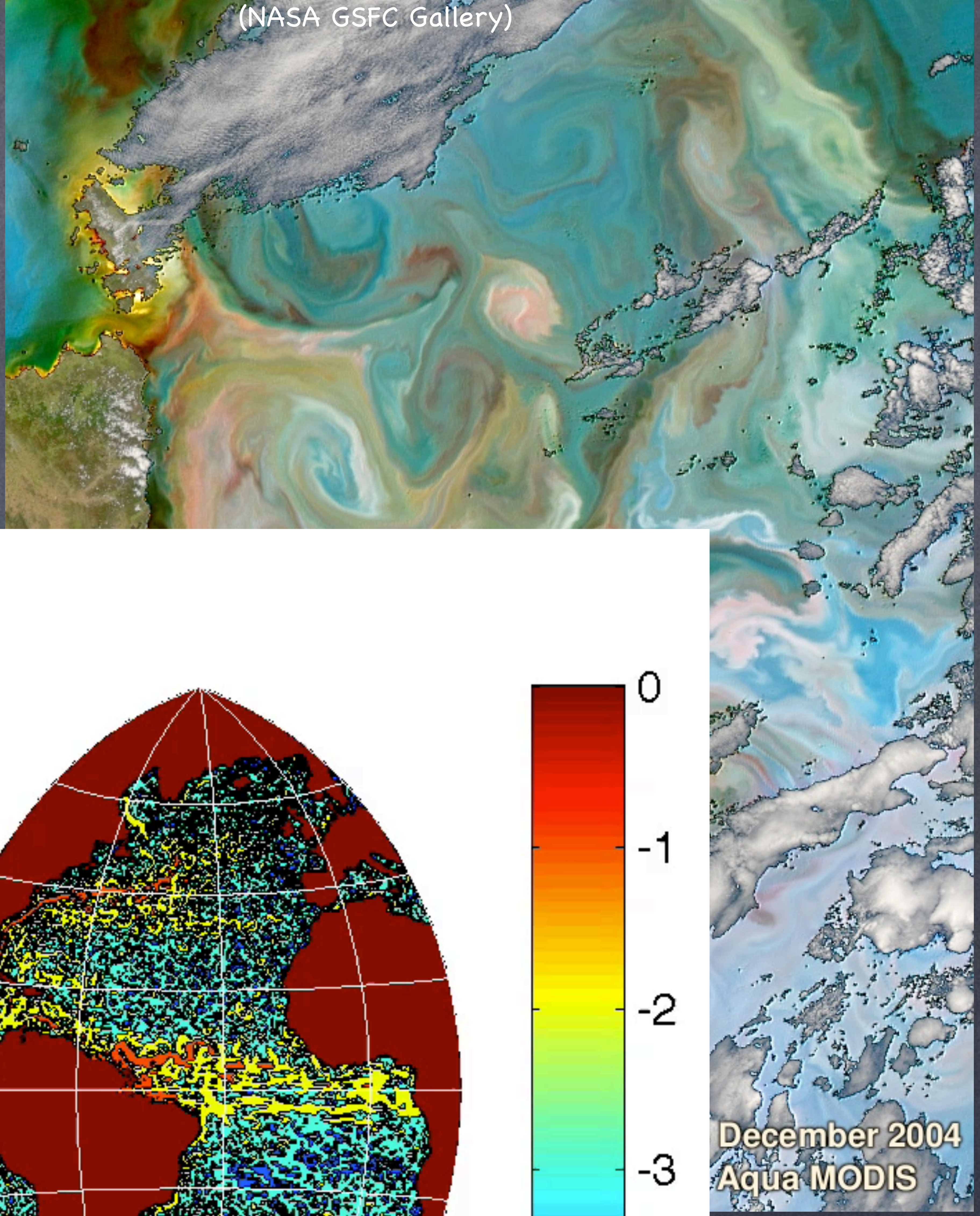


(Capet et al., 2008)

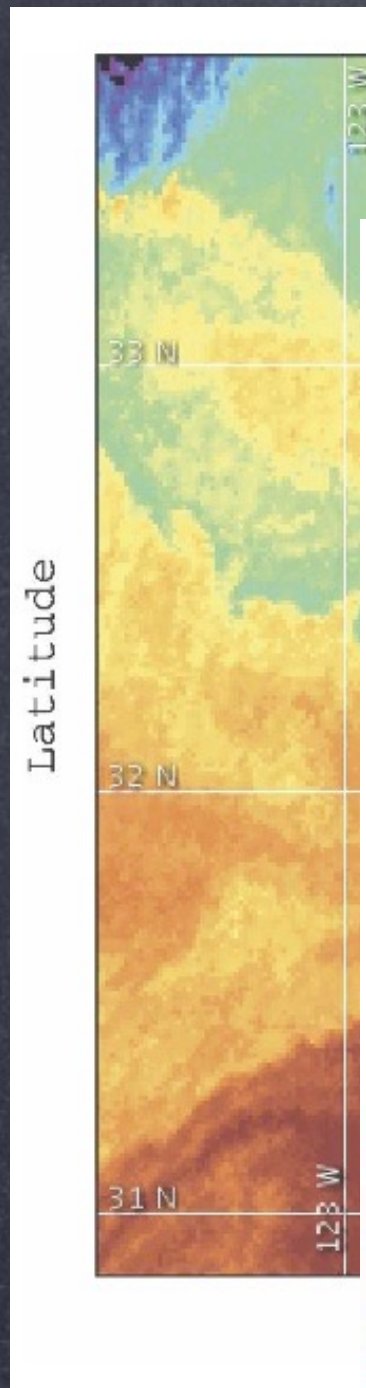


FIG. 16. Sea surface
California Current fro
upwelled water (i.e., 15
lengths around 30 km (
persistence of the insta

- Boundary Currents

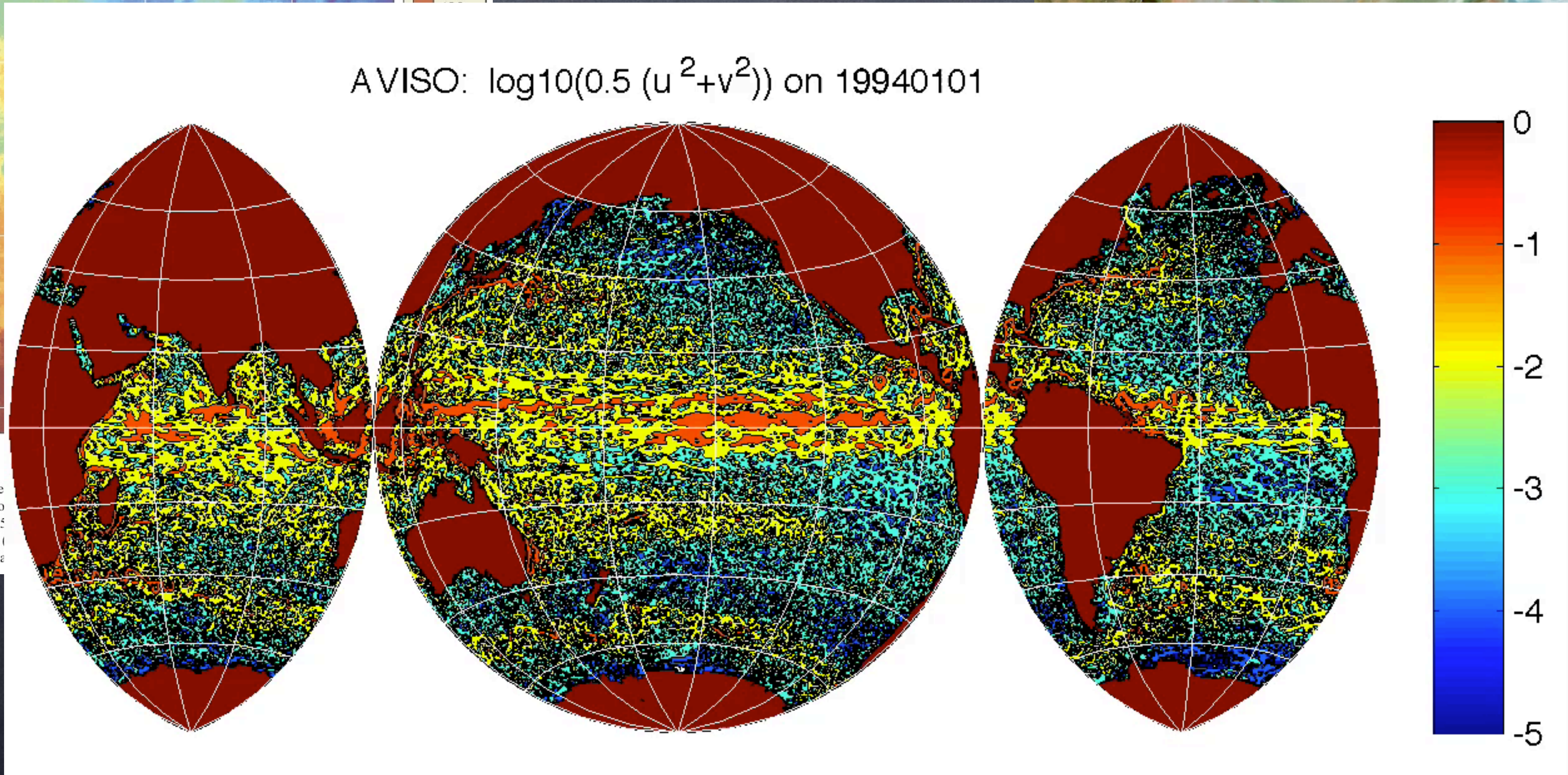

Th

(Ca

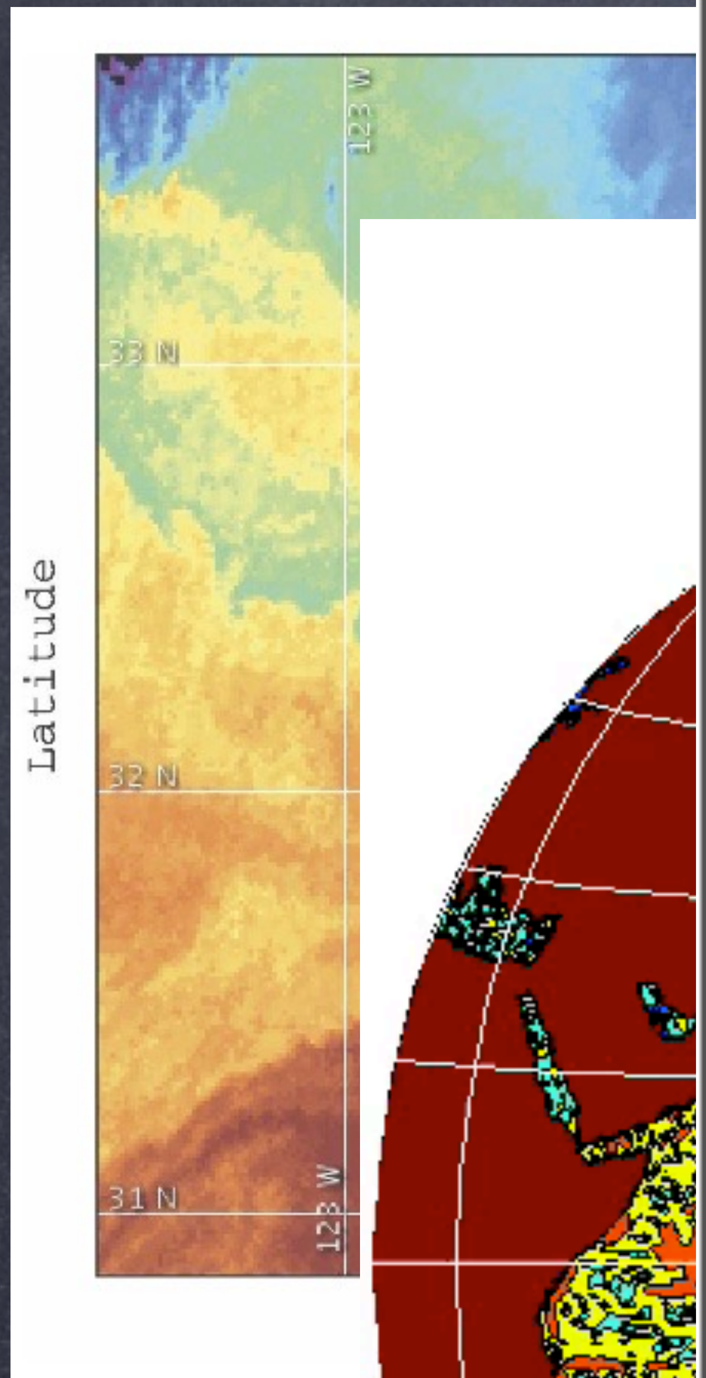


FIG. 16. Sea surface
California Current fro
upwelled water (i.e., 15
lengths around 30 km (
persistence of the insta

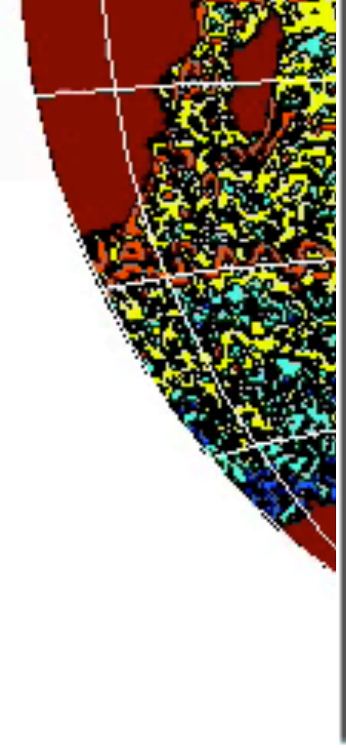

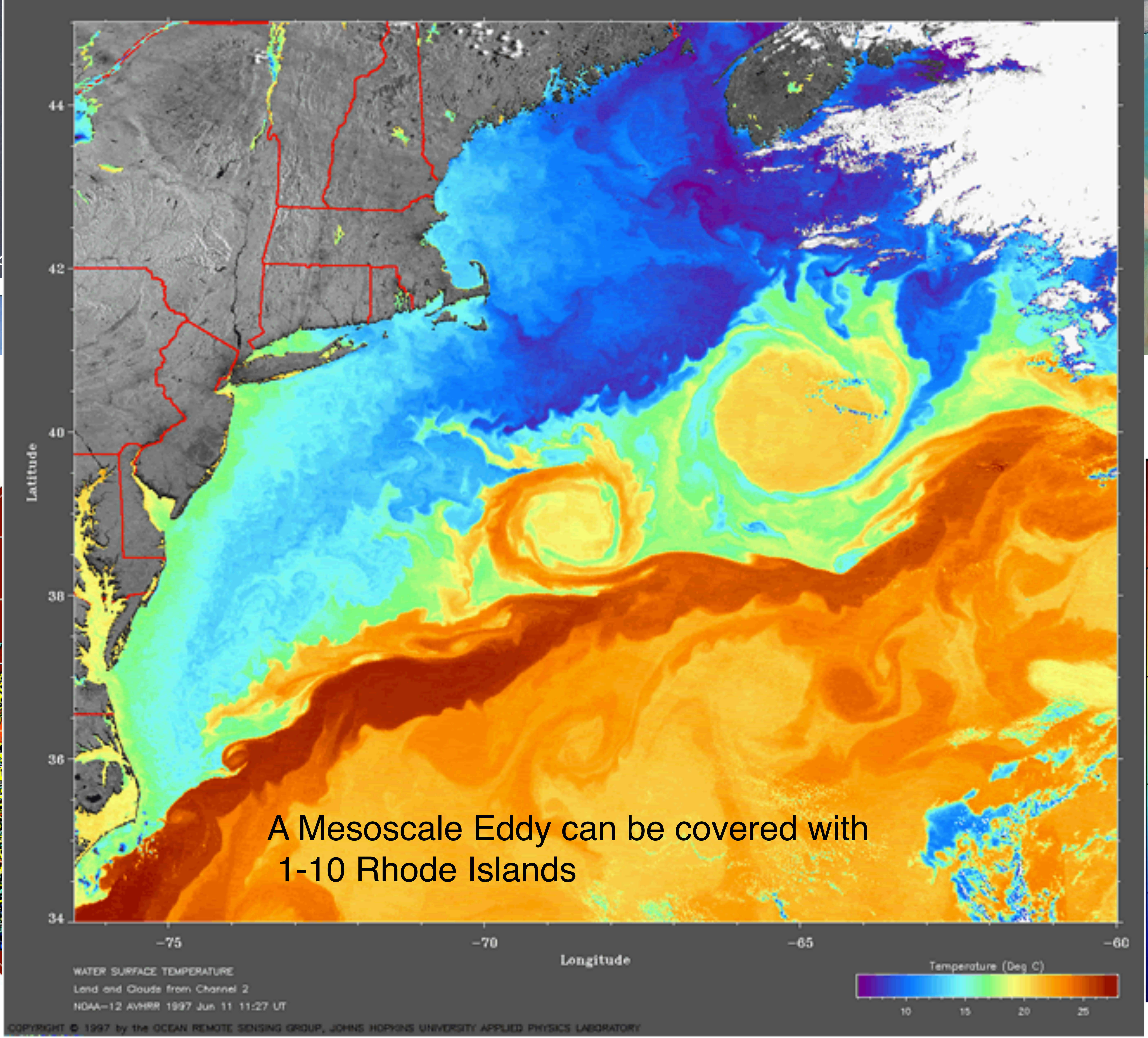


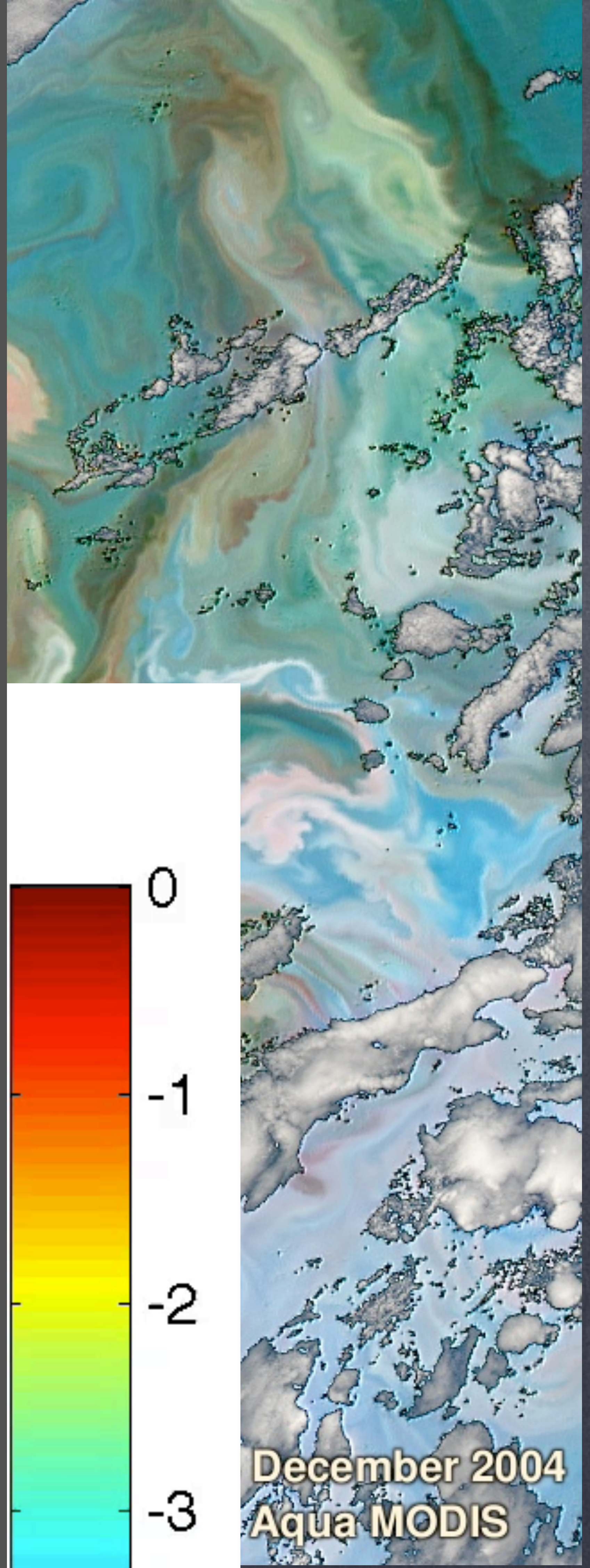


# 3D Turbulence Cascade

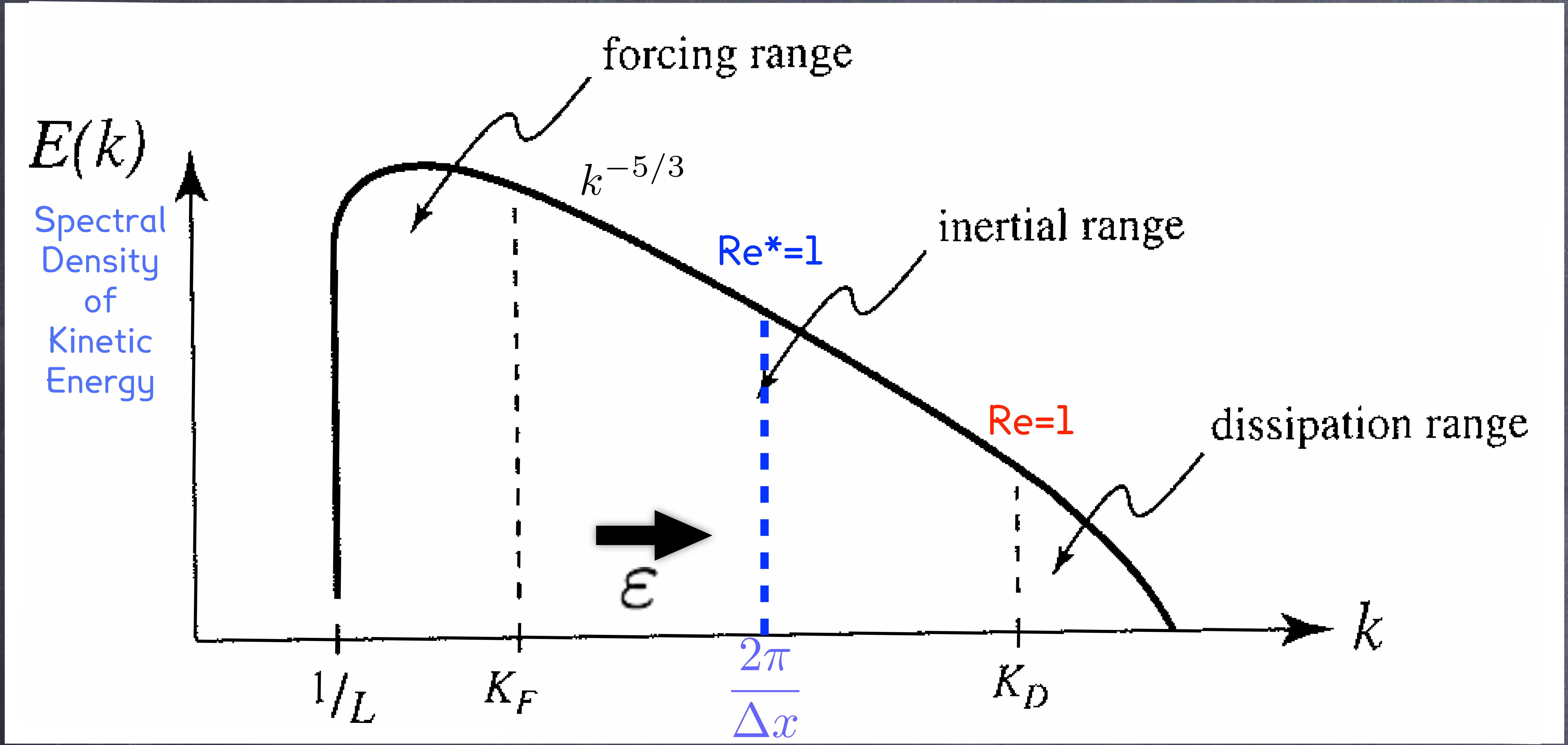


Suitable For Nonhydostatic Boussinesq; Wave-averaged

1963: Smagorinsky Scale & Flow Aware Viscosity Scaling,
So the Energy Cascade is Preserved,
but order-1 gridscale Reynolds #: $Re^* = UL/\nu_*$

$$\nu_{*h} = \left(\frac{\Upsilon_h \Delta x}{\pi}\right)^2 \sqrt{\left(\frac{\partial u_*}{\partial x} - \frac{\partial v_*}{\partial y}\right)^2 + \left(\frac{\partial u_*}{\partial y} + \frac{\partial v_*}{\partial x}\right)^2}$$

# Smagorinsky Viscosity (Cited by 17445) in 2 min

$$\frac{d\langle E_*\rangle}{dt} = -F_E|_0^{k_*} - \int_0^{k_*} \nu k^2 E(k)dk + \int_0^{k_*} S_E(k,t)dk.$$

Make k* Kolmogorov Scale

$$k_* = \Upsilon \varepsilon^{1/4} \nu_*^{-3/4},$$

All flux at k* "viscous"

$$\varepsilon = F_E(k_*) + \int_0^{k_*} \nu k^2 E(k)dk \equiv \int_0^{k_*} \nu_* k^2 E(k)dk$$

If the viscous term is evaluated in real space rather than wavenumber space, then

$$\int_0^{k_*} \nu_* k^2 E(k)\,dk = \left\langle \nu_* S_*^{ik} S_{*ik} \right\rangle, \qquad (20)$$

Finally, because the turbulence is assumed to be homogeneous, the domain-averaged friction is replaced with a local value, and the result for $\nu_*$ follows.

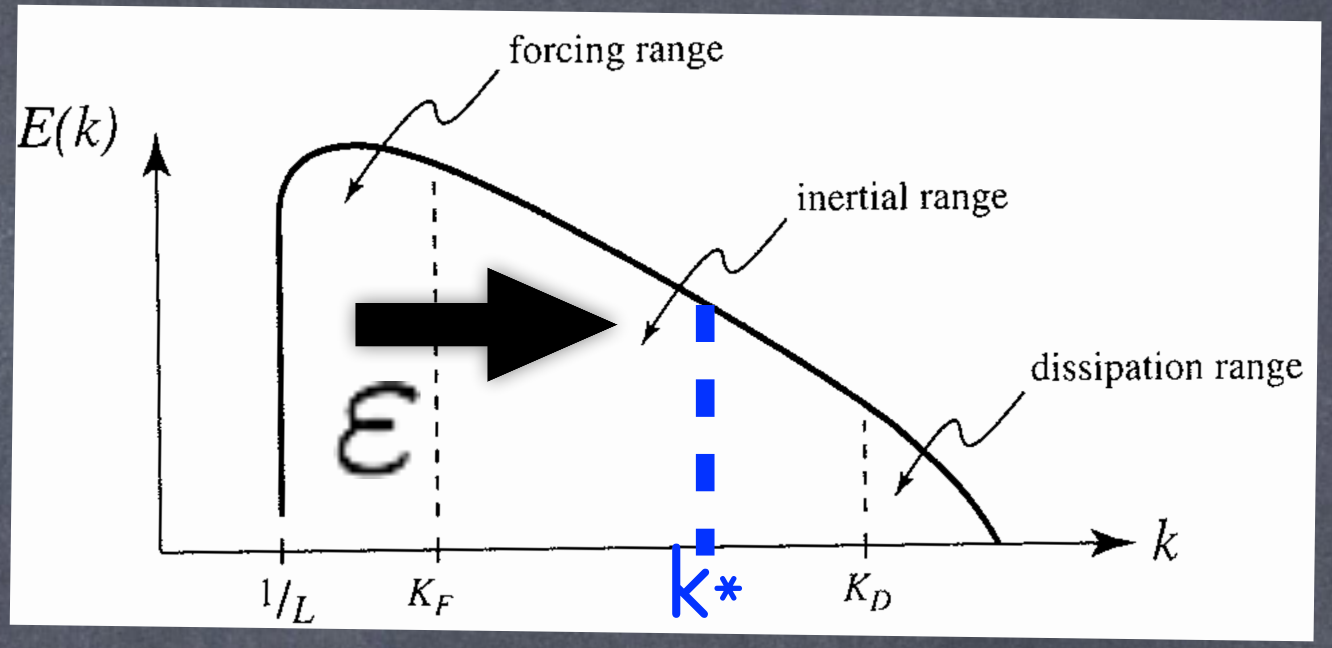


$$\nu_* = \left(\frac{\Upsilon}{k_*}\right)^2 |D_*|,$$

$$\nu_* = \left(\frac{\Upsilon \Delta x}{\pi}\right)^2 |D_*|,$$

$$|D_*| \equiv \sqrt{S_*^{ik} S_{*ik}}\ .$$

BFK and D. Menemenlis. Can large eddy simulation techniques improve mesoscale-rich ocean models? In M. Hecht and H. Hasumi, editors, Ocean Modeling in an Eddying Regime, volume 177, pages 319-338. AGU Geophysical Monograph Series, 2008.

# 2D Turbulence Differs

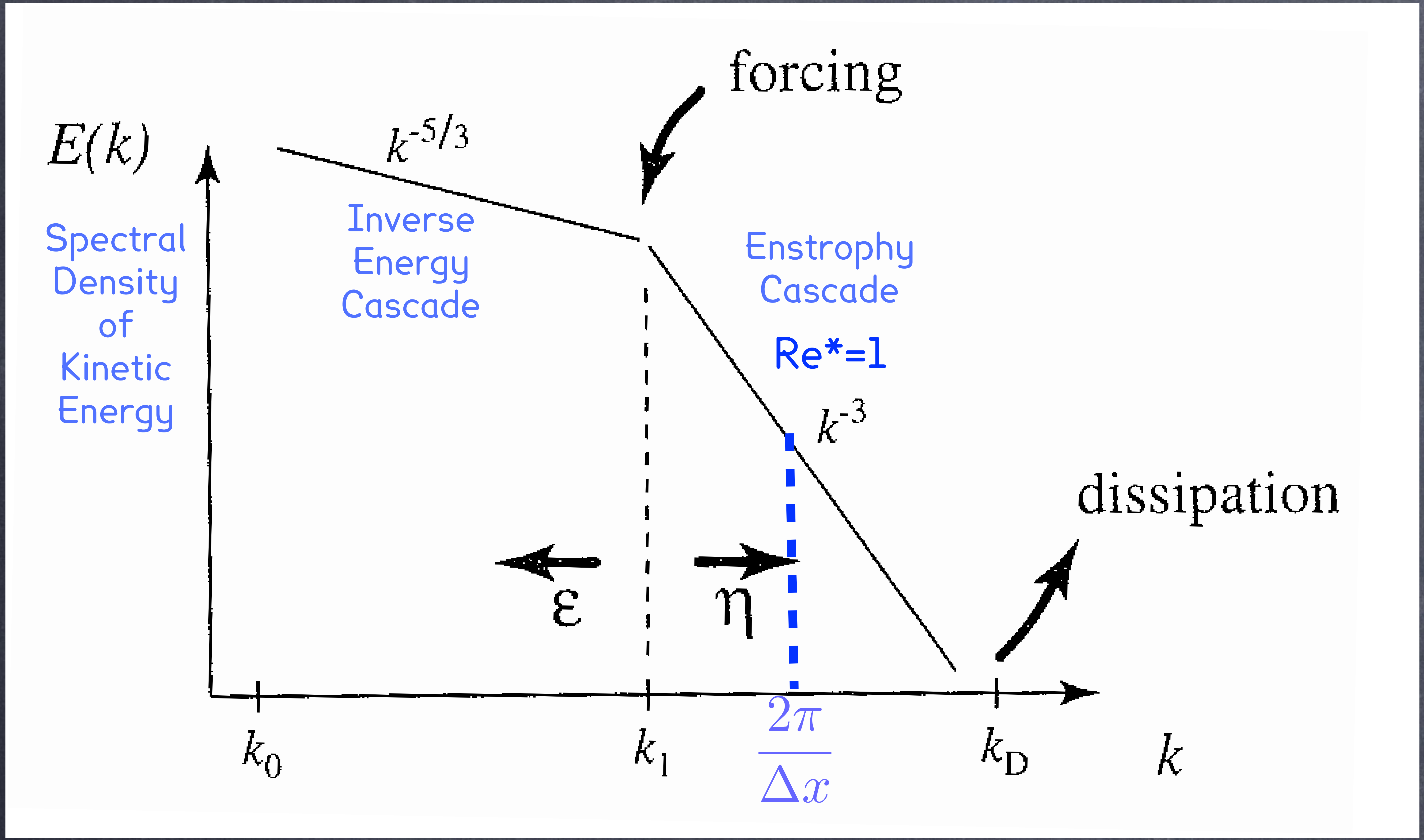


Suitable For 2D Oceans, E.g., Stommel & Munk Gyres

Best of: Graham & Ringler (2013)

1996: Leith Devises Viscosity Scaling,
So that the Enstrophy (vorticity²) Cascade is Preserved

R. Kraichnan, 1967 JFM
C.E. Leith, 1996 Physica D

$$\nu_* = \left(\frac{\Lambda \Delta x}{\pi}\right)^3 \left| \nabla_h \left( \frac{\partial u_*}{\partial y} - \frac{\partial v_*}{\partial x} \right) \right|$$

Barotropic or stacked layers

# Mesoscale Turbulence Like 2D cascade, but a little divergent

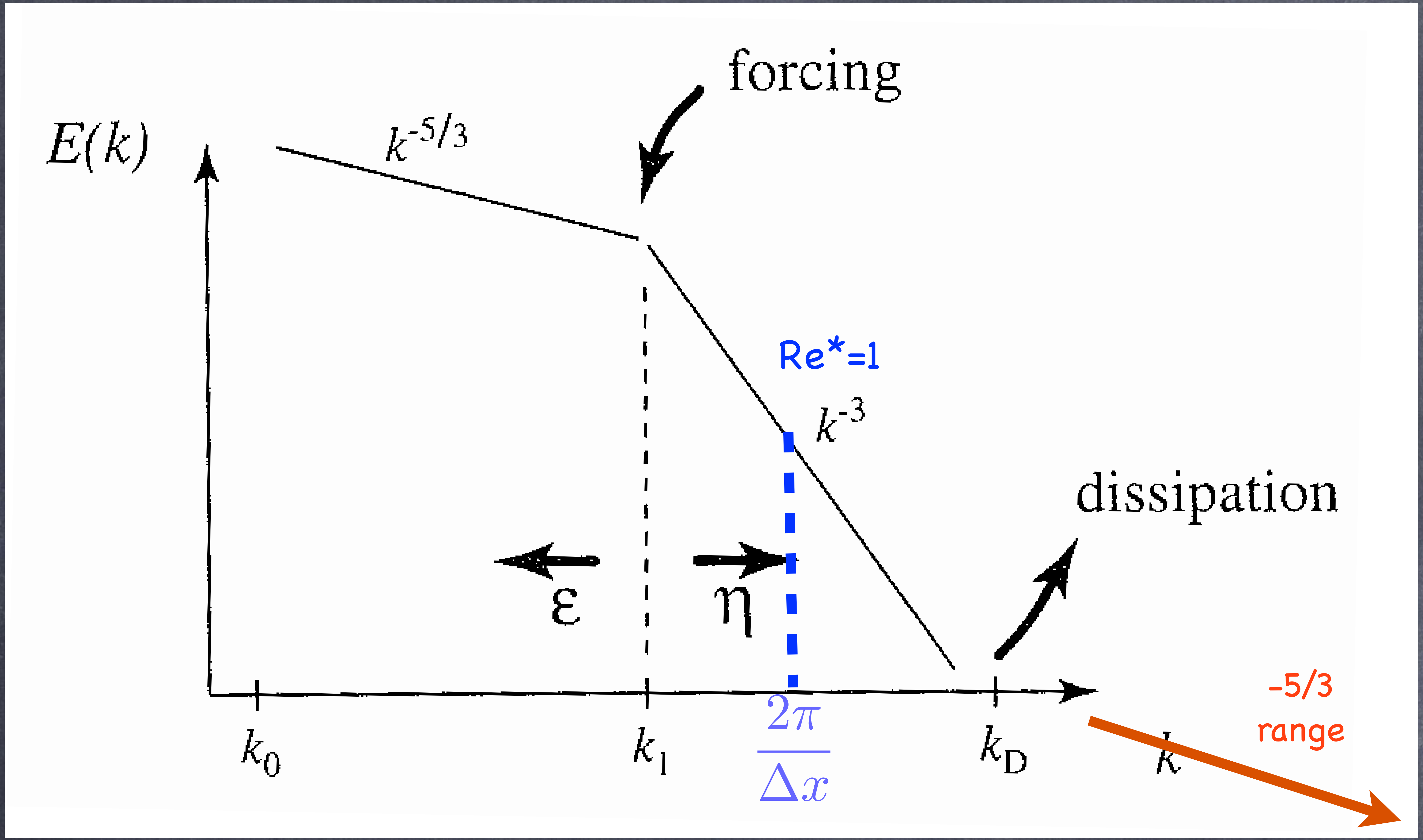


Suitable For 2D Oceans, Or Hydrostatic Boussinesq!

F-K & Menemenlis Revise Leith Viscosity Scaling,
So that diverging, vorticity-free, modes are also damped

$$\nu_* = \left(\frac{\Delta x}{\pi}\right)^3 \sqrt{\Lambda^6 |\nabla_h q_{2d}|^2 + \Lambda_d^6 |\nabla_h (\nabla_h \cdot \mathbf{u}_*)|^2}.$$

BFK and D. Menemenlis. Can large eddy simulation techniques improve mesoscale-rich ocean models? In M. Hecht and H. Hasumi, editors, Ocean Modeling in an Eddying Regime, volume 177, pages 319-338. AGU Geophysical Monograph Series, 2008.

# QGLeith: Pot'l Enstrophy cascade (efficient versions ready for Hydrostatic Boussinesq at 10km and finer)

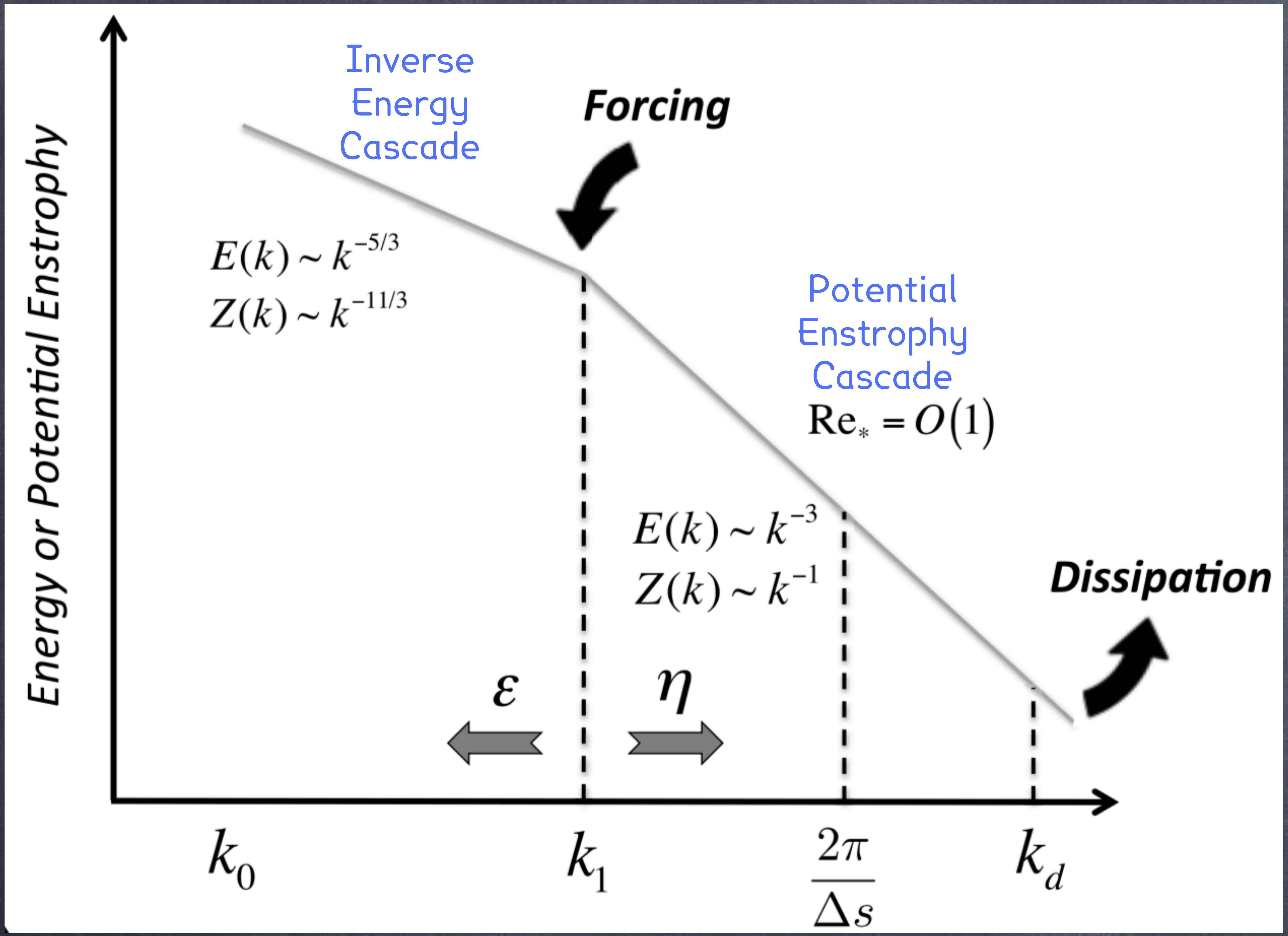


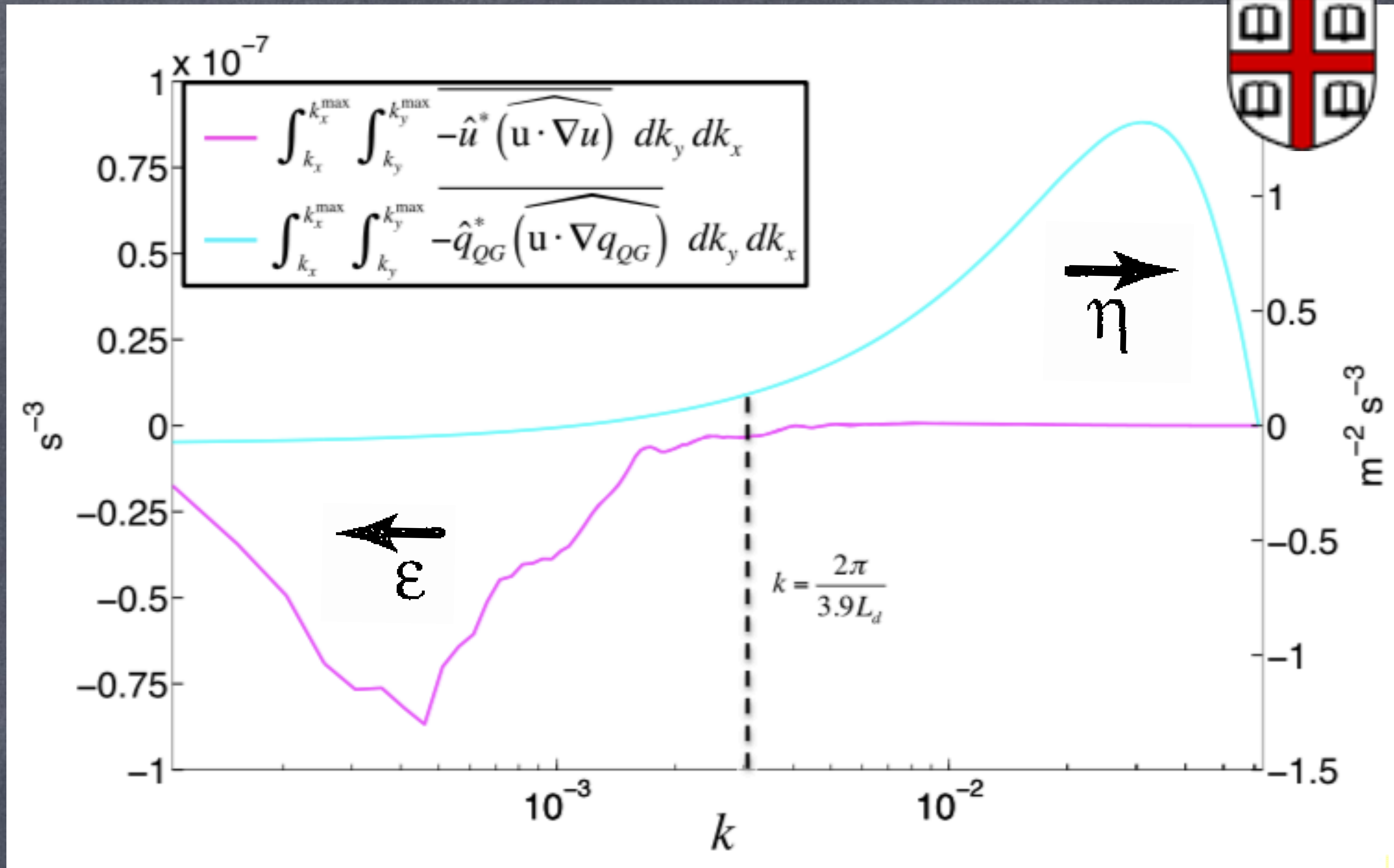


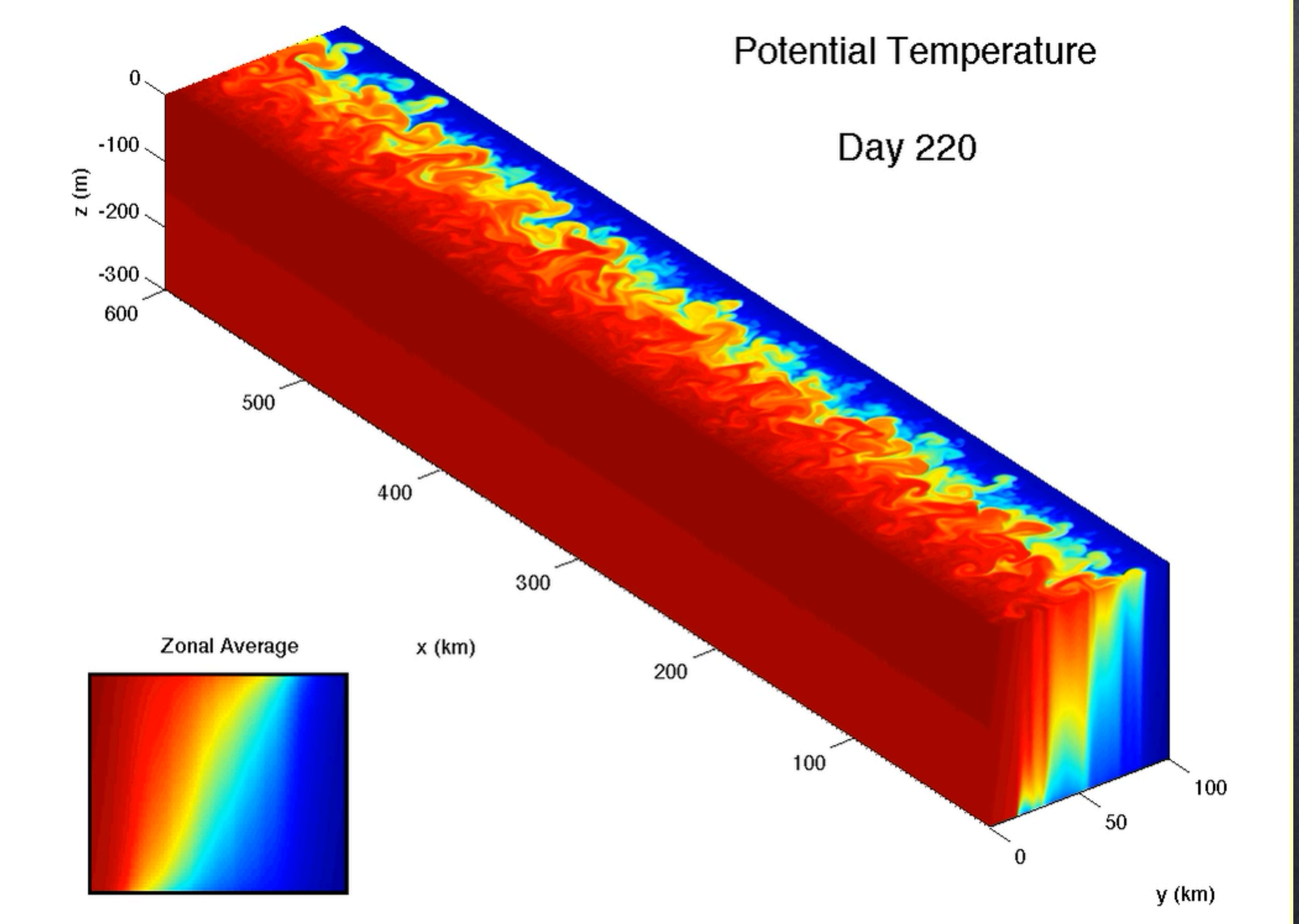


Provides lateral viscosity, diffusivity, and GM coefficient without overdamping resolved eddies


S. D. Bachman, B. Fox-Kemper, and B. Pearson. A scale-aware subgrid model for quasigeostrophic turbulence. Journal of Geophysical Research-Oceans, 122:1529-1554, March 2017.

B. Pearson, BFK, S. D. Bachman, and F. O. Bryan, 2017: Evaluation of scale-aware subgrid mesoscale eddy models in a global eddy-rich model. Ocean Modelling, 115:42–58.

# QGLeith: Pot'l Enstrophy cascade (efficient versions ready for Hydrostatic Boussinesq at 10km and finer)

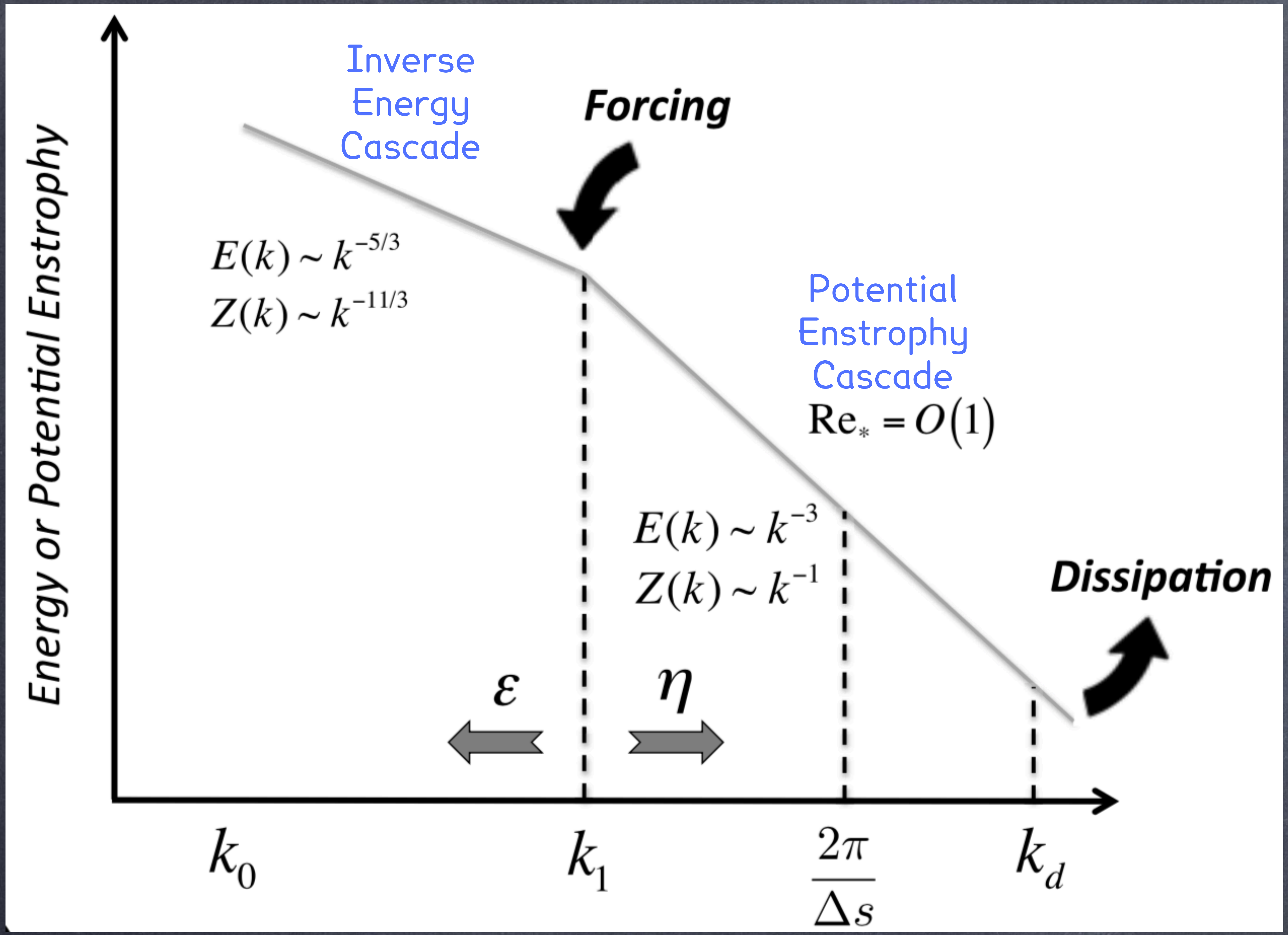


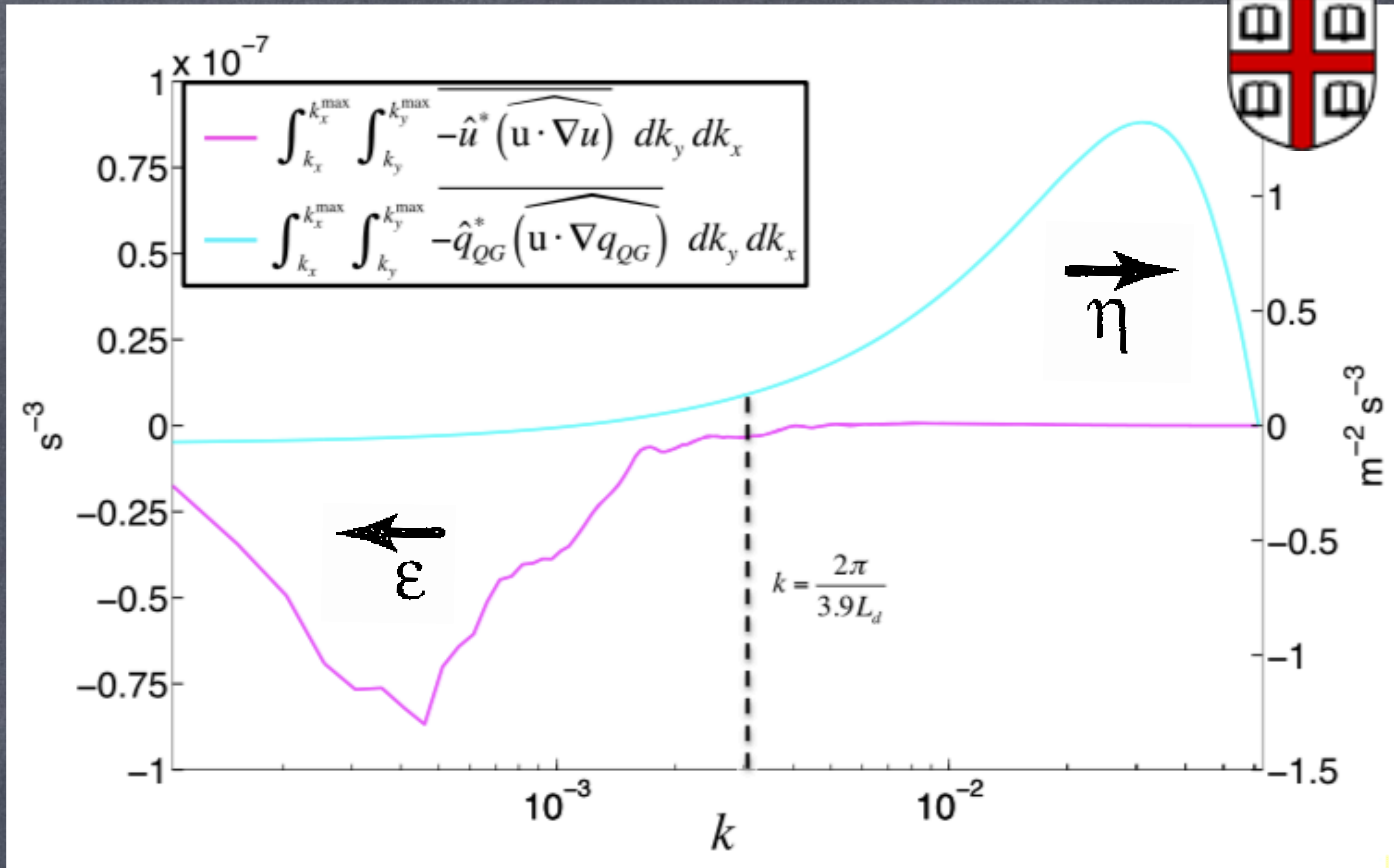


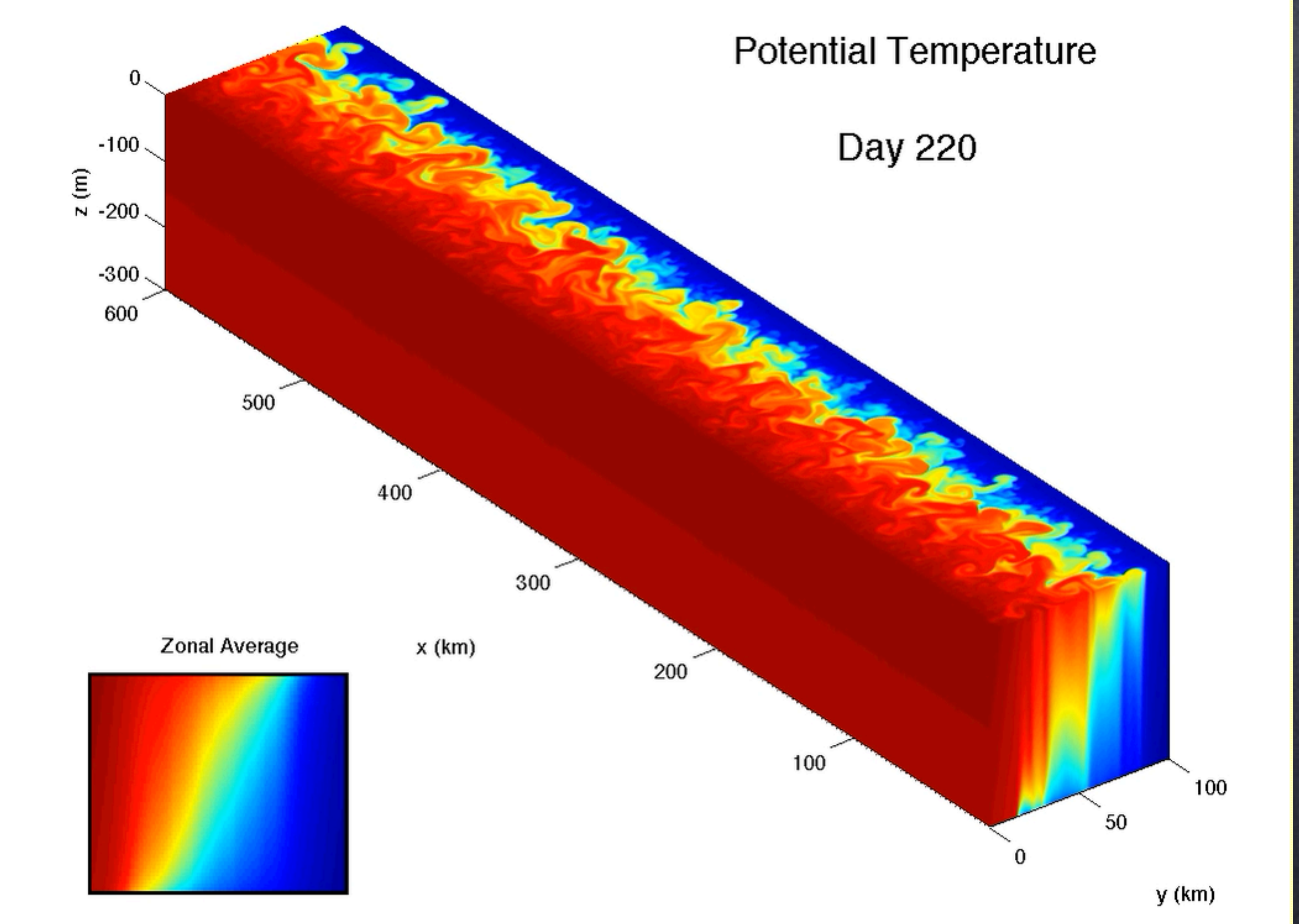


Provides lateral viscosity, diffusivity, and GM coefficient without overdamping resolved eddies


S. D. Bachman, B. Fox-Kemper, and B. Pearson. A scale-aware subgrid model for quasigeostrophic turbulence. Journal of Geophysical Research-Oceans, 122:1529-1554, March 2017.

B. Pearson, BFK, S. D. Bachman, and F. O. Bryan, 2017: Evaluation of scale-aware subgrid mesoscale eddy models in a global eddy-rich model. Ocean Modelling, 115:42-58.

# QG Turbulence: Pot'l Enstrophy cascade

## A Mesoscale Ocean Large Eddy Simulations Closure


BFK and D. Menemenlis. Can large eddy simulation techniques improve mesoscale-rich ocean models? In M. Hecht and H. Hasumi, editors, Ocean Modeling in an Eddying Regime, volume 177, pages 319-338. AGU Geophysical Monograph Series, 2008.

S. D. Bachman, B. Fox-Kemper, and B. Pearson. A scale-aware subgrid model for quasigeostrophic turbulence. Journal of Geophysical Research-Oceans, 122:1529-1554, March 2017.


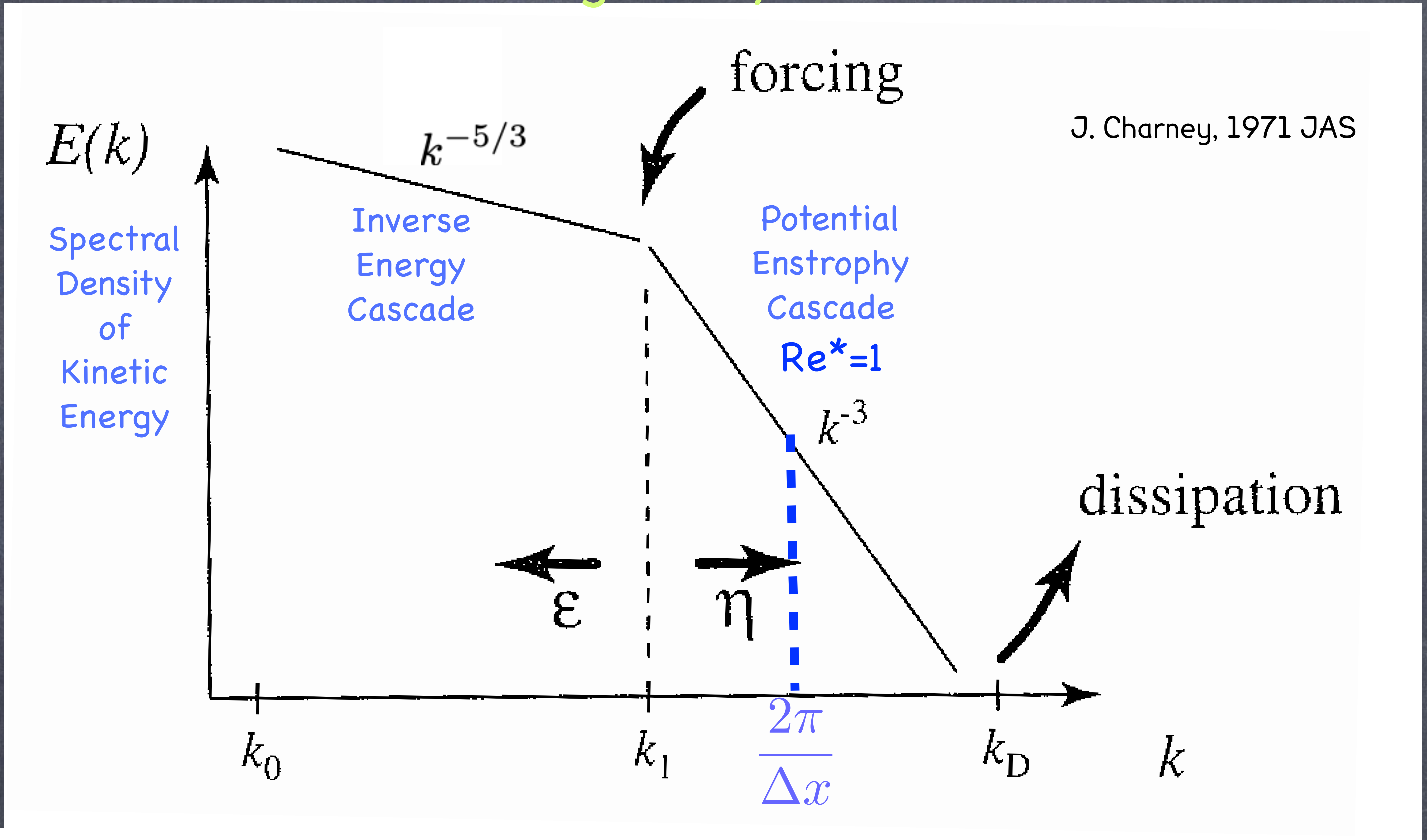


QG Leith Parameterization

$$\nu_{qg} = \left(\frac{\Lambda_{qg}\Delta x}{\pi}\right)^3 |\nabla q_{qg}|$$

$$q^*_{2d} = f + \hat{k}\cdot\nabla\times u^*$$
$$q^*_{qg} = f + \hat{k}\cdot\nabla\times u^* + \frac{\partial}{\partial z}\frac{f^2}{N^2}b^*$$

But, in QG, PV links buoyancy (diff.) to vorticity (visa.)

$$\nu_{qg} = \kappa_{Redi} = \kappa_{GM} = \left(\frac{\Lambda_{qg}\Delta x}{\pi}\right)^3 |\nabla q_{qg}|.$$

# Where does ocean energy go?

Spectrally speaking

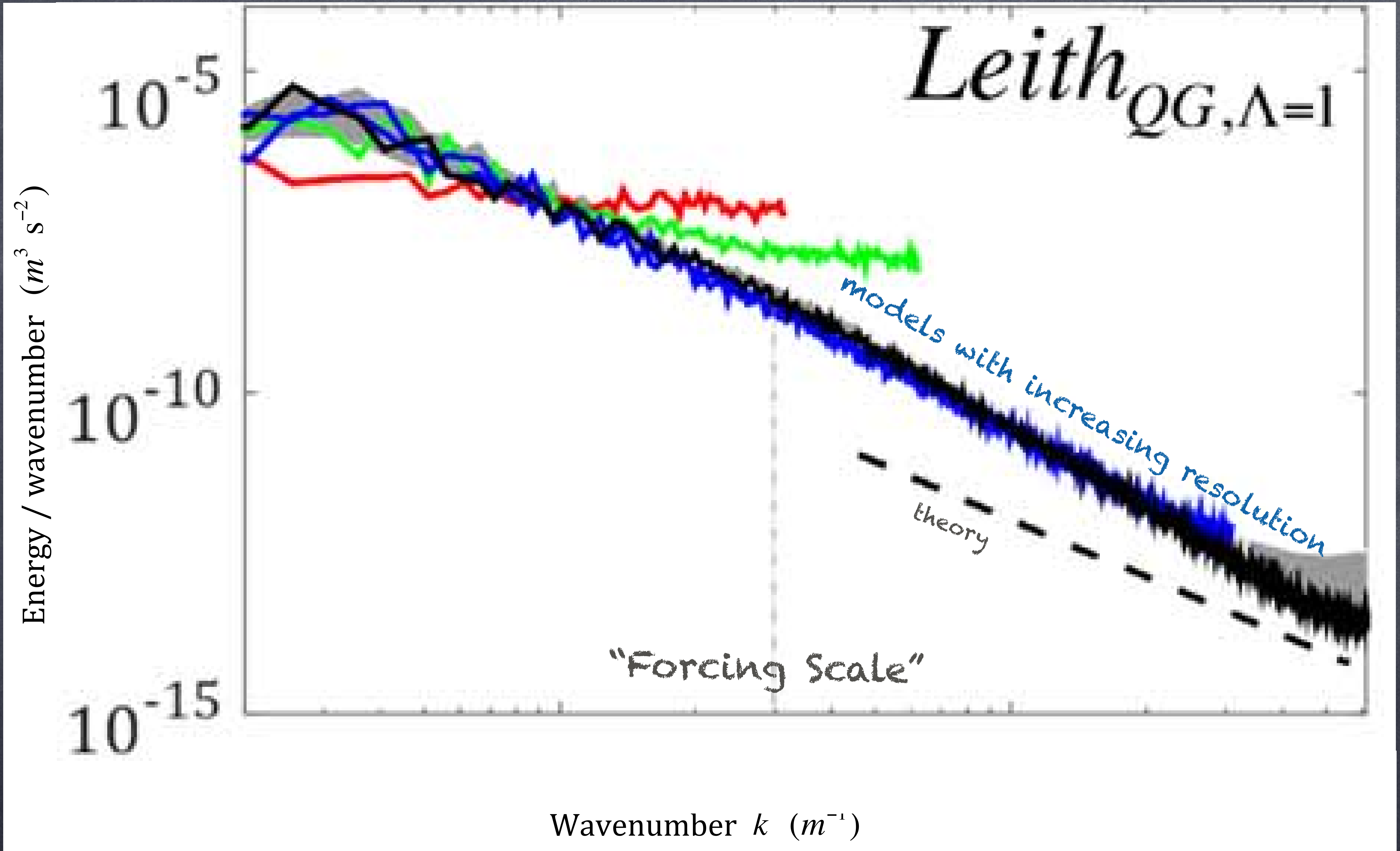


S. D. Bachman, B. Fox-Kemper, and B. Pearson, 2017: A scale-aware subgrid model for quasi- geostrophic turbulence. Journal of Geophysical Research–Oceans, 122:1529–1554. URL http: //dx.doi.org/10.1002/2016JC012265.

# Where does ocean energy go?

## Spectrally speaking

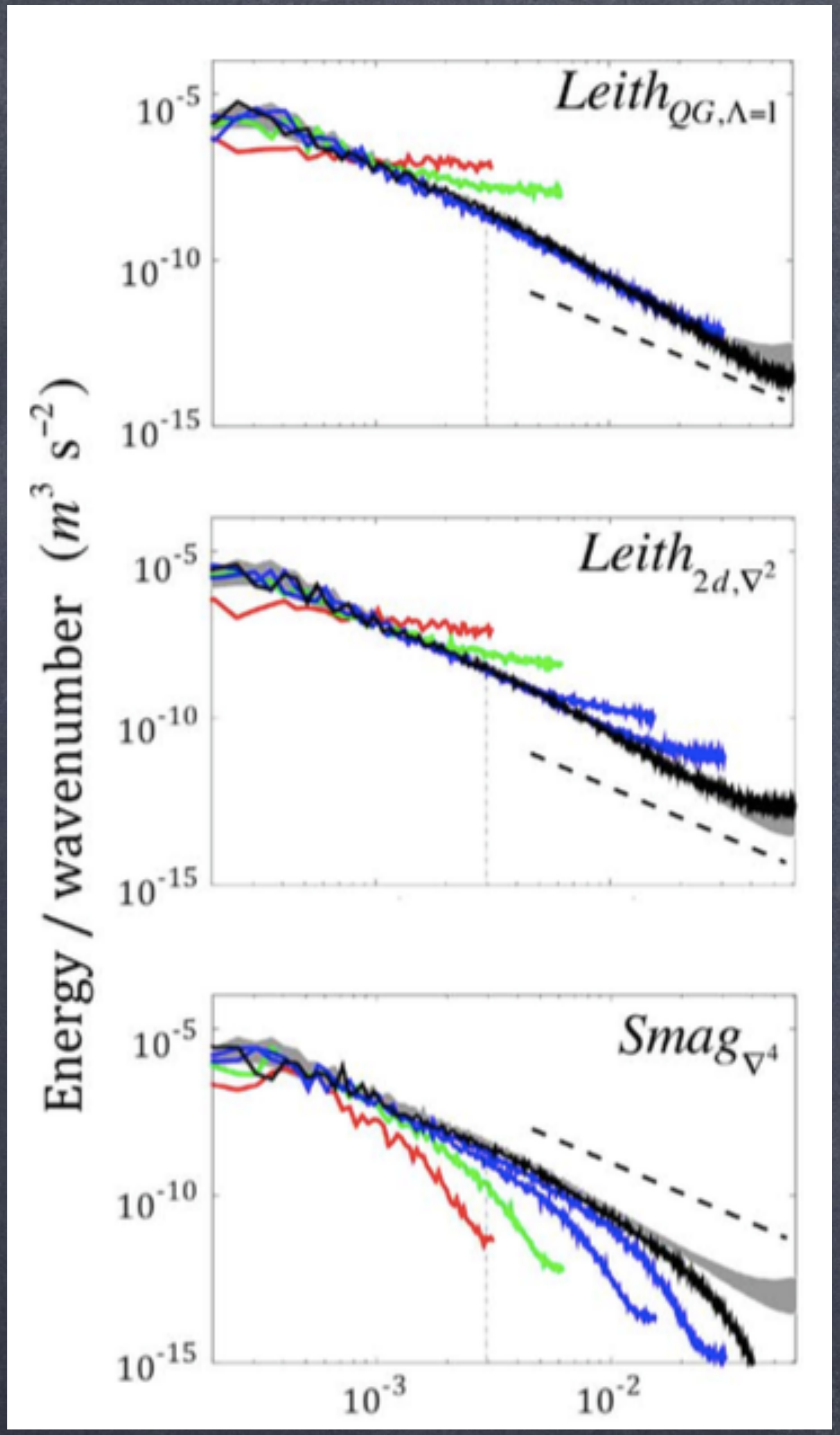


S. D. Bachman, B. Fox-Kemper, and B. Pearson, 2017: A scale-aware subgrid model for quasi- geostrophic turbulence. Journal of Geophysical Research–Oceans, 122:1529–1554. URL http: //dx.doi.org/10.1002/2016JC012265.

# Where does ocean energy go?

Spectrally speaking

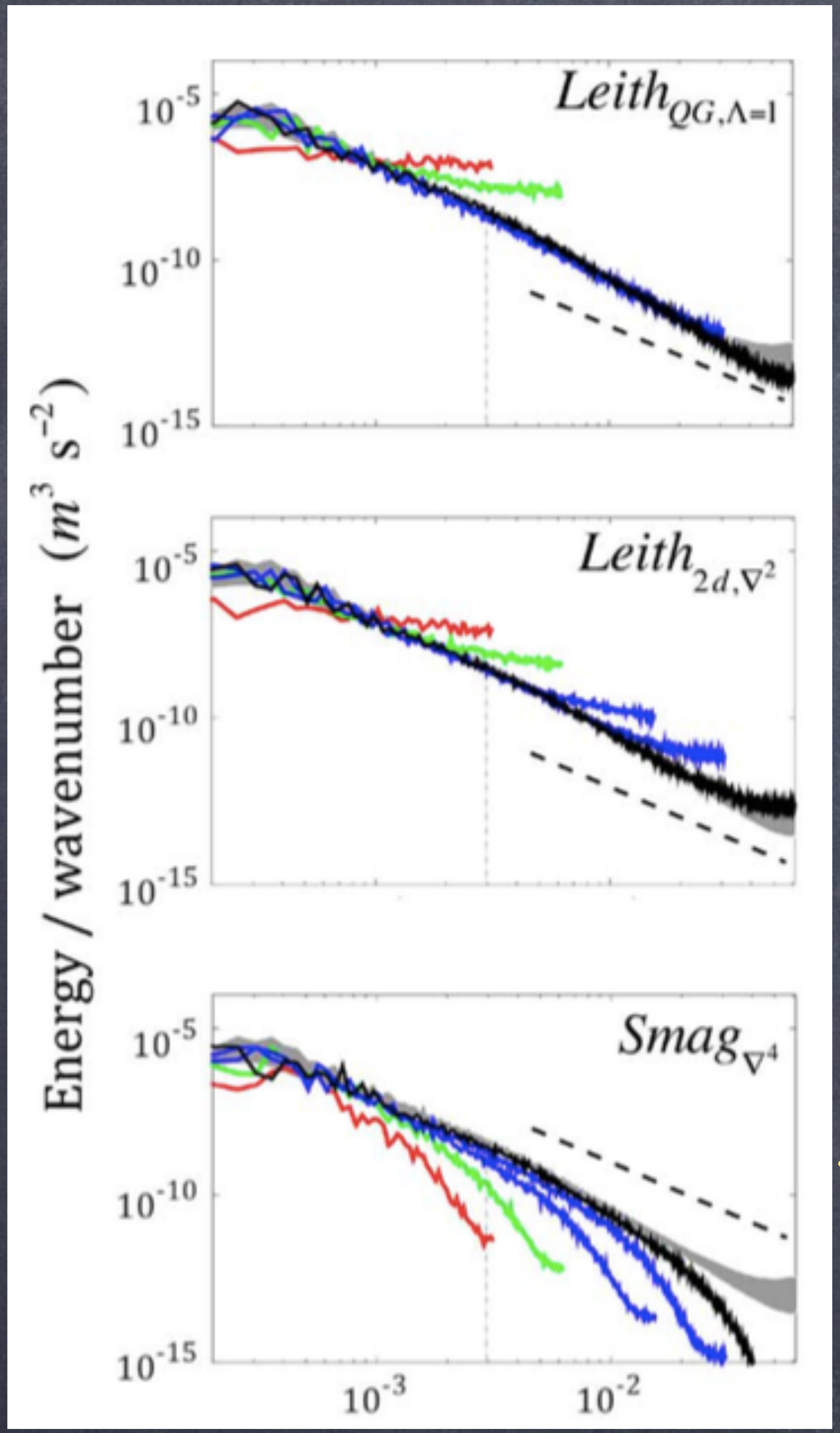


Too Smooth

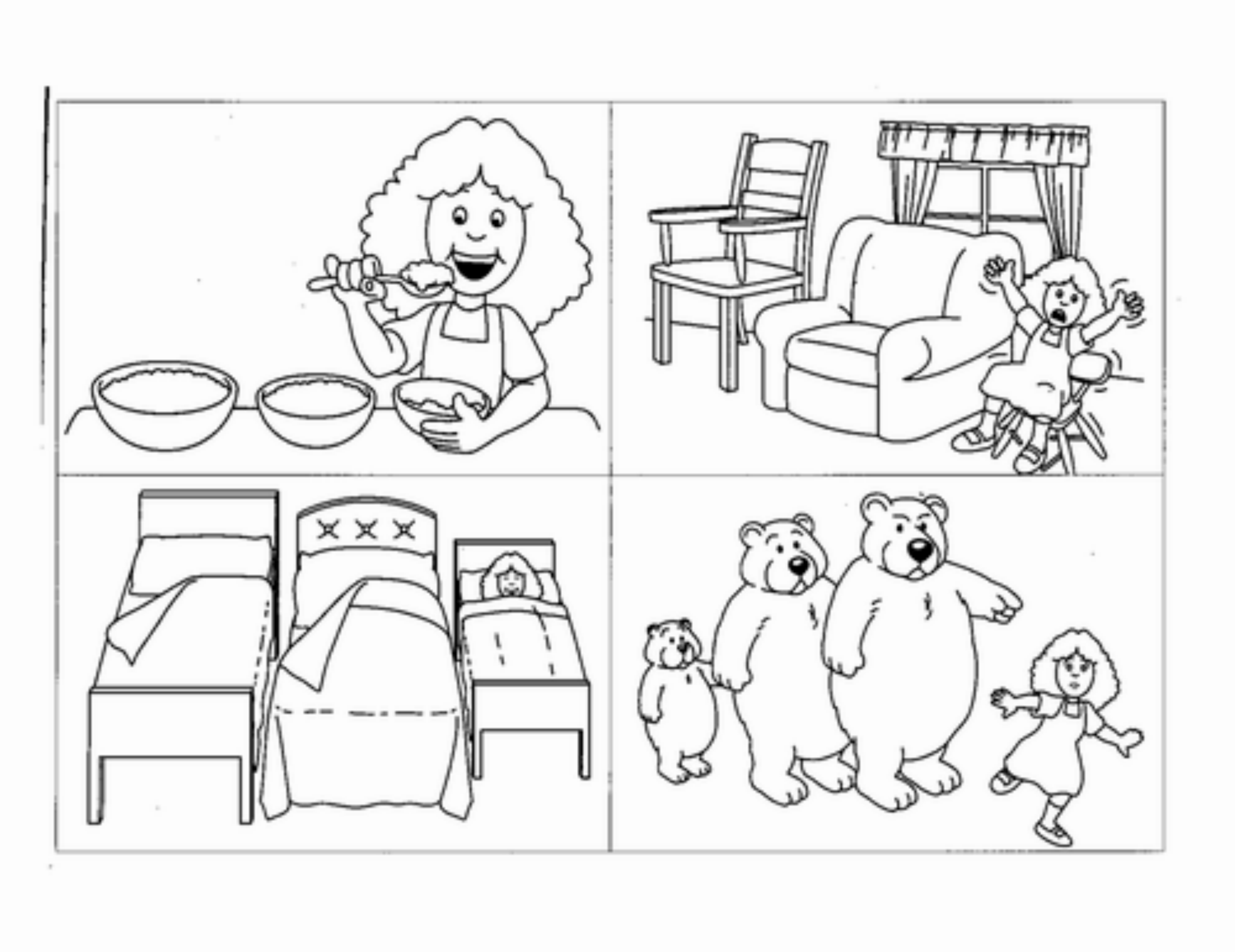

S. D. Bachman, B. Fox-Kemper, and B. Pearson, 2017: A scale-aware subgrid model for quasi- geostrophic turbulence. Journal of Geophysical Research–Oceans, 122:1529–1554. URL http: //dx.doi.org/10.1002/2016JC012265.

# Where does ocean energy go?

## Spectrally speaking

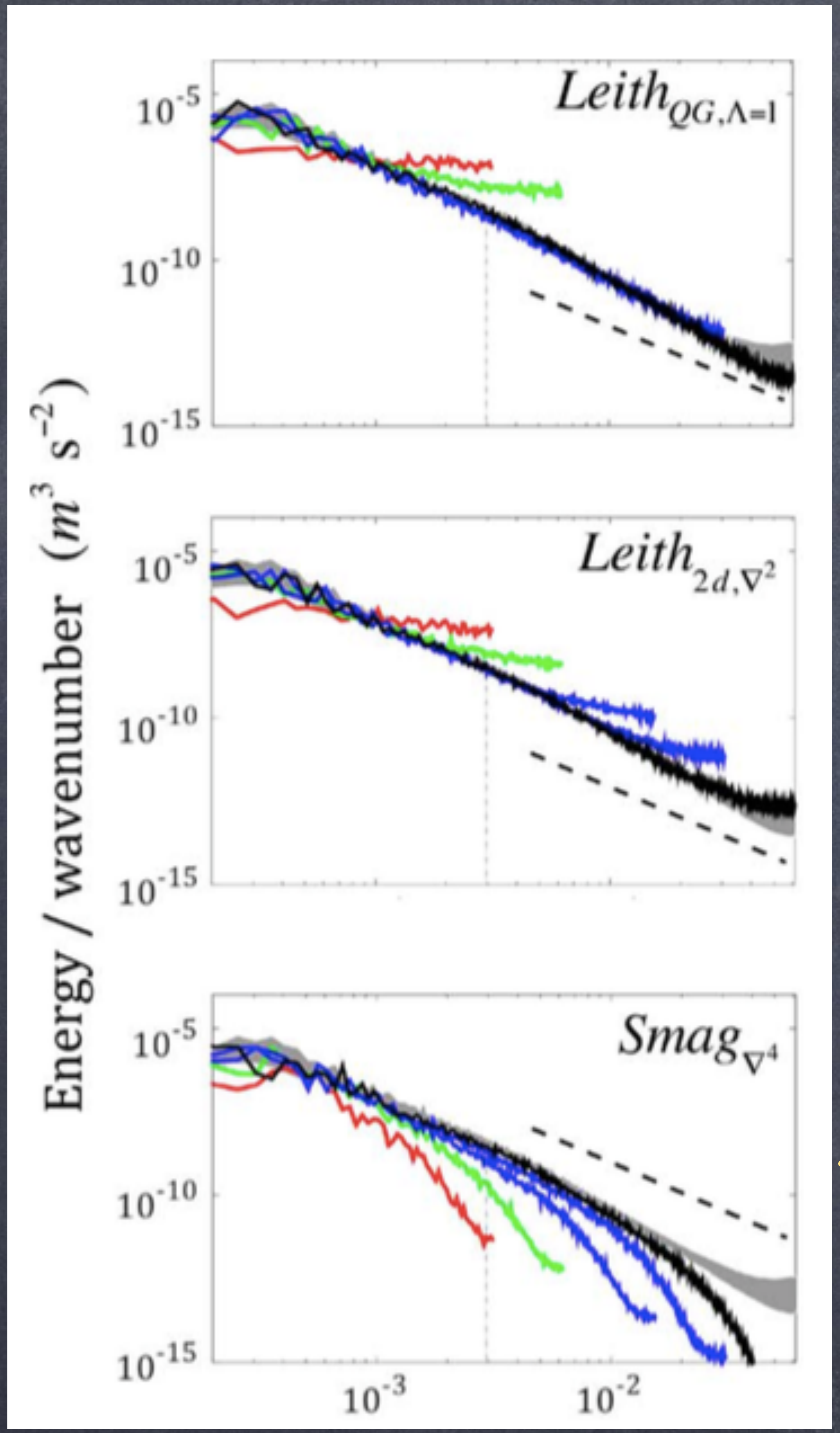


Too Noisy

Too Smooth

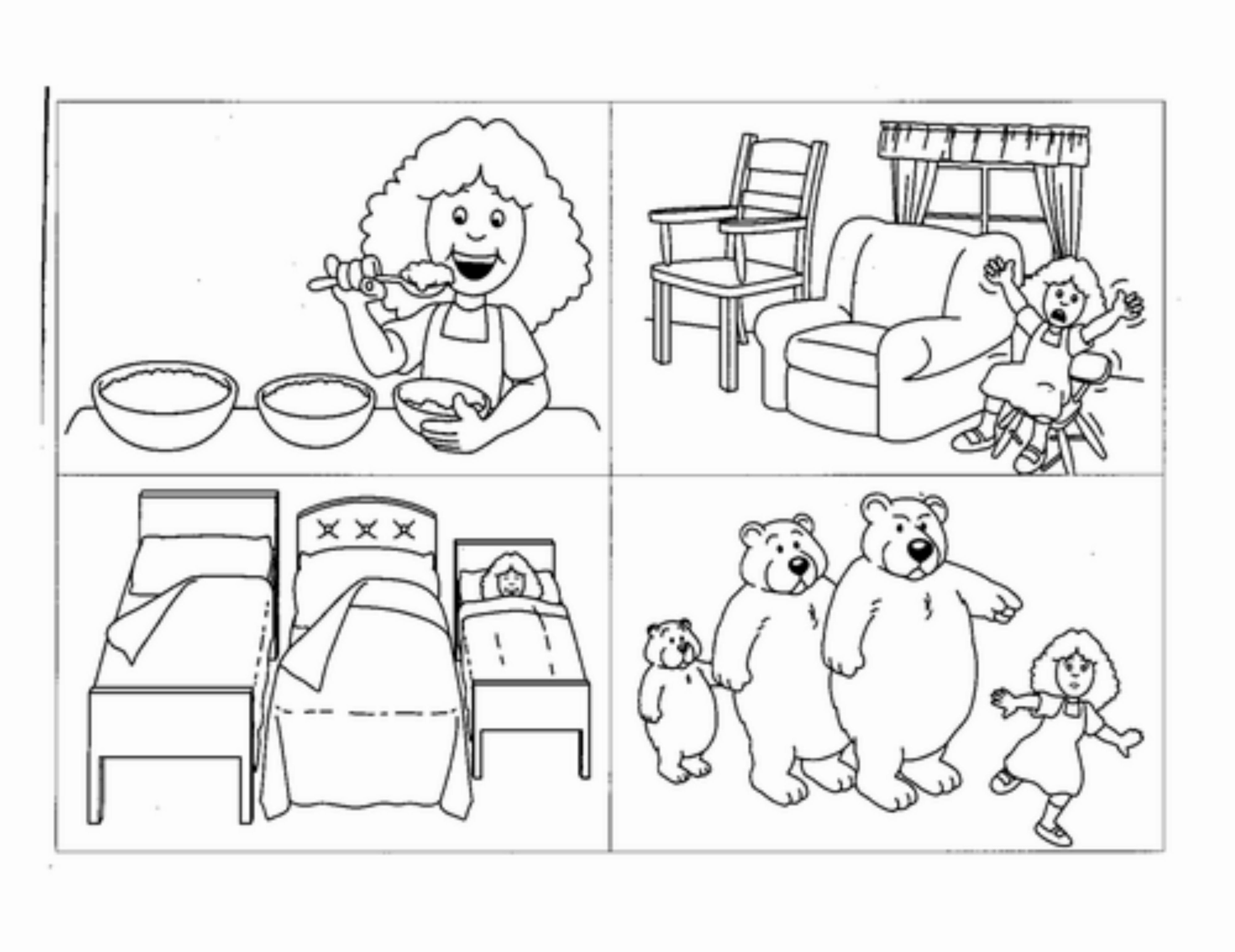

S. D. Bachman, B. Fox-Kemper, and B. Pearson, 2017: A scale-aware subgrid model for quasi- geostrophic turbulence. Journal of Geophysical Research–Oceans, 122:1529–1554. URL http: //dx.doi.org/10.1002/2016JC012265.

# Where does ocean energy go?

Spectrally speaking

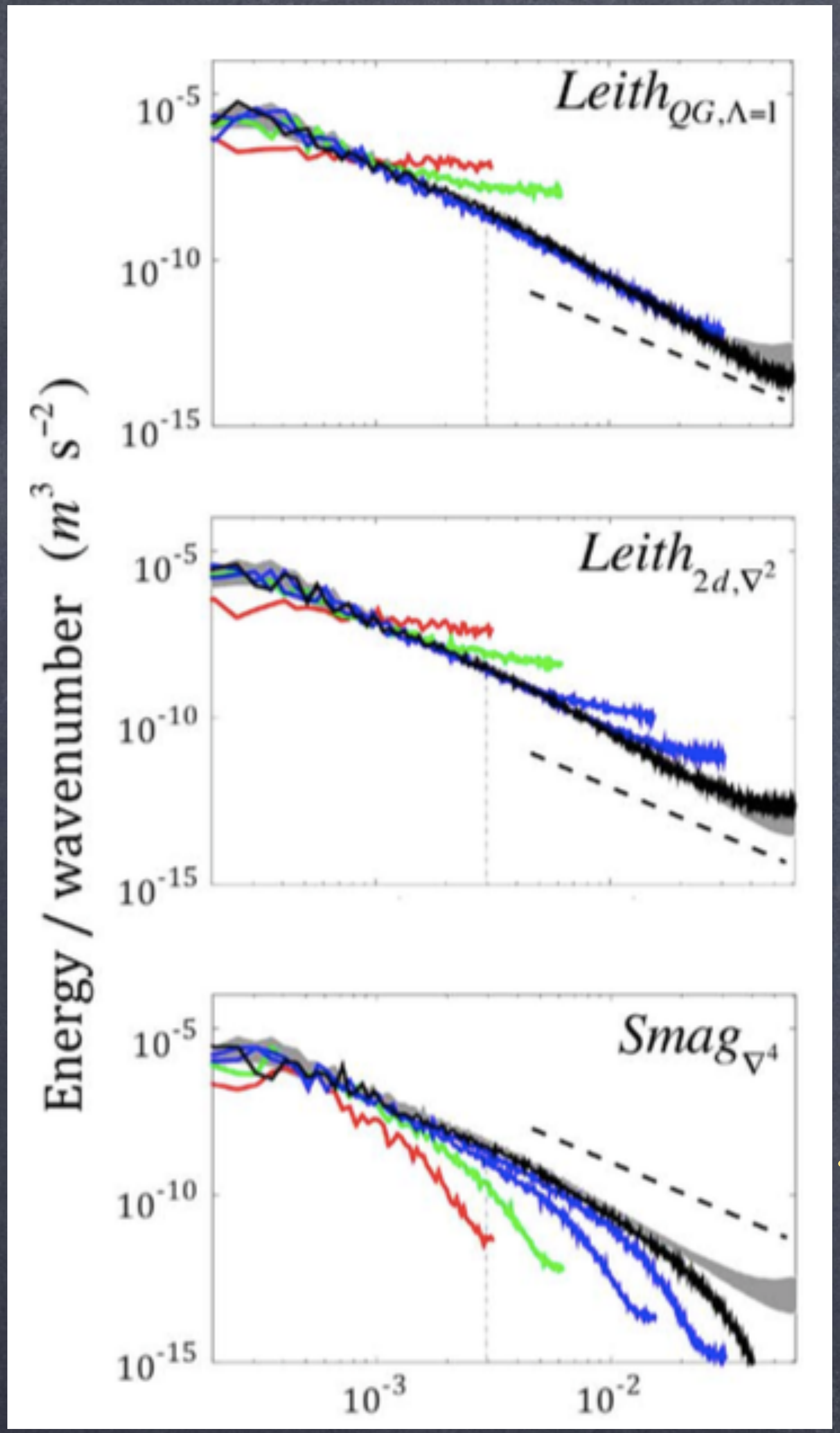


Just Right

Too Noisy

Too Smooth

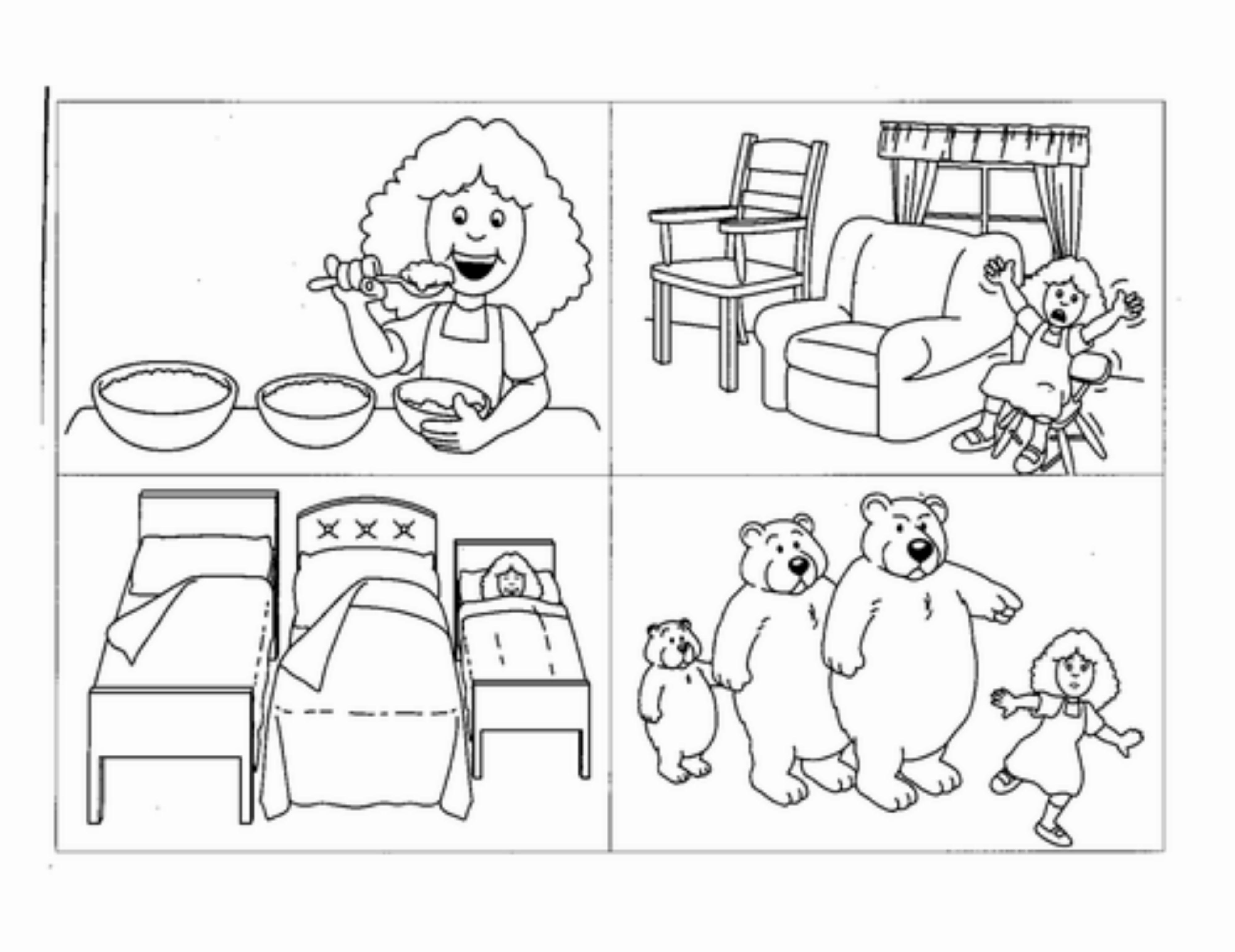

S. D. Bachman, B. Fox-Kemper, and B. Pearson, 2017: A scale-aware subgrid model for quasi- geostrophic turbulence. Journal of Geophysical Research–Oceans, 122:1529–1554. URL http: //dx.doi.org/10.1002/2016JC012265.

# QG Leith:

Works OK in an idealized flow:
Let's try it in a realistic, global model!

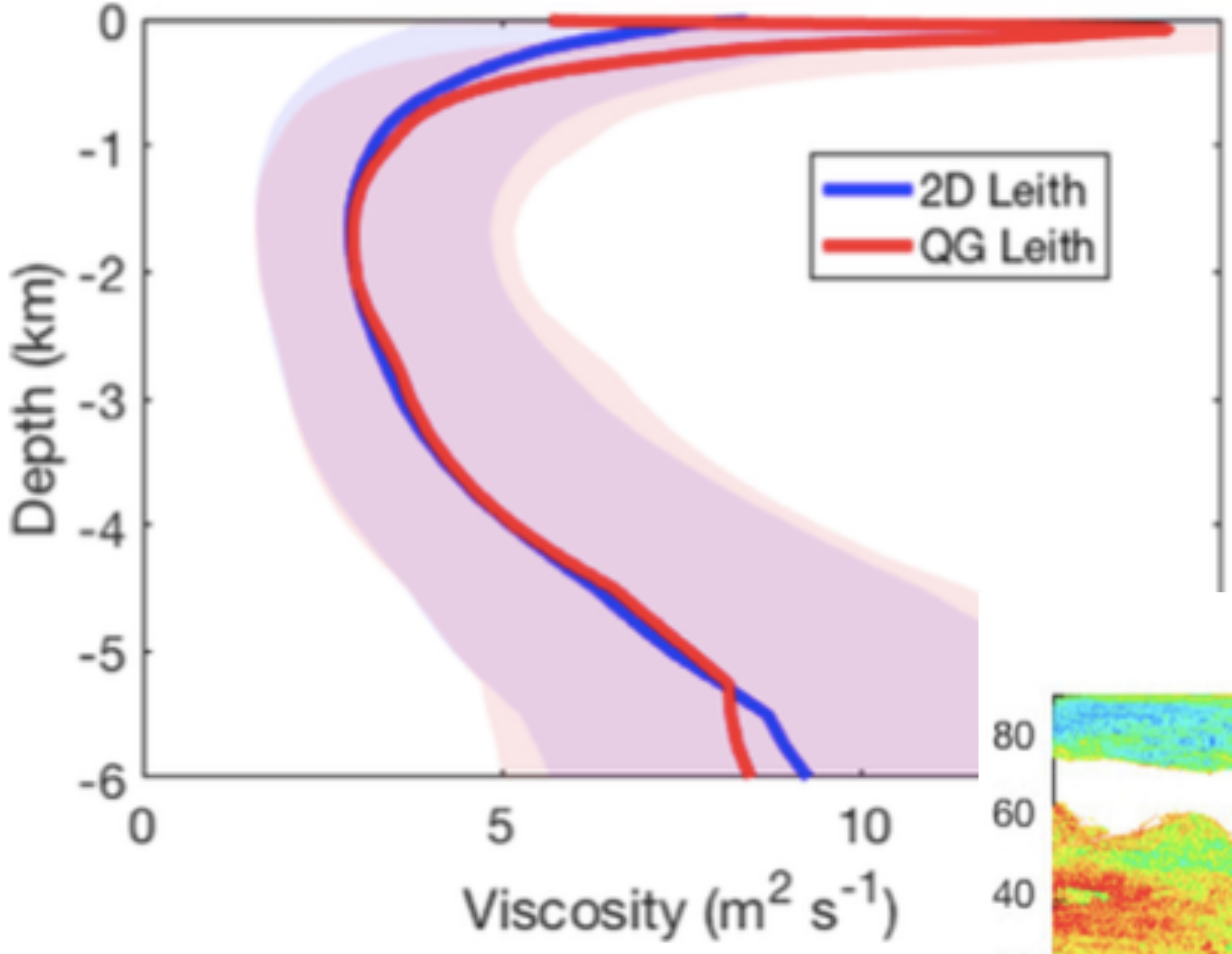


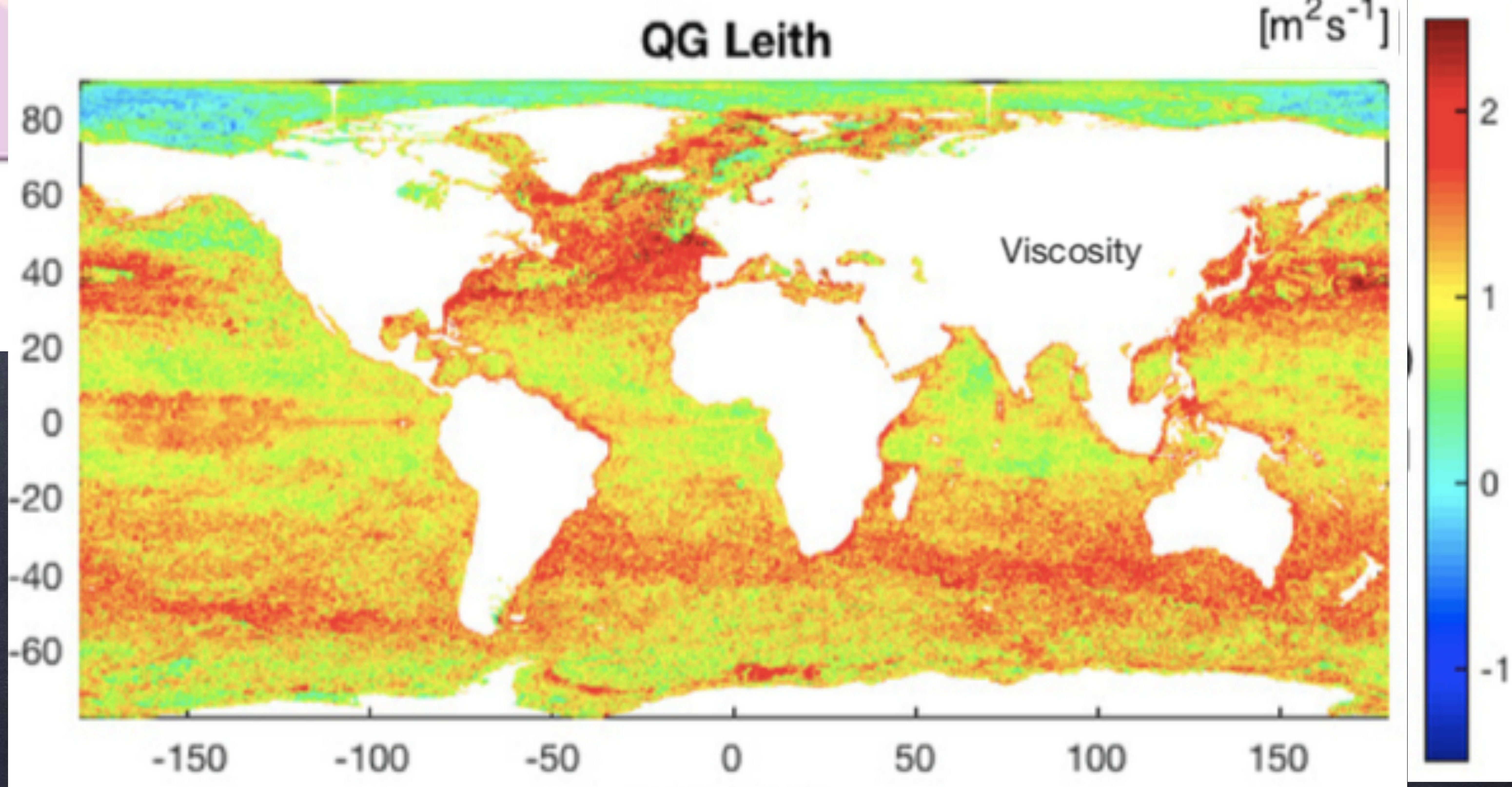


B. Pearson, BFK, S. D. Bachman, and F. O. Bryan, 2017: Evaluation of scale-aware subgrid mesoscale eddy models in a global eddy-rich model. Ocean Modelling, 115:42–58.

# Mesoscale Ocean LES: QGLeith

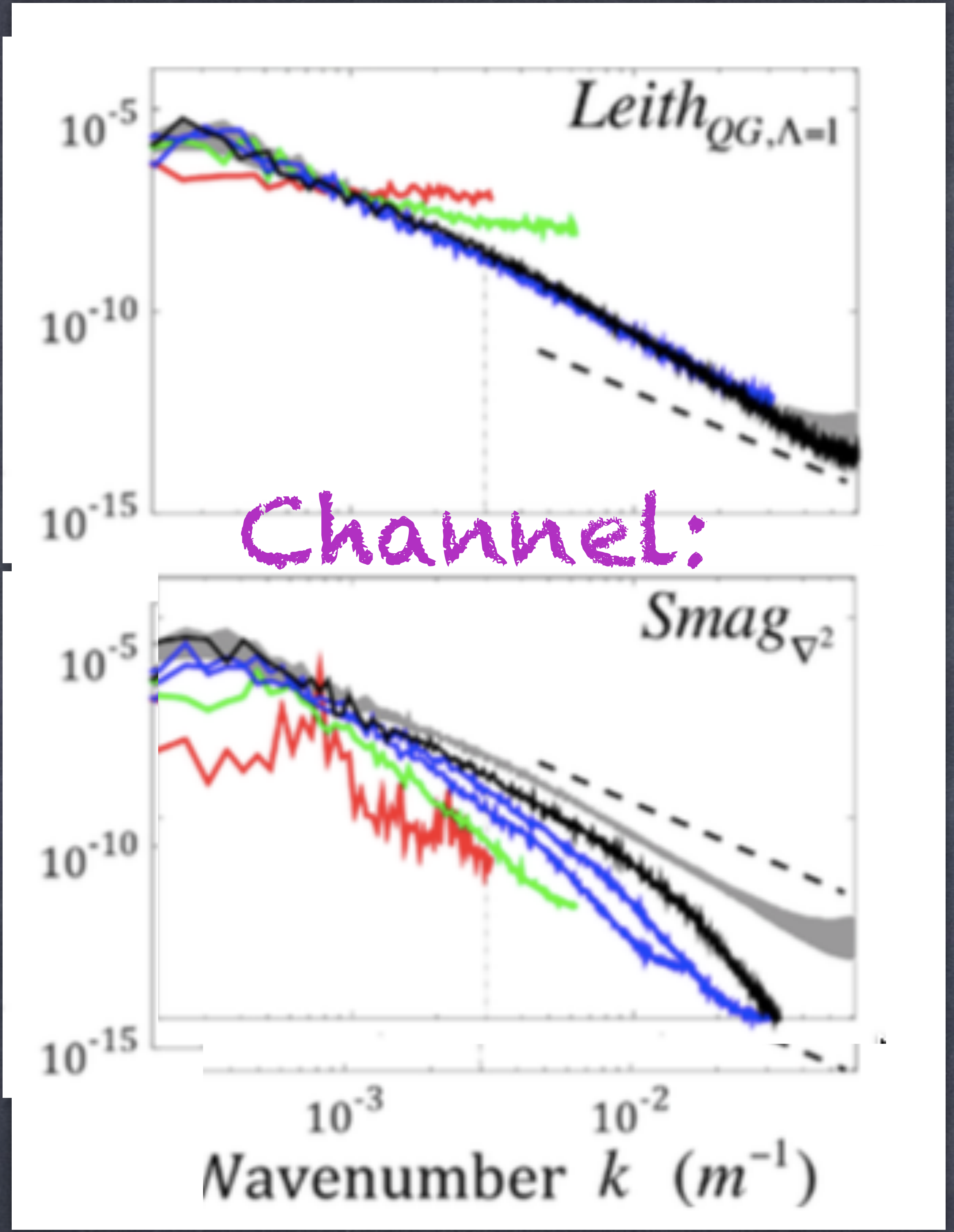


Channel:

LES for Pot'l Enstrophy

LES for EKE

ACC in Global!

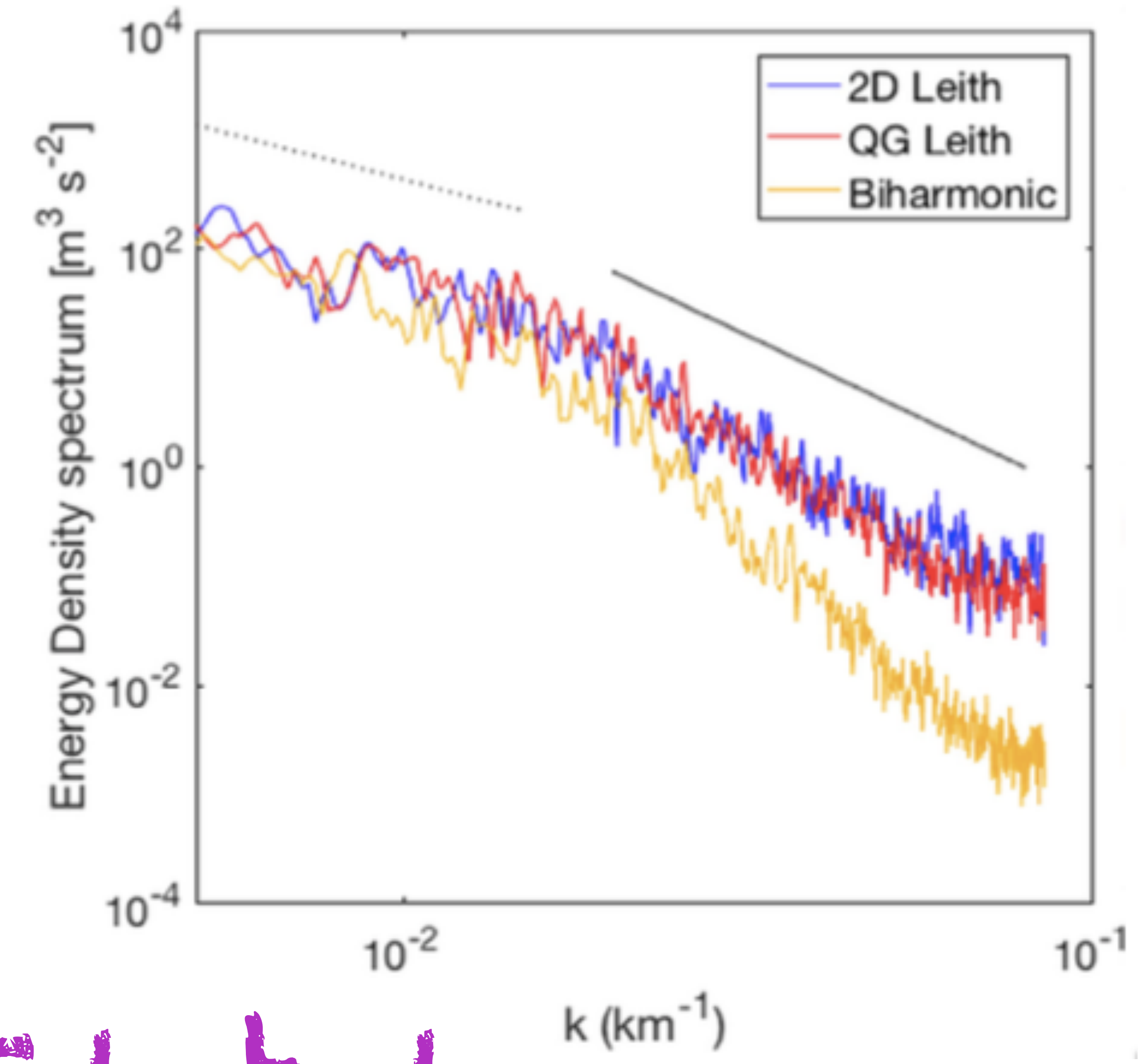


Global:
100m Dissipation

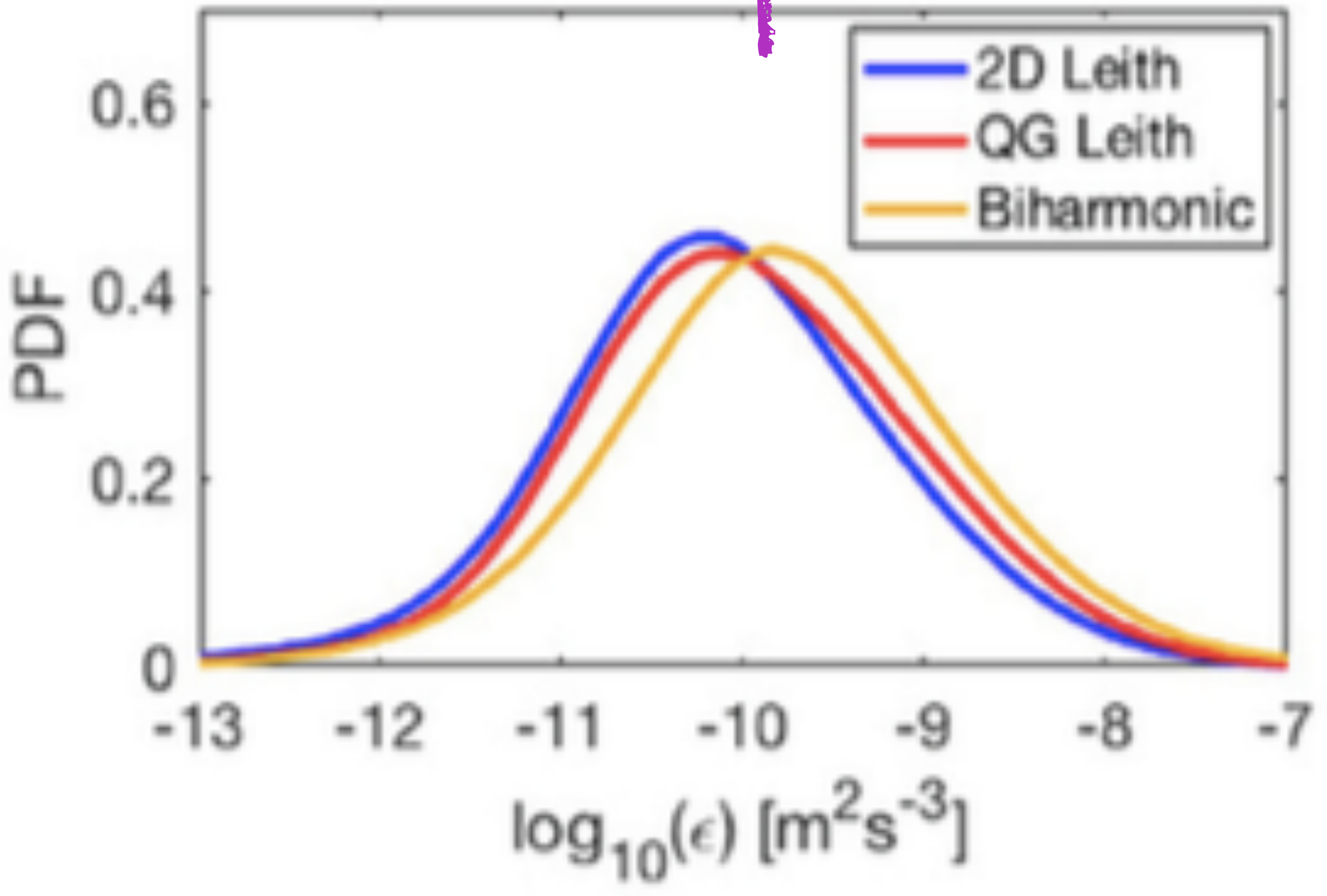


Global, POP, realistic forcing
10km (nominal) global
42 vertical levels
(most in upper 200m)


B. Pearson, BFK, S. D. Bachman, and F. O. Bryan, 2017: Evaluation of scale-aware subgrid mesoscale eddy models in a global eddy-rich model. Ocean Modelling, 115:42–58.

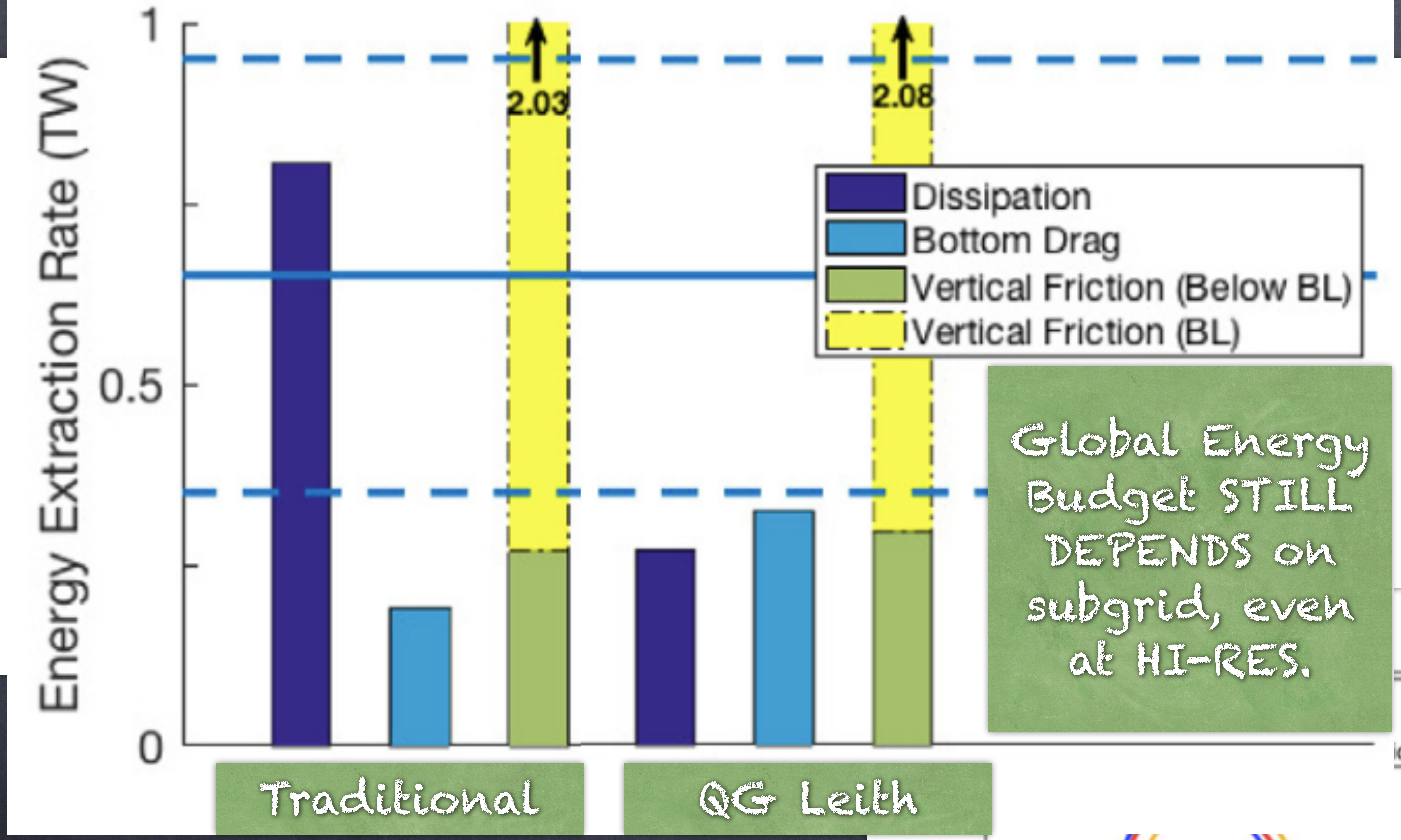


Global Energy Budget STILL DEPENDS on subgrid, even at HI-RES.

(most in upper 200m)

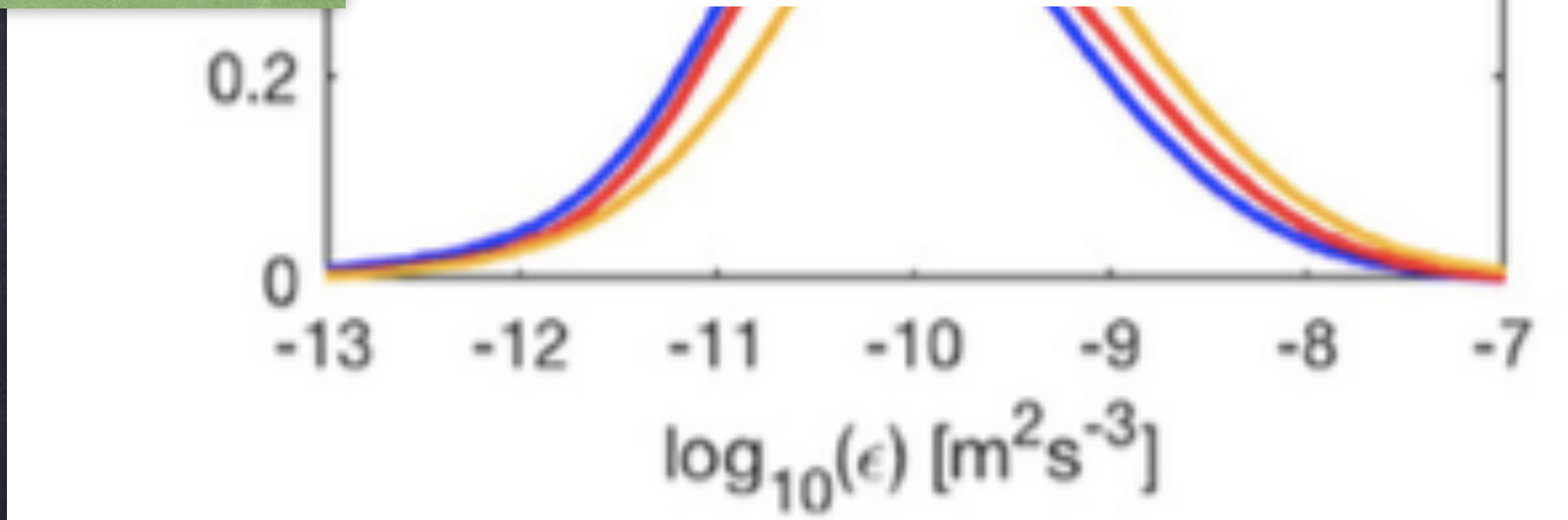


B. Pearson, BFK, S. D. Bachman, and F. O. Bryan, 2017: Evaluation of scale-aware subgrid mesoscale eddy models in a global eddy-rich model. Ocean Modelling, 115:42–58.

# A fun & meaningful result!

(Credit conversations with Royce in Dresden)

A (weak) dissipation of energy with pot'l enstrophy cascade

…

that's lognormally distributed

(super-Yaglom '66)

90% of KE dissipation in 10% of ocean

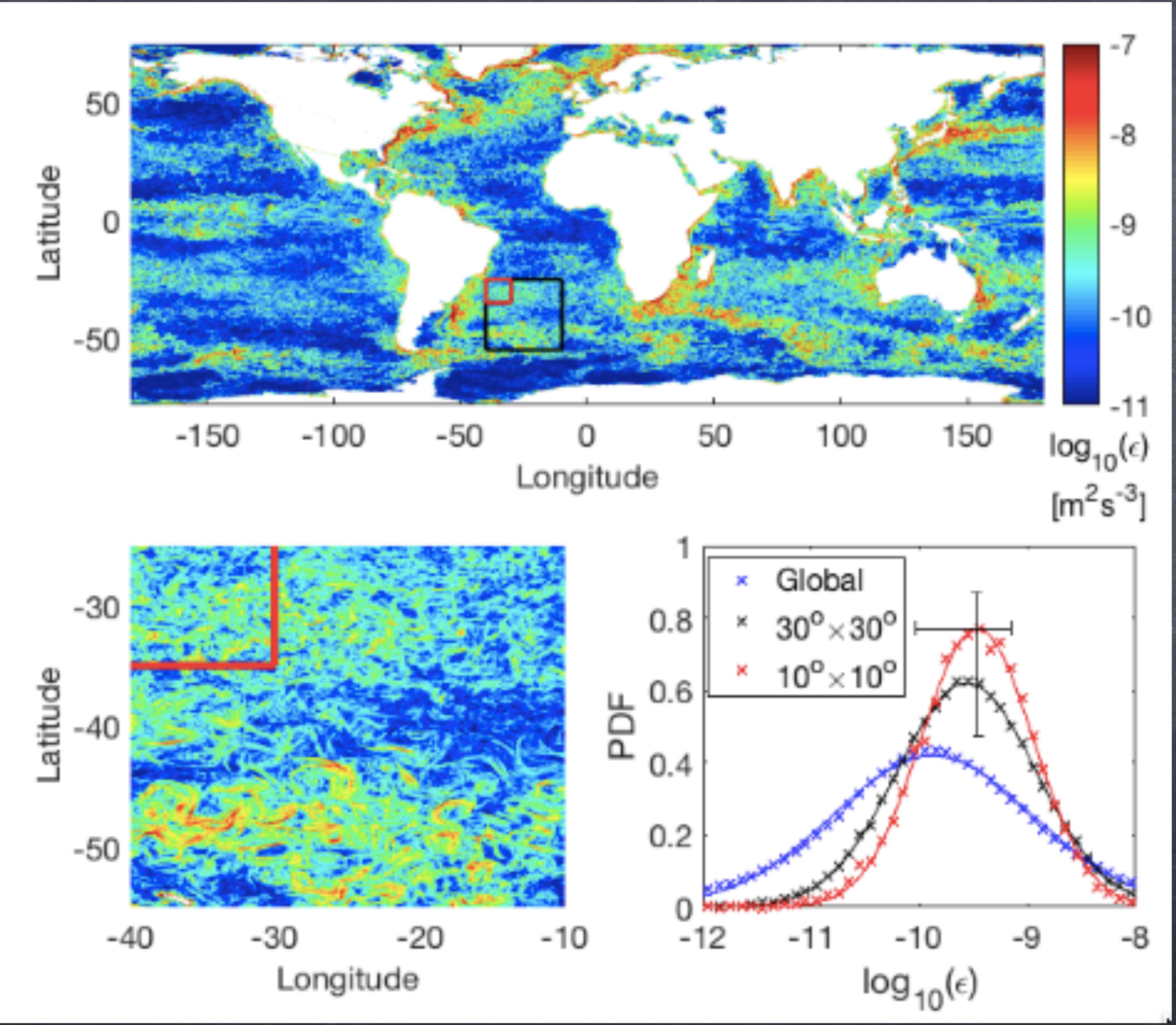


B. Pearson and BFK. Log-normal turbulence dissipation in global ocean models. Physical Review Letters, 120(9):094501, March 2018.

# Character of the Submesoscale

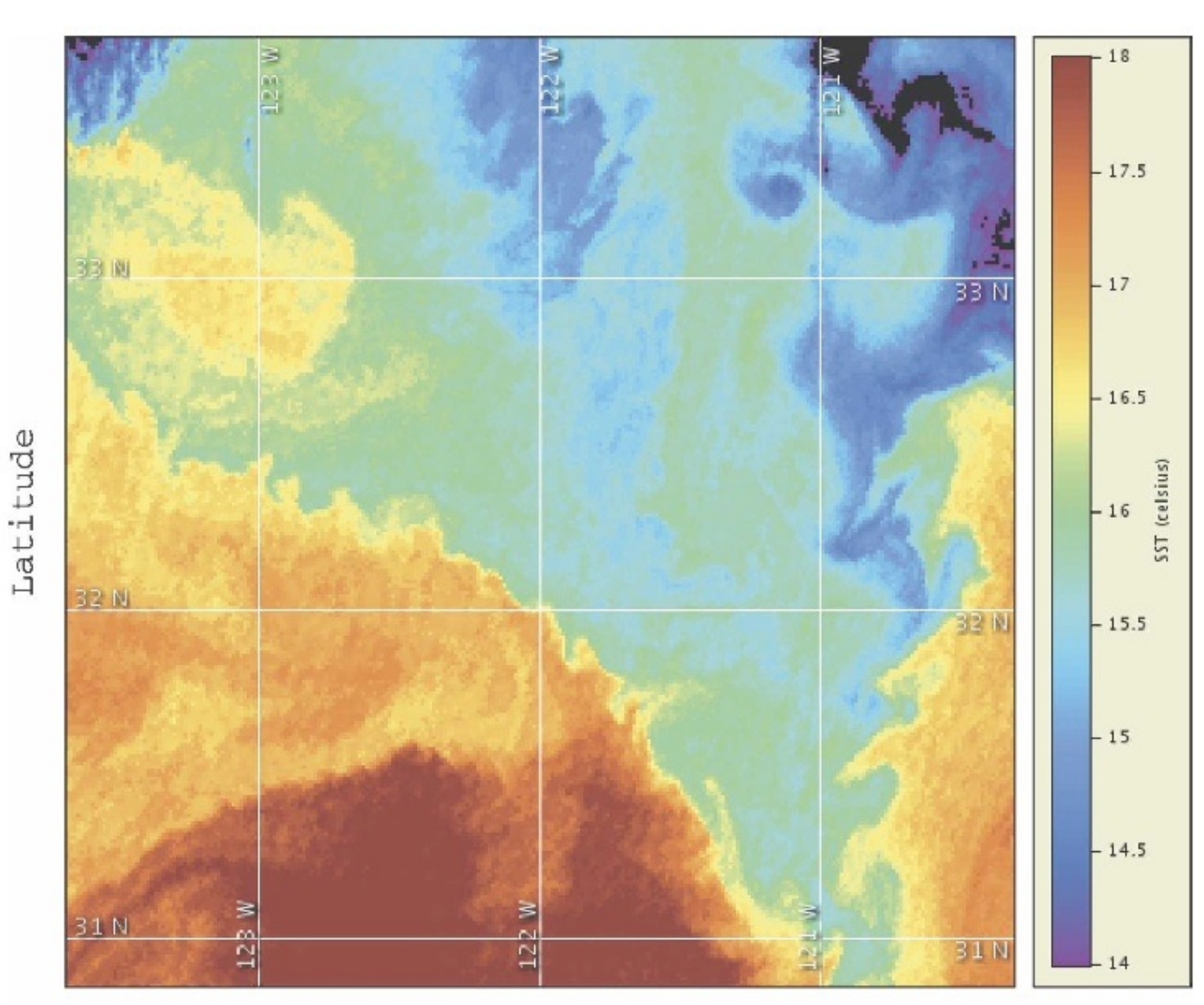


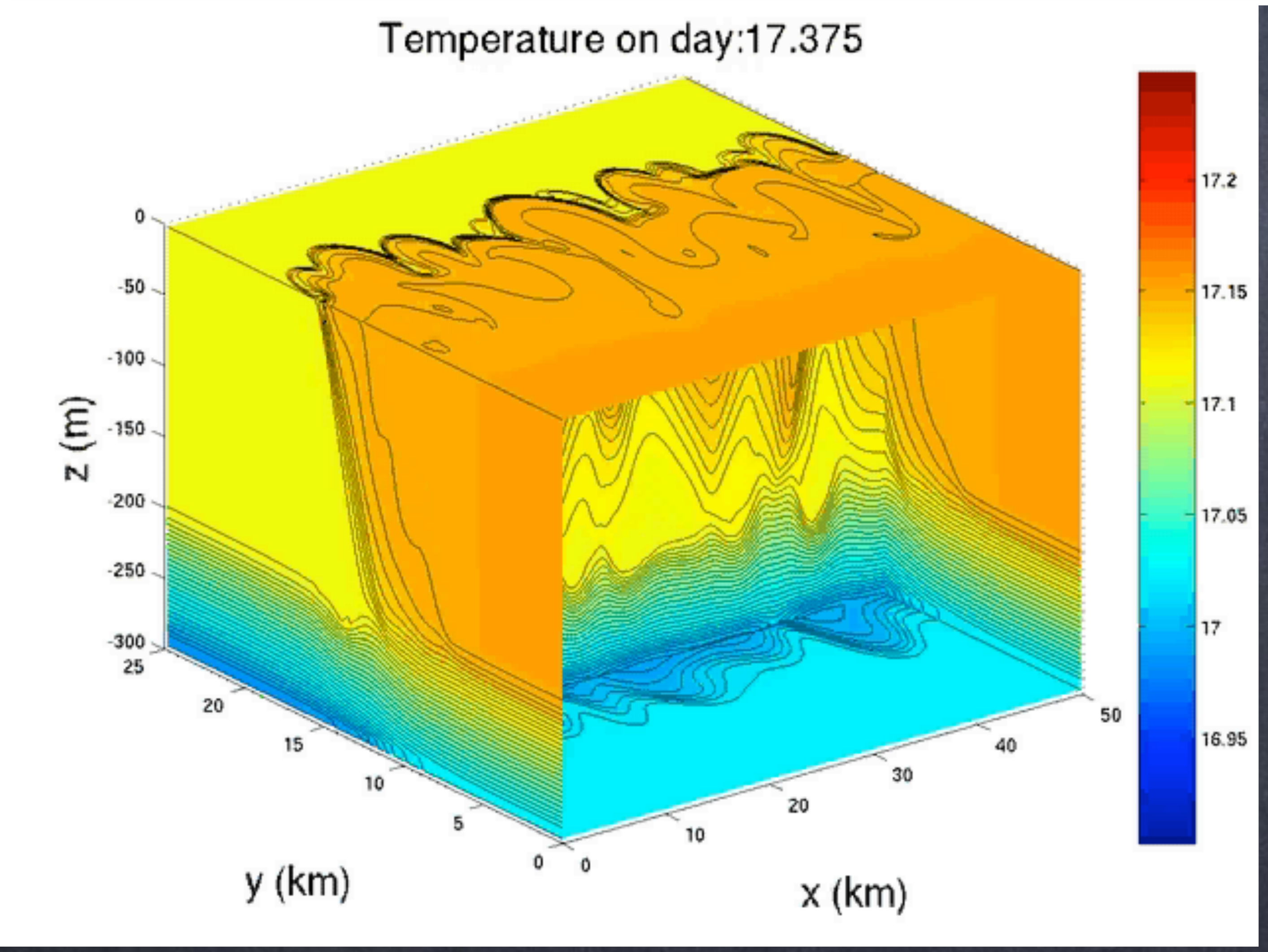


- Fronts
- Eddies
- Ro=O(1)
- Ri=O(1)
- near-surface (H=100m)
- 1-10km, days
- W/H~U/L
- hydrostatic
- Globally resolved in 2070-2100

⟵ 10 km

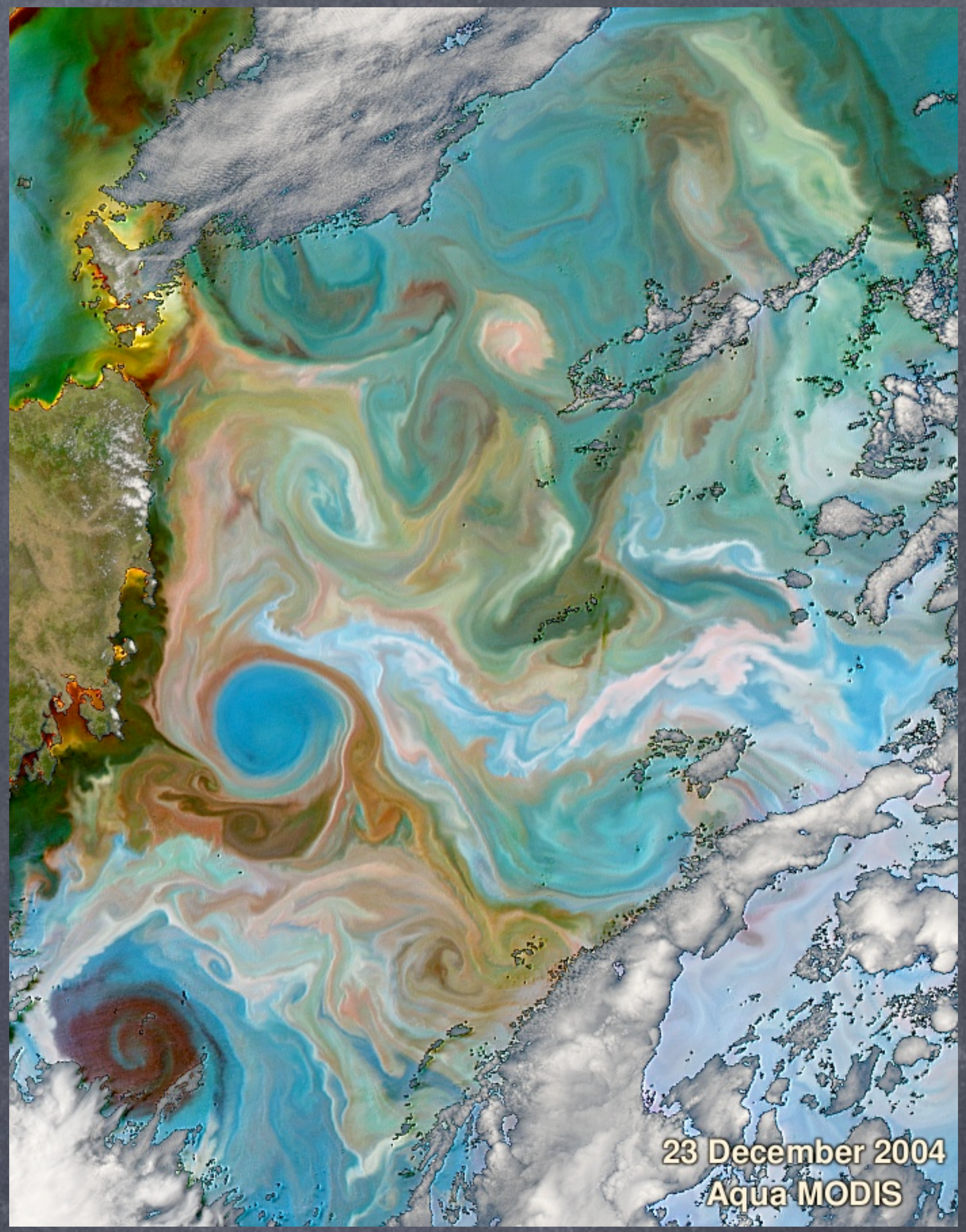


Eddy processes often baroclinic instability

BFK, R. Ferrari, and R. W. Hallberg. Parameterization of mixed layer eddies. Part I: Theory and diagnosis. Journal of Physical Oceanography, 38(6):1145-1165, 2008

BFK, G. Danabasoglu, R. Ferrari, S. M. Griffies, R. W. Hallberg, M. M. Holland, M. E. Maltrud, S. Peacock, and B. L. Samuels. Parameterization of mixed layer eddies. III: Implementation and impact in global ocean climate simulations. Ocean Modelling, 39:61-78, 2011.

# Character of the Submesoscale

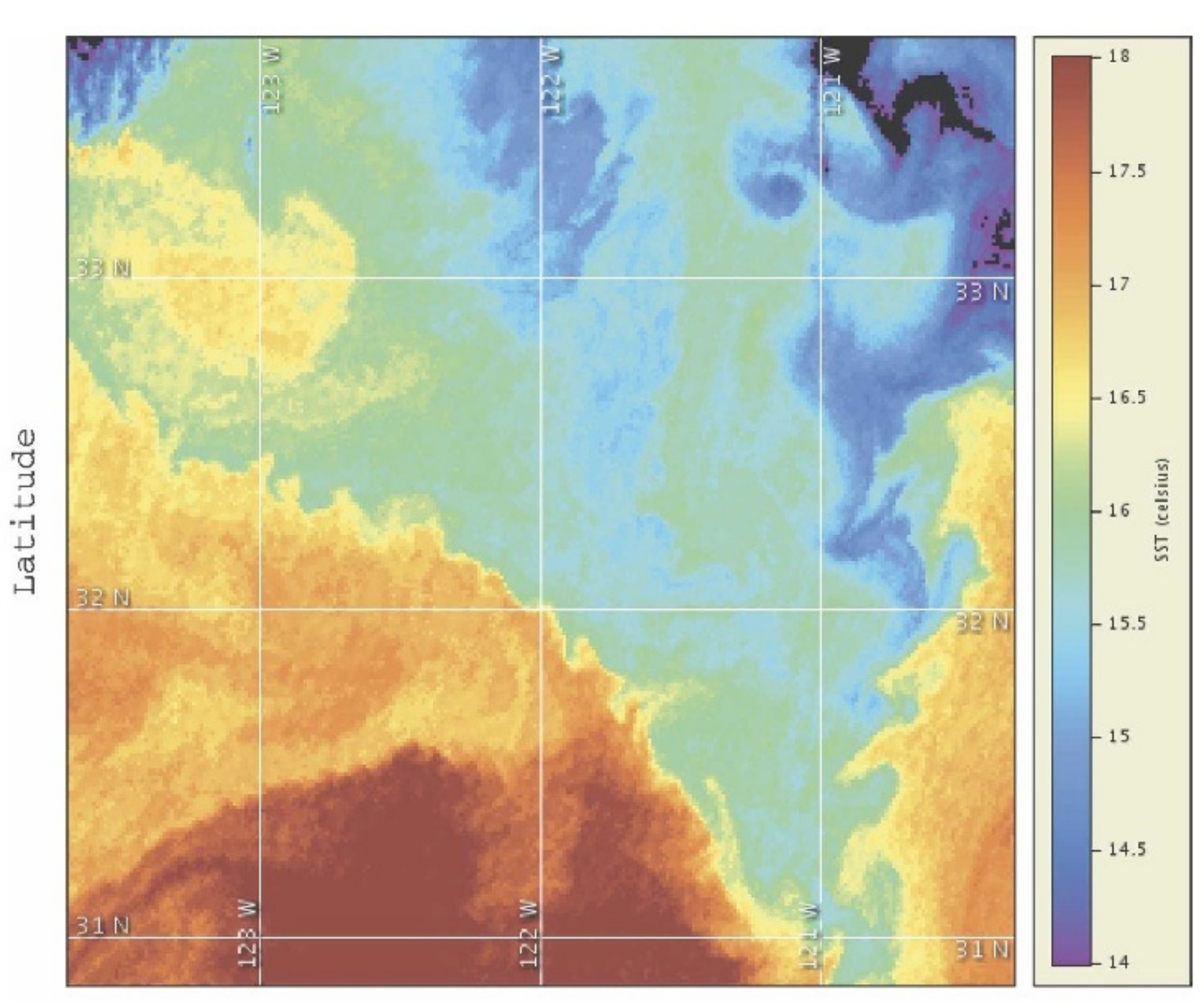


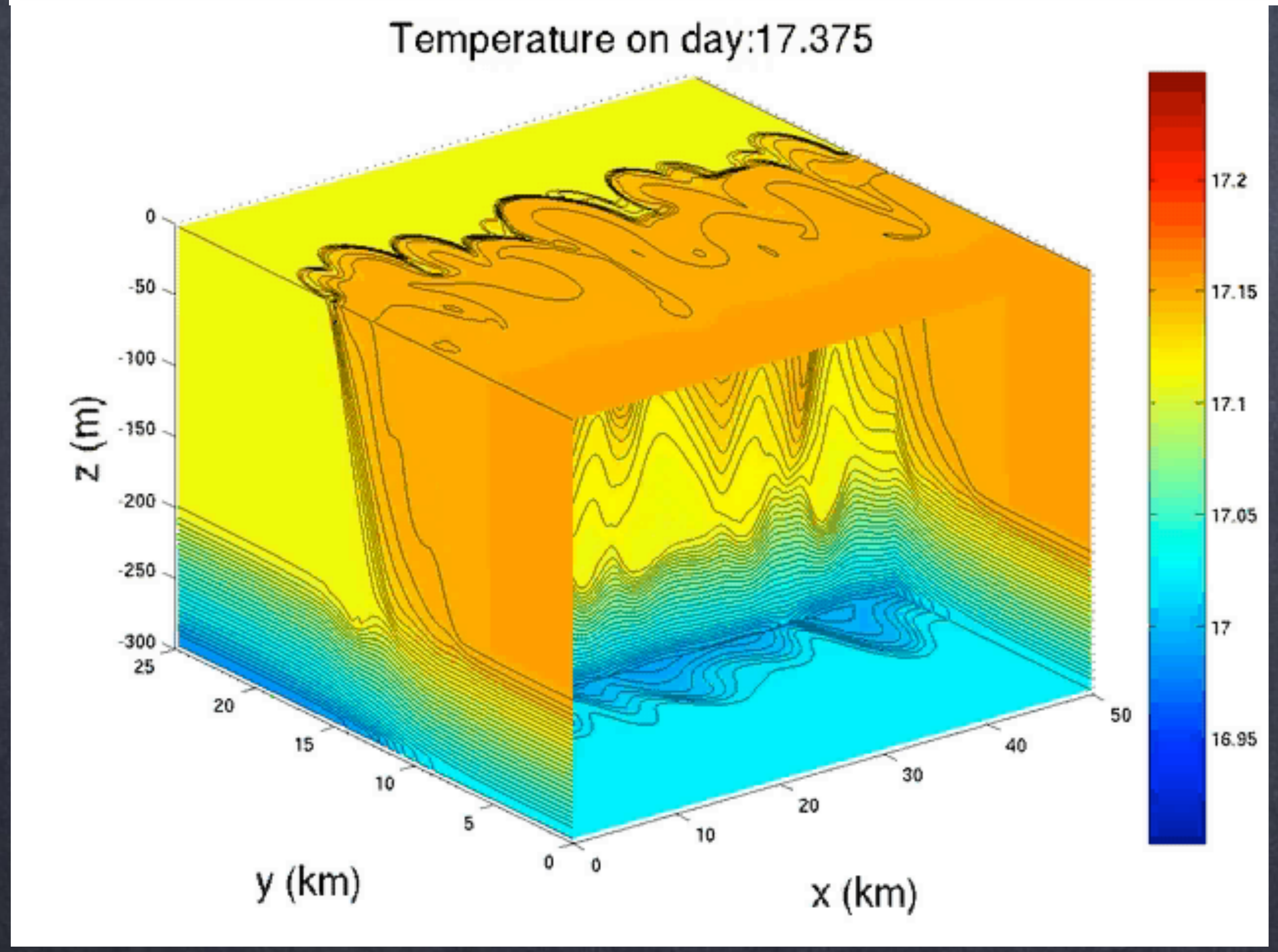


- Fronts
- Eddies
- Ro=O(1)
- Ri=O(1)
- near-surface (H=100m)
- 1-10km, days
- W/H~U/L
- hydrostatic
- Globally resolved in 2070-2100

← 10 km

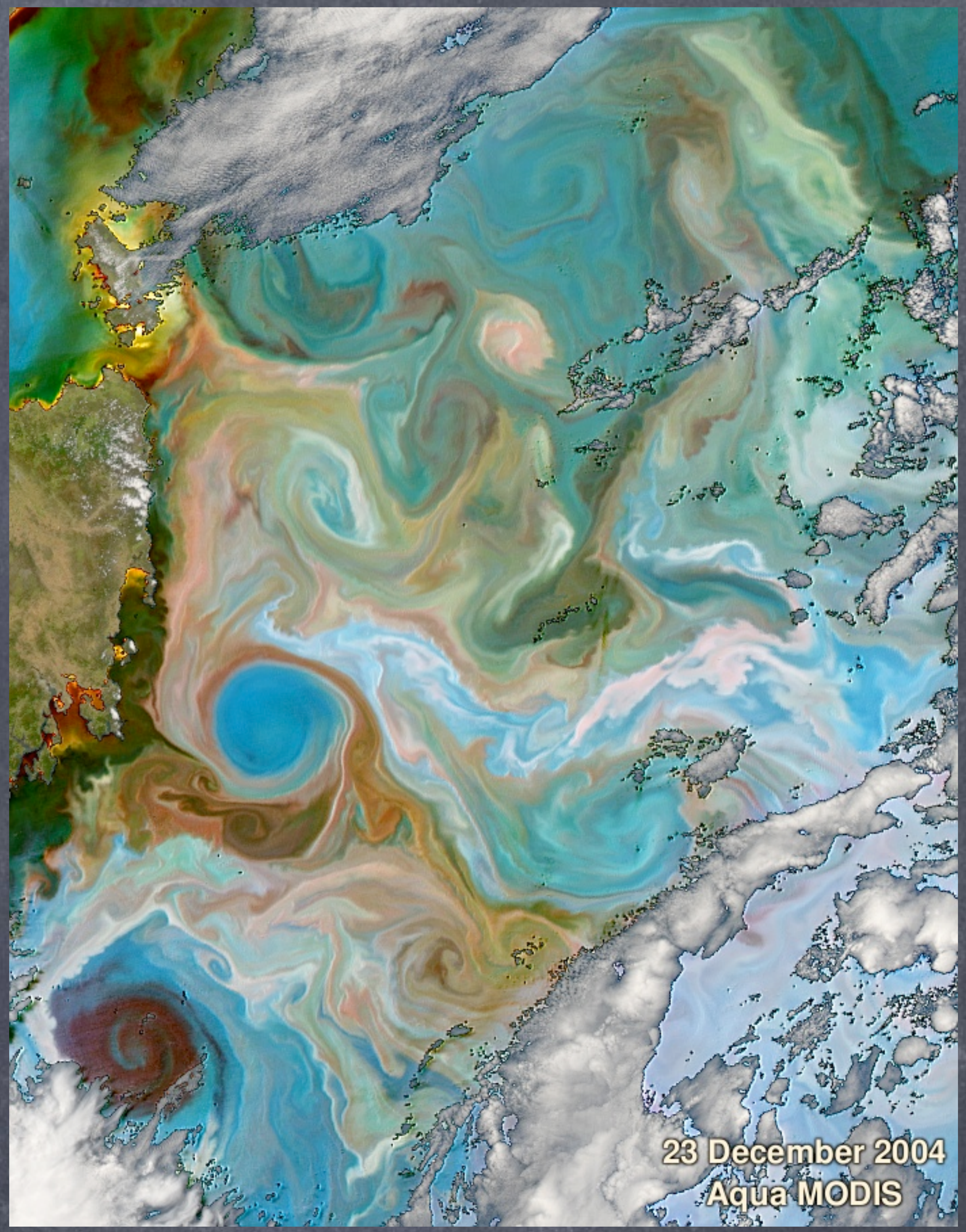


Eddy processes often
baroclinic instability

BFK, R. Ferrari, and R. W. Hallberg. Parameterization of mixed layer eddies. Part I: Theory and diagnosis. Journal of Physical Oceanography, 38(6):1145-1165, 2008

BFK, G. Danabasoglu, R. Ferrari, S. M. Griffies, R. W. Hallberg, M. M. Holland, M. E. Maltrud, S. Peacock, and B. L. Samuels. Parameterization of mixed layer eddies. III: Implementation and impact in global ocean climate simulations. Ocean Modelling, 39:61-78, 2011.

# Character of the Submesoscale

Fronts

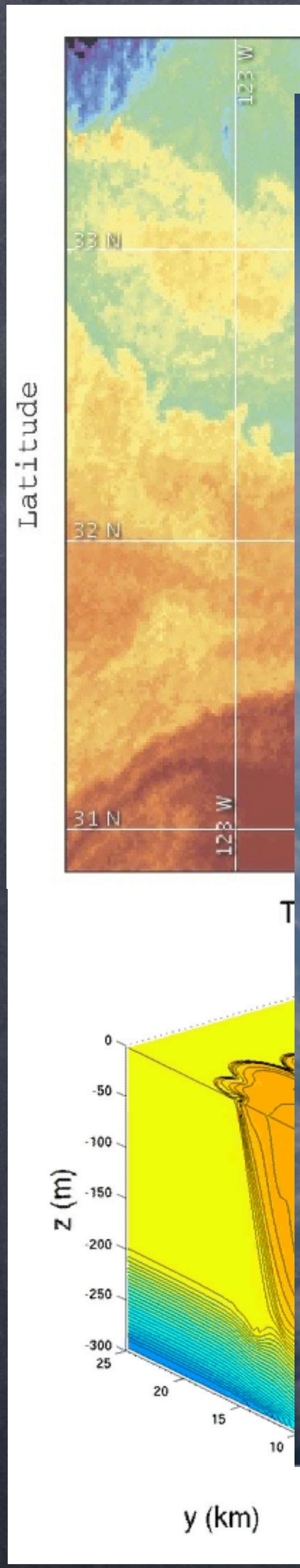


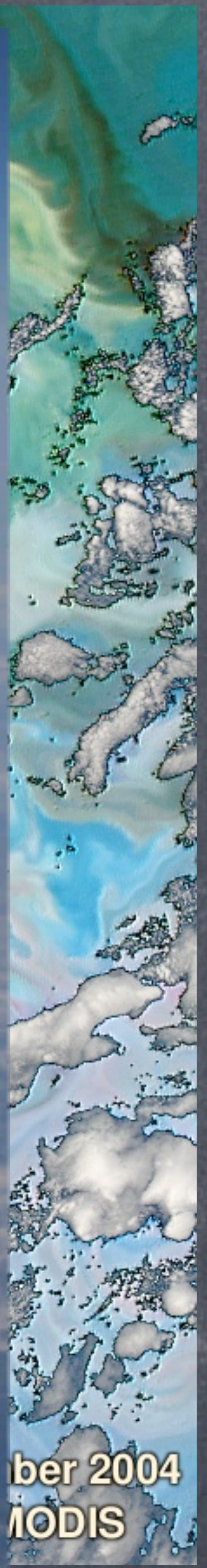



M. M. Holland, M. E. Maltrud, S. Peacock, and B. L. Samuels. Parameterization of mixed layer eddies. III: Implementation and impact in global ocean climate simulations. Ocean Modelling, 39:61-78, 2011.

B. Fox-Kemper, R. Ferrari, and R. W. Hallberg. Parameterization of mixed layer eddies. Part I: Theory and diagnosis. Journal of Physical Oceanography, 38(6):1145-1165, 2008.

# Having a Mixed Layer Counts!

The vertical buoyancy flux in the ML (<w′b′>) without diurnal cycle is not less than with cycle (ML)

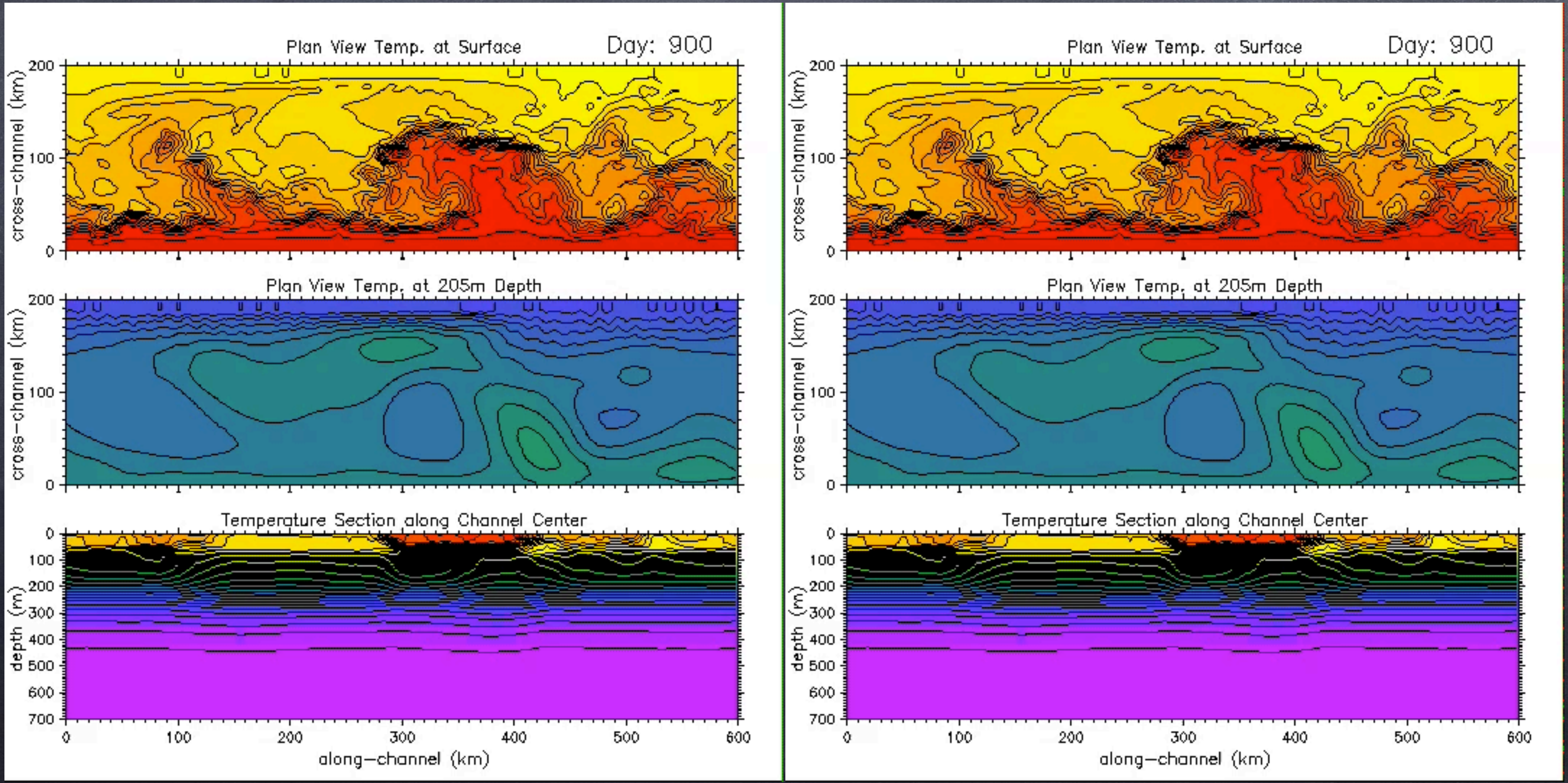

B. Fox-Kemper, R. Ferrari, and R. W. Hallberg. Parameterization of mixed layer eddies. Part I: Theory and diagnosis. Journal of Physical Oceanography, 38(6):1145-1165, 2008.

# Having a Mixed Layer Counts!

## The vertical buoyancy flux in the ML (<w′b′>) without diurnal cycle is 4x less than with cycle (ML)

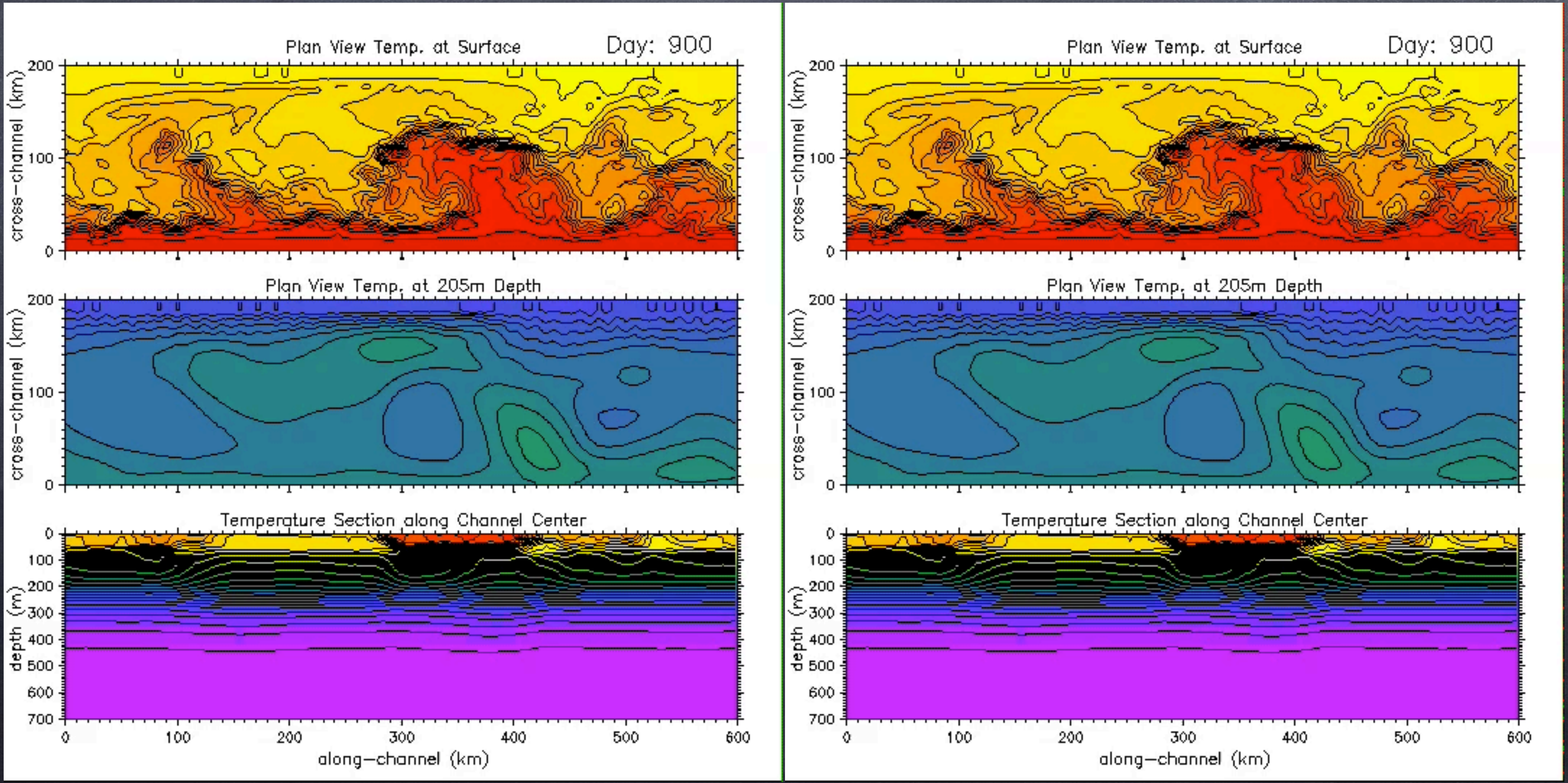

# GMST: Surface Energy Budget=Ocean Heat Content Budget

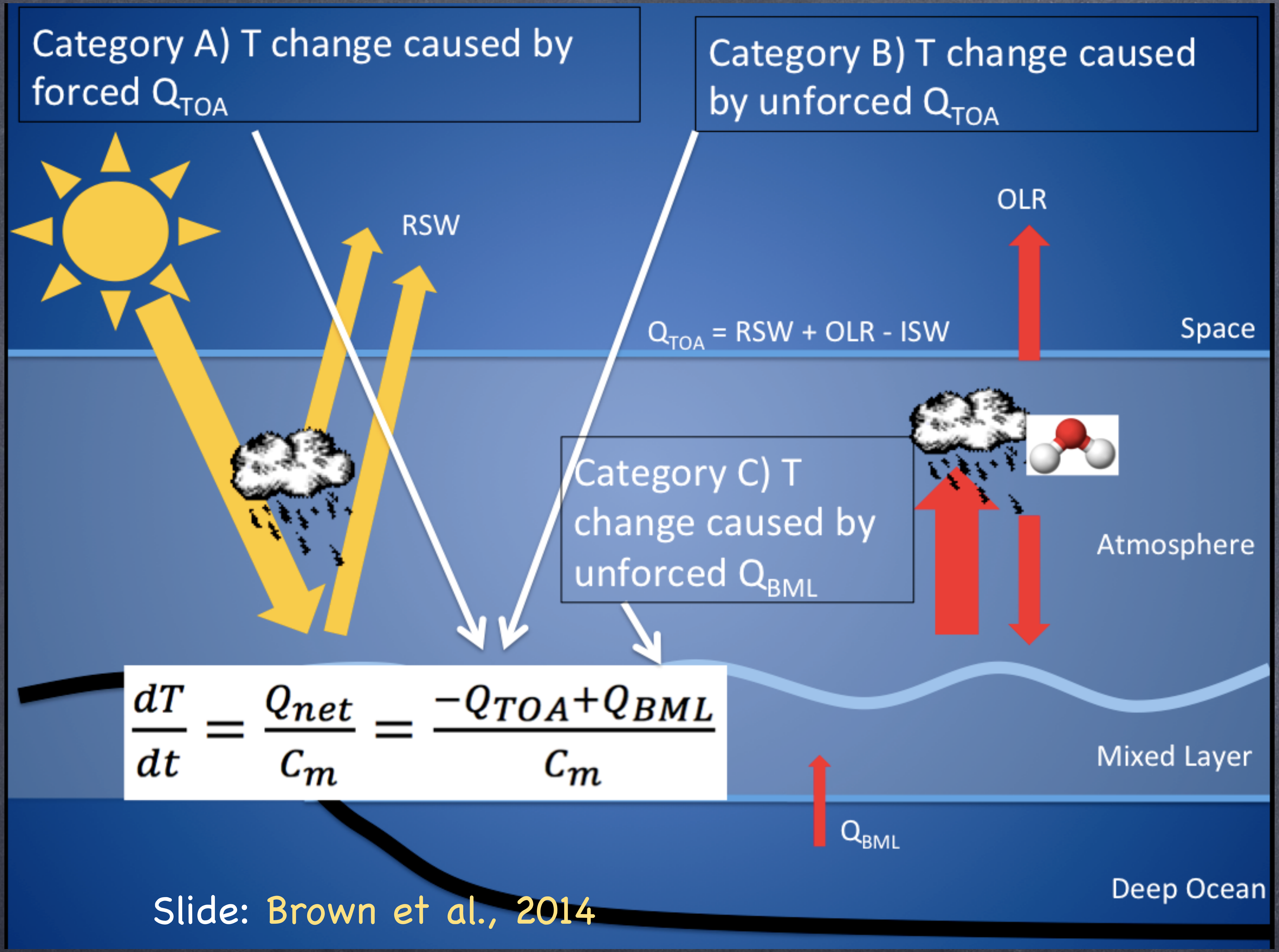


Top of Atmosphere Imbalance!!

341.3-101.9-238.5=0.9

This equals net absorbed

- 3.4m of ocean has heat capacity of whole atmosphere
- Ocean Mixed Layer is about 100m deep.

# Surface, Mixed Layer, Seasons?

0.7 W/m²

=

Atmosphere: 1.9K/yr

=

3.4m Ocean: 1.9K/yr

=

34m Ocean: 0.19K/yr

=1% of mixed layer seasonality

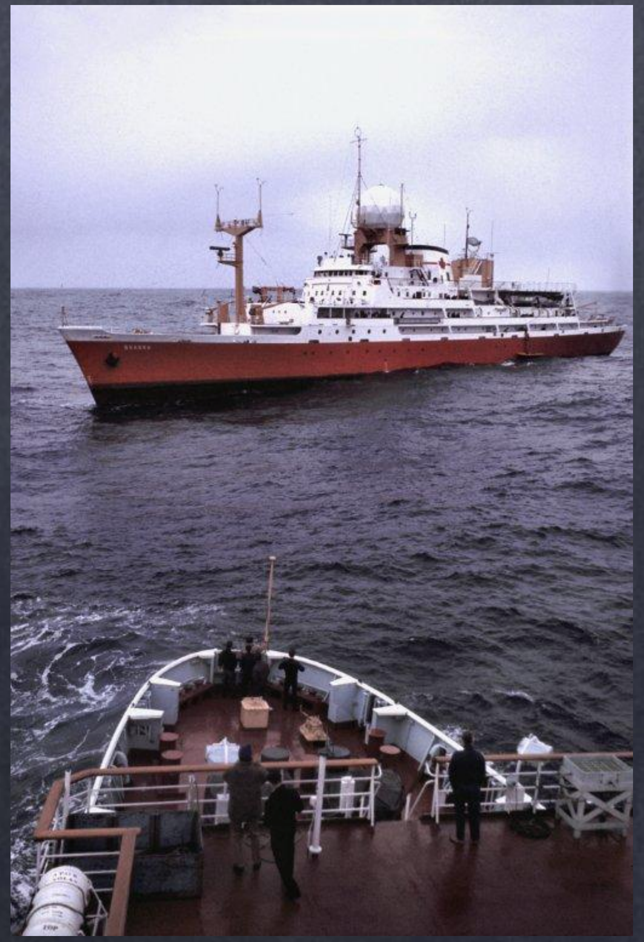

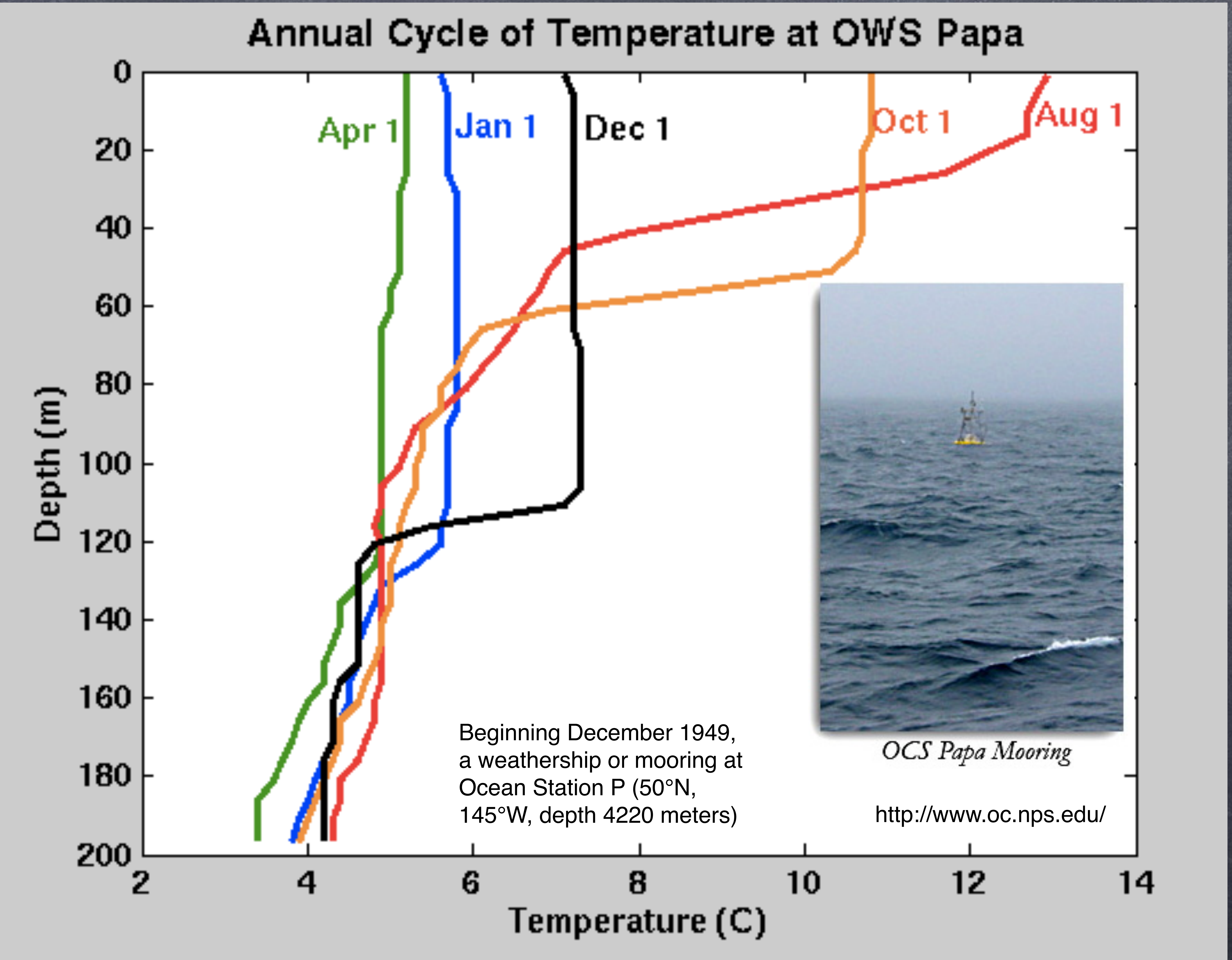

# The Ocean Mixed Layer is home to submesoscales & Langmuir

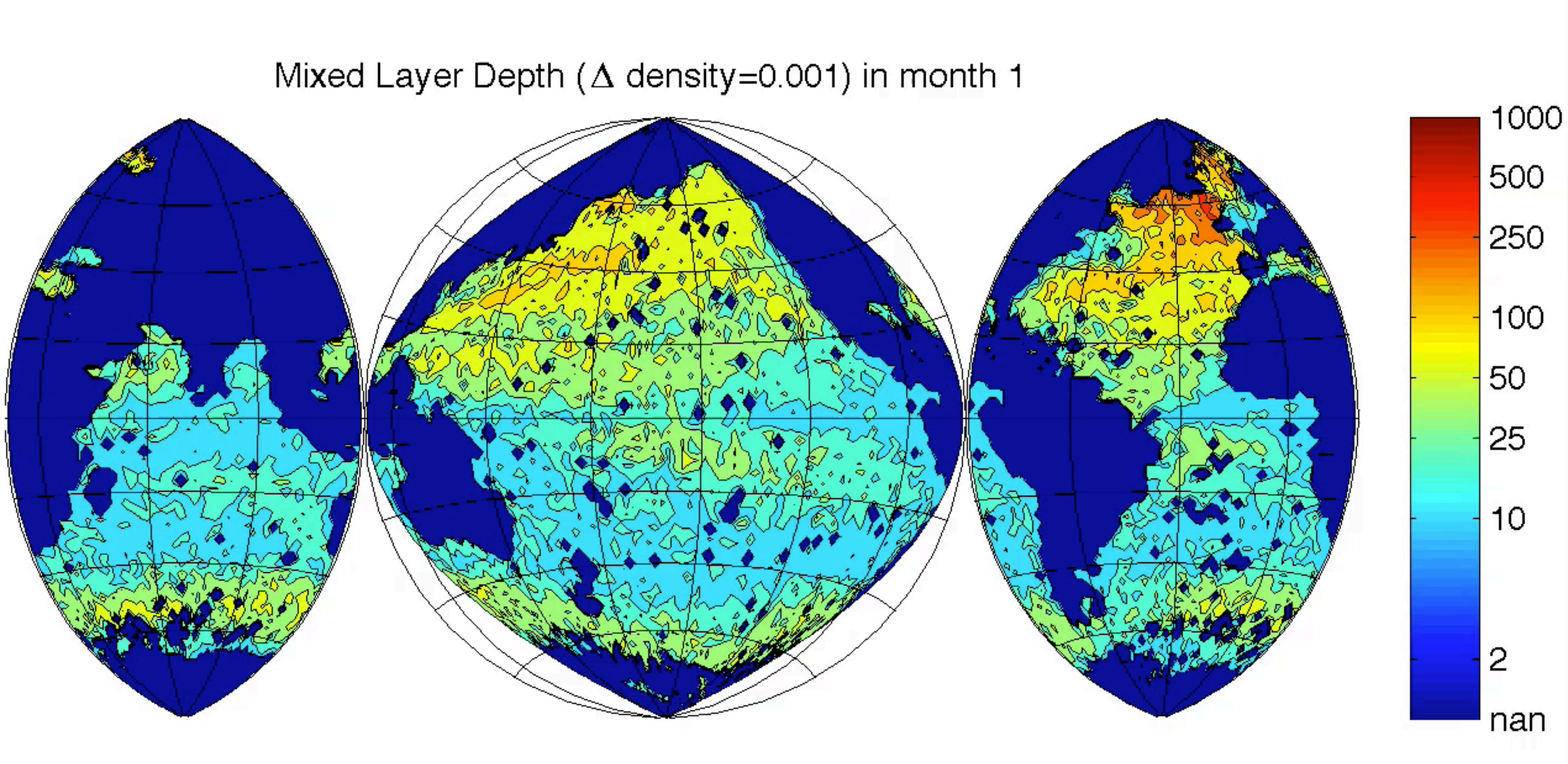


Mixed Layer Depth climatology
From Argo float data courtesy C. de Boyer-Montegut

# The Ocean Mixed Layer is home to submesoscales & Langmuir

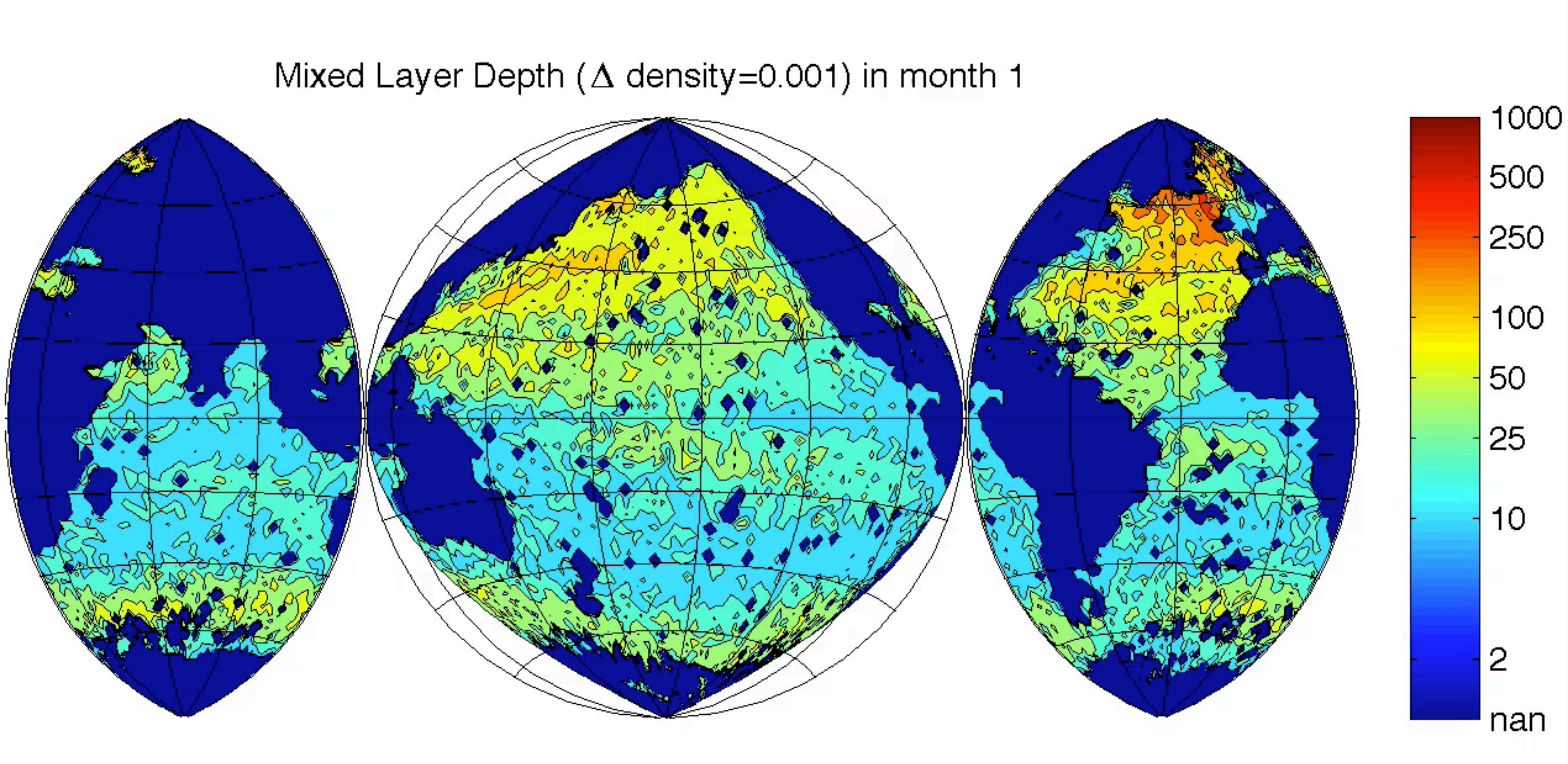


Mixed Layer Depth climatology
From Argo float data courtesy C. de Boyer-Montegut

# Ocean Mixed Layer Depth (MLD) in Winter and Summer

Observed MLD, model MLD biases, and projected changes in MLD


**Mixed layer depth in (a-d) winter and (e-h) summer.** (a, e) Observed climatological mean mixed layer depth (based on density threshold) from the Argo Mixed Layer Depth (Holte et al., 2017) **from** observations 2000-2019. (b, f) Bias between the observation-based estimate (2000-2019) and the 1995-2014 CMIP6 climatological mean mixed layer depth. (c, d, g, h) Projected MLD change from 1995-2014 to 2081-2100 under (c, g) SSP1-2.6 and (d, h) SSP5-8.5 scenarios.

B. Fox-Kemper, R. Ferrari, and R. W. Hallberg. Parameterization of mixed layer eddies. Part I: Theory and diagnosis. Journal of Physical Oceanography, 38(6):1145-1165, 2008.

# Prototype: Mixed Layer Front Adjustment

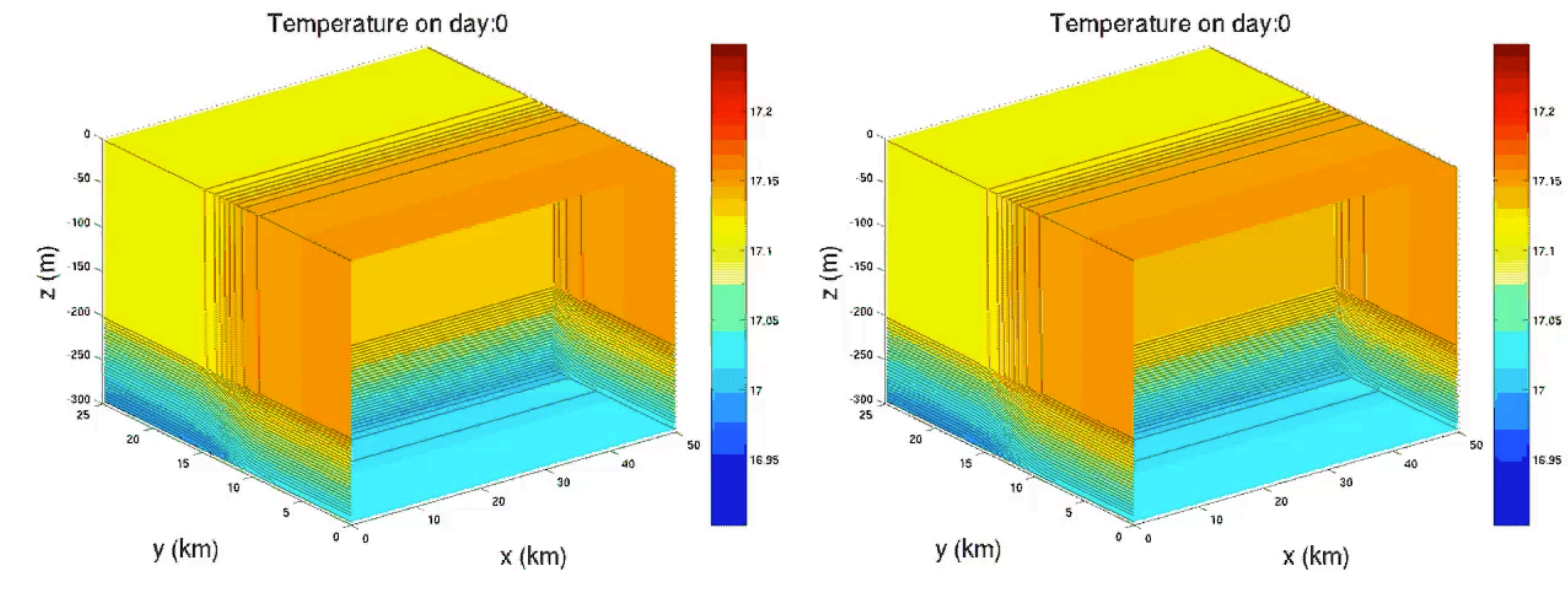


Simple Spindown

Plus, Diurnal Cycle and Parameterized Mixing

Note: initial geostrophic adjustment overwhelmed by eddy restratification

B. Fox-Kemper, R. Ferrari, and R. W. Hallberg. Parameterization of mixed layer eddies. Part I: Theory and diagnosis. Journal of Physical Oceanography, 38(6):1145-1165, 2008.

# Prototype: Mixed Layer Front Adjustment

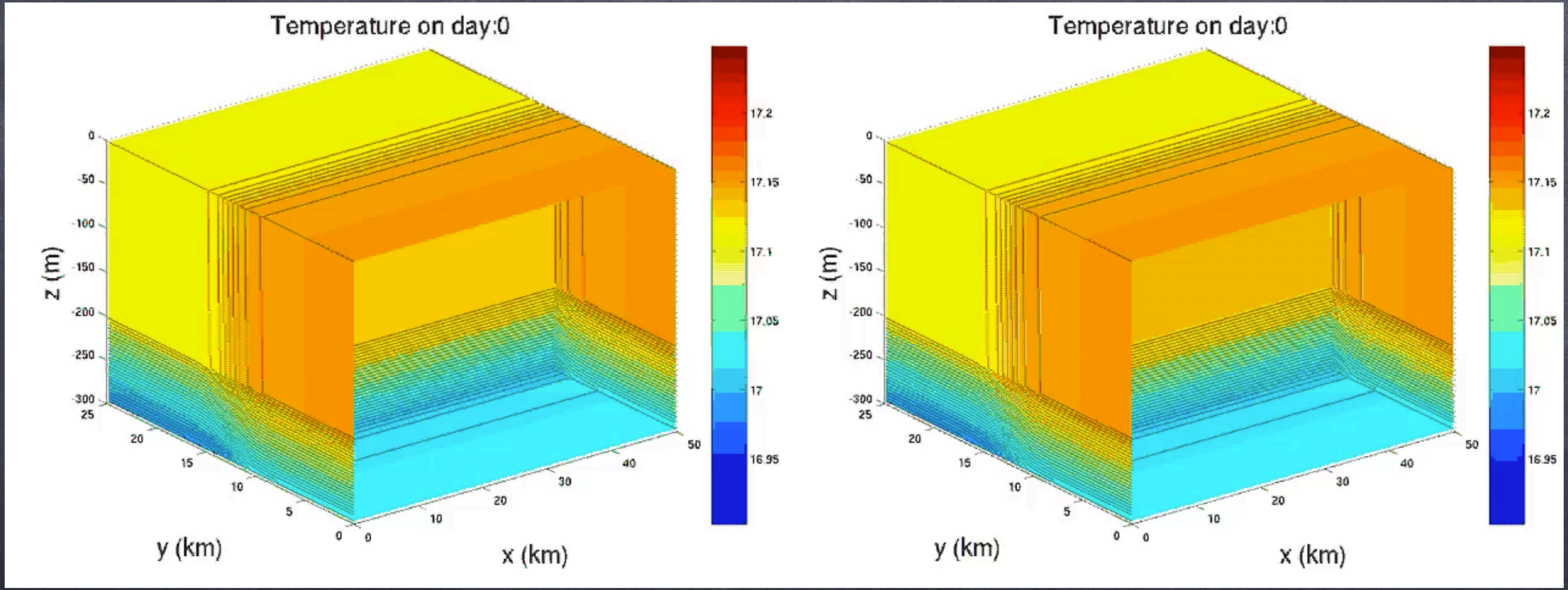


Simple Spindown

Plus, Diurnal Cycle and Parameterized Mixing

Note: initial geostrophic adjustment overwhelmed by eddy restratification

# Parameterization of Finite Amp. Eddies: Ingredients

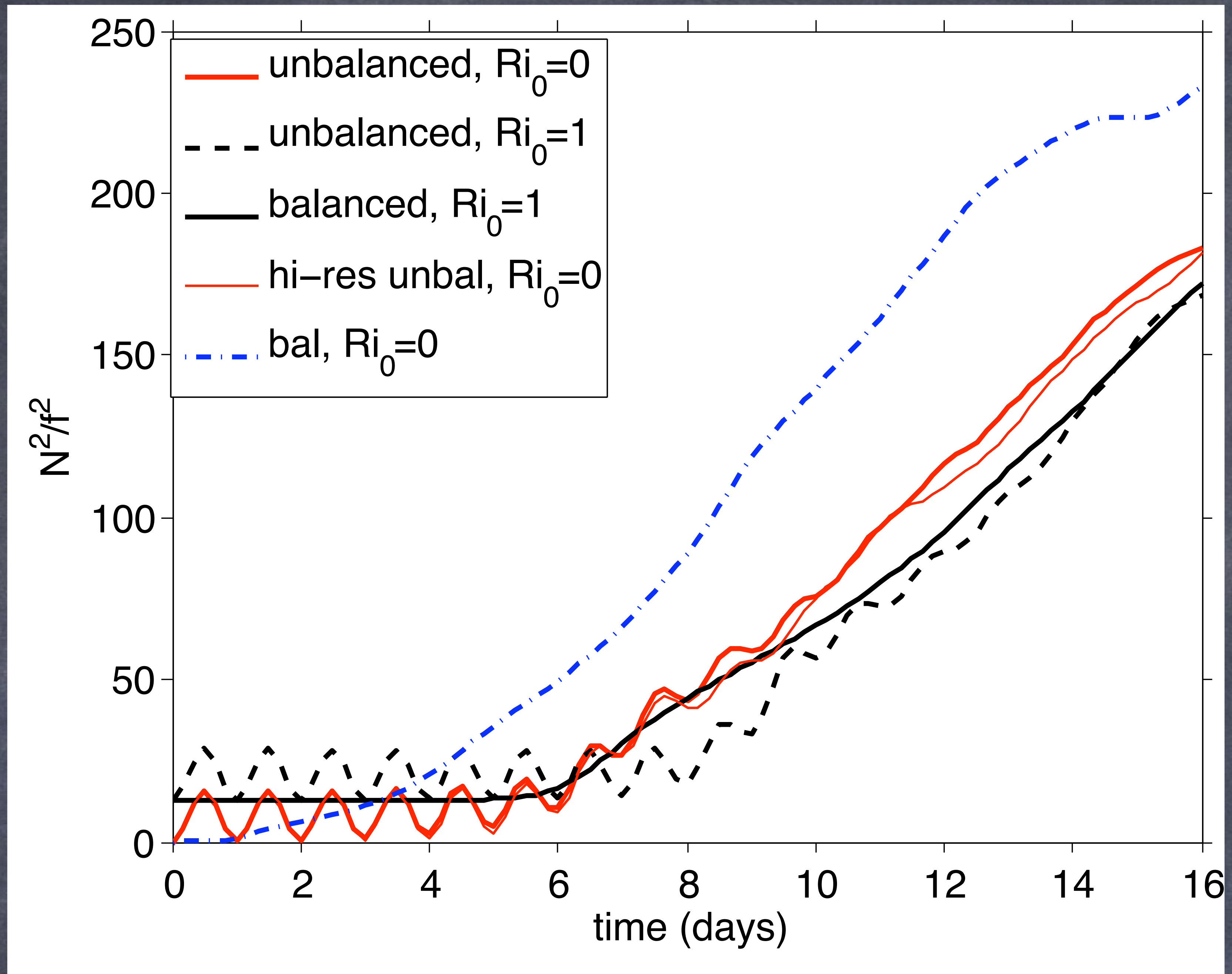


B. Fox-Kemper, R. Ferrari, and R. W. Hallberg. Parameterization of mixed layer eddies. Part I: Theory and diagnosis. Journal of Physical Oceanography, 38(6):1145-1165, 2008.

# Parameterization of Finite Amp. Eddies: Ingredients

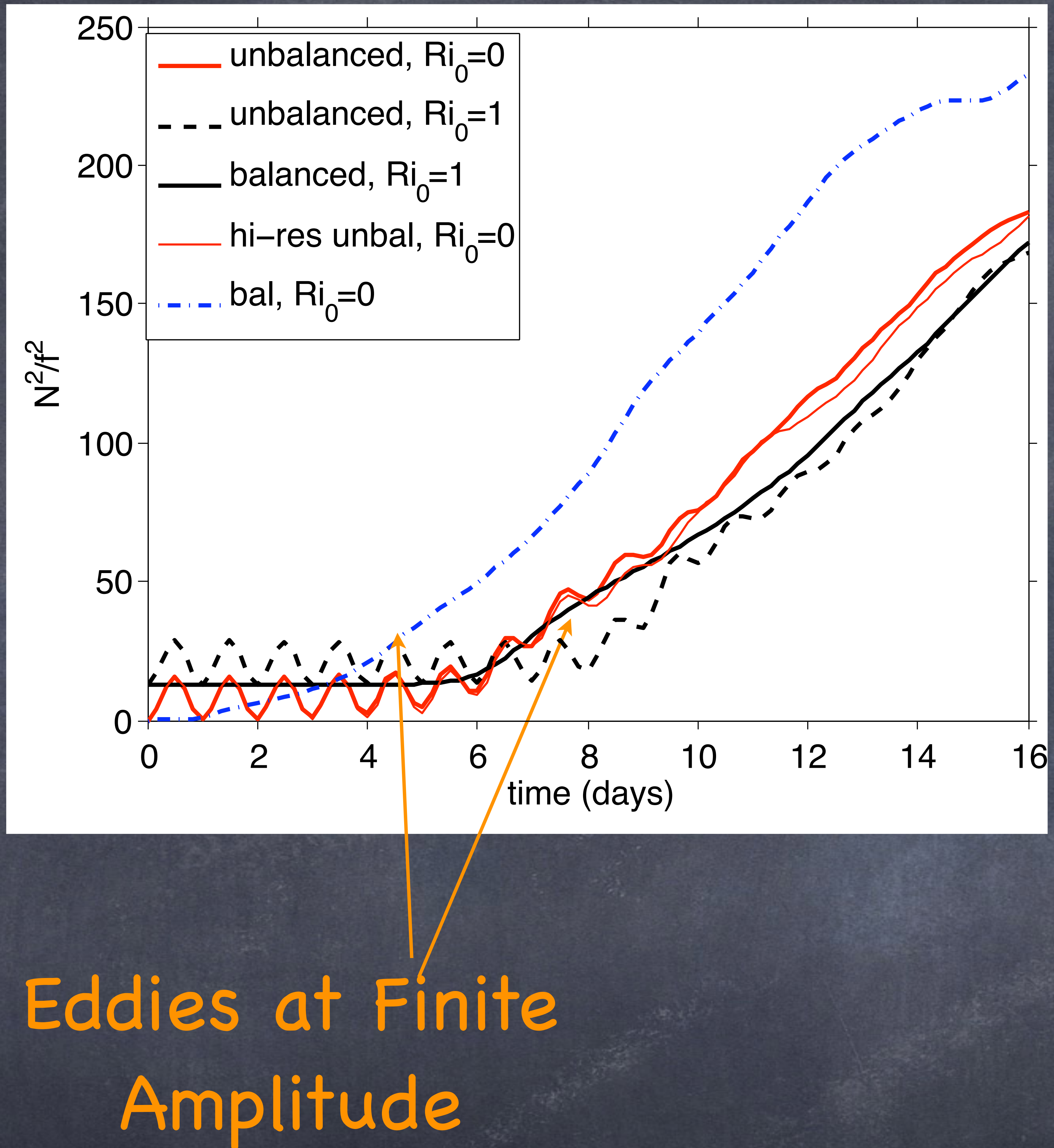


B. Fox-Kemper, R. Ferrari, and R. W. Hallberg. Parameterization of mixed layer eddies. Part I: Theory and diagnosis. Journal of Physical Oceanography, 38(6):1145-1165, 2008.

# Parameterization of Finite Amp. Eddies: Ingredients

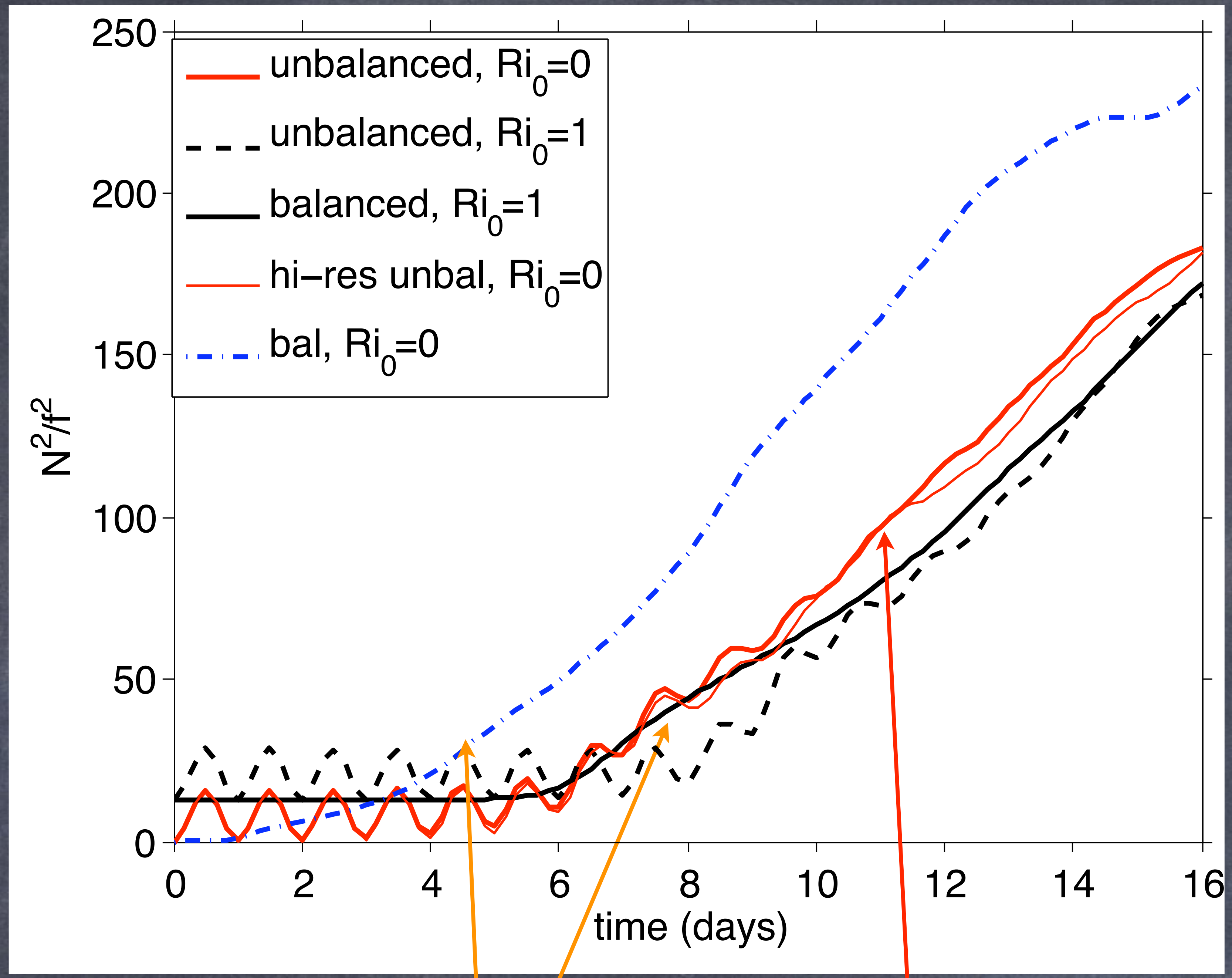


Resolution Convergence

Eddies at Finite Amplitude

B. Fox-Kemper, R. Ferrari, and R. W. Hallberg. Parameterization of mixed layer eddies. Part I: Theory and diagnosis. Journal of Physical Oceanography, 38(6):1145-1165, 2008.

# Parameterization of Finite Amp. Eddies: Ingredients

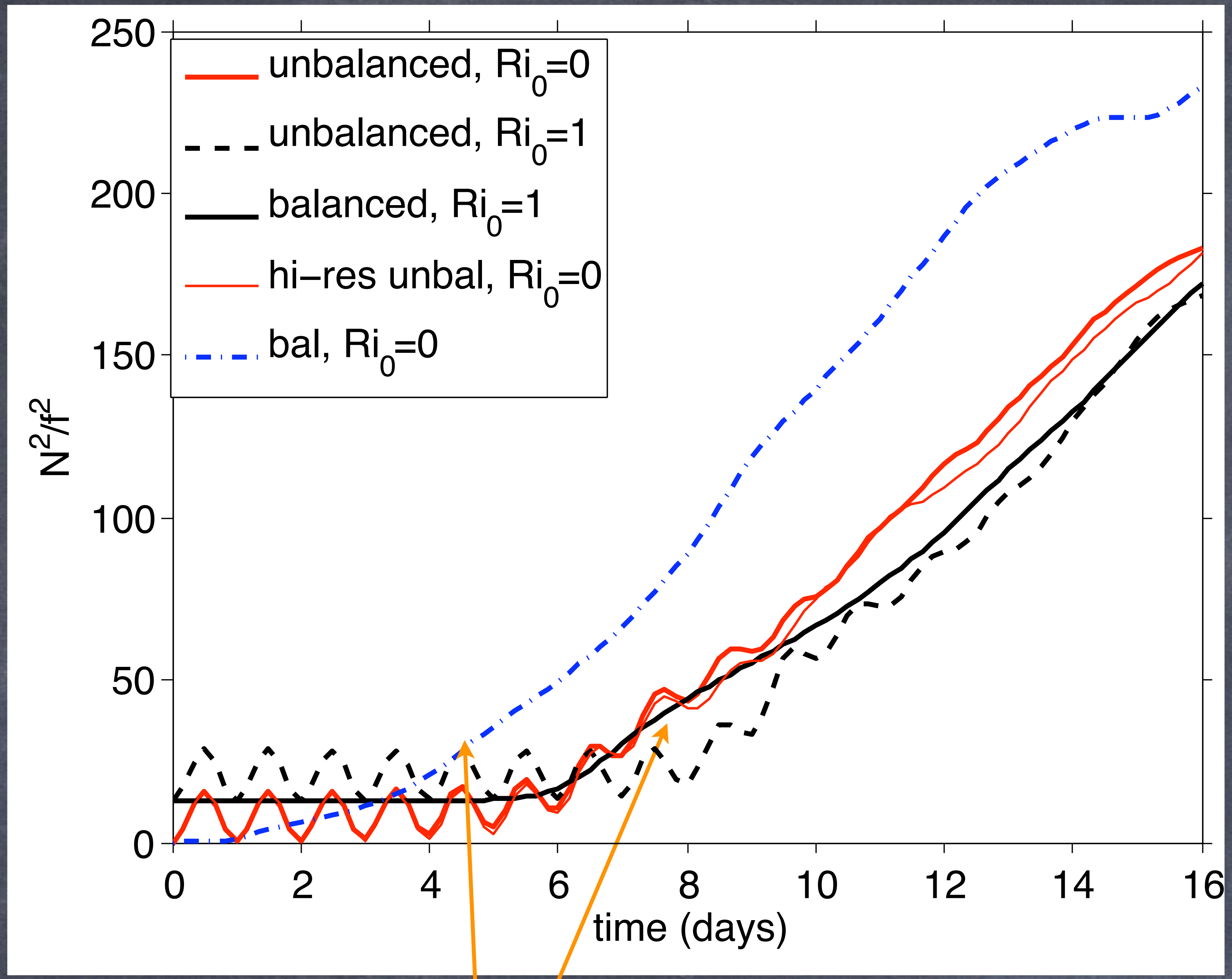


## Power Spectrum of KE

Eddies at Finite Amplitude

B. Fox-Kemper, R. Ferrari, and R. W. Hallberg. Parameterization of mixed layer eddies. Part I: Theory and diagnosis. Journal of Physical Oceanography, 38(6):1145-1165, 2008.

# Parameterization of Finite Amp. Eddies: Ingredients

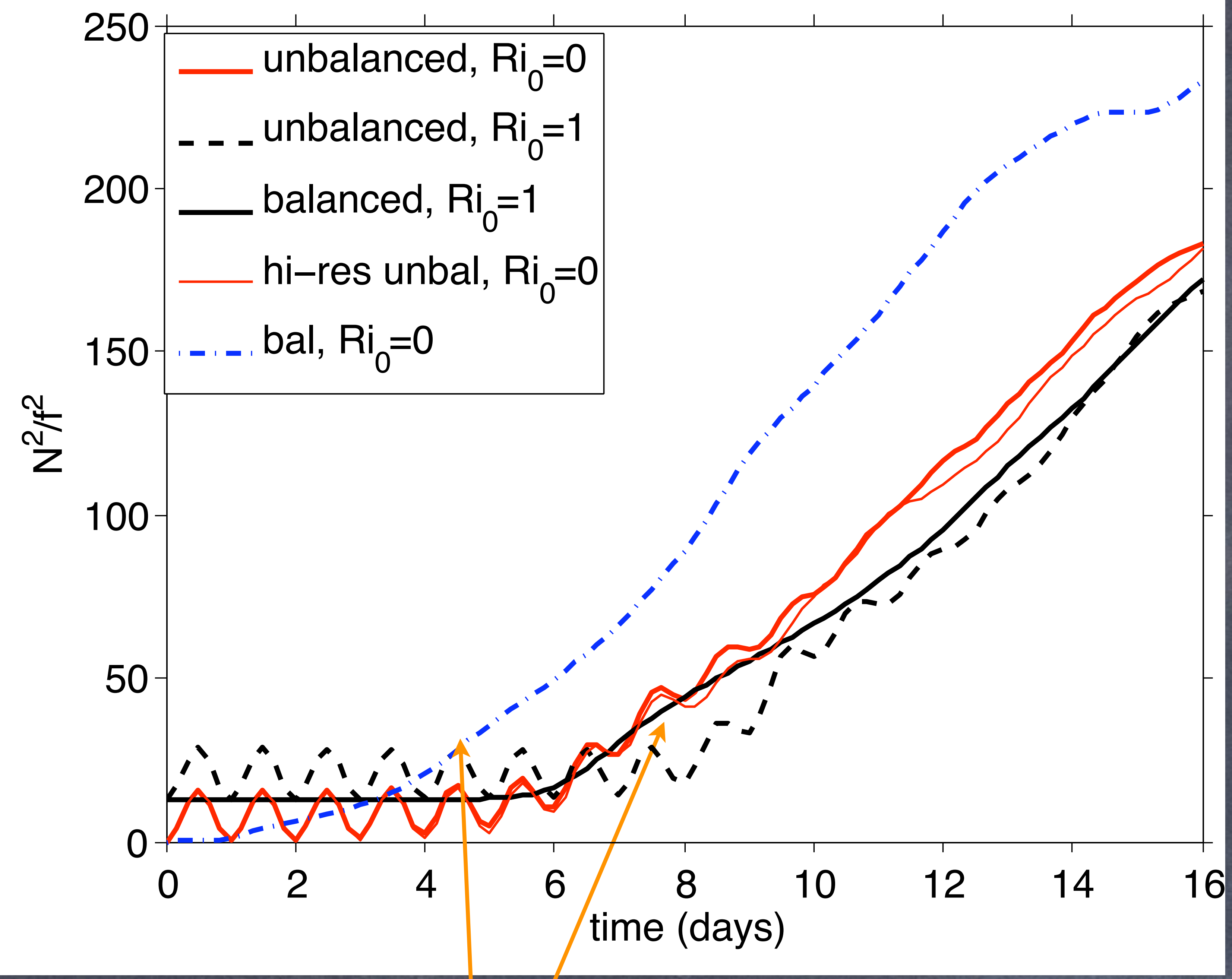


Eddies at Finite Amplitude

## Power Spectrum of KE

At Finite Amplitude Horizontal Scale Unclear

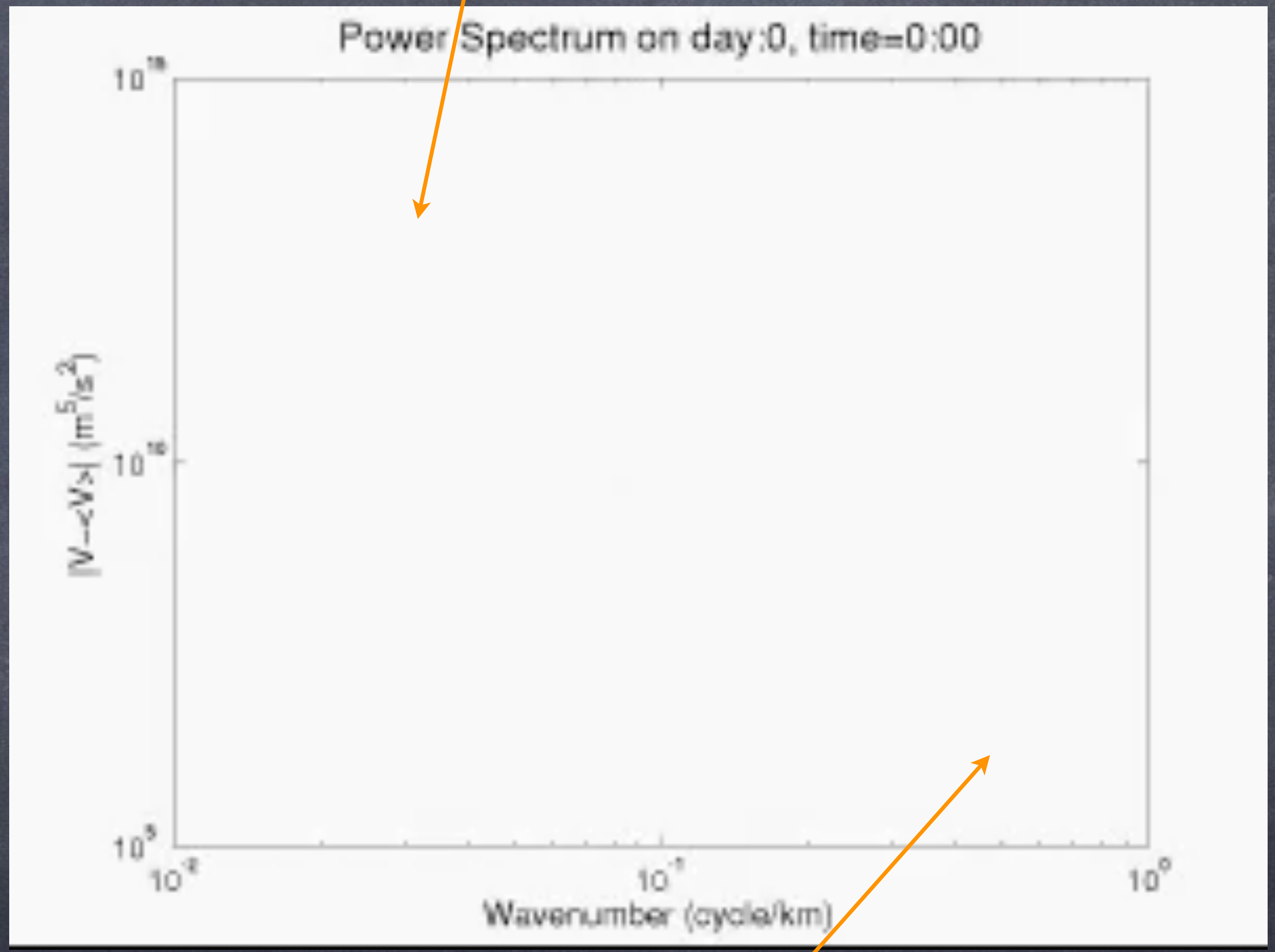


Initially, Linear Prediction of Lengthscale good

B. Fox-Kemper, R. Ferrari, and R. W. Hallberg. Parameterization of mixed layer eddies. Part I: Theory and diagnosis. Journal of Physical Oceanography, 38(6):1145-1165, 2008.

# Parameterization of Finite Amp. Eddies: Ingredients

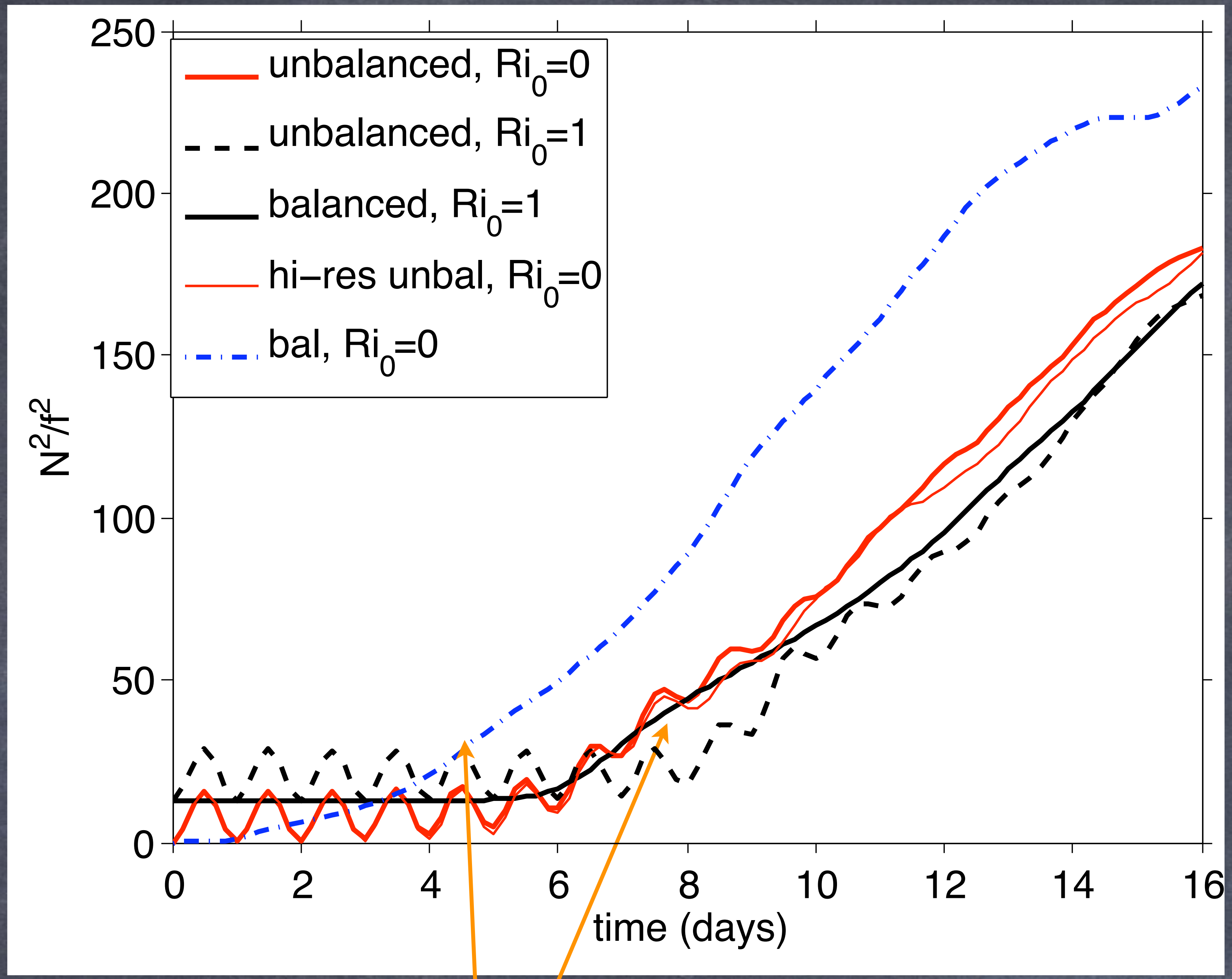


Eddies at Finite Amplitude

## Power Spectrum of KE

At Finite Amplitude Horizontal Scale Unclear

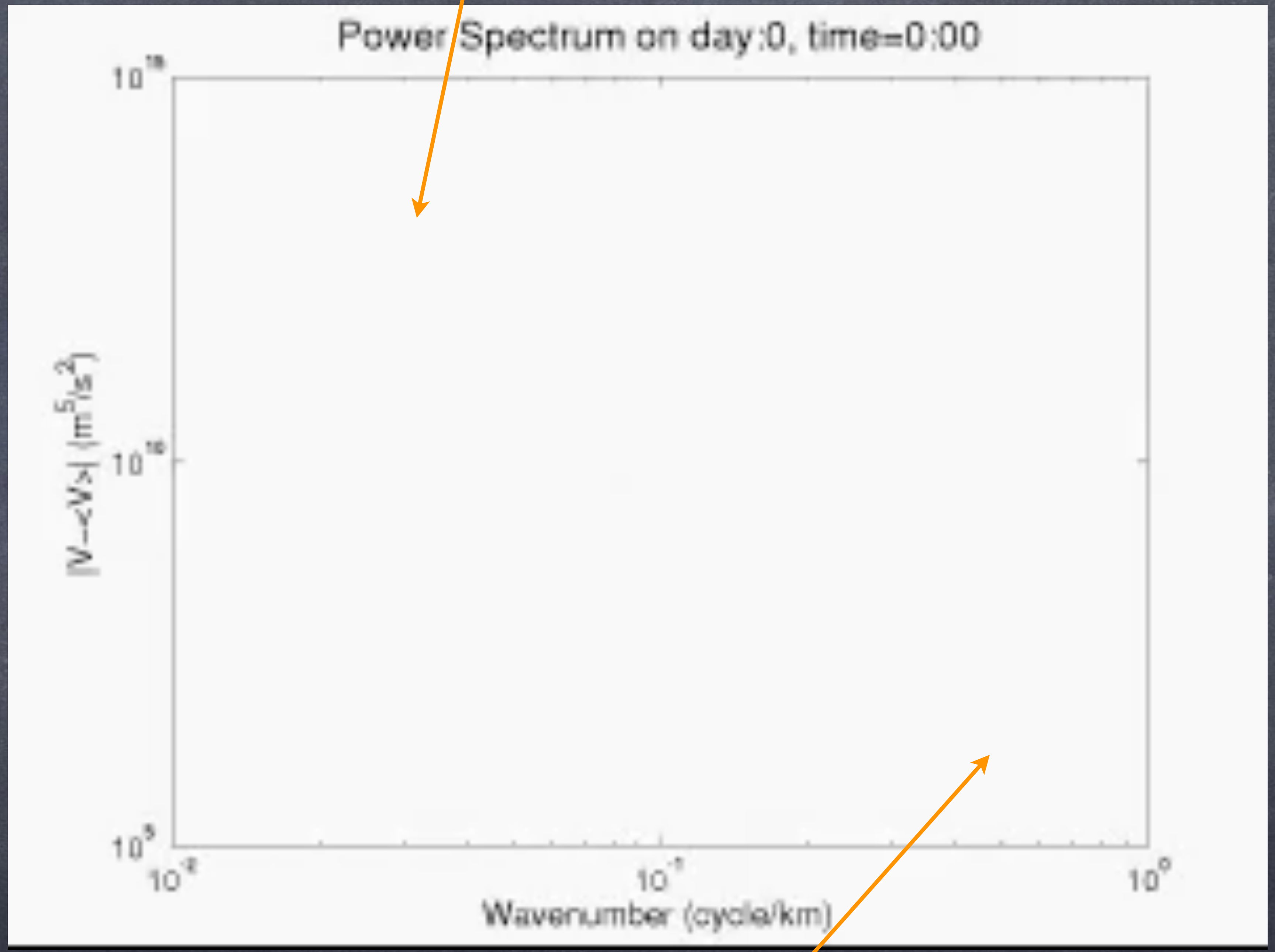


Initially, Linear Prediction of Lengthscale good

B. Fox-Kemper, R. Ferrari, and R. W. Hallberg. Parameterization of mixed layer eddies. Part I: Theory and diagnosis. Journal of Physical Oceanography, 38(6):1145-1165, 2008.

Inverse Cascade => No Results from Linear Instability Ingredients

B. Fox-Kemper, R. Ferrari, and R. W. Hallberg. Parameterization of mixed layer eddies. Part I: Theory and diagnosis. Journal of Physical Oceanography, 38(6):1145-1165, 2008.

# What lengthscale dominates <w'b'>?

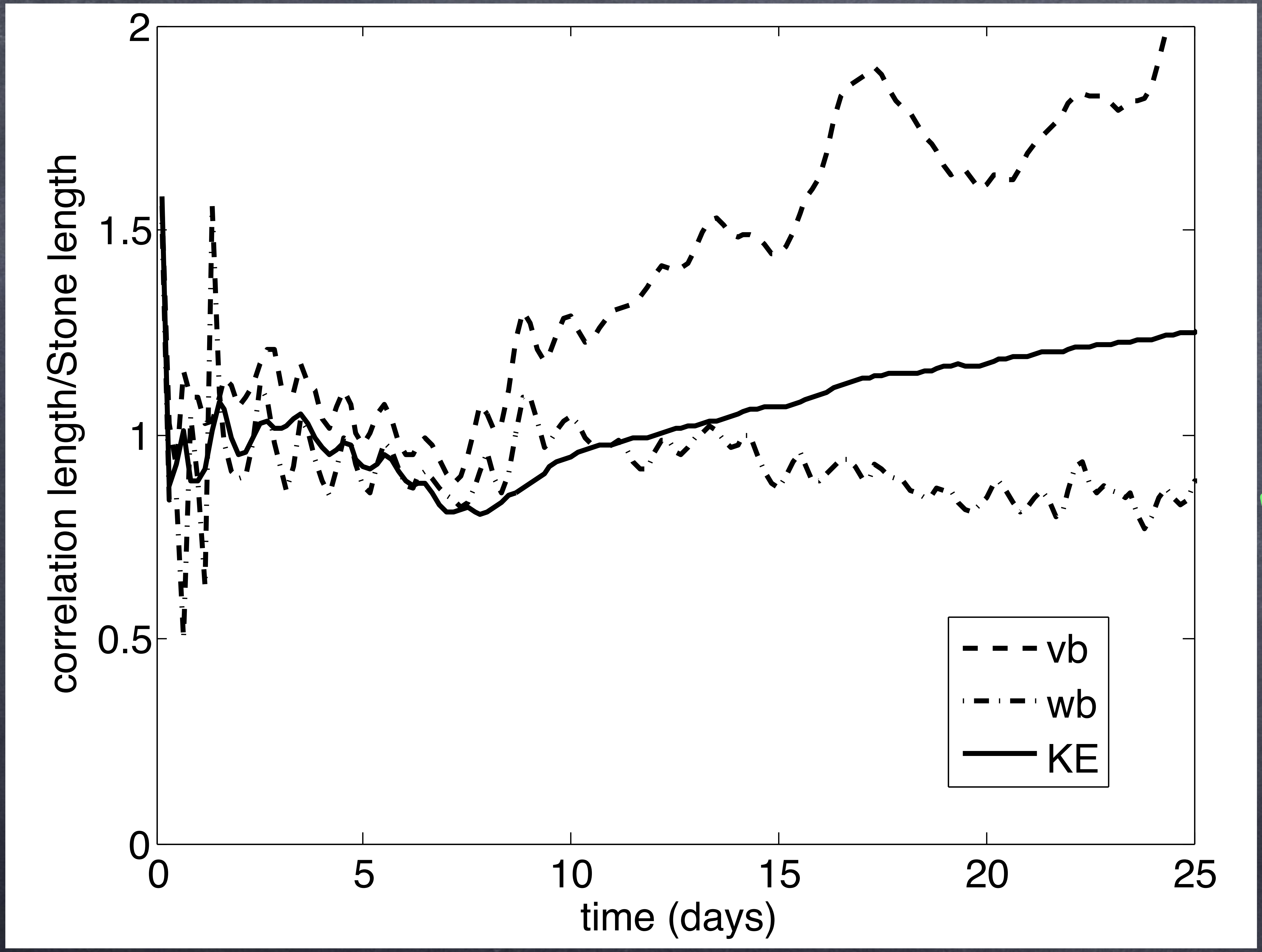


vb

KE

wb

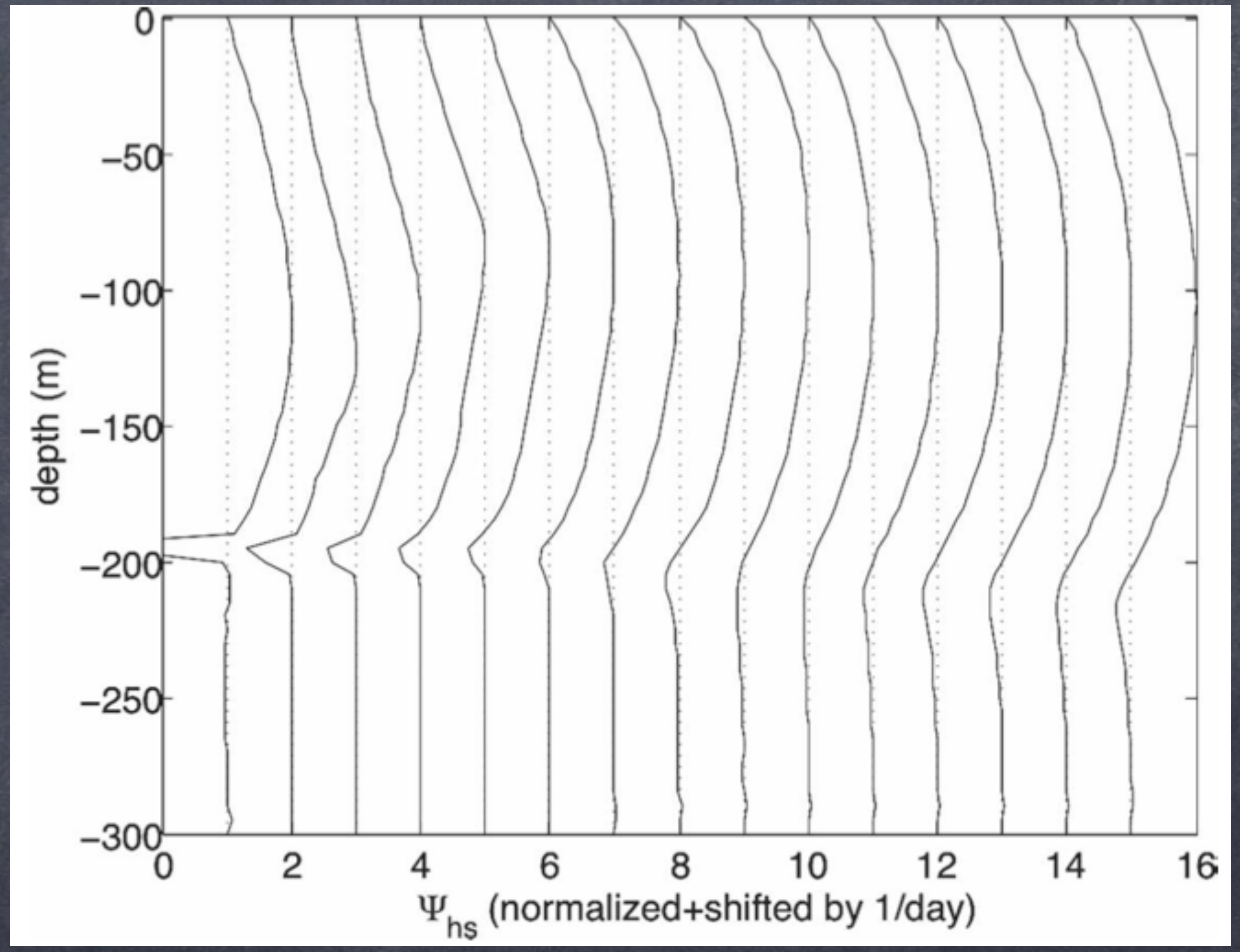

# What lengthscale dominates <w'b'>?

B. Fox-Kemper, R. Ferrari, and R. W. Hallberg. Parameterization of mixed layer eddies. Part I: Theory and diagnosis. Journal of Physical Oceanography, 38(6):1145-1165, 2008.

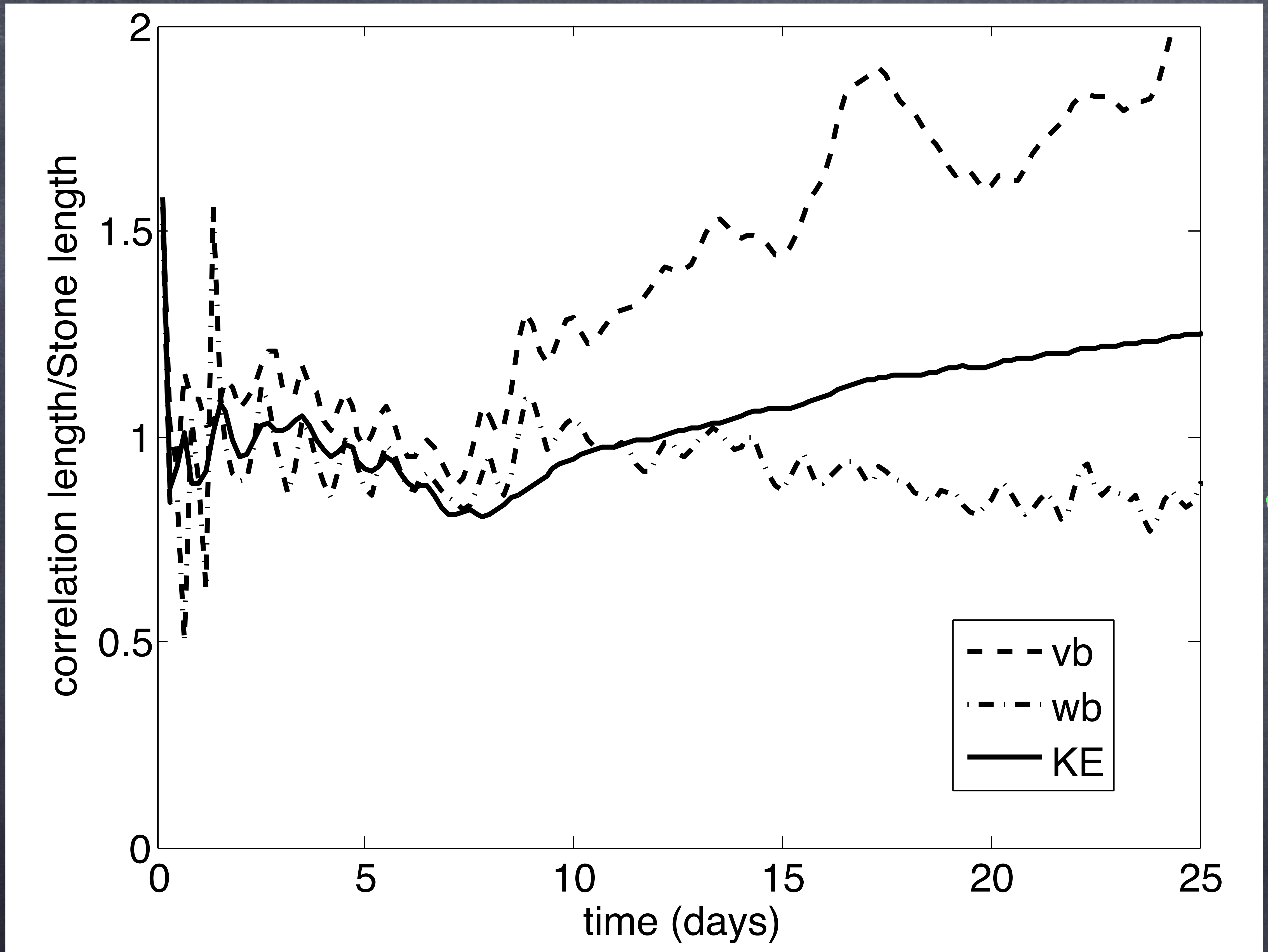


vb

KE

wb

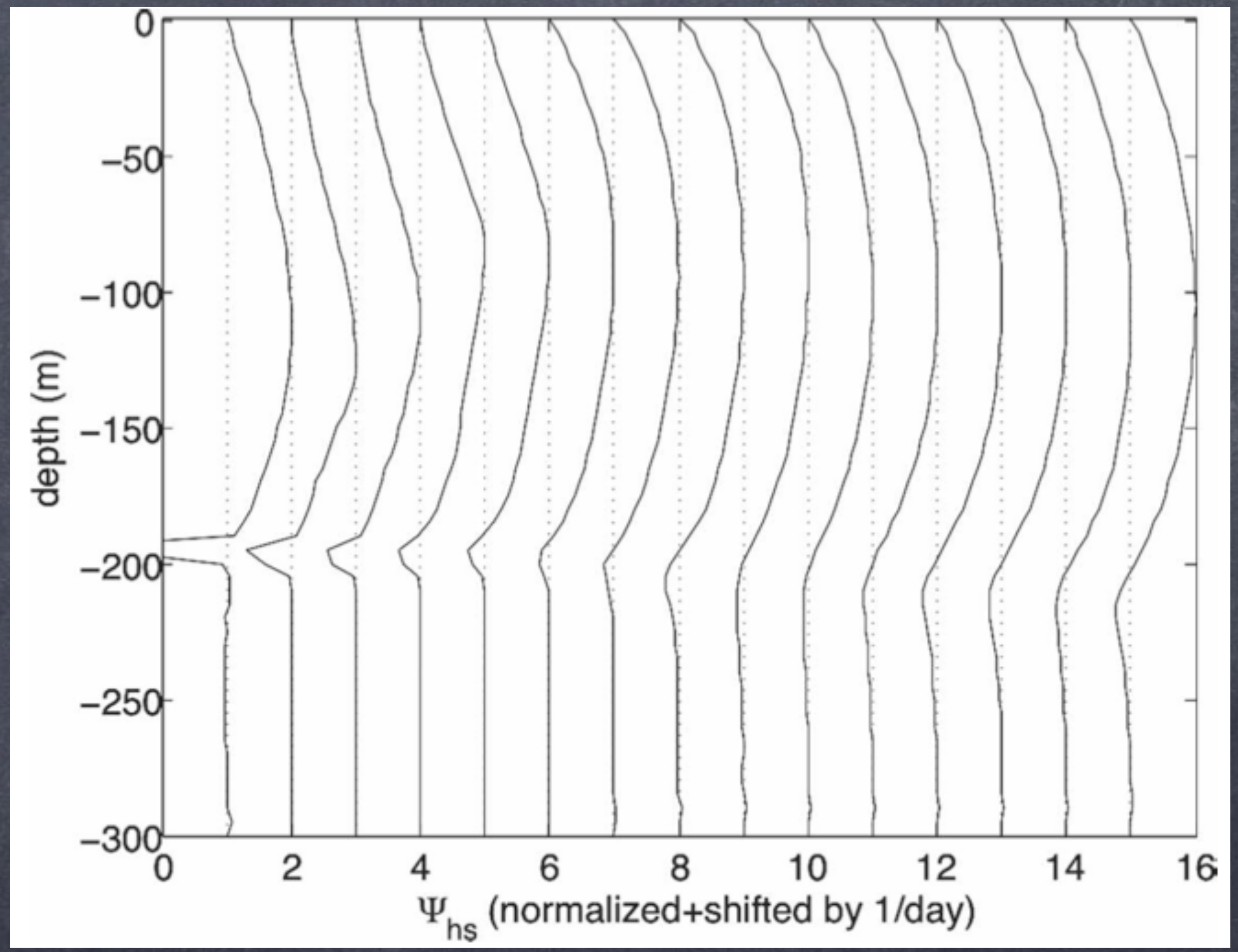


Stone fastest-mode Soln OK!

$$\mu(z) = \left[1 - \left(\frac{2z}{H} + 1\right)^2\right]\left[1 + \frac{5}{21}\left(\frac{2z}{H} + 1\right)^2\right]$$

# Parameterization of Finite Amp. Eddies: Ingredients

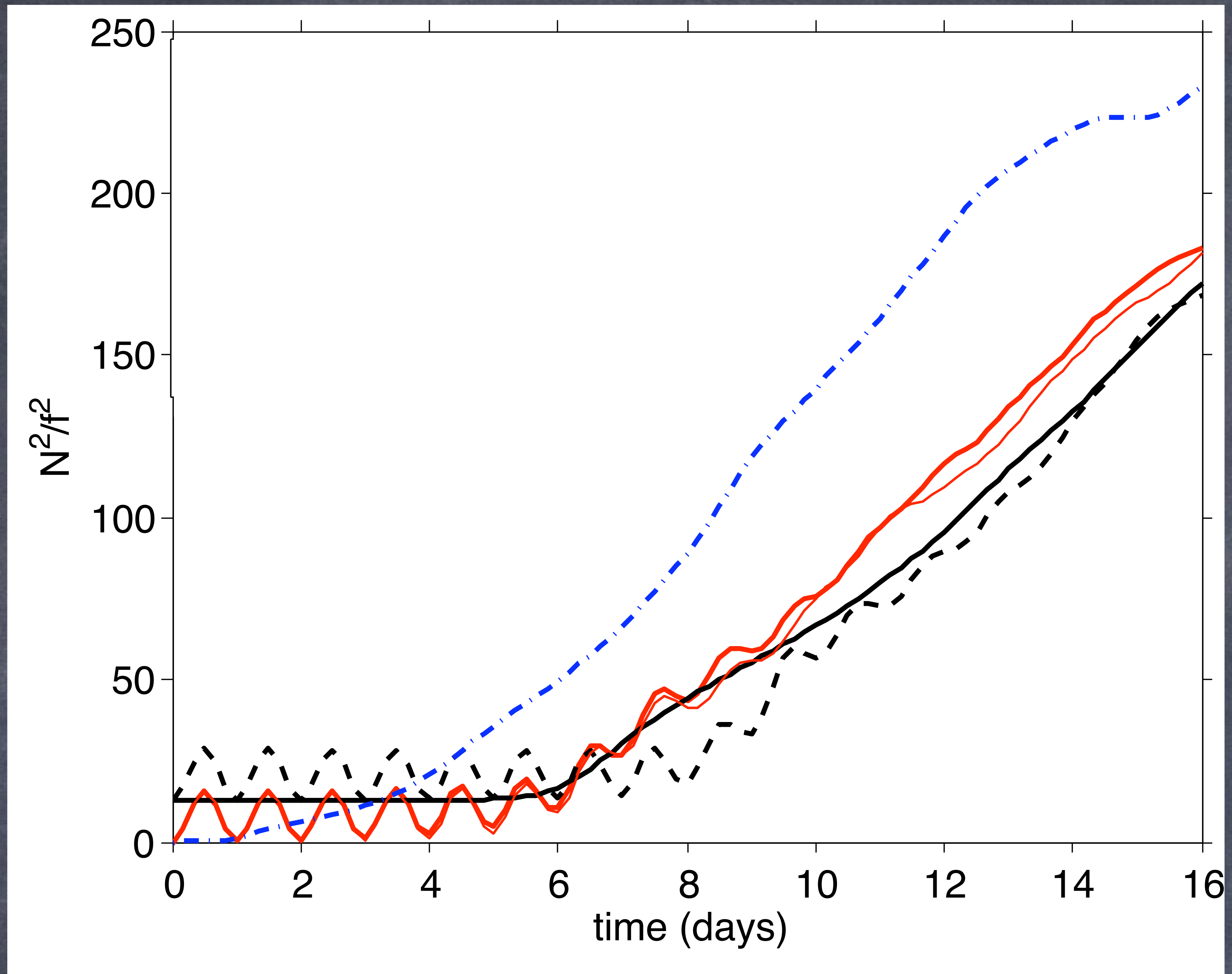

# Parameterization of Finite Amp. Eddies: Ingredients

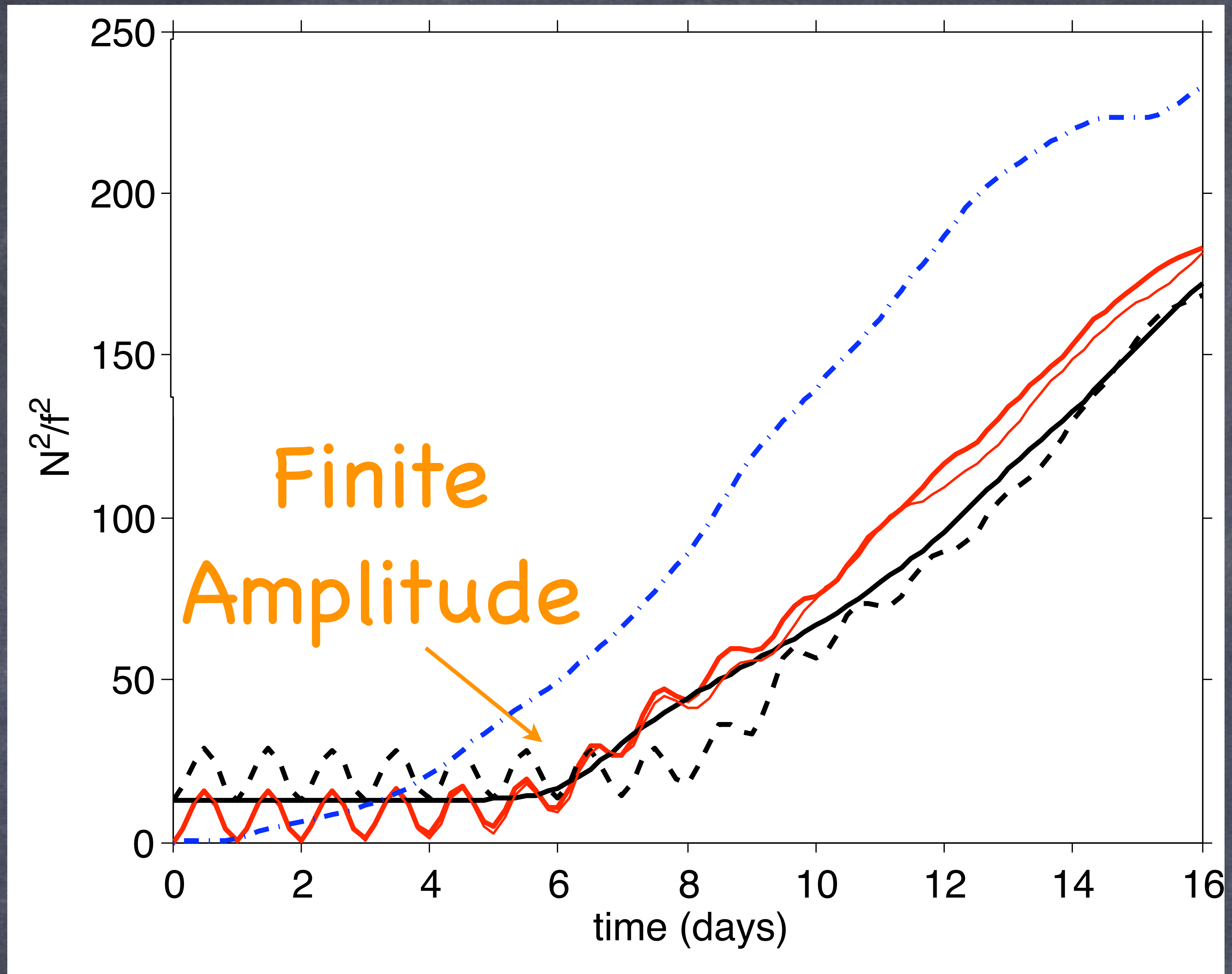

# Parameterization of Finite Amp. Eddies: Ingredients

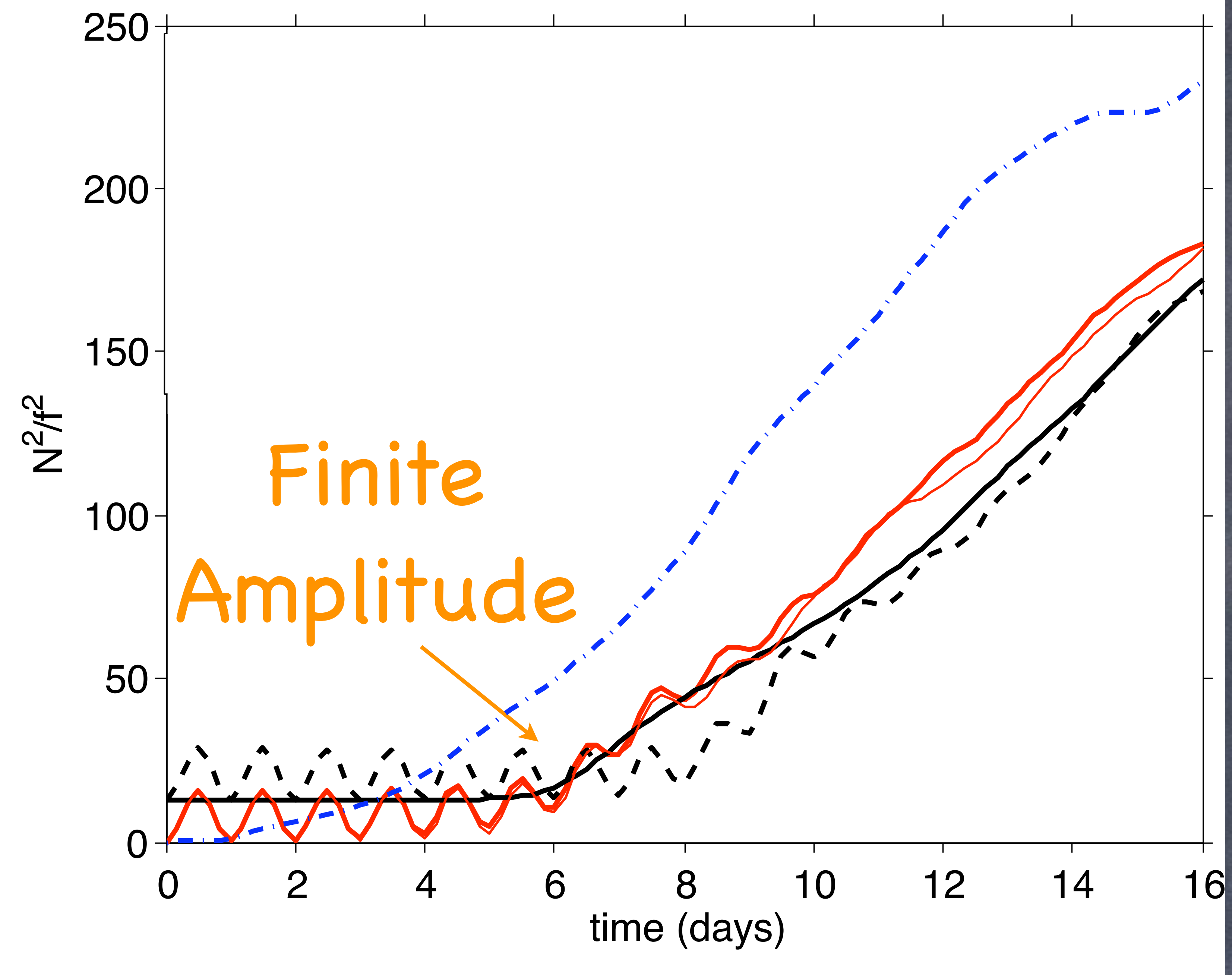


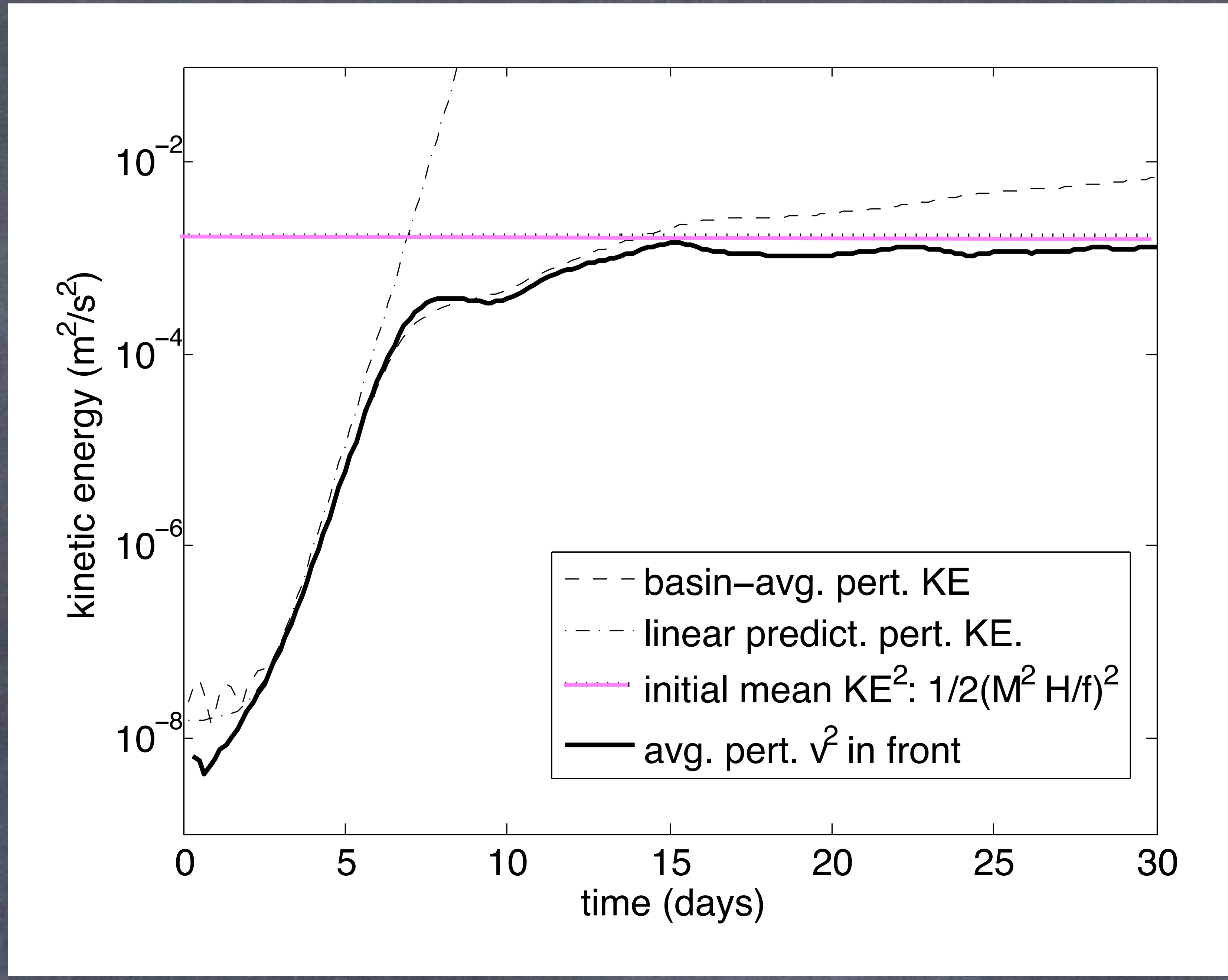

# Parameterization of Finite Amp. Eddies: Ingredients

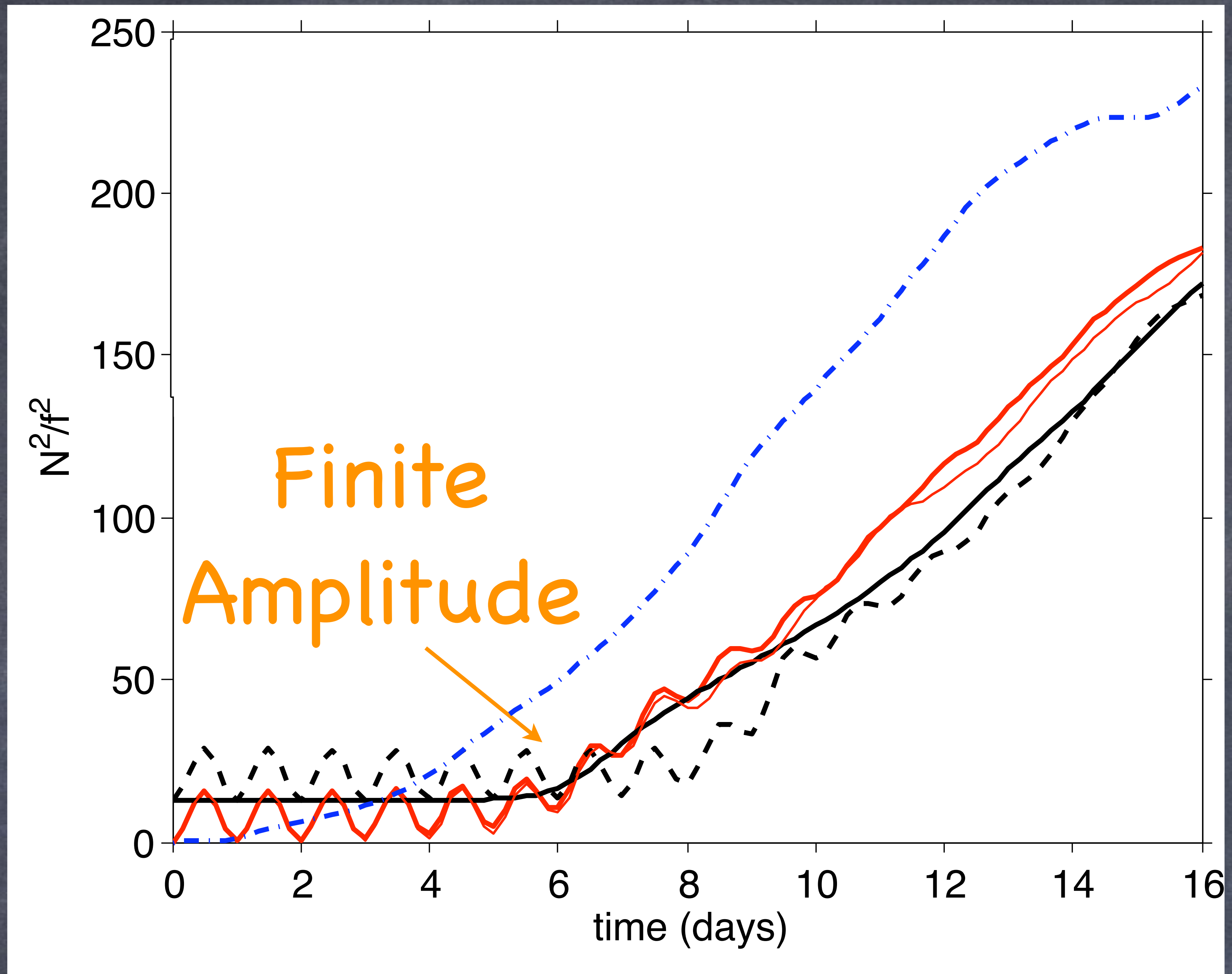


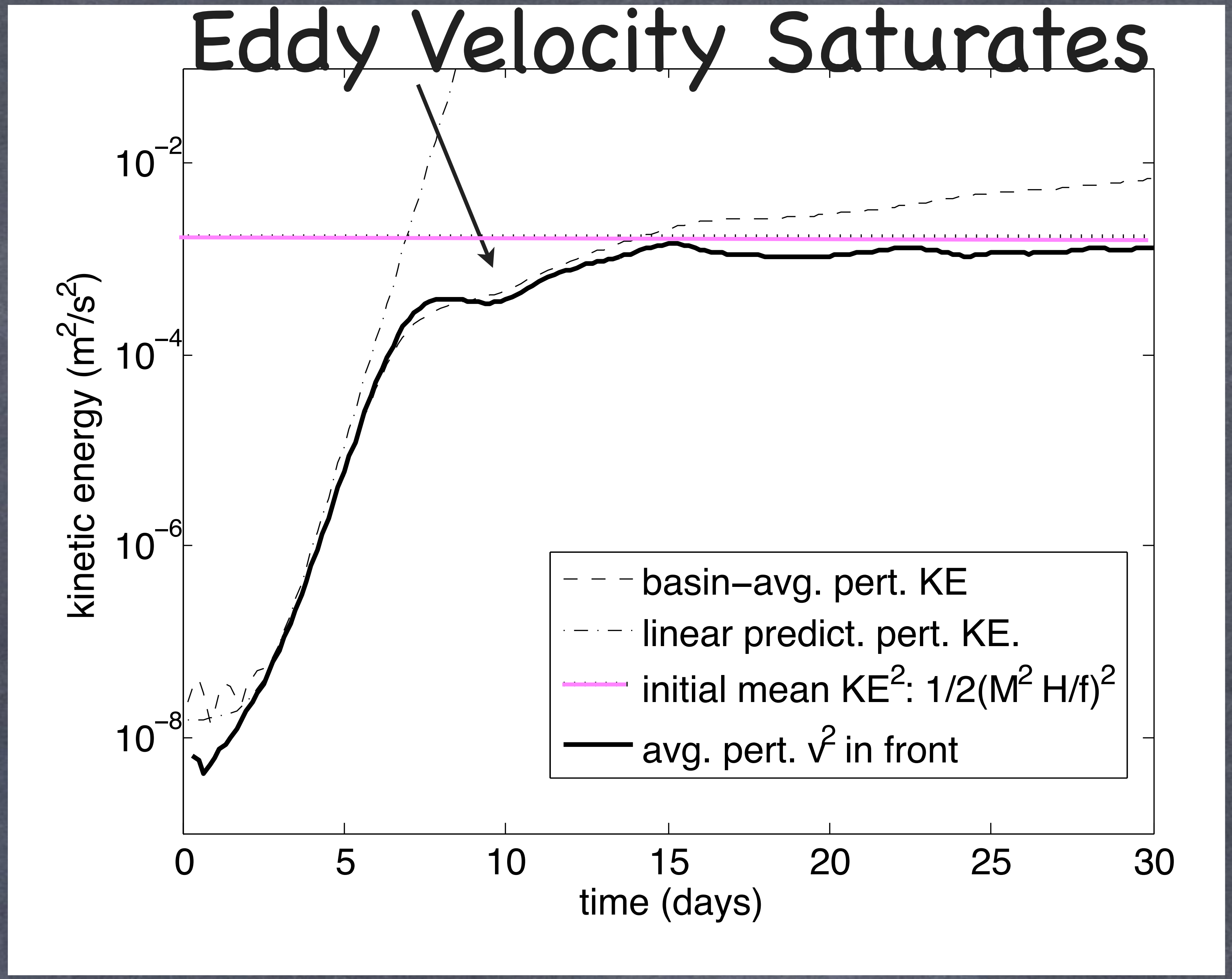

# Parameterization of Finite Amp. Eddies: Ingredients

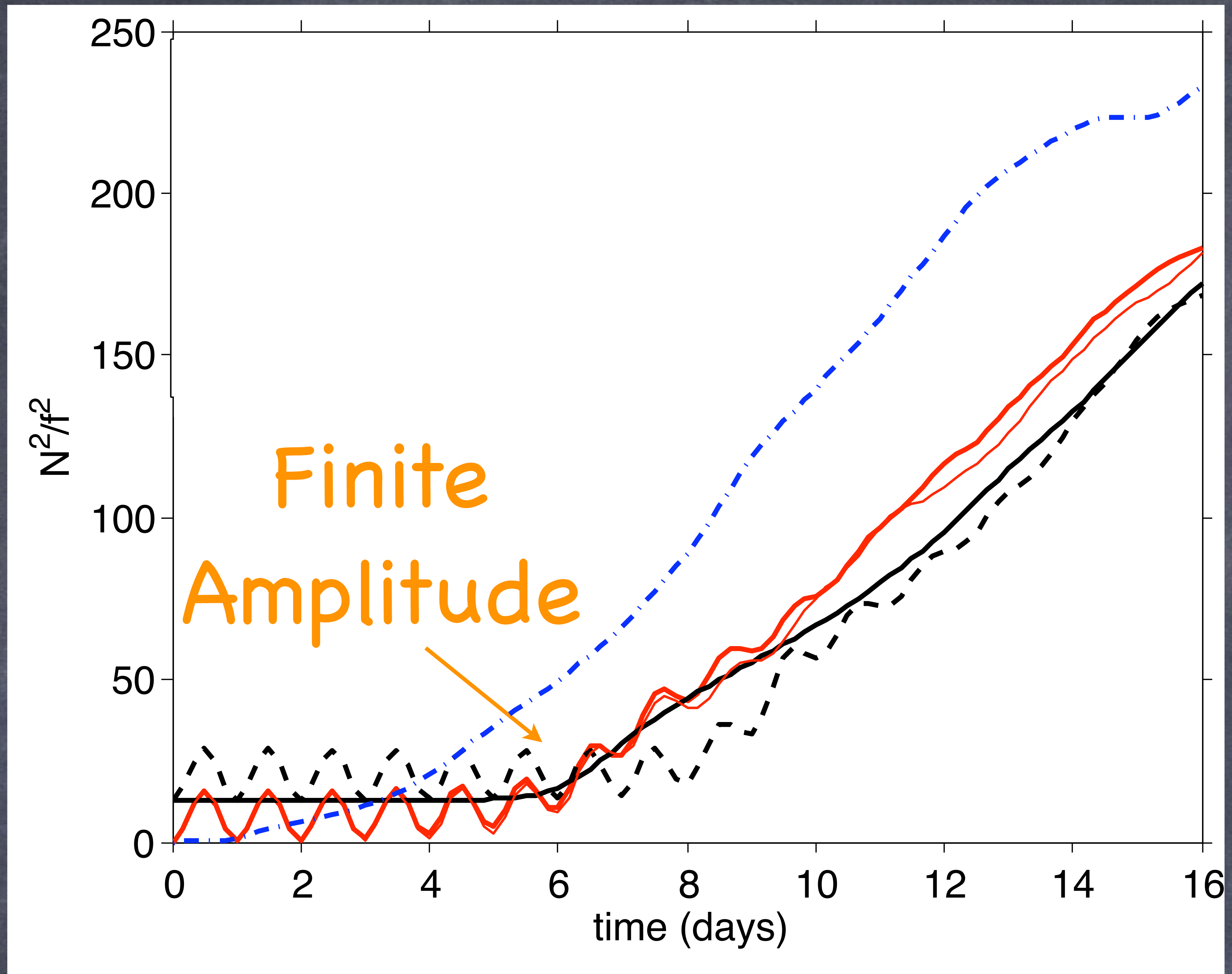


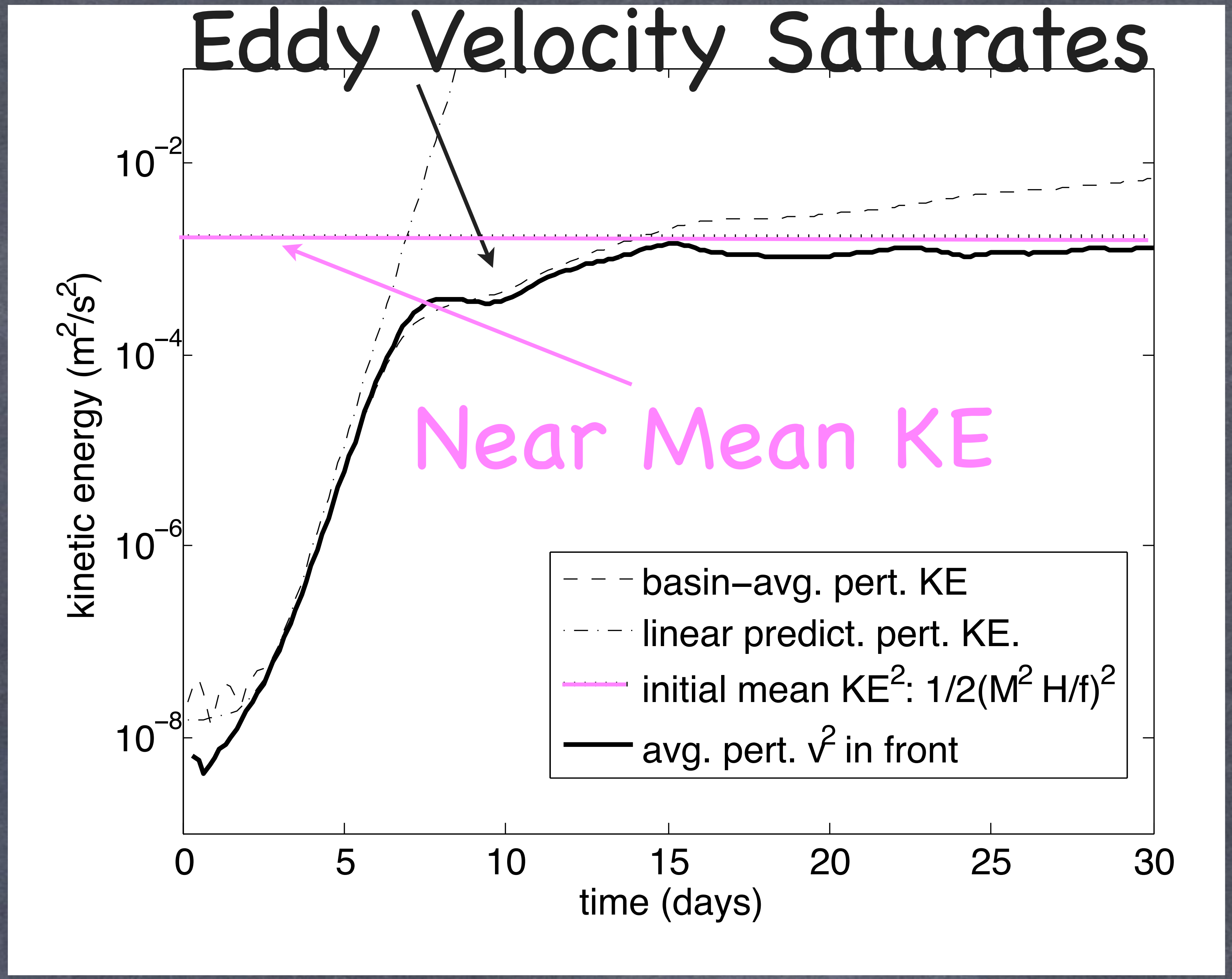

# Parameterization of Finite Amp. Eddies: Ingredients

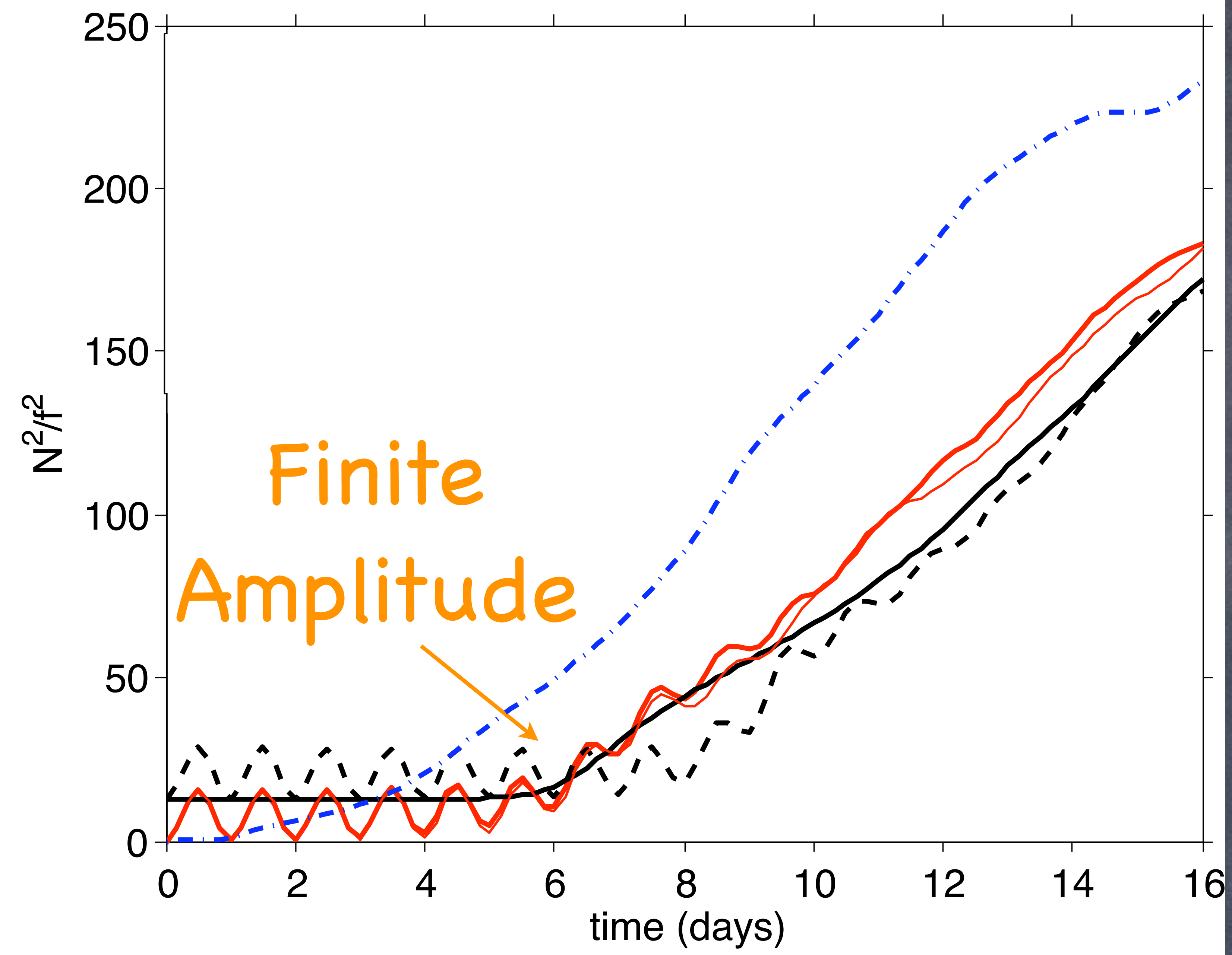


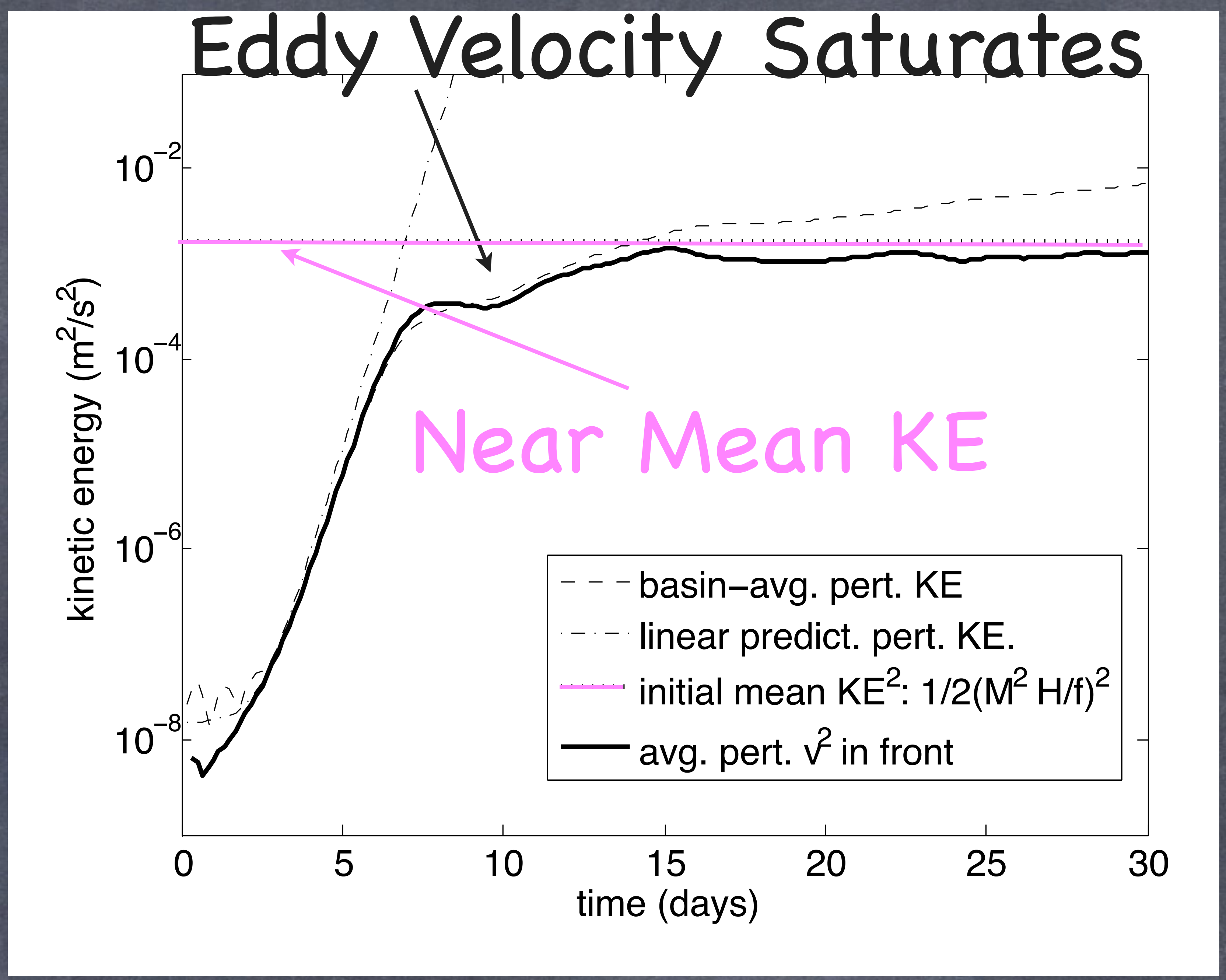


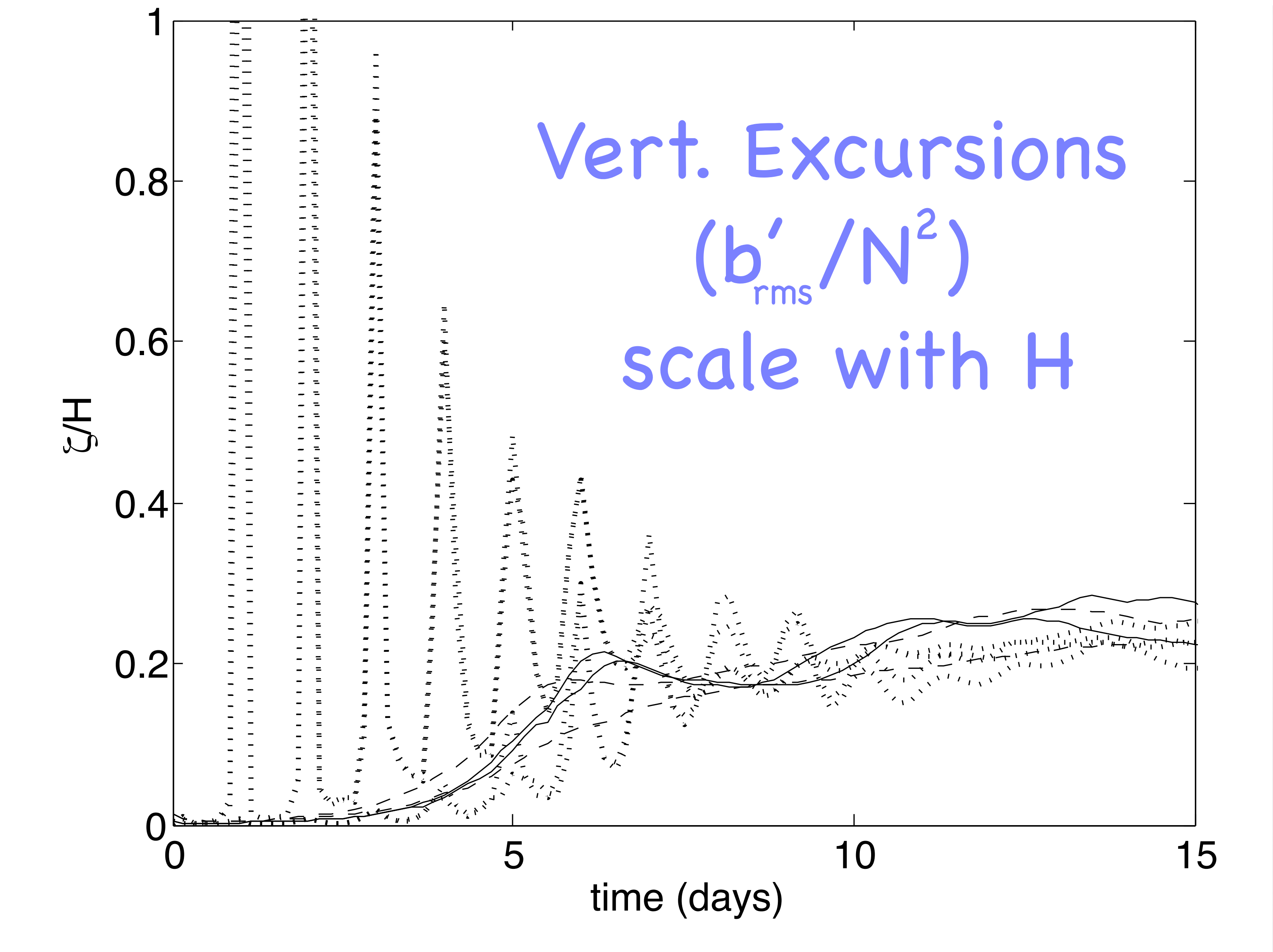

# Parameterization of Finite Amp. Eddies: Ingredients

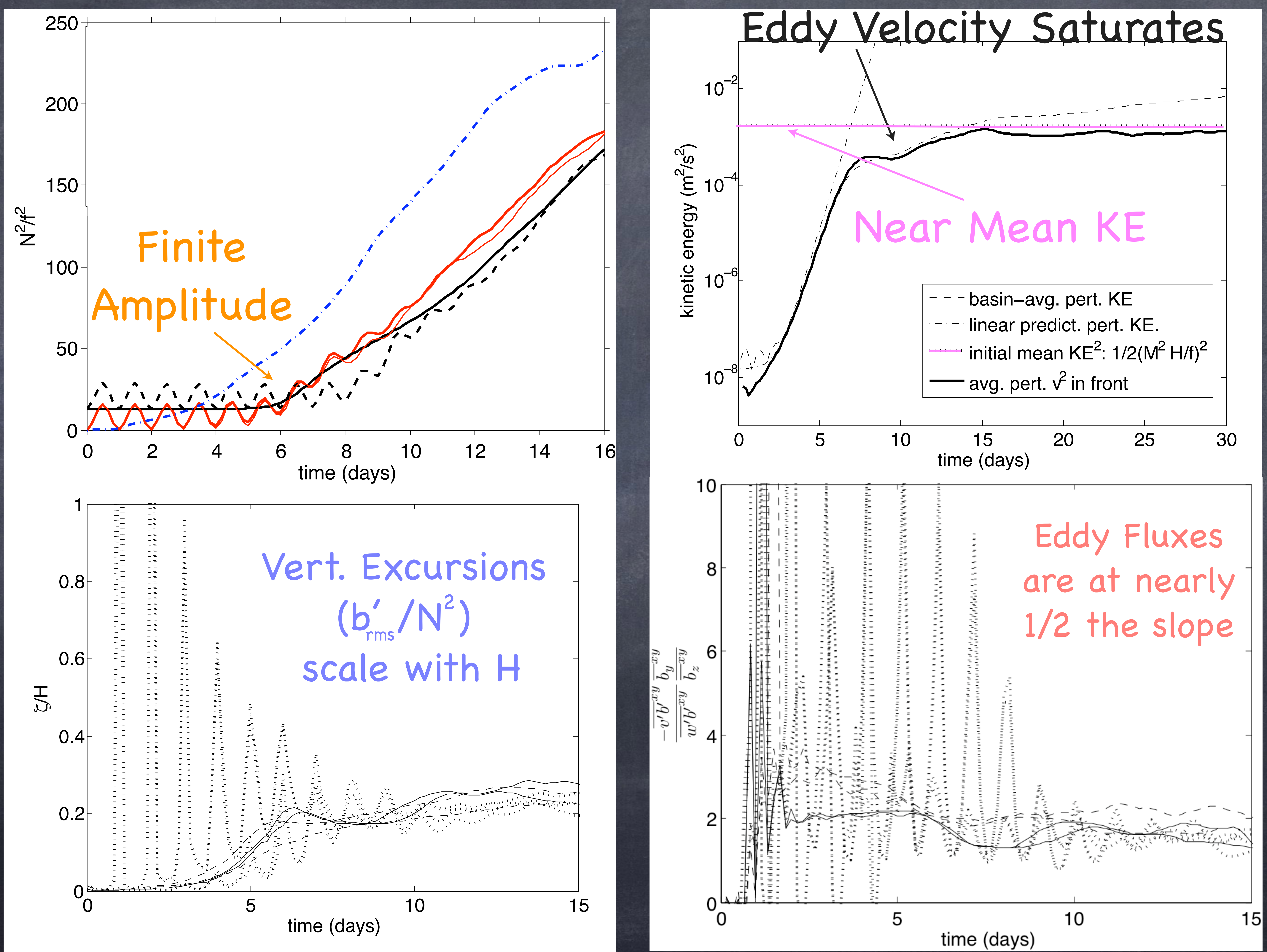

B. Fox-Kemper, R. Ferrari, and R. W. Hallberg. Parameterization of mixed layer eddies. Part I: Theory and diagnosis. Journal of Physical Oceanography, 38(6):1145-1165, 2008.

# Magnitude Analysis: Vert. Fluxes

Extraction of potential energy by submesoscale eddies:

$$-\langle wb \rangle = \frac{\partial \langle PE \rangle}{\partial t} \approx \frac{\Delta PE}{\Delta t} \propto \frac{\Delta z \Delta b}{\Delta t}$$

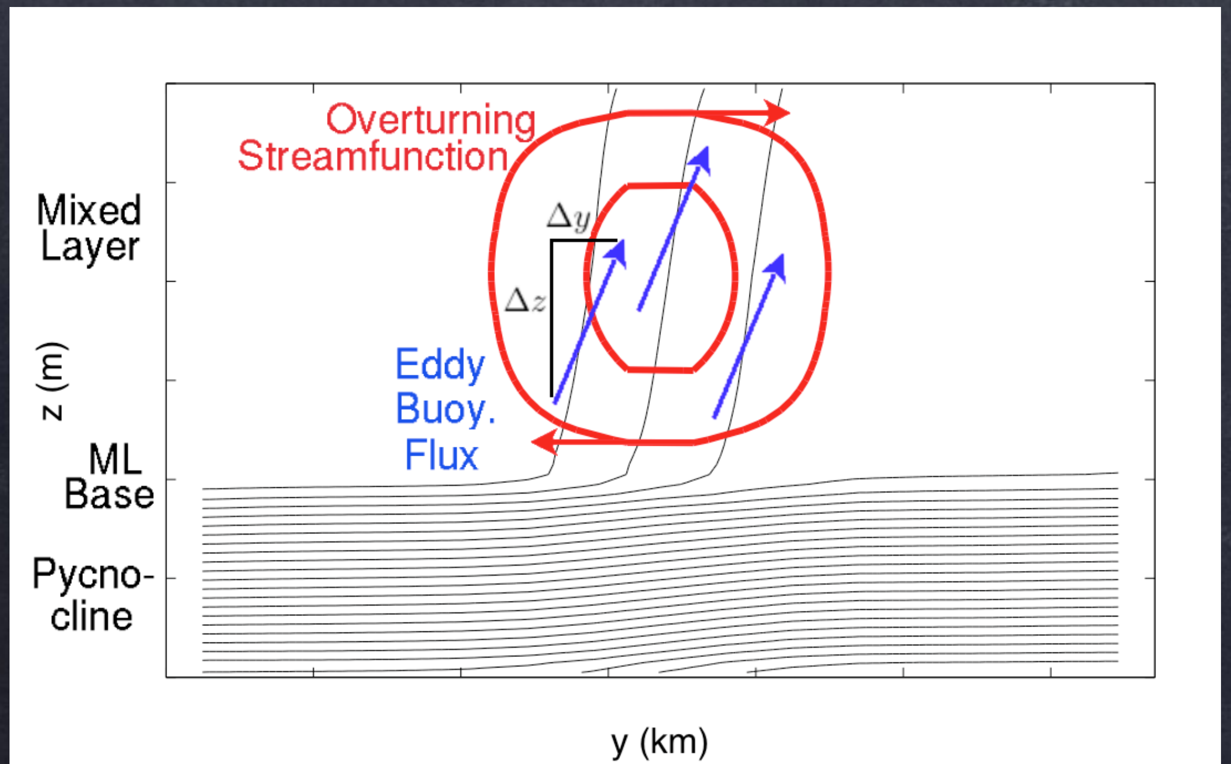


$$\langle wb \rangle \propto \frac{-\Delta z \Delta b}{\Delta t}$$

B. Fox-Kemper, R. Ferrari, and R. W. Hallberg. Parameterization of mixed layer eddies. Part I: Theory and diagnosis. Journal of Physical Oceanography, 38(6):1145-1165, 2008.

# Magnitude Analysis: Vert. Fluxes

Extraction of potential energy by submesoscale eddies:

$$-\langle wb \rangle = \frac{\partial \langle PE \rangle}{\partial t} \approx \frac{\Delta PE}{\Delta t} \propto \frac{\Delta z \Delta b}{\Delta t}$$

Buoy. diff just parcel exchange of large-scale buoy.

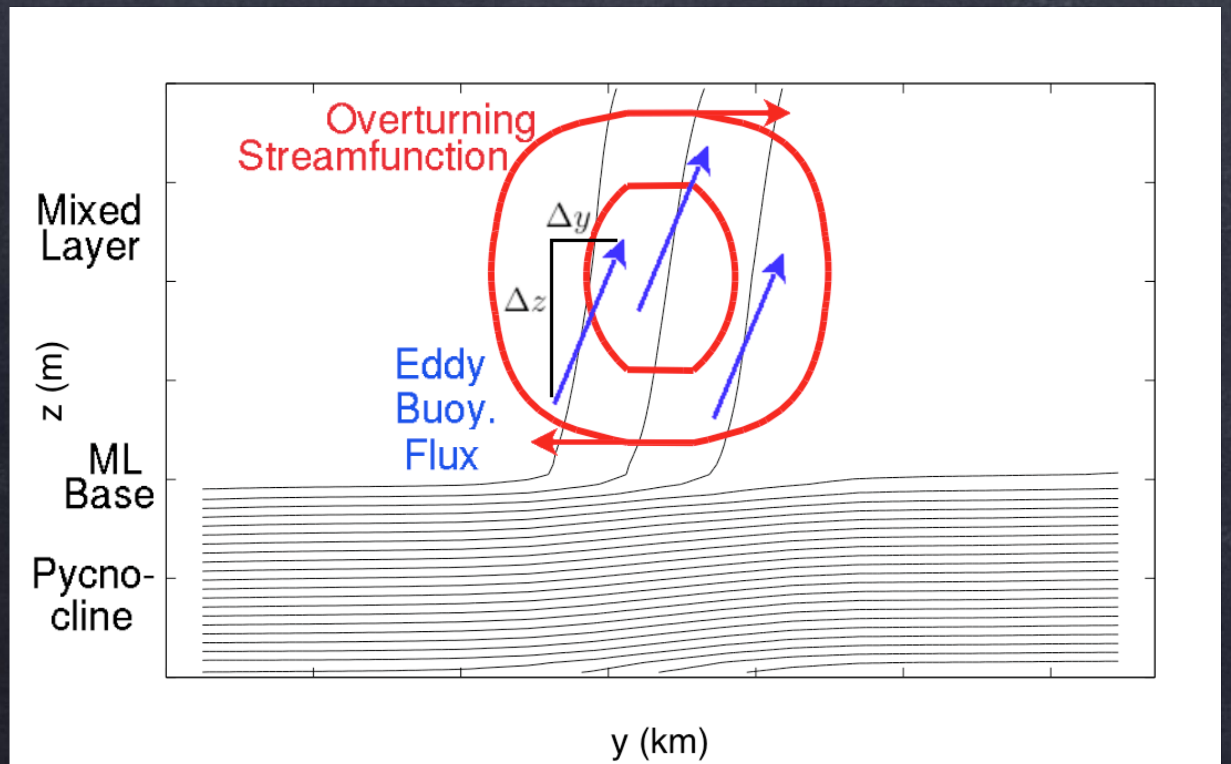


$$\langle wb \rangle \propto \frac{-\Delta z \Delta b}{\Delta t}$$

B. Fox-Kemper, R. Ferrari, and R. W. Hallberg. Parameterization of mixed layer eddies. Part I: Theory and diagnosis. Journal of Physical Oceanography, 38(6):1145-1165, 2008.

# Magnitude Analysis: Vert. Fluxes

Extraction of potential energy by submesoscale eddies:

$$-\langle wb\rangle = \frac{\partial\langle PE\rangle}{\partial t} \approx \frac{\Delta PE}{\Delta t} \propto \frac{\Delta z \Delta b}{\Delta t}$$

Buoy. diff just parcel exchange of large-scale buoy.

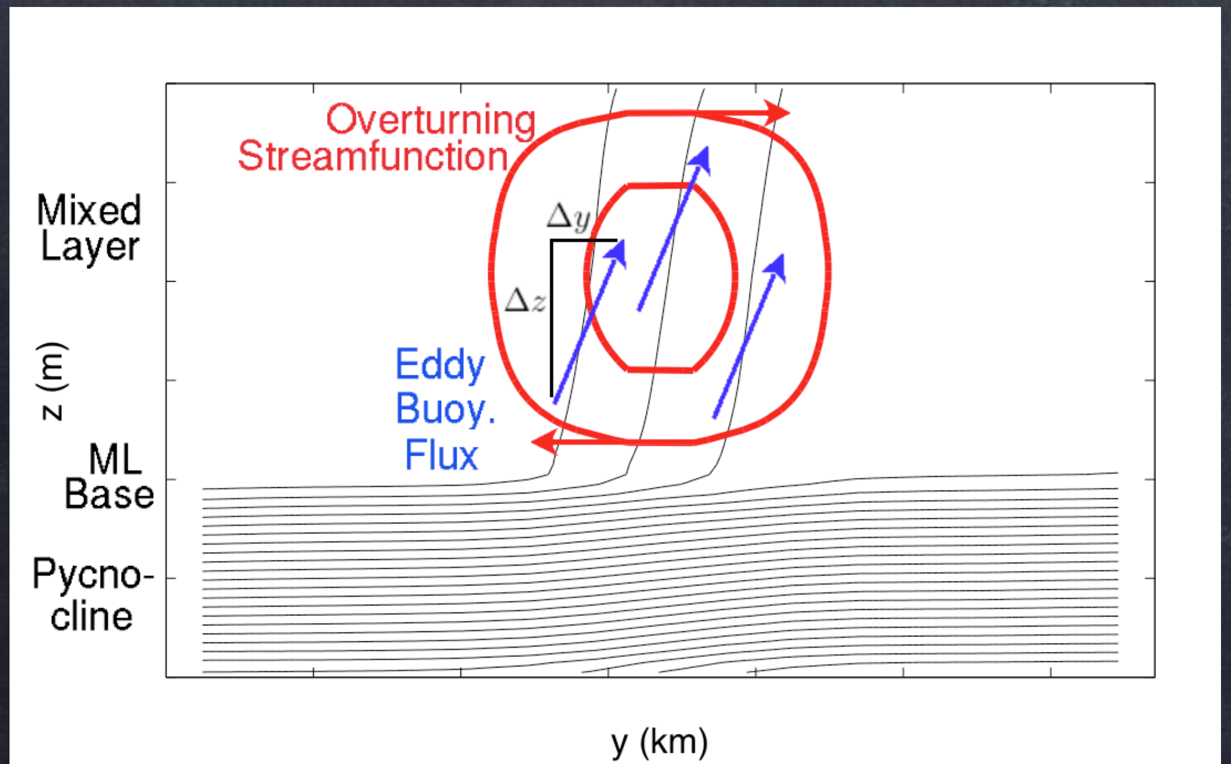


$$\langle wb\rangle \propto \frac{-\Delta z\left(\Delta y \frac{\partial \bar{b}}{\partial y} + \Delta z \frac{\partial \bar{b}}{\partial z}\right)}{\Delta t}$$

B. Fox-Kemper, R. Ferrari, and R. W. Hallberg. Parameterization of mixed layer eddies. Part I: Theory and diagnosis. Journal of Physical Oceanography, 38(6):1145-1165, 2008.

# Magnitude Analysis: Vert. Fluxes

Extraction of potential energy by submesoscale eddies:

$$-\langle wb\rangle = \frac{\partial\langle PE\rangle}{\partial t} \approx \frac{\Delta PE}{\Delta t} \propto \frac{\Delta z \Delta b}{\Delta t}$$

Buoy. diff just parcel exchange of large-scale buoy.

Flux slope scales with the buoy. slope: $\frac{\Delta y}{\Delta z} \propto \frac{-\frac{\partial \bar{b}}{\partial z}}{\frac{\partial \bar{b}}{\partial y}}$

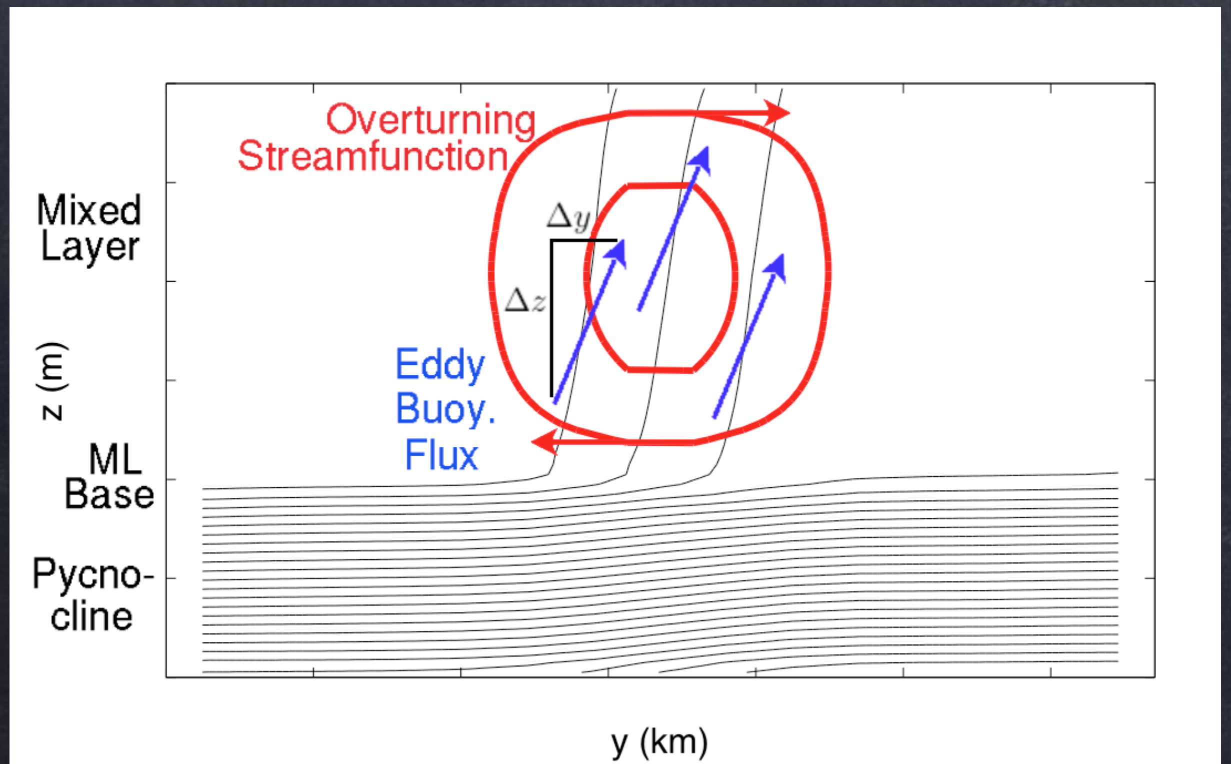


$$\langle wb\rangle \propto \frac{-\Delta z\left(\Delta y \frac{\partial \bar{b}}{\partial y} + \Delta z \frac{\partial \bar{b}}{\partial z}\right)}{\Delta t}$$

B. Fox-Kemper, R. Ferrari, and R. W. Hallberg. Parameterization of mixed layer eddies. Part I: Theory and diagnosis. Journal of Physical Oceanography, 38(6):1145-1165, 2008.

# Magnitude Analysis: Vert. Fluxes

Extraction of potential energy by submesoscale eddies:

$$-\langle wb \rangle = \frac{\partial \langle PE \rangle}{\partial t} \approx \frac{\Delta PE}{\Delta t} \propto \frac{\Delta z \Delta b}{\Delta t}$$

Buoy. diff just parcel exchange of large-scale buoy.

Flux slope scales with the buoy. slope: $\dfrac{\Delta y}{\Delta z} \propto \dfrac{-\frac{\partial \bar{b}}{\partial z}}{\frac{\partial \bar{b}}{\partial y}}$

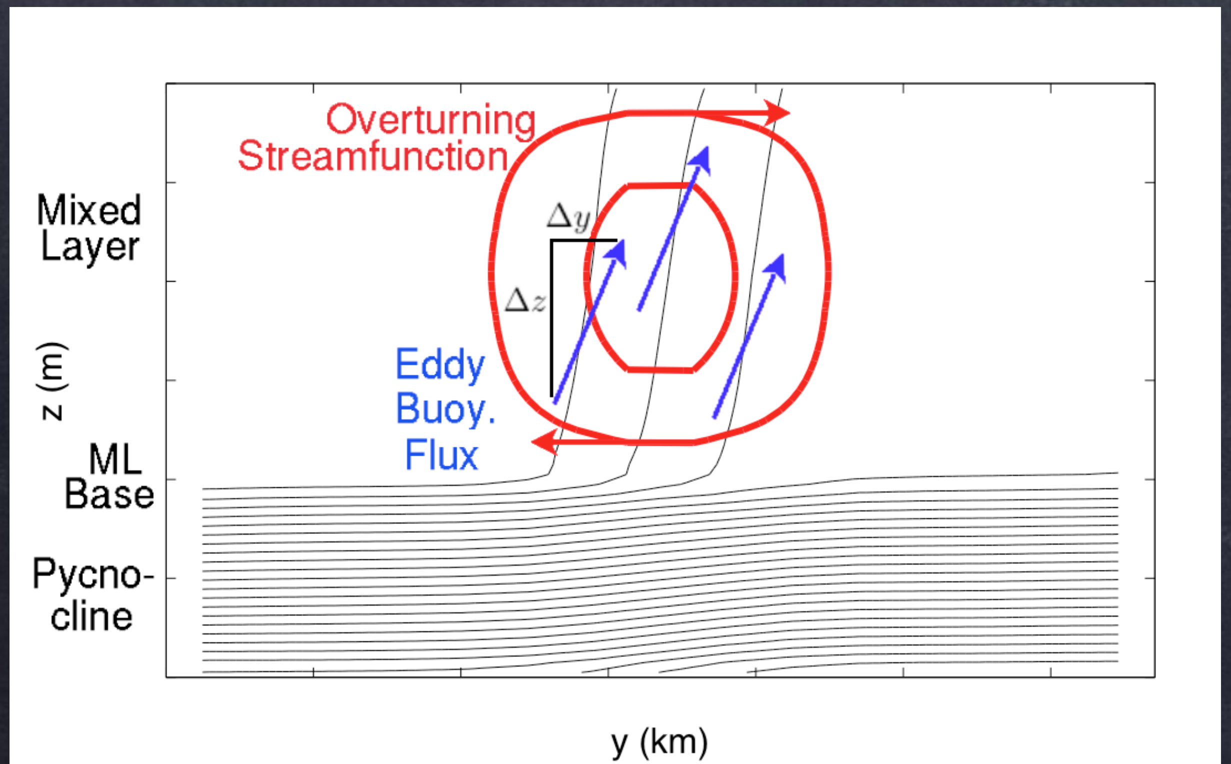


$$\langle wb \rangle \propto \frac{\Delta z \Delta y \frac{\partial \bar{b}}{\partial y}}{\Delta t}$$

B. Fox-Kemper, R. Ferrari, and R. W. Hallberg. Parameterization of mixed layer eddies. Part I: Theory and diagnosis. Journal of Physical Oceanography, 38(6):1145-1165, 2008.

# Magnitude Analysis: Vert. Fluxes

Extraction of potential energy by submesoscale eddies:

$$-\langle wb\rangle = \frac{\partial\langle PE\rangle}{\partial t} \approx \frac{\Delta PE}{\Delta t} \propto \frac{\Delta z \Delta b}{\Delta t}$$

Buoy. diff just parcel exchange of large-scale buoy.

Flux slope scales with the buoy. slope: $\frac{\Delta y}{\Delta z} \propto \frac{-\frac{\partial \bar{b}}{\partial z}}{\frac{\partial \bar{b}}{\partial y}}$

Time scale is turnover time

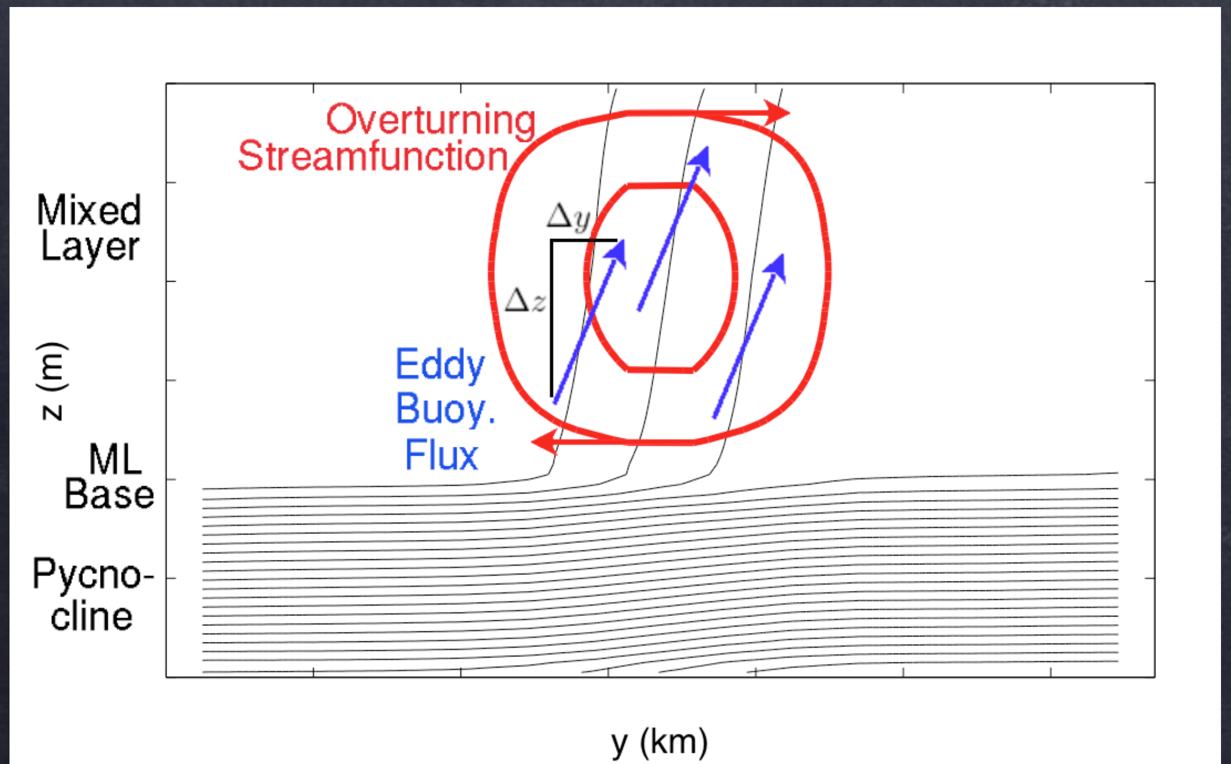


$$\langle wb\rangle \propto \frac{\Delta z \Delta y \frac{\partial \bar{b}}{\partial y}}{\Delta t}$$

B. Fox-Kemper, R. Ferrari, and R. W. Hallberg. Parameterization of mixed layer eddies. Part I: Theory and diagnosis. Journal of Physical Oceanography, 38(6):1145-1165, 2008.

# Magnitude Analysis: Vert. Fluxes

Extraction of potential energy by submesoscale eddies:

$$-\langle wb \rangle = \frac{\partial \langle PE \rangle}{\partial t} \approx \frac{\Delta PE}{\Delta t} \propto \frac{\Delta z \Delta b}{\Delta t}$$

Buoy. diff just parcel exchange of large-scale buoy.

Flux slope scales with the buoy. slope: $\frac{\Delta y}{\Delta z} \propto \frac{-\frac{\partial \bar{b}}{\partial z}}{\frac{\partial \bar{b}}{\partial y}}$

Time scale is turnover time

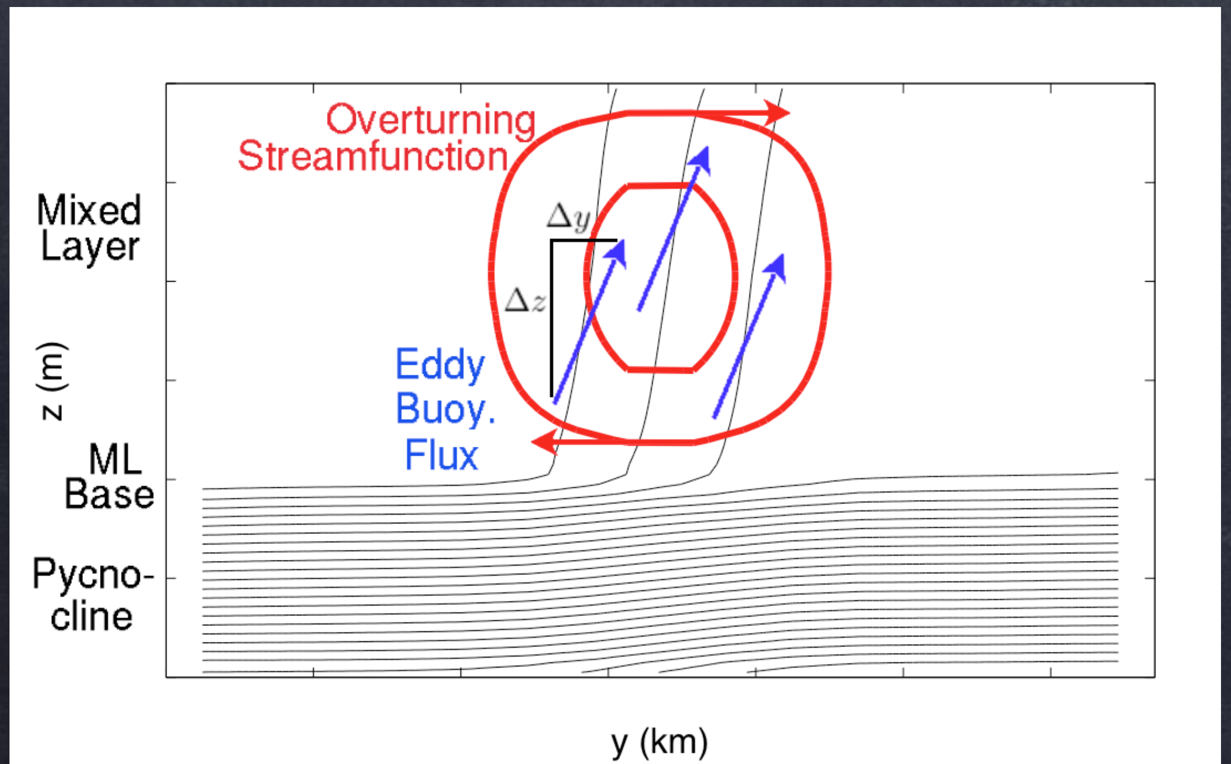


$$\langle wb \rangle \propto \frac{\Delta z \Delta y \frac{\partial \bar{b}}{\partial y}}{\Delta y / V}$$

B. Fox-Kemper, R. Ferrari, and R. W. Hallberg. Parameterization of mixed layer eddies. Part I: Theory and diagnosis. Journal of Physical Oceanography, 38(6):1145-1165, 2008.

# Magnitude Analysis: Vert. Fluxes

Extraction of potential energy by submesoscale eddies:

$$-\langle wb\rangle = \frac{\partial\langle PE\rangle}{\partial t} \approx \frac{\Delta PE}{\Delta t} \propto \frac{\Delta z \Delta b}{\Delta t}$$

Buoy. diff just parcel exchange of large-scale buoy.

Flux slope scales with the buoy. slope: $\frac{\Delta y}{\Delta z} \propto \frac{-\frac{\partial \bar b}{\partial z}}{\frac{\partial \bar b}{\partial y}}$

Time scale is turnover time from mean thermal wind:

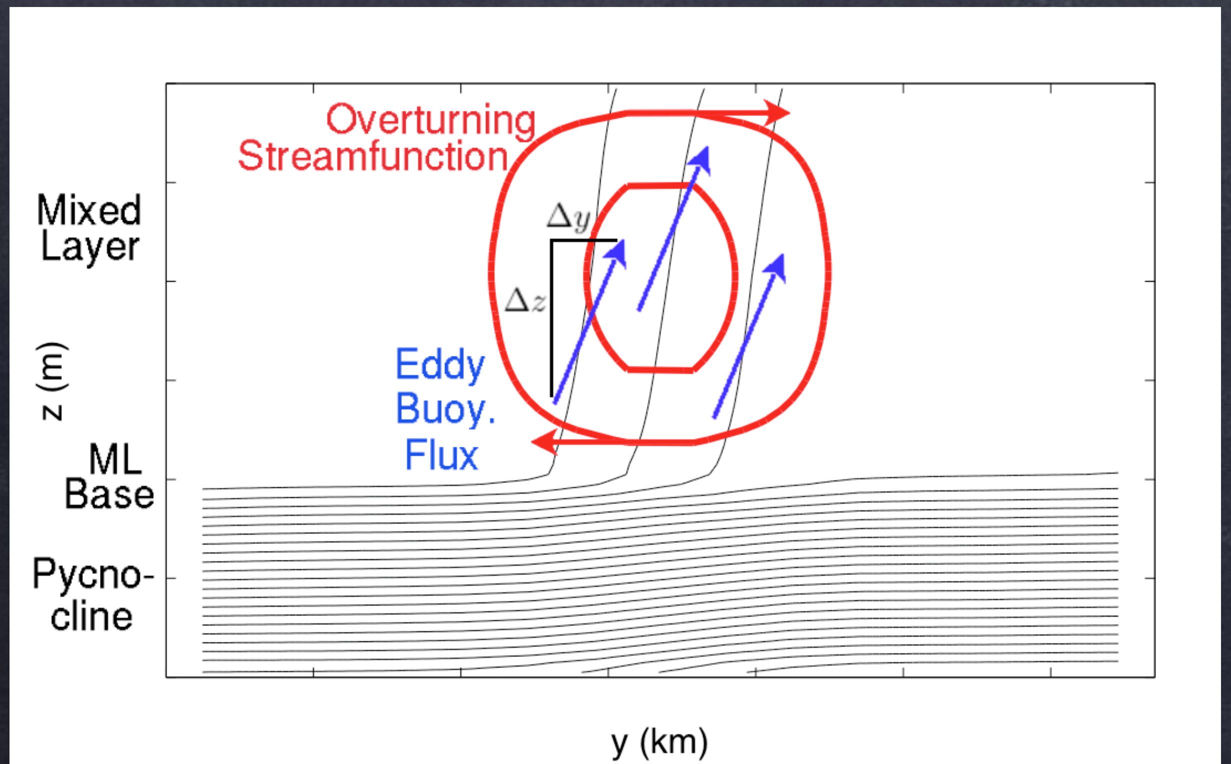


$$\langle wb\rangle \propto \frac{\Delta z H}{|f|}\left[\frac{\partial \bar b}{\partial y}\right]^2$$

B. Fox-Kemper, R. Ferrari, and R. W. Hallberg. Parameterization of mixed layer eddies. Part I: Theory and diagnosis. Journal of Physical Oceanography, 38(6):1145-1165, 2008.

# Magnitude Analysis: Vert. Fluxes

Extraction of potential energy by submesoscale eddies:

$$-\langle wb\rangle = \frac{\partial\langle PE\rangle}{\partial t} \approx \frac{\Delta PE}{\Delta t} \propto \frac{\Delta z \Delta b}{\Delta t}$$

Buoy. diff just parcel exchange of large-scale buoy.

Flux slope scales with the buoy. slope: $\frac{\Delta y}{\Delta z} \propto \frac{-\frac{\partial \bar{b}}{\partial z}}{\frac{\partial \bar{b}}{\partial y}}$

Time scale is turnover time from mean thermal wind:

Vertical scale known: $\Delta z \propto H$

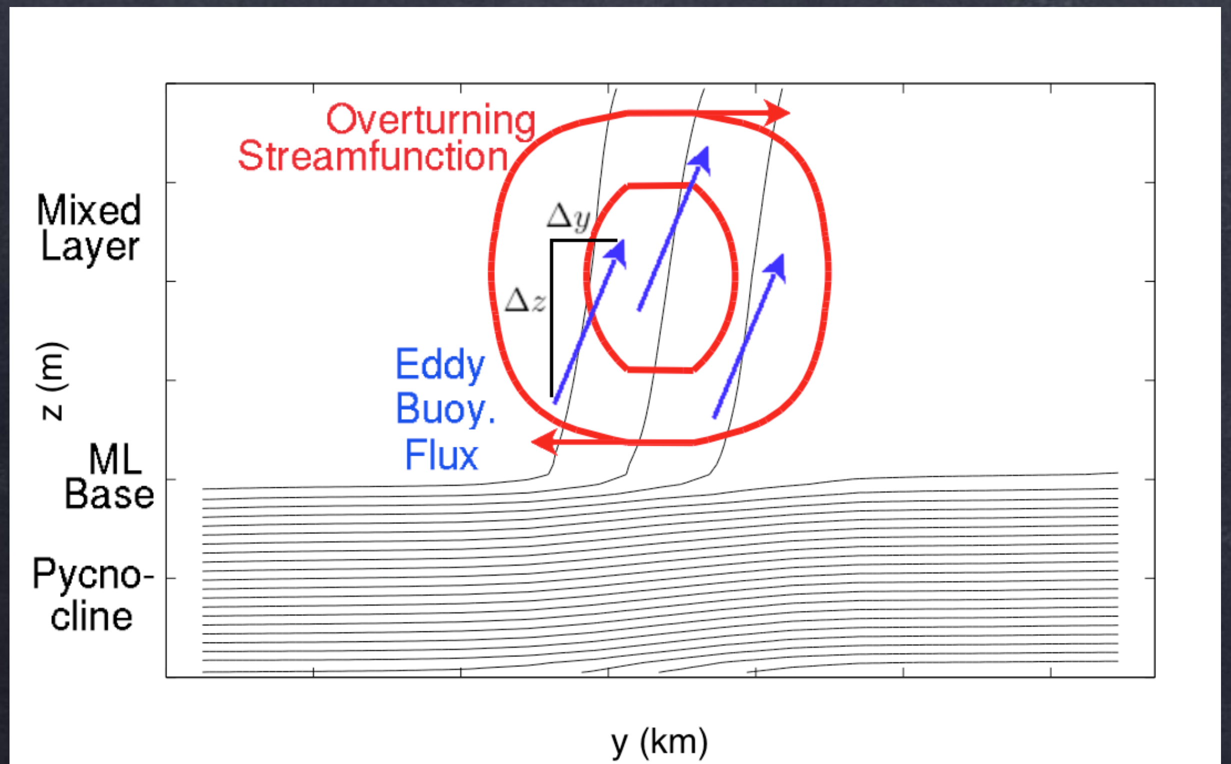


$$\langle wb\rangle \propto \frac{\Delta z H}{|f|}\left[\frac{\partial \bar{b}}{\partial y}\right]^2$$

B. Fox-Kemper, R. Ferrari, and R. W. Hallberg. Parameterization of mixed layer eddies. Part I: Theory and diagnosis. Journal of Physical Oceanography, 38(6):1145-1165, 2008.

# Magnitude Analysis: Vert. Fluxes

Extraction of potential energy by submesoscale eddies:

$$-\langle wb\rangle = \frac{\partial\langle PE\rangle}{\partial t} \approx \frac{\Delta PE}{\Delta t} \propto \frac{\Delta z \Delta b}{\Delta t}$$

Buoy. diff just parcel exchange of large-scale buoy.

Flux slope scales with the buoy. slope: $\frac{\Delta y}{\Delta z} \propto \frac{-\frac{\partial \bar{b}}{\partial z}}{\frac{\partial \bar{b}}{\partial y}}$

Time scale is turnover time from mean thermal wind:

Vertical scale known: $\Delta z \propto H$

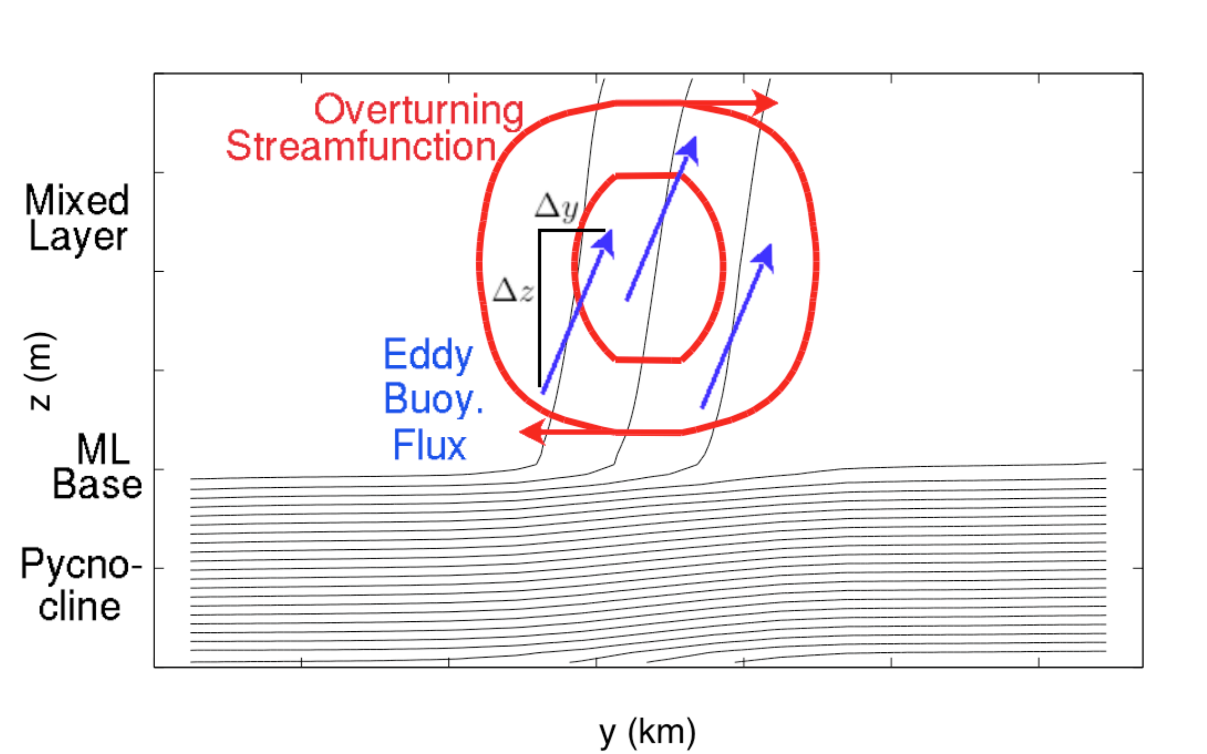


$$\langle wb\rangle \propto \frac{H^2}{|f|}\left[\frac{\partial \bar{b}}{\partial y}\right]^2$$

Fox-Kemper et al., 2008

B. Fox-Kemper, R. Ferrari, and R. W. Hallberg. Parameterization of mixed layer eddies. Part I: Theory and diagnosis. Journal of Physical Oceanography, 38(6):1145-1165, 2008.

# Eddies effect a largely adiabatic transfer: thus representable by a streamfunction

$$\mathbf{\Psi} \propto \frac{H^2 \nabla \bar{b} \times \hat{\mathbf{z}}}{|f|} \longrightarrow \overline{\mathbf{u}' b'} \equiv \mathbf{\Psi} \times \nabla \bar{b}$$

$$\overline{w' b'} \propto \frac{H^2}{|f|} \left| \nabla_H \bar{b} \right|^2$$

$$\overline{\mathbf{u}'_H b'} \propto \frac{-H^2 \frac{\partial \bar{b}}{\partial z}}{|f|} \nabla_H \bar{b}$$

B. Fox-Kemper, R. Ferrari, and R. W. Hallberg. Parameterization of mixed layer eddies. Part I: Theory and diagnosis. Journal of Physical Oceanography, 38(6):1145-1165, 2008.

# Eddies effect a largely adiabatic transfer: thus representable by a streamfunction

$$\boldsymbol{\Psi} \propto \frac{H^2 \nabla \bar{b} \times \hat{\mathbf{z}}}{|f|} \longrightarrow \overline{\mathbf{u}' b'} \equiv \boldsymbol{\Psi} \times \nabla \bar{b}$$

For a consistently upward,

$$\overline{w' b'} \propto \frac{H^2}{|f|} \left| \nabla_H \bar{b} \right|^2$$

$$\overline{\mathbf{u}'_H b'} \propto \frac{-H^2 \frac{\partial \bar{b}}{\partial z}}{|f|} \nabla_H \bar{b}$$

B. Fox-Kemper, R. Ferrari, and R. W. Hallberg. Parameterization of mixed layer eddies. Part I: Theory and diagnosis. Journal of Physical Oceanography, 38(6):1145-1165, 2008.

# Eddies effect a largely adiabatic transfer: thus representable by a streamfunction

$$\mathbf{\Psi} \propto \frac{H^2 \nabla \bar{b} \times \hat{\mathbf{z}}}{|f|} \longrightarrow \overline{\mathbf{u}' b'} \equiv \mathbf{\Psi} \times \nabla \bar{b}$$

For a consistently upward,

$$\overline{w' b'} \propto \frac{H^2}{|f|} \left|\nabla_H \bar{b}\right|^2$$

And horizontally downgradient flux.

$$\overline{\mathbf{u}'_H b'} \propto \frac{-H^2 \frac{\partial \bar{b}}{\partial z}}{|f|} \nabla_H \bar{b}$$

# What does it look like?

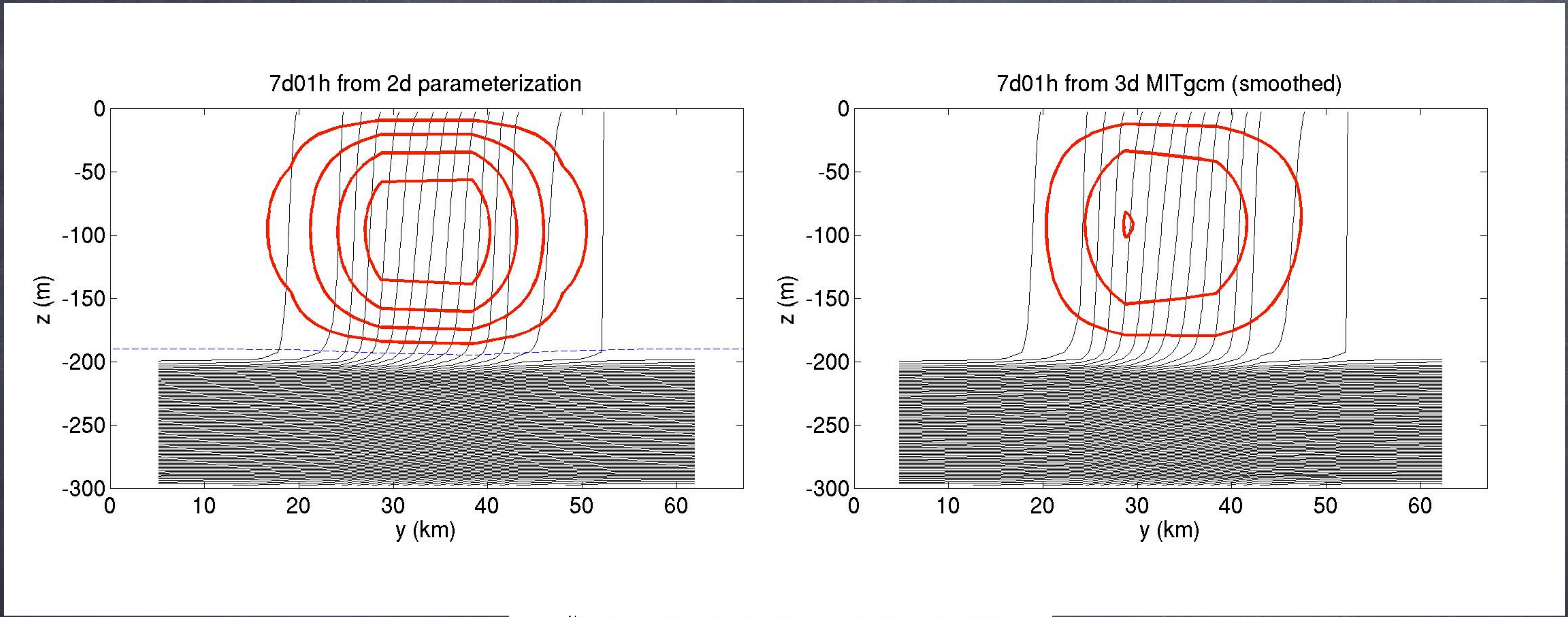


N²

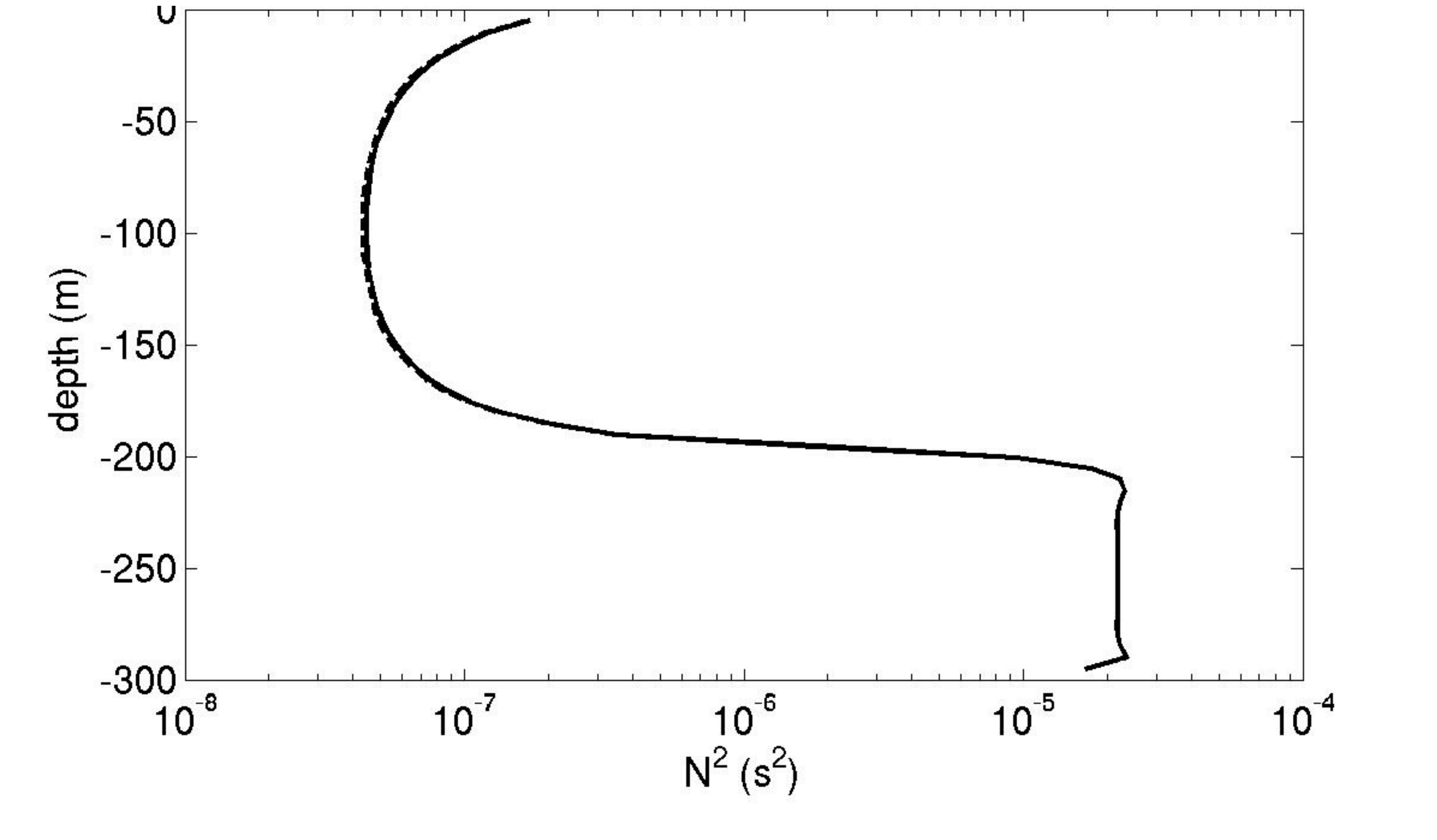


B. Fox-Kemper and R. Ferrari. Parameterization of mixed layer eddies. Part II: Prognosis and impact. Journal of Physical Oceanography, 38(6):1166-1179, 2008.

# What does it look like?

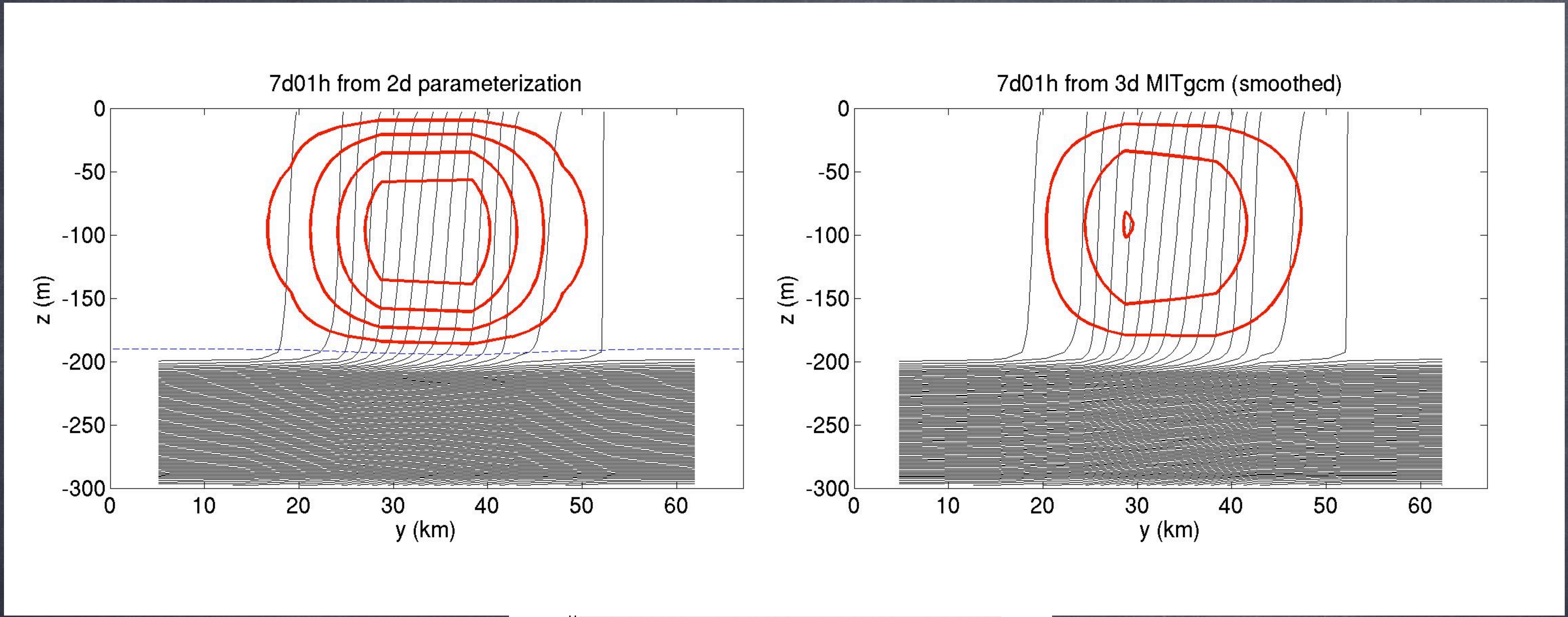


$N^2$

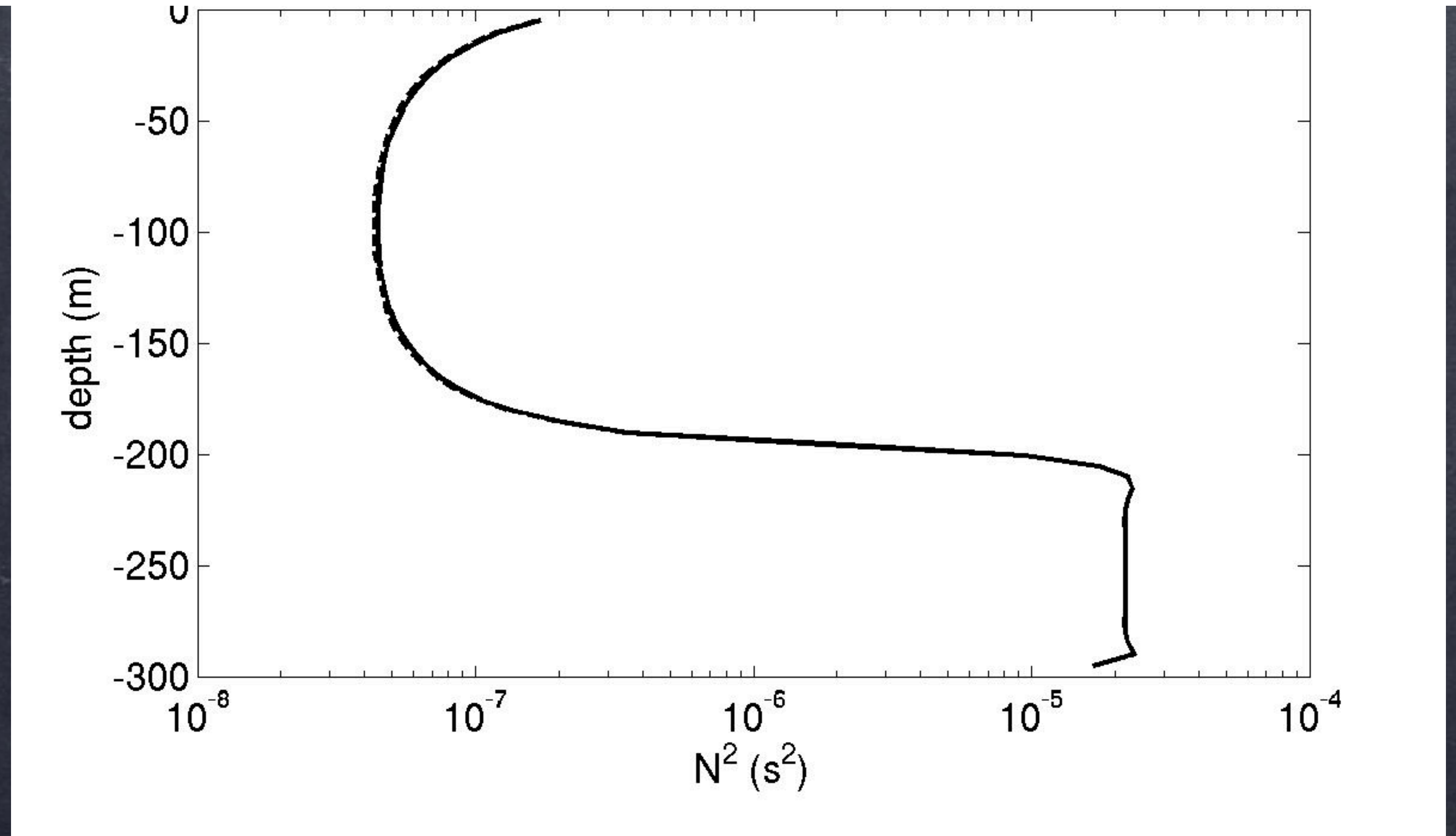


B. Fox-Kemper and R. Ferrari. Parameterization of mixed layer eddies. Part II: Prognosis and impact. Journal of Physical Oceanography, 38(6):1166-1179, 2008.

# Global Ocean Climate is SENSITIVE to these Mixed Layer Eddies! At least as parameterized

Implemented in IPCC AR5 & 6: NCAR, GFDL, Hadley, NEMO,...

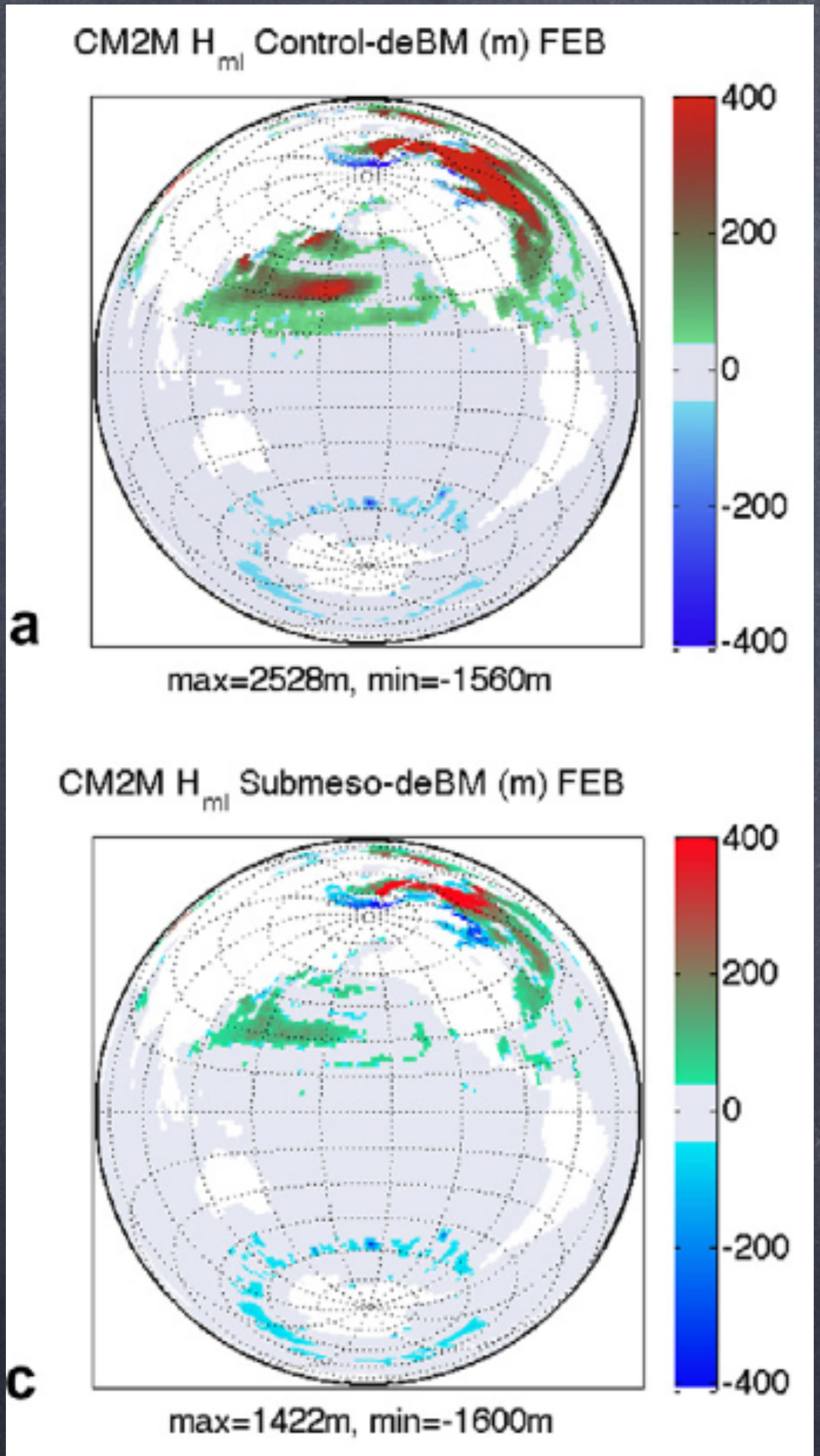


February Mixed layer depth Bias w/o MLE

February MLD Bias With MLE Parameterization

O(0.1 W/m²) change to global mean net fluxes,

Regional: 5 to 50 W/m²

Deep Mixed Layer Bias reduced

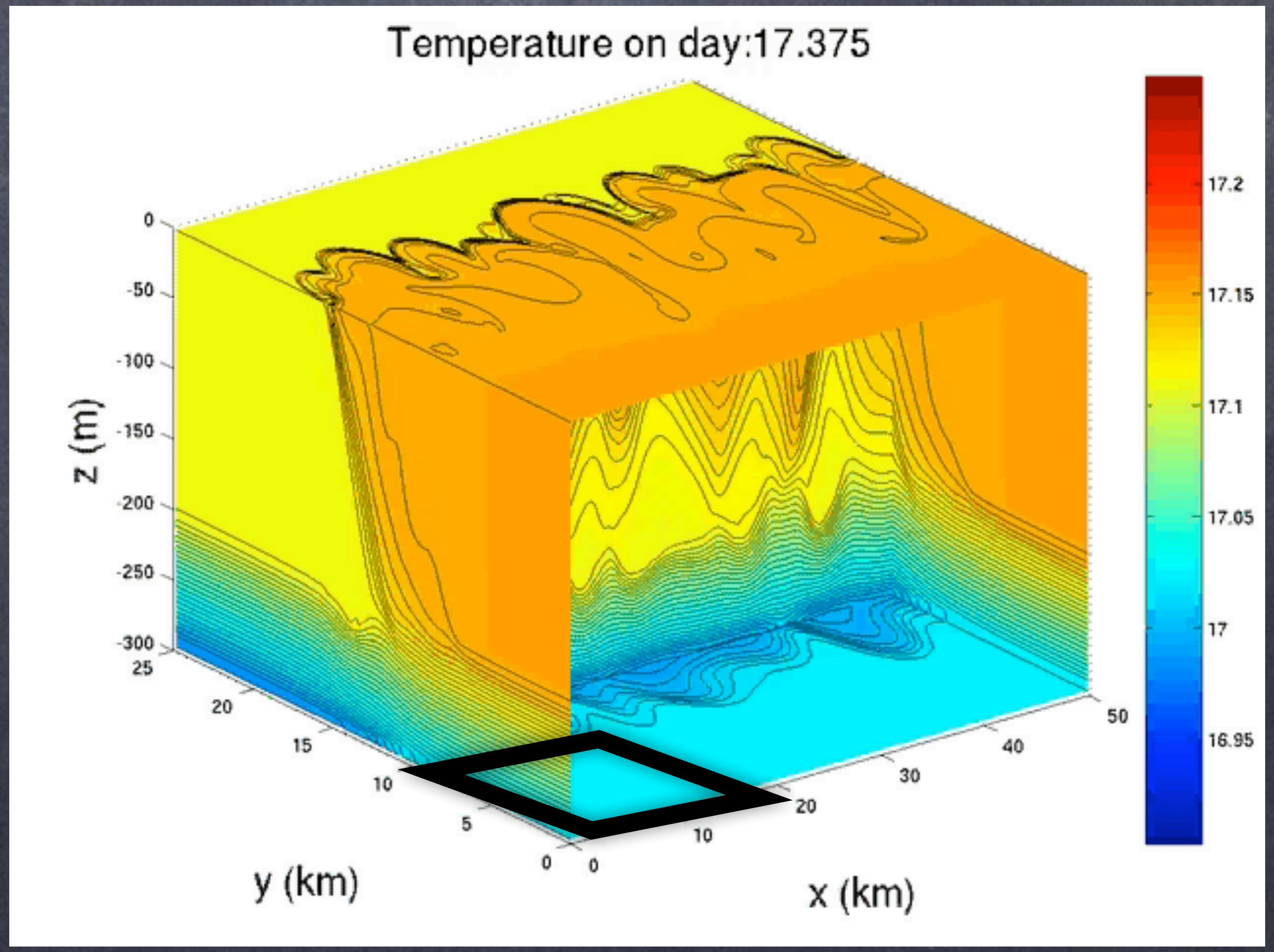


BFK, G. Danabasoglu, R. Ferrari, S. M. Griffies, R. W. Hallberg, M. M. Holland, M. E. Maltrud, S. Peacock, and B. L. Samuels. Parameterization of mixed layer eddies. III: Implementation and impact in global ocean climate simulations. Ocean Modelling, 39:61-78, 2011.

# Global Ocean Climate is SENSITIVE to these Mixed Layer Eddies! At least as parameterized

Implemented in IPCC AR5 & 6: NCAR, GFDL, Hadley, NEMO,...

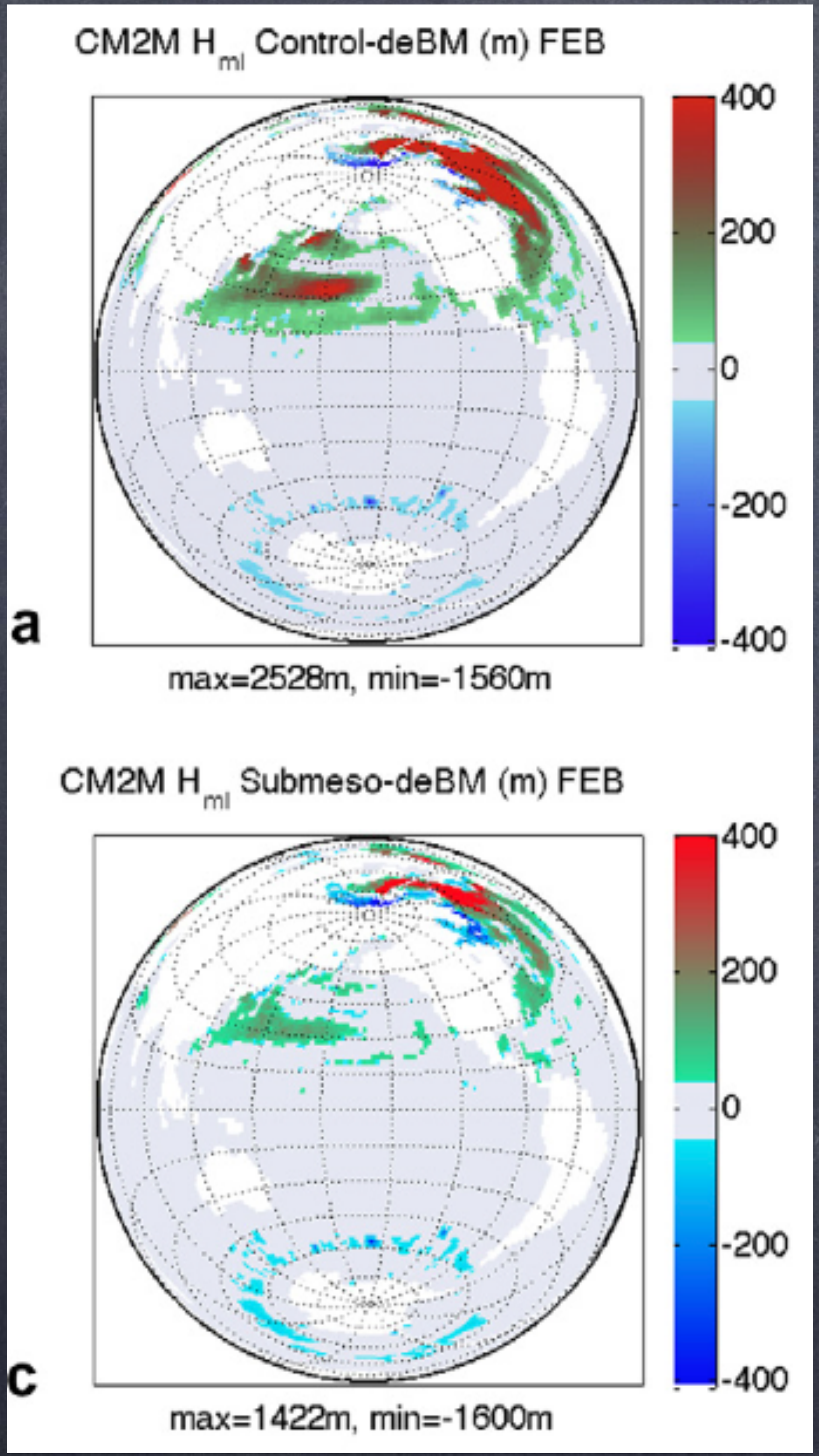


February Mixed layer depth Bias w/o MLE

February MLD Bias With MLE Parameterization

O(0.1 W/m$^2$) change to global mean net fluxes,
Regional: 5 to 50 W/m$^2$

Deep Mixed Layer Bias reduced

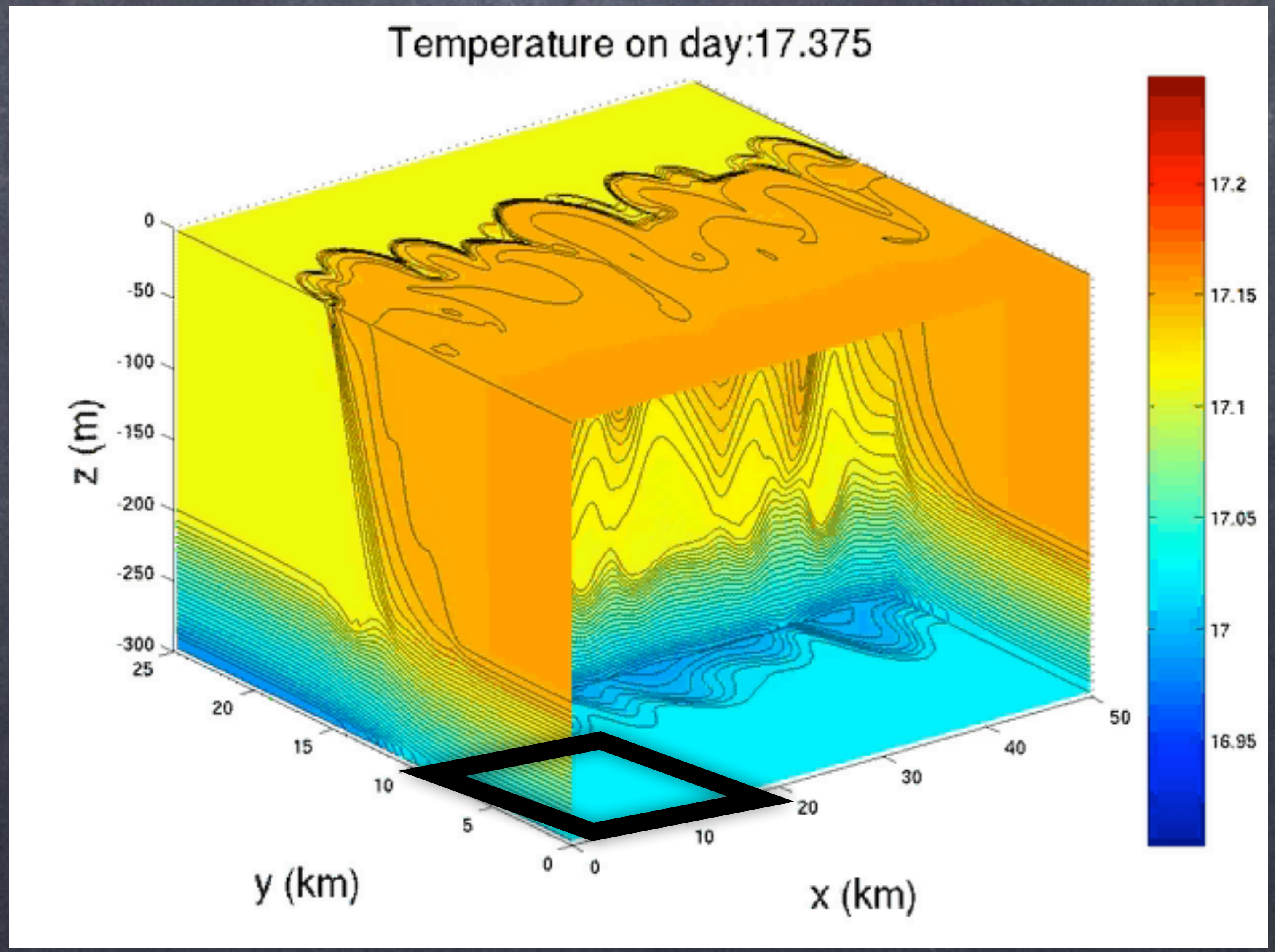


BFK, G. Danabasoglu, R. Ferrari, S. M. Griffies, R. W. Hallberg, M. M. Holland, M. E. Maltrud, S. Peacock, and B. L. Samuels. Parameterization of mixed layer eddies. III: Implementation and impact in global ocean climate simulations. Ocean Modelling, 39:61-78, 2011.

# MLEs on Mixing Layer Depth in Eddy-Resolving Southern Ocean Model

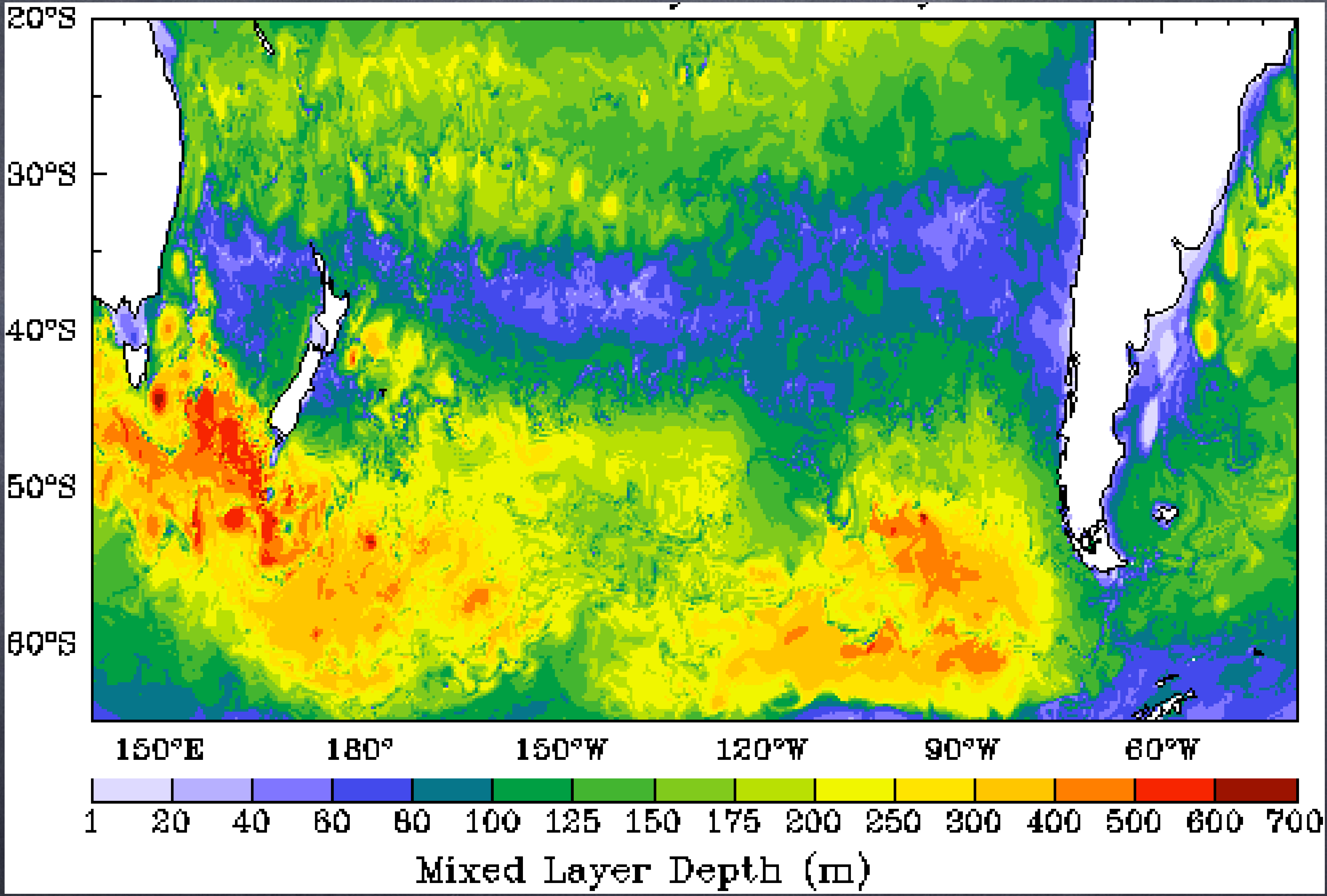


BFK, G. Danabasoglu, R. Ferrari, S. M. Griffies, R. W. Hallberg, M. M. Holland, M. E. Maltrud, S. Peacock, and B. L. Samuels. Parameterization of mixed layer eddies. III: Implementation and impact in global ocean climate simulations. Ocean Modelling, 39:61-78, 2011.

# MLEs on Mixing Layer Depth in Eddy-Resolving Southern Ocean Model

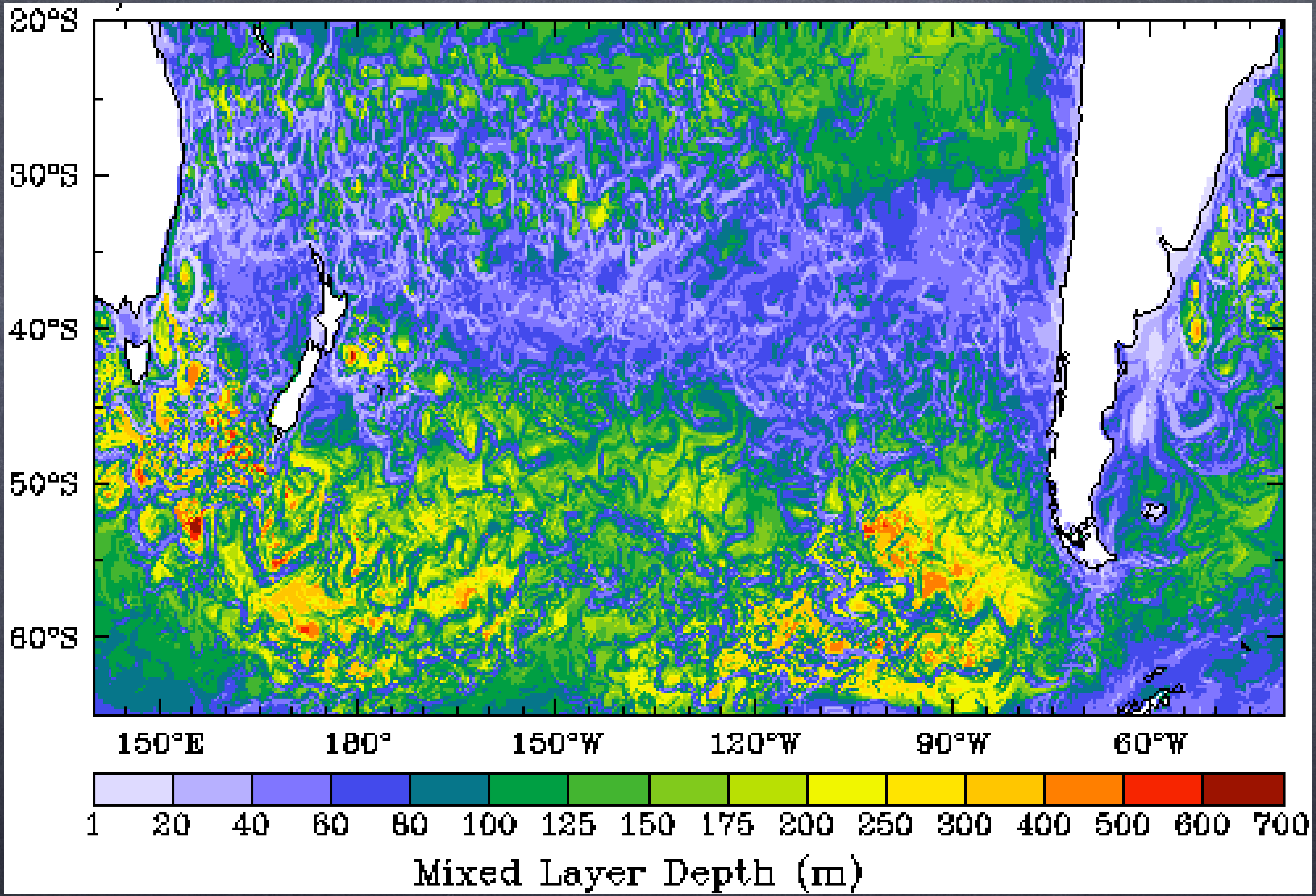


BFK, G. Danabasoglu, R. Ferrari, S. M. Griffies, R. W. Hallberg, M. M. Holland, M. E. Maltrud, S. Peacock, and B. L. Samuels. Parameterization of mixed layer eddies. III: Implementation and impact in global ocean climate simulations. Ocean Modelling, 39:61-78, 2011.

# SI are roughly 10x smaller than MLI

## MLI Scale (km)

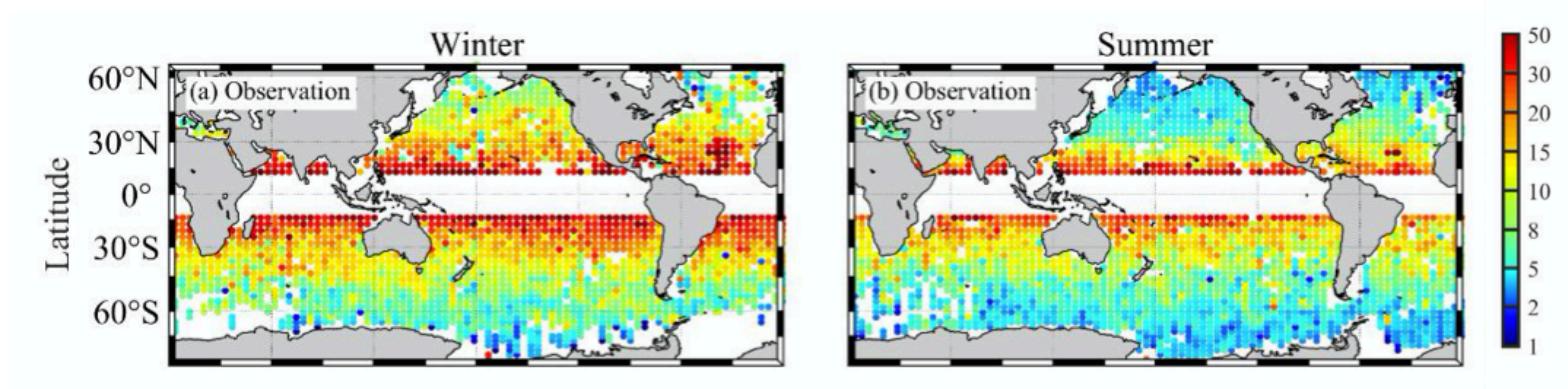


## SI Scale (km)

February

August

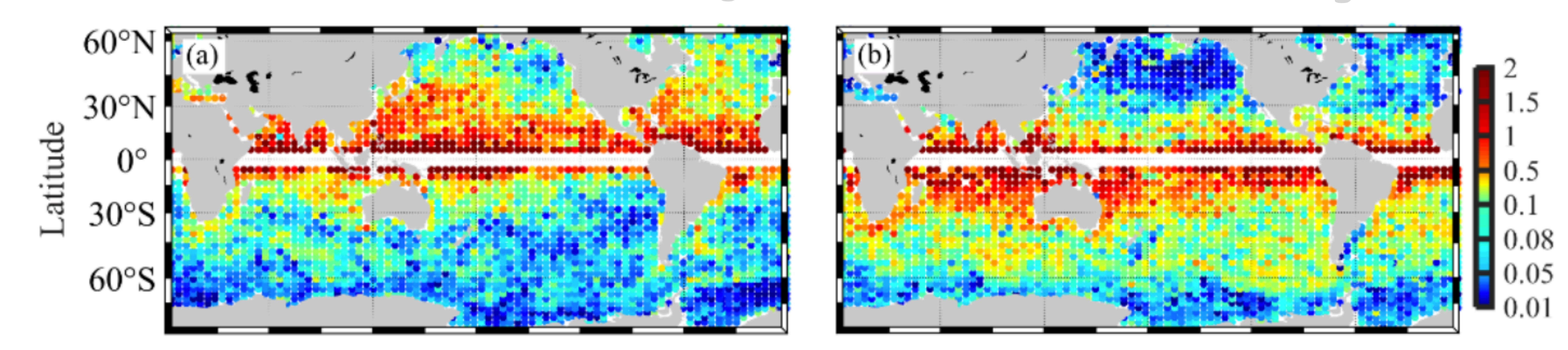


J. Dong, BFK, H. Zhang, and C. Dong. The scale of submesoscale baroclinic instability globally. JPO, 50(9):2649-2667, 2020. dx.doi.org/10.1175/JPO-D-20-0043.1
J. Dong, BFK, H. Zhang, and C. Dong. The Scale and Activity of Symmetric Instability Estimated from a Global Submesoscale-Permitting Ocean Model. JPO, 2021. dx.doi.org/10.1175/JPO-D-20-0159.1

# Sensitivity of Climate to Submeso: AMOC & Cryosphere Impacts

May Stabilize AMOC

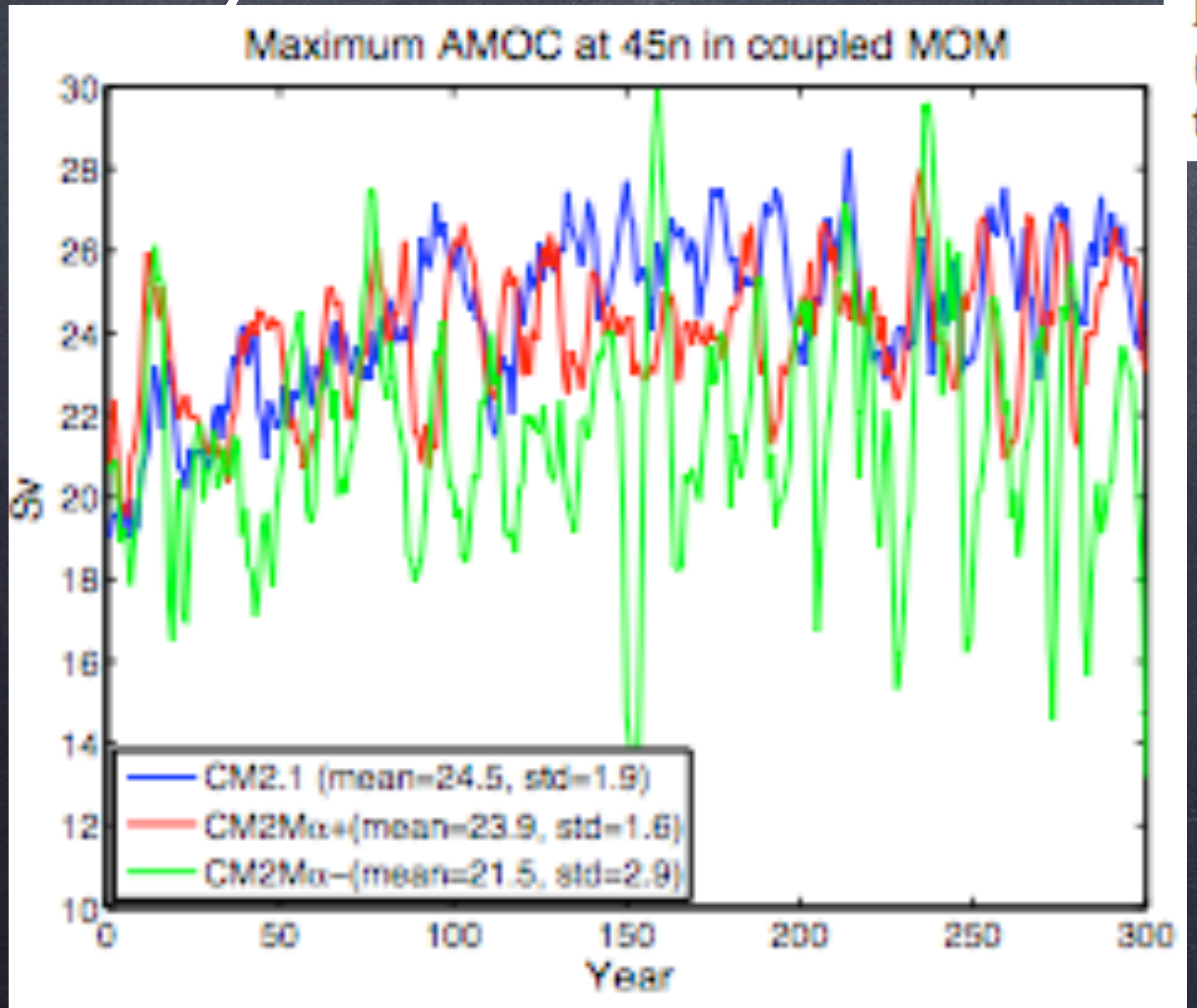


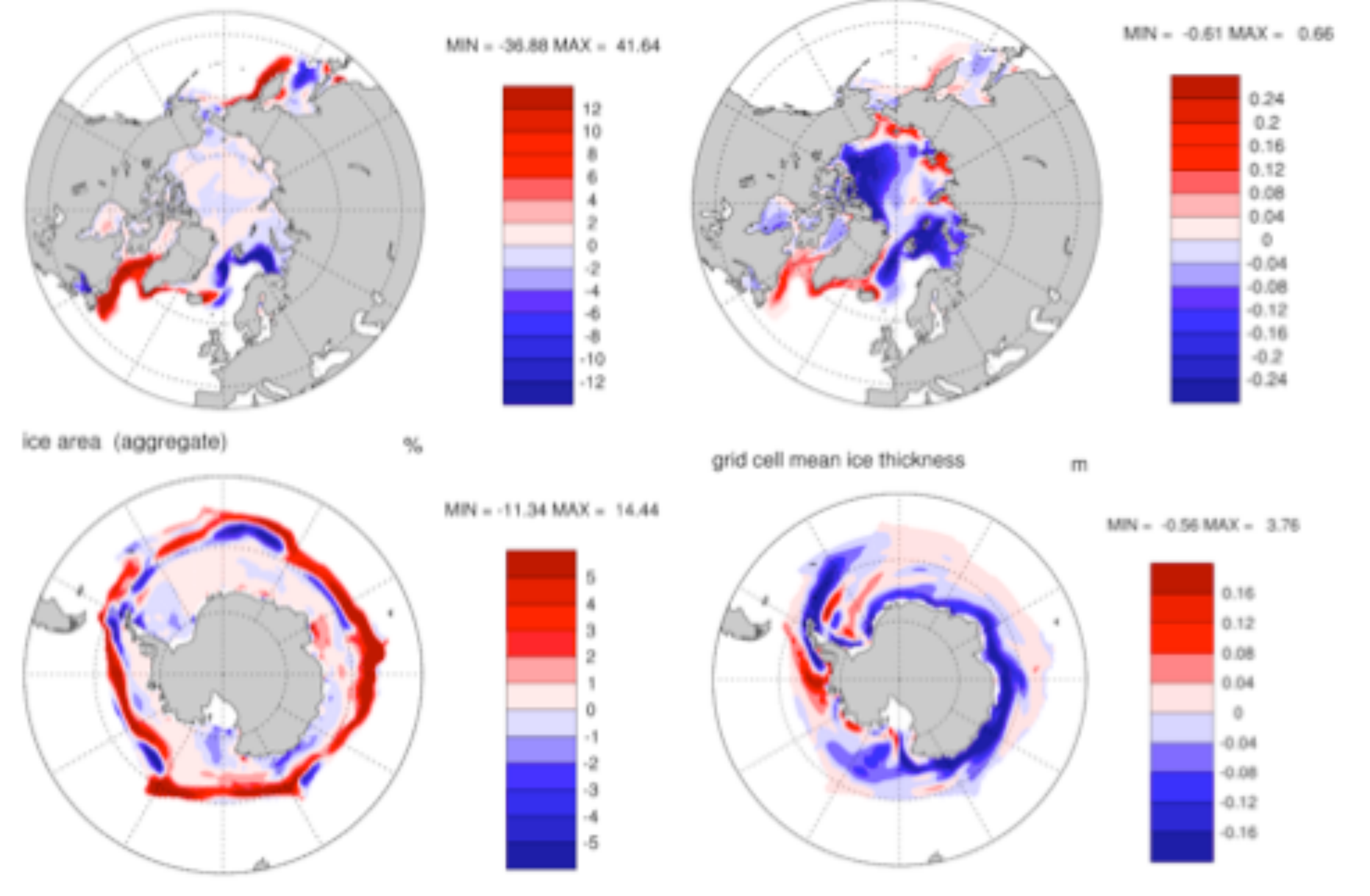


Figure 10: Wintertime sea ice sensitivity to introduction of MLE parameterization ($CCSM^+$ minus $CCSM^-$): January to March Northern Hemisphere a) ice area and b) thickness and July to September Southern Hemisphere c) ice area and d) thickness.

Affects sea ice

B. Fox-Kemper, G. Danabasoglu, R. Ferrari, S. M. Griffies, R. W. Hallberg, M. M. Holland, M. E. Maltrud, S. Peacock, and B. L. Samuels. Parameterization of mixed layer eddies. III: Implementation and impact in global ocean climate simulations. Ocean Modelling, 39:61-78, 2011.

NO RETUNING NEEDED!!!

These are impacts: bias change unknown

Physical Sensitivity of Ocean Climate to Submesoscale Mixed Layer Eddy Restratification:

Improves CFC uptake (water masses)

So, affects ocean heat & carbon uptake, too!

With MLE Parameterization

Bias w/o MLE

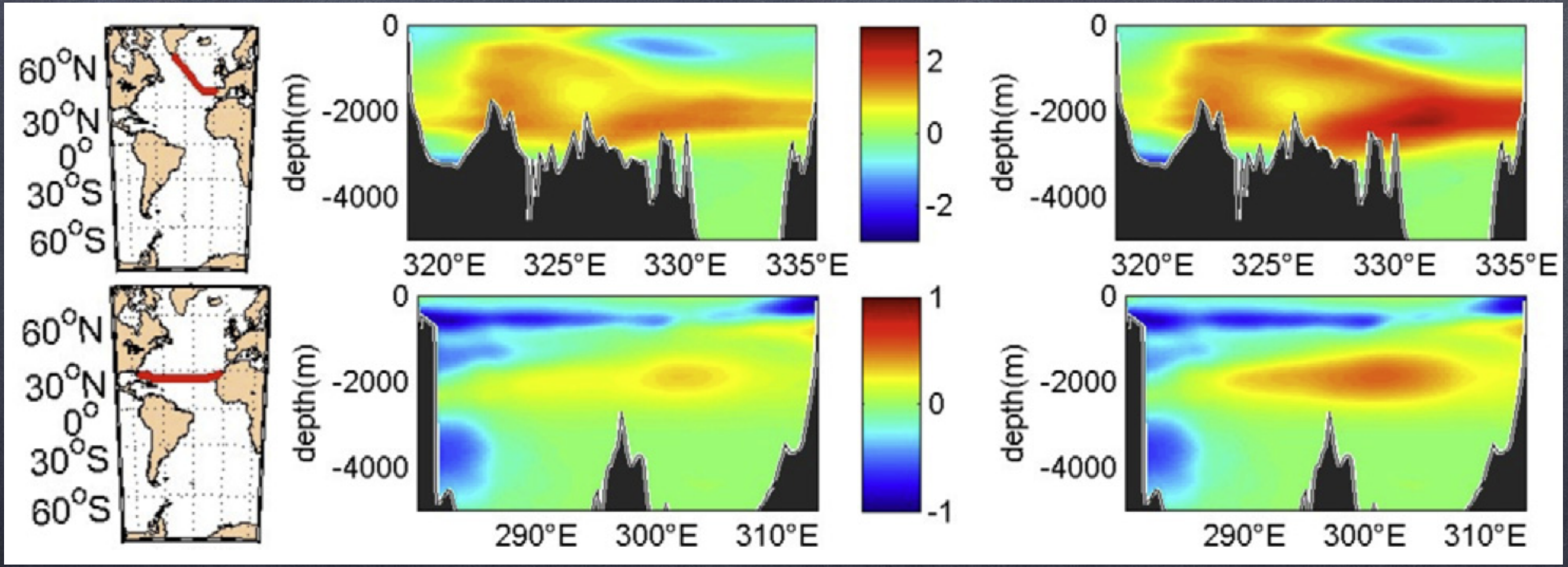


BFK, G. Danabasoglu, R. Ferrari, S. M. Griffies, R. W. Hallberg, M. M. Holland, M. E. Maltrud, S. Peacock, and B. L. Samuels. Parameterization of mixed layer eddies. III: Implementation and impact in global ocean climate simulations. *Ocean Modelling*, 39:61-78, 2011.

# Waves, Langmuir, and Climate

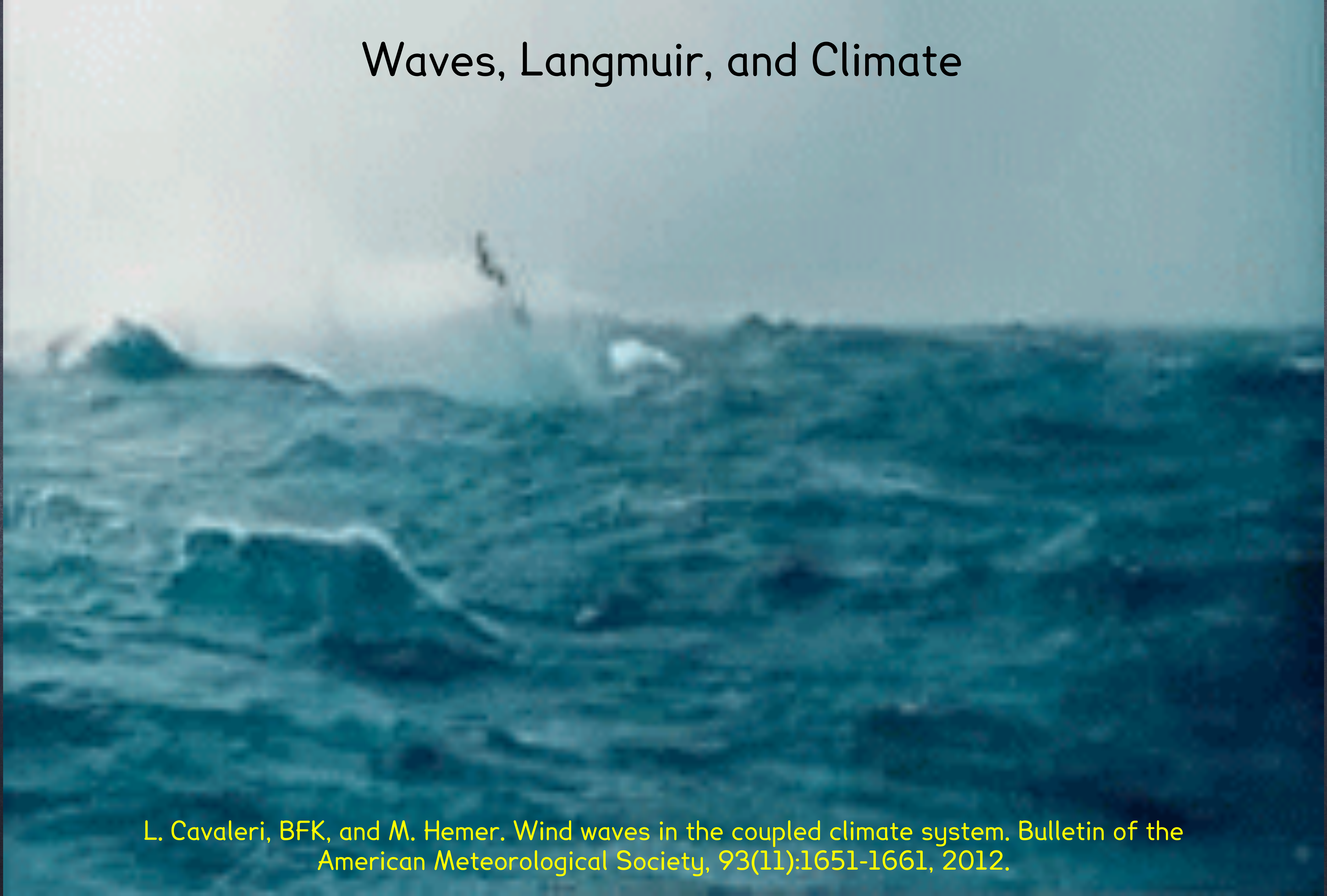

L. Cavaleri, BFK, and M. Hemer. Wind waves in the coupled climate system. Bulletin of the American Meteorological Society, 93(11):1651-1661, 2012.

# Waves, Langmuir, and Climate

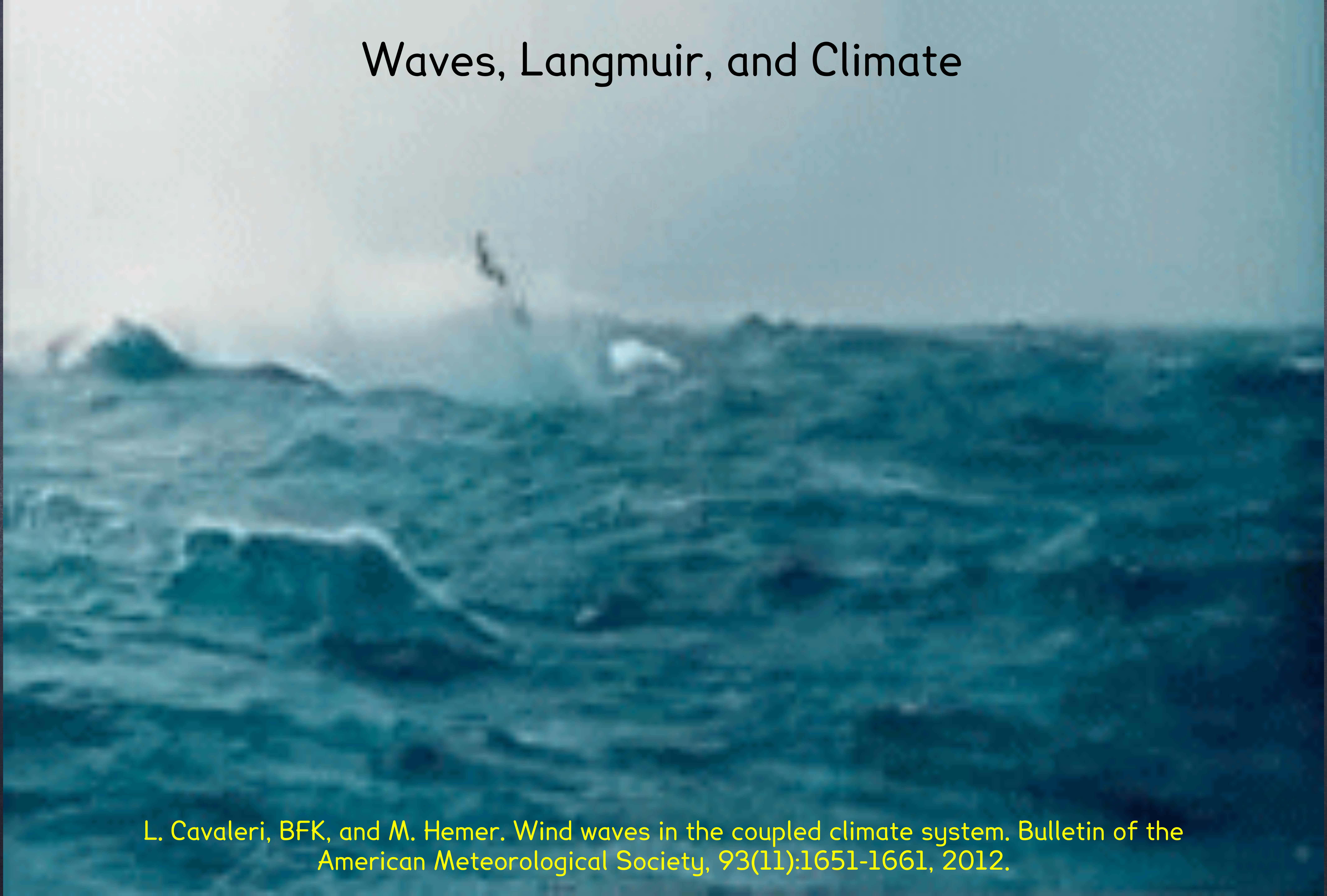

L. Cavaleri, BFK, and M. Hemer. Wind waves in the coupled climate system. Bulletin of the American Meteorological Society, 93(11):1651-1661, 2012.

# The Character of Langmuir Turbulence

- Near-surface
- Langmuir Cells & Langmuir Turb.
- $Ro \gg 1$
- $Ri < 1$
- 1-100m (H=L)
- 10s to 1hr
- $w \sim u = O(10 cm/s)$
- Nonhydrostatic
- Stokes drift
- Eqtns: Wave-Averaged aka Craik-Leibovich

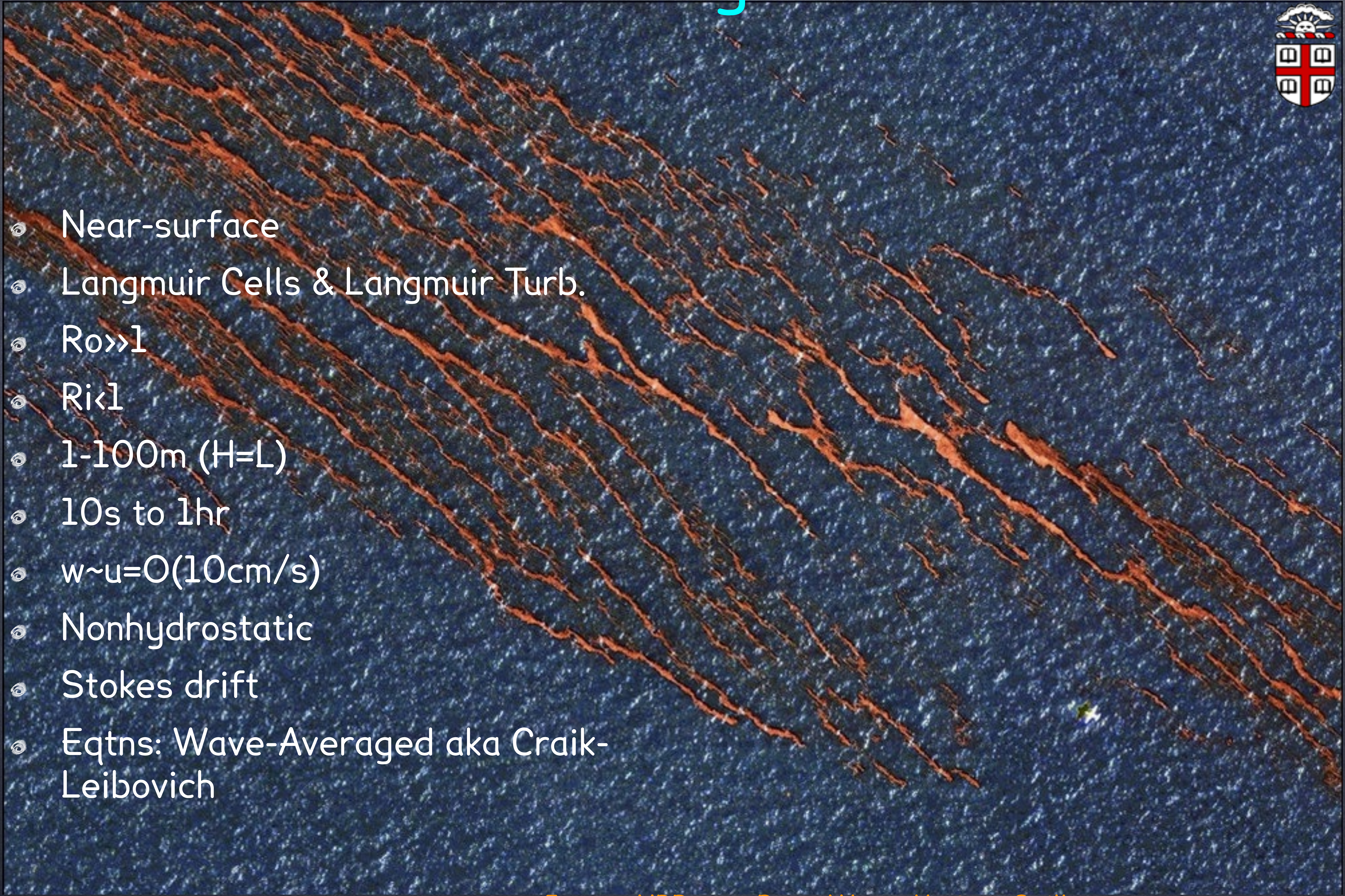

Image: NPR.org,  Deep Water Horizon Spill

# Diverse types of interaction: Stronger Langmuir (small) Turbulence, Fronts vary from place to place, one orientation is stronger?

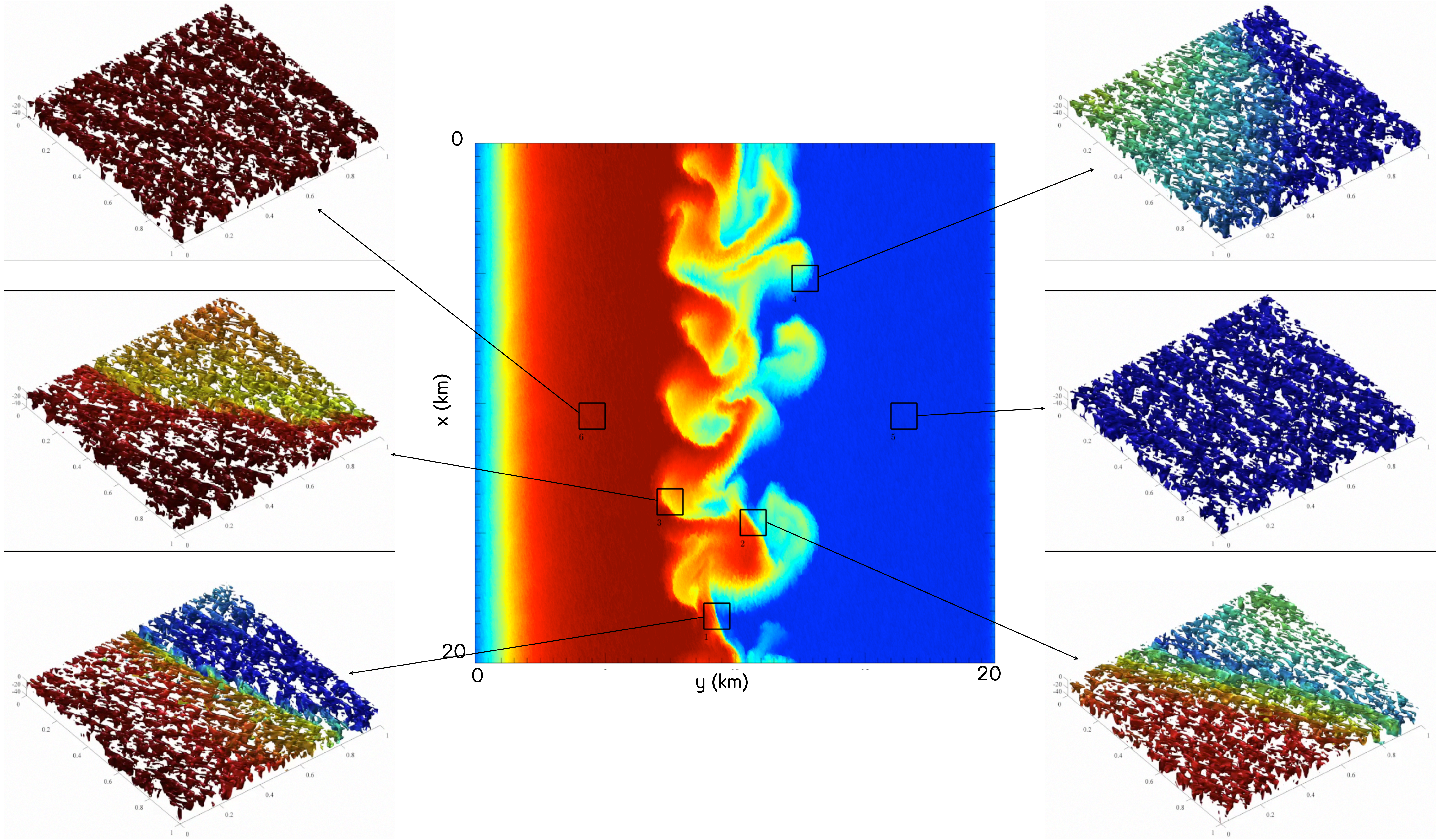


P. E. Hamlington, L. P. Van Roekel, BFK, K. Julien, and G. P. Chini. Langmuir-submesoscale interactions: Descriptive analysis of multiscale frontal spin-down simulations. Journal of Physical Oceanography, 44(9):2249-2272, September 2014.

# Diverse types of interaction: Stronger Langmuir (small) Turbulence, Fronts vary from place to place, one orientation is stronger?

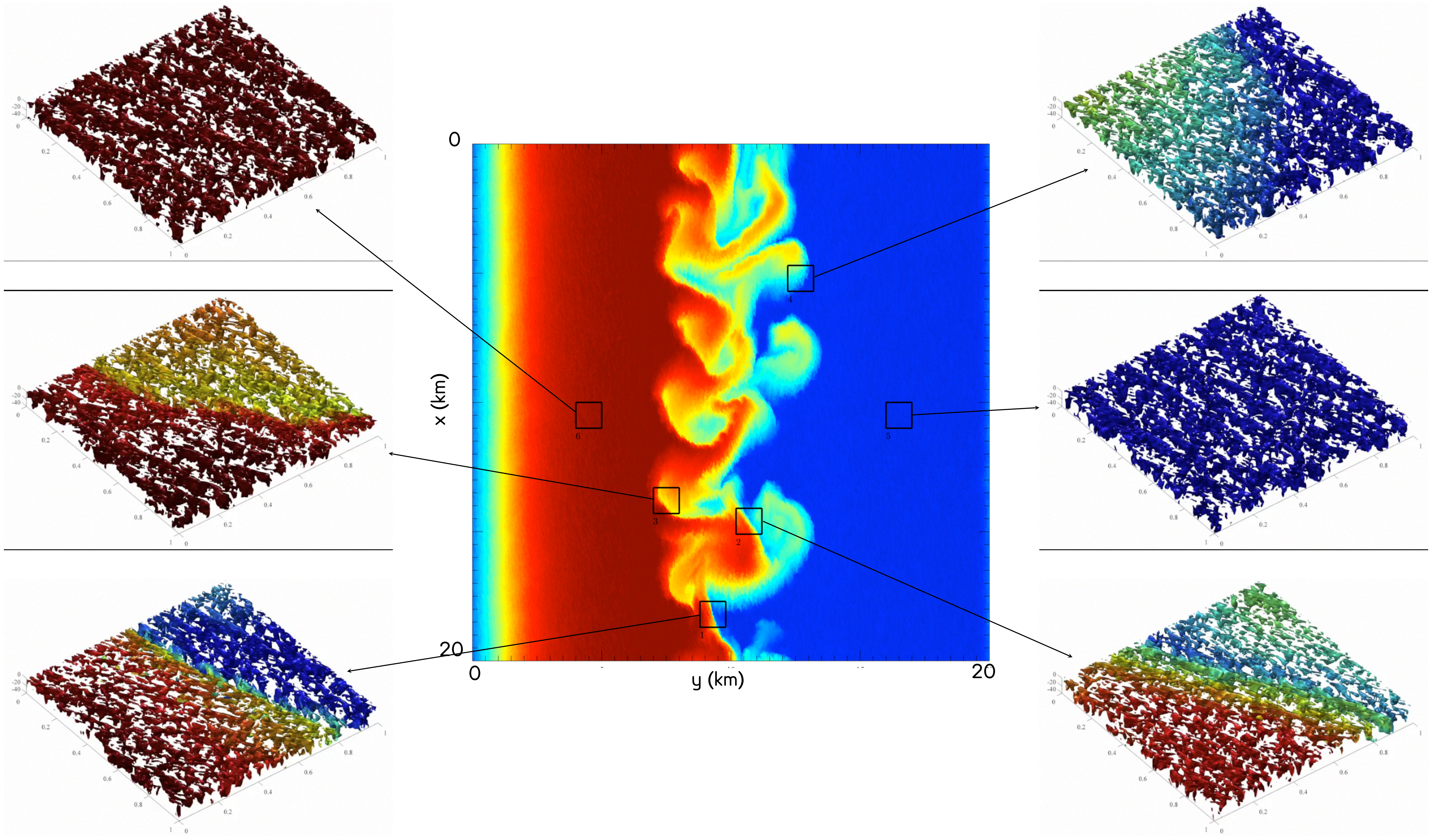


P. E. Hamlington, L. P. Van Roekel, BFK, K. Julien, and G. P. Chini. Langmuir-submesoscale interactions: Descriptive analysis of multiscale frontal spin-down simulations. Journal of Physical Oceanography, 44(9):2249-2272, September 2014.

A photo of Langmuir windrows impinging a front in Narragansett Bay, Rhode Island (courtesy P. Cornillon)

# What Pays the Bills:

## Parameterizing Turbulence to Improve Climate and Weather Models

- These turbulent phenomena aren't only pretty—they accumulate into sizable effects onto global properties, especially boundary layer depth.
- The boundary layer in turn filters the exchange of energy, carbon, momentum, etc., between the changing atmosphere and the ocean reservoir.
- Langmuir Turbulence is an excellent recent example, which energizes the boundary layer turbulence, so entrainment and mixing are faster.

Q. Li, B. G. Reichl, BFK, A. J. Adcroft, S. Belcher, G. Danabasoglu, A. Grant, S. M. Griffies, R. W. Hallberg, T. Hara, R. Harcourt, T. Kukulka, W. G. Large, J. C. McWilliams, B. Pearson, P. Sullivan, L. V. Roekel, P. Wang, and Z. Zheng. Comparing ocean boundary vertical mixing schemes including Langmuir turbulence. Journal of Advances in Modeling Earth Systems (JAMES), 11(11):3545-3592, 2019.

# 3 Effects Dominate open ocean "Wave-Averaged Equations": (Craik, Leibovich, McWilliams et al. 1997)

All rely only on Stokes drift of waves

1: Stokes Advection: parcels, tracers, momentum move with Lagrangian, not Eulerian flow

2: Stokes Coriolis: water parcels experience Coriolis force during this motion

3: Stokes Shear Force

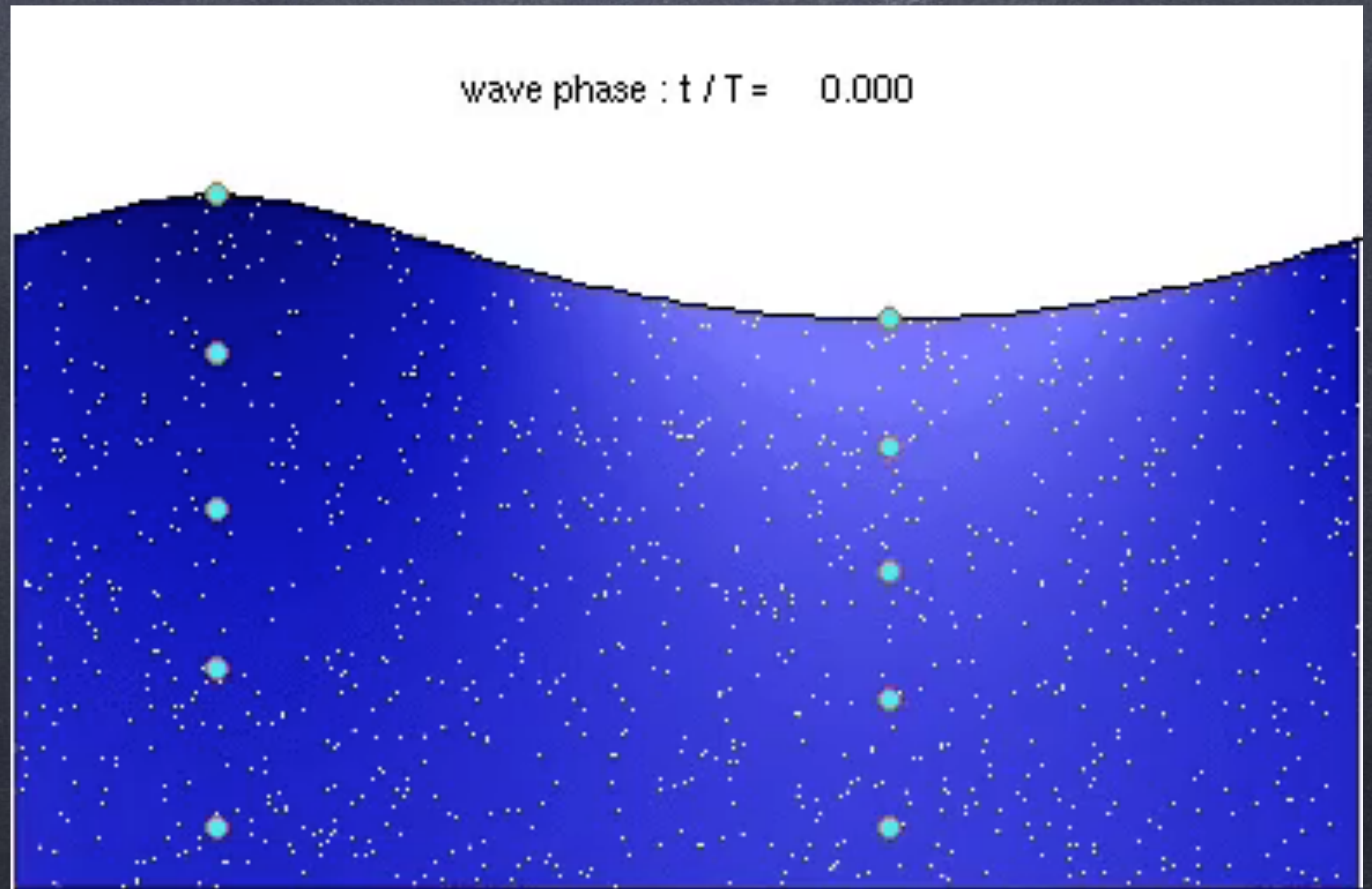


N. Suzuki and BFK. Understanding Stokes forces in the wave-averaged equations. Journal of Geophysical Research-Oceans, 121:1-18, 2016.

# 3 Effects Dominate open ocean "Wave-Averaged Equations": (Craik, Leibovich, McWilliams et al. 1997)

All rely only on Stokes drift of waves

1: Stokes Advection: parcels, tracers, momentum move with Lagrangian, not Eulerian flow

2: Stokes Coriolis: water parcels experience Coriolis force during this motion

3: Stokes Shear Force

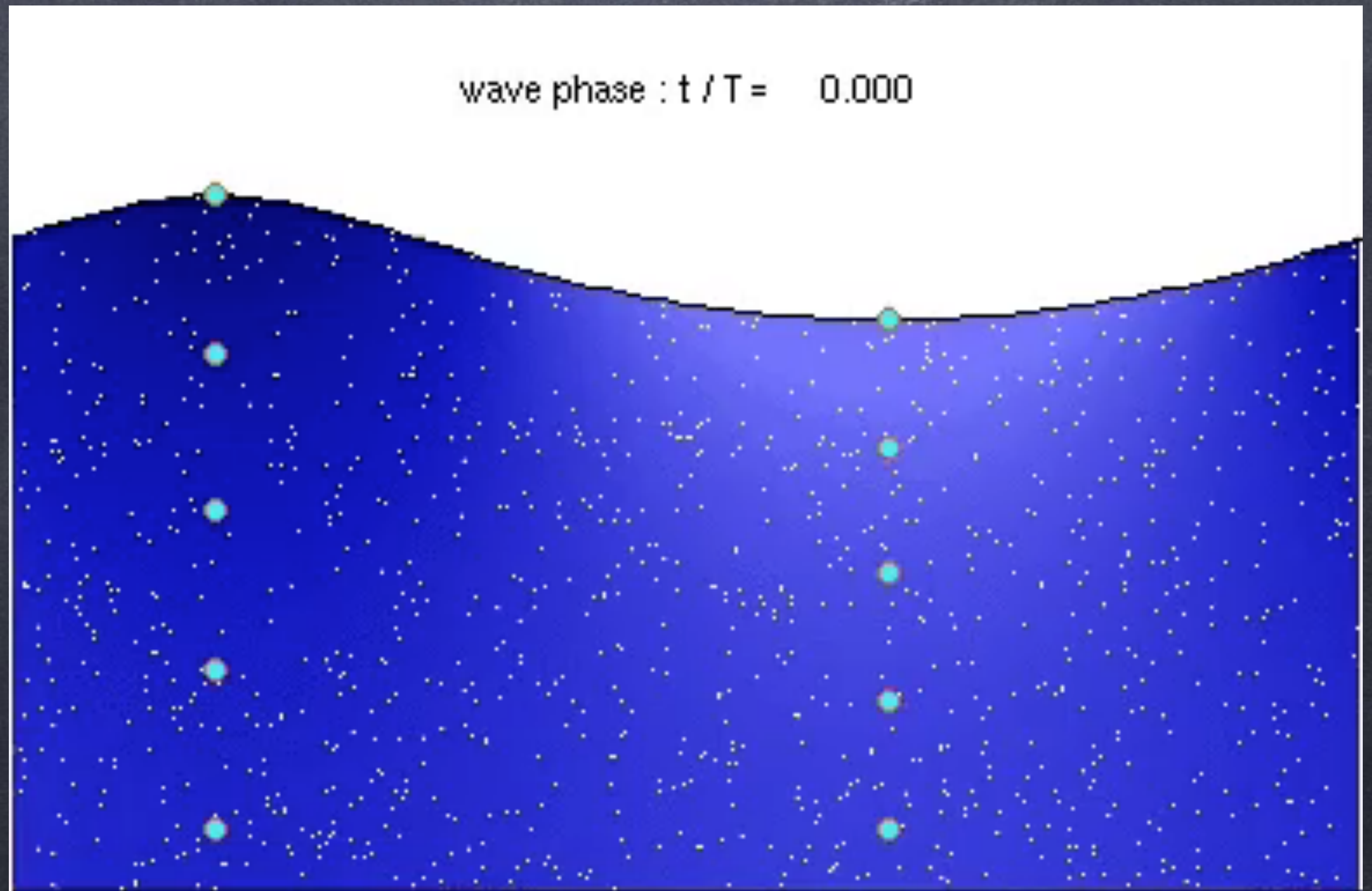


N. Suzuki and BFK. Understanding Stokes forces in the wave-averaged equations. Journal of Geophysical Research-Oceans, 121:1-18, 2016.

image:
Thorpe, 04

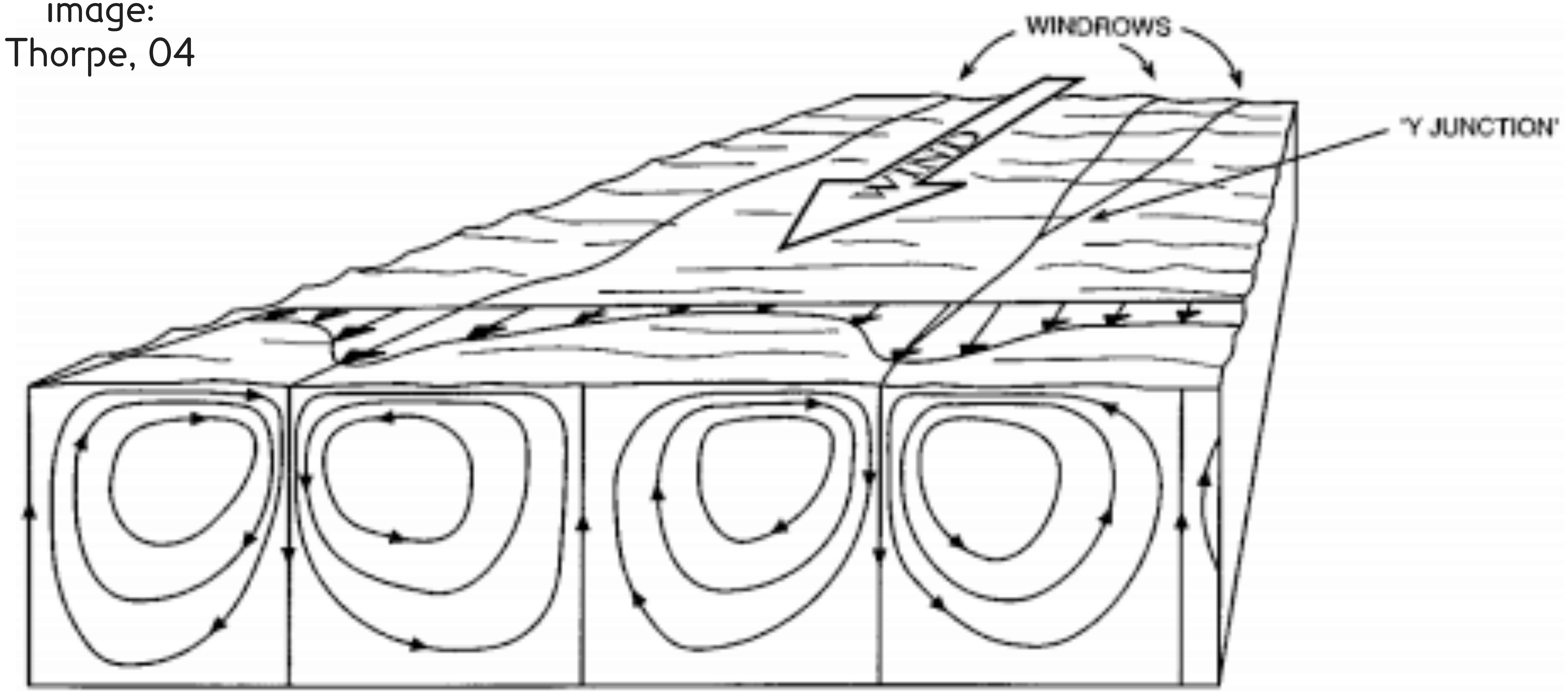


**Figure 1** Sketch showing the pattern of mean flow in idealized Langmuir circulation. The windrows may be 2 m to 300 m apart, and the cell form is roughly square (as shown). In practice the flow is turbulent, especially near the water surface, and the windrows (Figure 2) amalgamate and meander in space and time. Bands of bubbles or buoyant algae may form within the downward-going (or downwelling) flow (see Figure 3).

$$\frac{\alpha^2}{Ri}\left[w_{,t} + v_j^L w_{,j} + \frac{M_{Ro}}{RoRi} w w_{,z}\right] = -\pi_{,z} + b - \varepsilon v_j^L v^s_{j,z} + \frac{\alpha^2}{ReRi} w_{,jj}$$

N. Suzuki and BFK. Understanding Stokes forces in the wave-averaged equations. Journal of Geophysical Research-Oceans, 121:1-18, 2016.

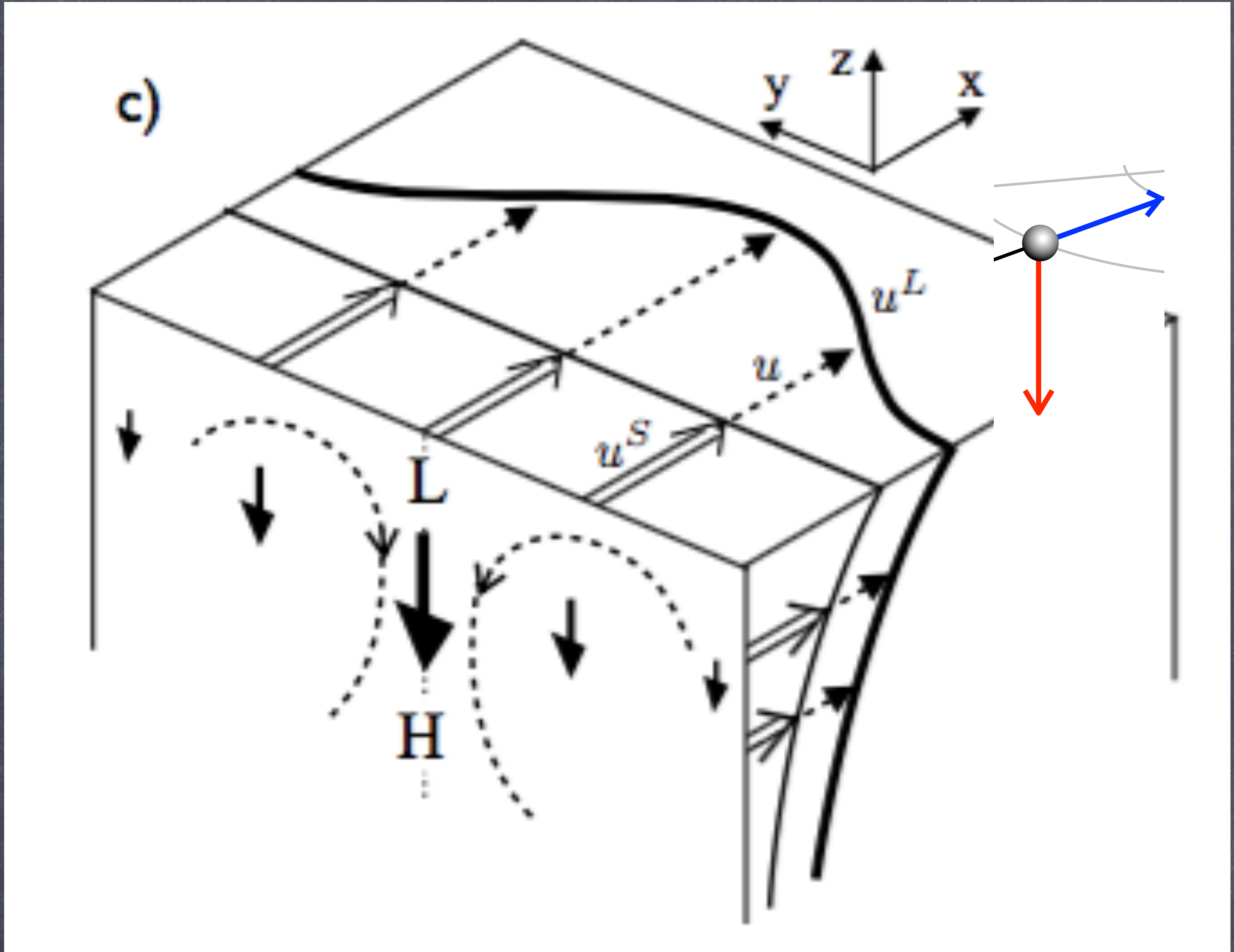


$$\frac{\alpha^2}{Ri}\left[w_{,t}+v_j^L w_{,j}+\frac{M_{Ro}}{RoRi}ww_{,z}\right]=-\pi_{,z}+b-\varepsilon v_j^L v_{j,z}^s+\frac{\alpha^2}{ReRi}w_{,jj}$$

N. Suzuki and BFK. Understanding Stokes forces in the wave-averaged equations. Journal of Geophysical Research-Oceans, 121:1-18, 2016.

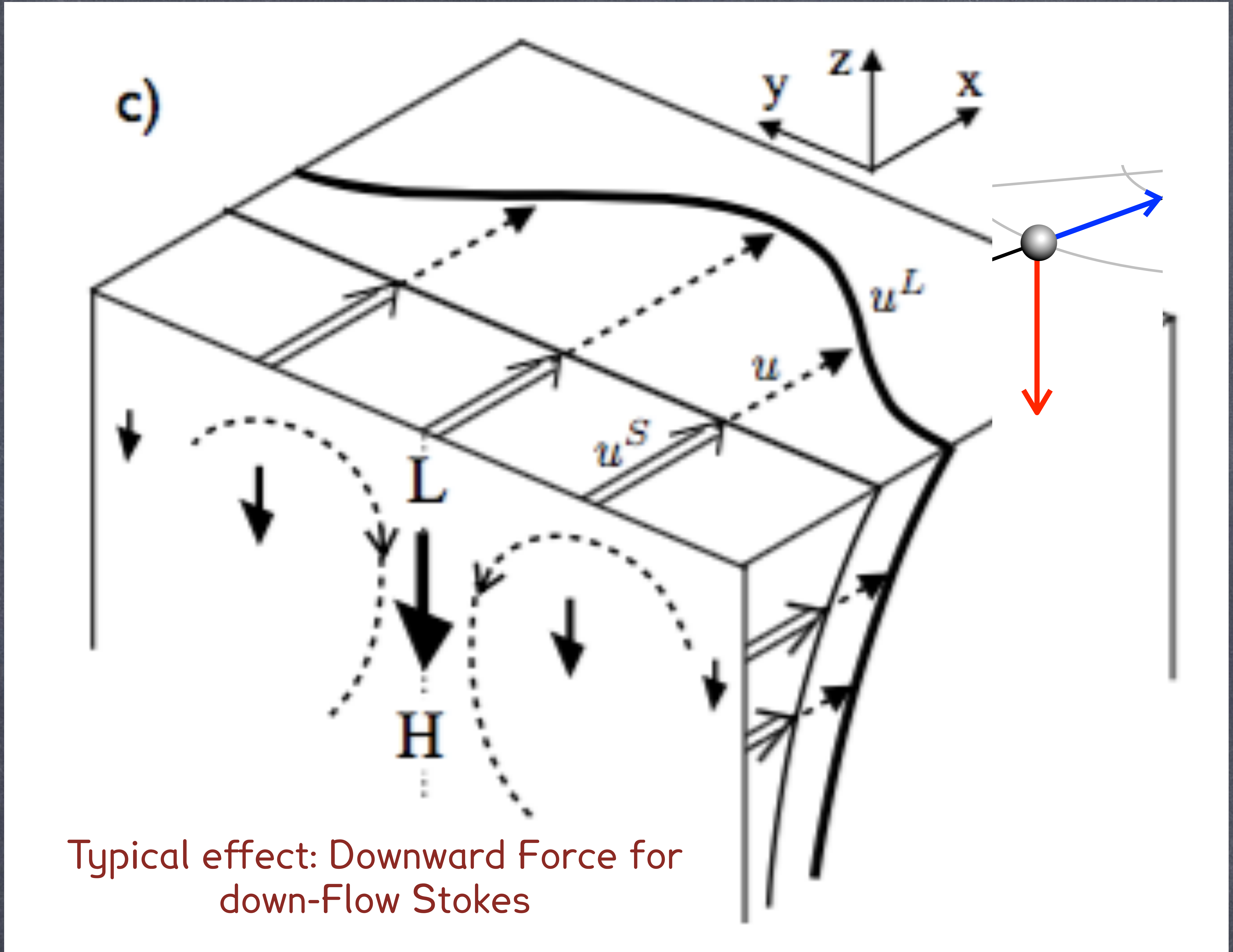

Typical effect: Downward Force for down-Flow Stokes

$$\frac{\alpha^2}{Ri}\left[w_{,t}+v_j^L w_{,j}+\frac{M_{Ro}}{RoRi}ww_{,z}\right]=-\pi_{,z}+b-\varepsilon v_j^L v^s_{j,z}+\frac{\alpha^2}{ReRi}w_{,jj}$$

N. Suzuki and BFK. Understanding Stokes forces in the wave-averaged equations. Journal of Geophysical Research-Oceans, 121:1-18, 2016.

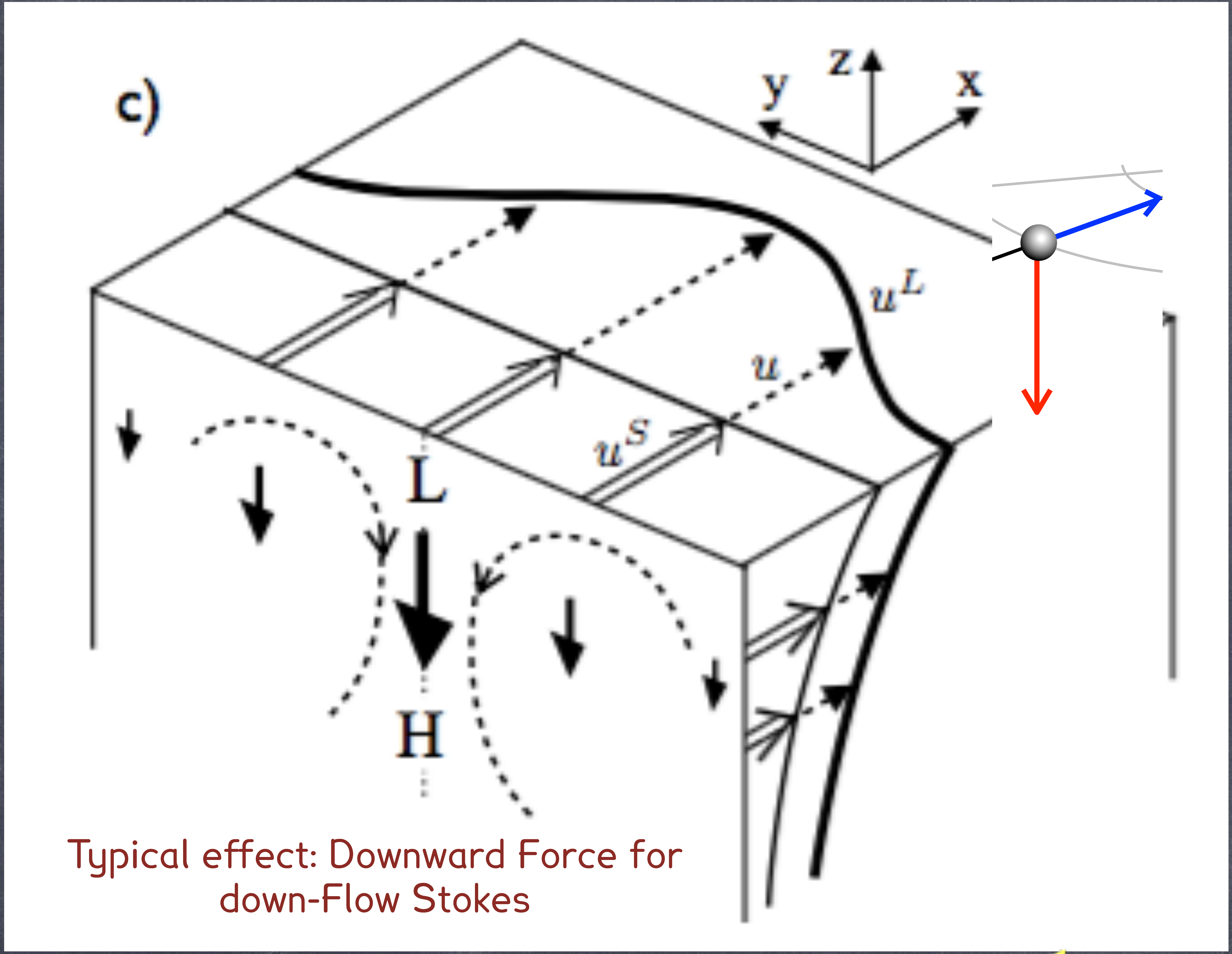


Typical effect: Downward Force for down-Flow Stokes

"wavy hydrostatic" if $\epsilon \gg 1$

$$\frac{\alpha^2}{Ri}\left[w_{,t} + v_j^L w_{,j} + \frac{M_{Ro}}{RoRi} w w_{,z}\right] = \boxed{-\pi_{,z} + b - \varepsilon v_j^L v^s_{j,z}} + \frac{\alpha^2}{ReRi} w_{,jj}$$

N. Suzuki and BFK. Understanding Stokes forces in the wave-averaged equations. Journal of Geophysical Research-Oceans, 121:1-18, 2016.

# Langmuir Mixing in Climate: Boundary Layer Depth Improved (RMS error tabulated)

| | | Summer | | | Winter | | |
|---|---|---|---|---|---|---|---|
| | Case | Global | South of 30°S | 30°S-30°N | Global | South of 30°S | 30°S-30°N |
| Control | CTRL | $10.28 \pm 0.29$ | $16.00 \pm 0.48$ | $6.57 \pm 0.23$ | $50.24 \pm 1.42$ | $52.52 \pm 0.54$ | $15.89 \pm 0.33$ |
| Old Scheme Mixing | VR12-MA | $9.31 \pm 0.28$ | $10.64 \pm 0.49$ | $9.60 \pm 0.33$ | $47.65 \pm 1.15$ | $48.47 \pm 0.49$ | $22.98 \pm 0.42$ |
| Bad Entrain. | VR12-EN | $11.65 \pm 0.29$ | $11.91 \pm 0.83$ | $12.79 \pm 0.39$ | $56.85 \pm 0.93$ | $61.30 \pm 1.21$ | $33.60 \pm 0.55$ |
| New Entrain. | LF17 | $8.48 \pm 0.24$ | $8.92 \pm 0.39$ | $9.15 \pm 0.30$ | $47.78 \pm 1.08$ | $49.98 \pm 0.77$ | $22.43 \pm 0.43$ |

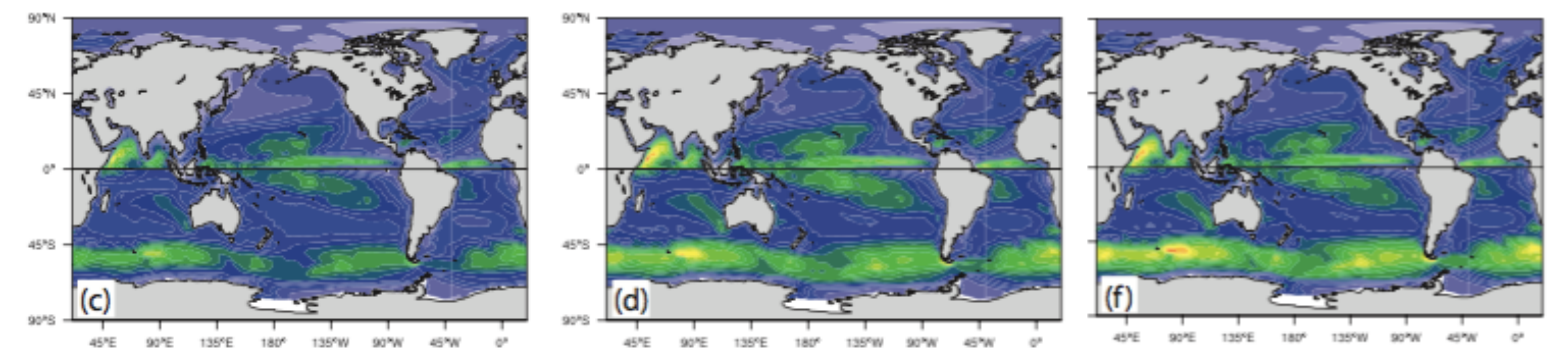


CTRL (No Lang.)    Mixing w/o Entrain Eval.    Mixing & Refined Entrainment


L. P. Van Roekel, BFK, P. P. Sullivan, P. E. Hamlington, and S. R. Haney. The form and orientation of Langmuir cells for misaligned winds and waves. Journal of Geophysical Research-Oceans, 117:C05001, 22pp, May 2012.

Q. Li, A. Webb, BFK, A. Craig, G. Danabasoglu, W. G. Large, and M. Vertenstein. Langmuir mixing effects on global climate: WAVEWATCH III in CESM. Ocean Modelling, 103:145-160, July 2016.

Q. Li & BFK. Assessing the effects of Langmuir turbulence on the entrainment buoyancy flux in the ocean surface boundary layer. Journal of Physical Oceanography, 47:2863-2886, December 2017.

Q. Li and B. Fox-Kemper. Anisotropy of Langmuir turbulence and the Langmuir-enhanced mixed layer entrainment. Physical Review Fluids, 5:013803, January 2020.

# Langmuir Mixing in Climate: Boundary Layer Depth Improved (RMS error tabulated)

| | | Summer | | | Winter | | |
|---|---|---|---|---|---|---|---|
| | Case | Global | South of 30°S | 30°S-30°N | Global | South of 30°S | 30°S-30°N |
| Control | CTRL | 10.28 ± 0.29 | 16.00 ± 0.48 | 6.57 ± 0.23 | 50.24 ± 1.42 | 52.52 ± 0.54 | 15.89 ± 0.33 |
| Old Scheme Mixing | VR12-MA | 9.31 ± 0.28 | 10.64 ± 0.49 | 9.60 ± 0.33 | 47.65 ± 1.15 | 48.47 ± 0.49 | 22.98 ± 0.42 |
| Bad Entrain. | VR12-EN | 11.65 ± 0.29 | 11.91 ± 0.83 | 12.79 ± 0.39 | 56.85 ± 0.93 | 61.30 ± 1.21 | 33.60 ± 0.55 |
| New Entrain. | LF17 | 8.48 ± 0.24 | 8.92 ± 0.39 | 9.15 ± 0.30 | 47.78 ± 1.08 | 49.98 ± 0.77 | 22.43 ± 0.43 |

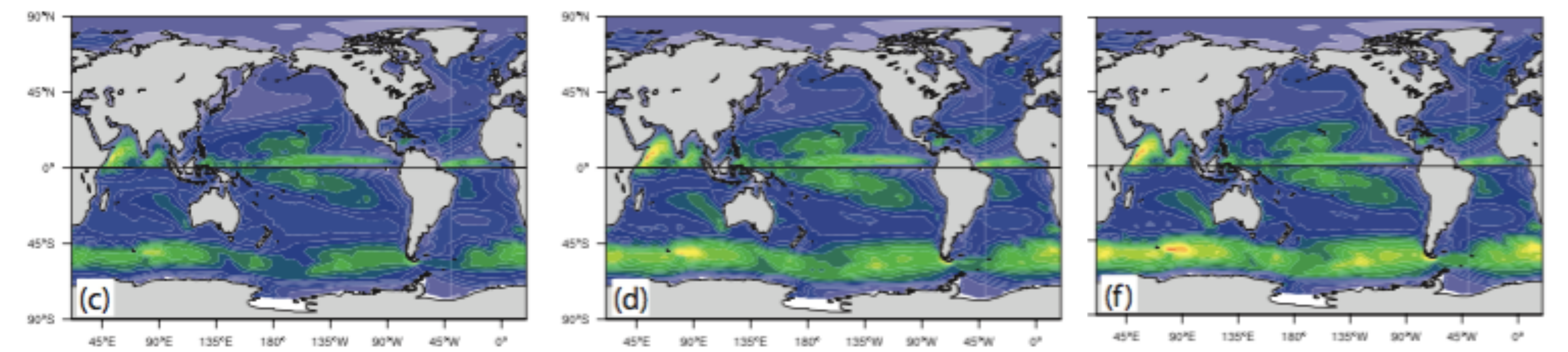


CTRL (No Lang.) | Mixing w/o Entrain Eval. | Mixing & Refined Entrainment


L. P. Van Roekel, BFK, P. P. Sullivan, P. E. Hamlington, and S. R. Haney. The form and orientation of Langmuir cells for misaligned winds and waves. Journal of Geophysical Research-Oceans, 117:C05001, 22pp, May 2012.

Q. Li, A. Webb, BFK, A. Craig, G. Danabasoglu, W. G. Large, and M. Vertenstein. Langmuir mixing effects on global climate: WAVEWATCH III in CESM. Ocean Modelling, 103:145-160, July 2016.

Q. Li & BFK. Assessing the effects of Langmuir turbulence on the entrainment buoyancy flux in the ocean surface boundary layer. Journal of Physical Oceanography, 47:2863-2886, December 2017.

Q. Li and B. Fox-Kemper. Anisotropy of Langmuir turbulence and the Langmuir-enhanced mixed layer entrainment. Physical Review Fluids, 5:013803, January 2020.

# Langmuir Mixing in Climate: Boundary Layer Depth Improved (RMS error tabulated)

| | Case | Summer Global | Summer South of 30°S | Summer 30°S-30°N | Winter Global | Winter South of 30°S | Winter 30°S-30°N |
|---|---|---|---|---|---|---|---|
| Control | CTRL | 10.28 ± 0.29 | 16.00 ± 0.48 | 6.57 ± 0.23 | 50.24 ± 1.42 | 52.52 ± 0.54 | 15.89 ± 0.33 |
| Old Scheme Mixing | VR12-MA | 9.31 ± 0.28 | 10.64 ± 0.49 | 9.60 ± 0.33 | 47.65 ± 1.15 | 48.47 ± 0.49 | 22.98 ± 0.42 |
| Bad Entrain. | VR12-EN | 11.65 ± 0.29 | 11.91 ± 0.83 | 12.79 ± 0.39 | 56.85 ± 0.93 | 61.30 ± 1.21 | 33.60 ± 0.55 |
| New Entrain. | LF17 | 8.48 ± 0.24 | 8.92 ± 0.39 | 9.15 ± 0.30 | 47.78 ± 1.08 | 49.98 ± 0.77 | 22.43 ± 0.43 |

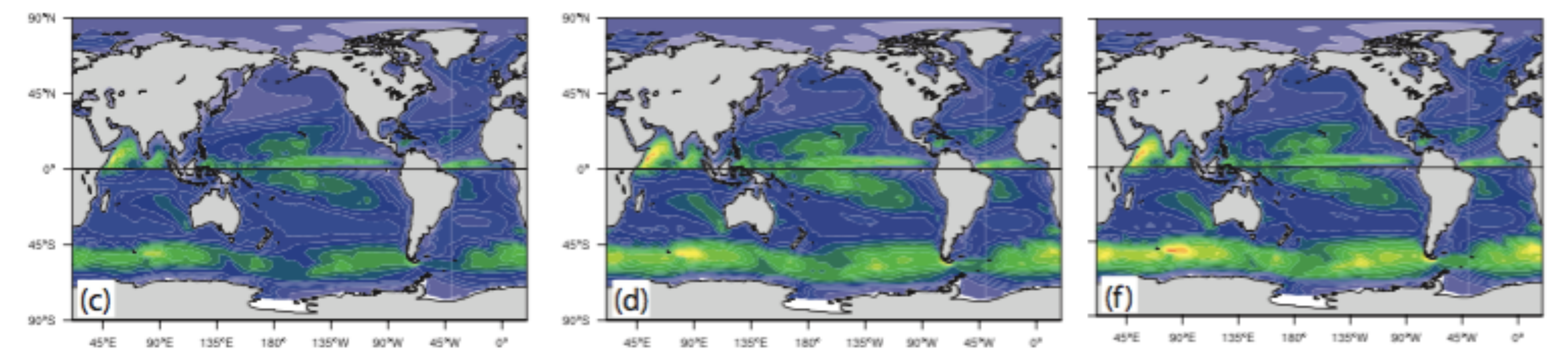


CTRL (No Lang.) | Mixing w/o Entrain Eval. | Mixing & Refined Entrainment


L. P. Van Roekel, BFK, P. P. Sullivan, P. E. Hamlington, and S. R. Haney. The form and orientation of Langmuir cells for misaligned winds and waves. Journal of Geophysical Research-Oceans, 117:C05001, 22pp, May 2012.

Q. Li, A. Webb, BFK, A. Craig, G. Danabasoglu, W. G. Large, and M. Vertenstein. Langmuir mixing effects on global climate: WAVEWATCH III in CESM. Ocean Modelling, 103:145-160, July 2016.

Q. Li & BFK. Assessing the effects of Langmuir turbulence on the entrainment buoyancy flux in the ocean surface boundary layer. Journal of Physical Oceanography, 47:2863-2886, December 2017.

Q. Li and B. Fox-Kemper. Anisotropy of Langmuir turbulence and the Langmuir-enhanced mixed layer entrainment. Physical Review Fluids, 5:013803, January 2020.

# GMST: Surface Energy Budget=Ocean Heat Content Budget

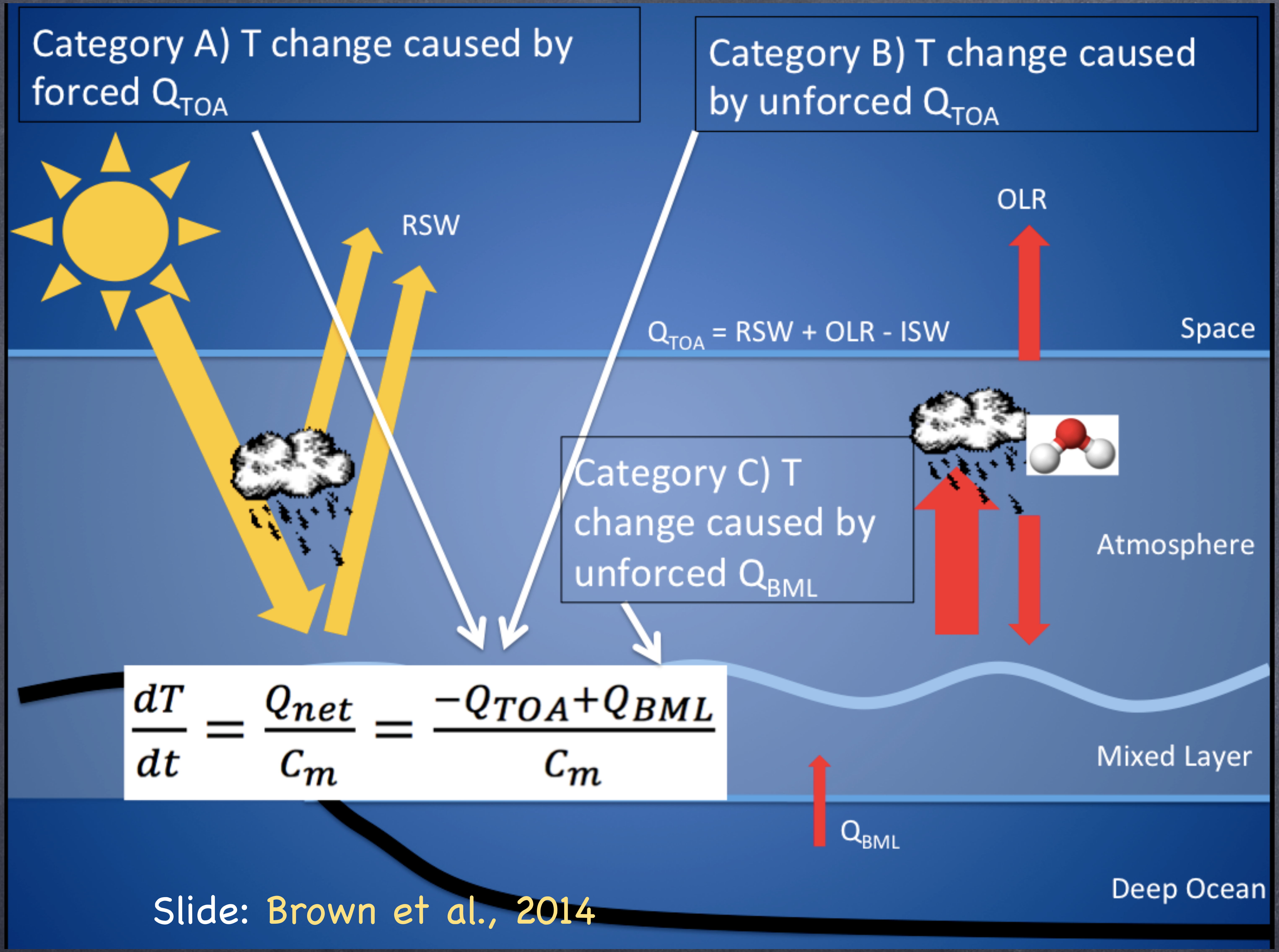


$$\frac{dT}{dt} = \frac{Q_{net}}{C_m} = \frac{-Q_{TOA}+Q_{BML}}{C_m}$$

So, we've improved the mixed layer, shouldn't it improve the climate projections somehow?

- 3.4m of ocean has heat capacity of whole atmosphere
- Ocean Mixed Layer is about 100m deep.

# Modeling of variability

A stochastic, predictable persistence model:
Frankignoul & Hasselmann (77)

Temp Change — Random Atmosphere — Restoring — Mixed Layer

$$\frac{dT}{dt} = \frac{f_1'}{h} - \lambda T$$

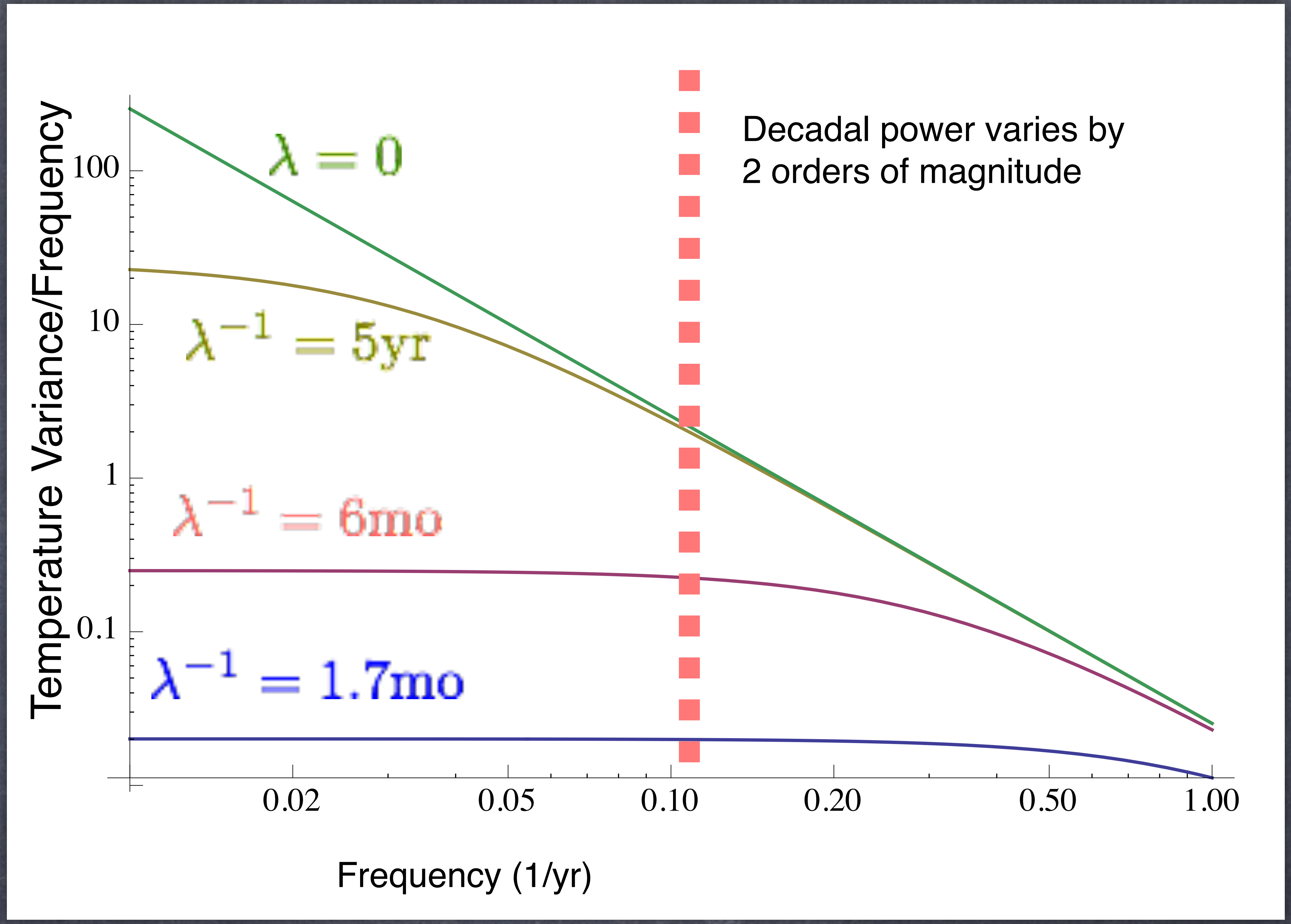


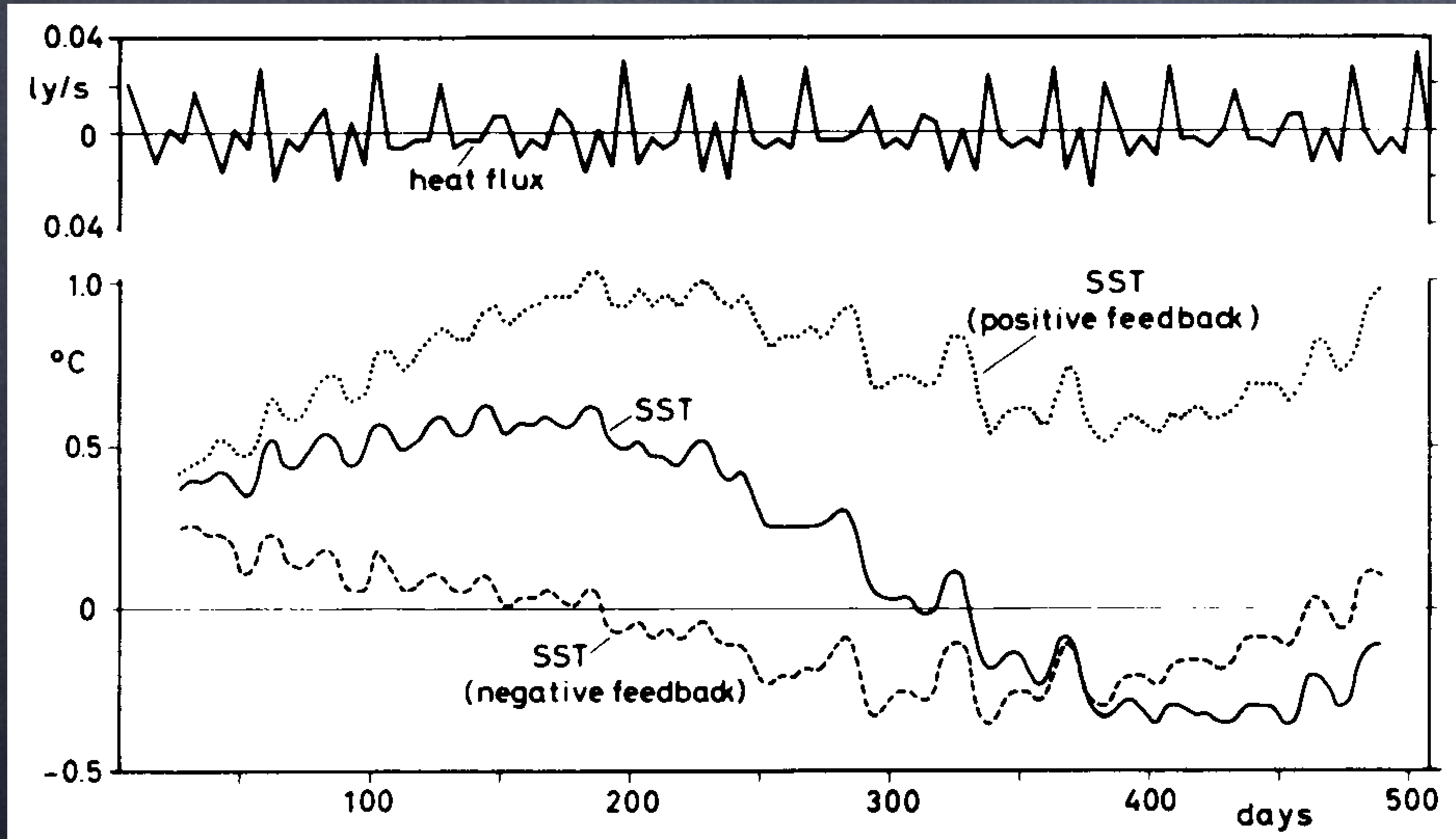


$$\lambda = \rho^a C_p^a (\rho^w C_p^w)^{-1} C_H (1 + B) \langle |U| \rangle h^{-1}$$

$$= (1.7 \text{ month})^{-1}$$

# World Ocean

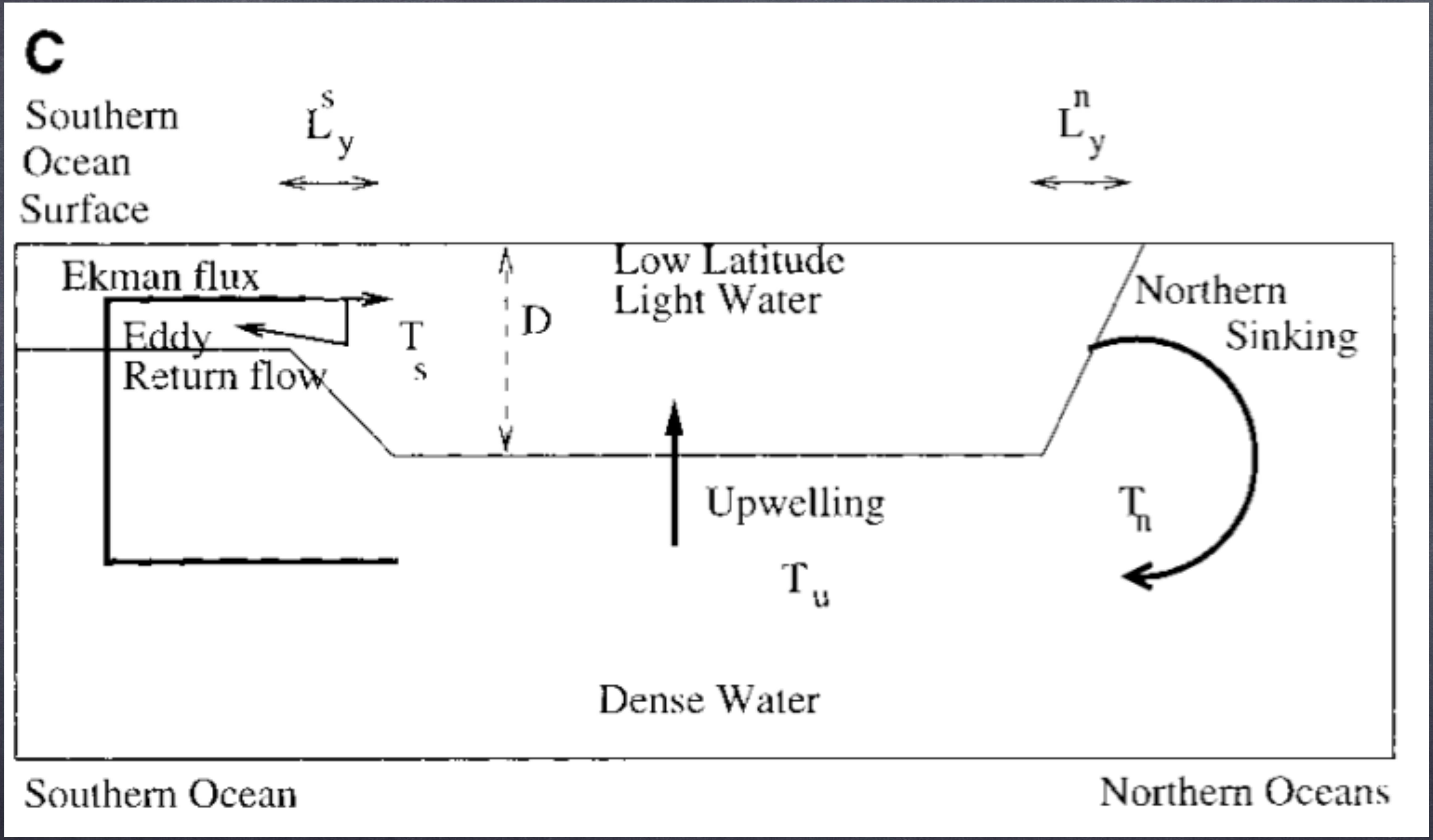


Gnanadesikan SCIENCE VOL 283 26 MARCH 1999

Even Simpler: 2-Layer Homogeneous Energy Balance Model (Gregory, 2000)

# Even Simpler: 2-Layer Homogeneous EBM (Gregory, 2000; Winton et al. 2010; Geoffroy et al. 2013)

G. Hall and BFK. Regional mixed layer depth as a climate diagnostic and emergent constraint. GRL, 2021. Submitted.

The 2-layer model parameters are estimated from 25 CMIP6 model timeseries–
None of the parameters are observable
9 further CMIP6 models are used as out-of-sample validation

$$C_S \frac{d\Delta T}{dt} = F - \lambda \Delta T - \varepsilon\gamma(\Delta T - \Delta T_D),$$
$$C_D \frac{d\Delta T_D}{dt} = \gamma(\Delta T - \Delta T_D);$$

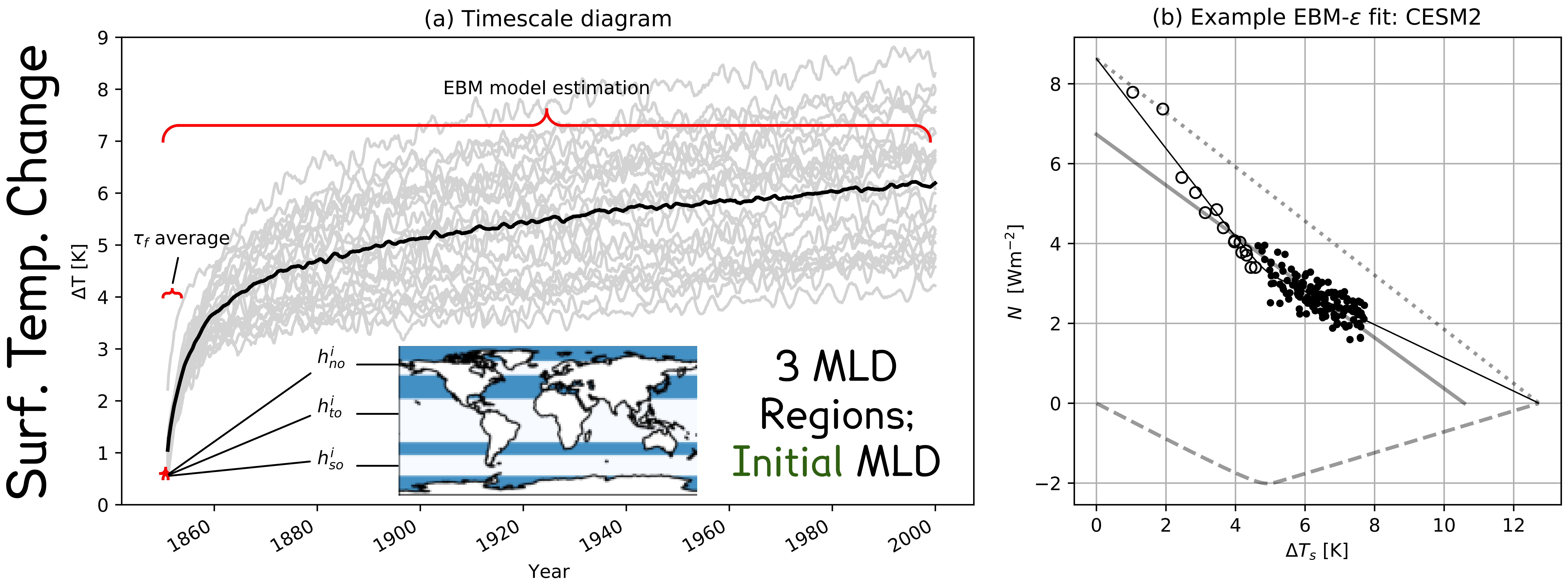

# We can use the mixed layer depth as An EMERGENT CONSTRAINT

That is, an observable that correlates or constrains the other properties useful for projections.

## CMIP6 GCMs give MLD & 2-Layer Model Properties

G. Hall and BFK. Regional mixed layer depth as a climate diagnostic and emergent constraint. GRL, 2021. Submitted.

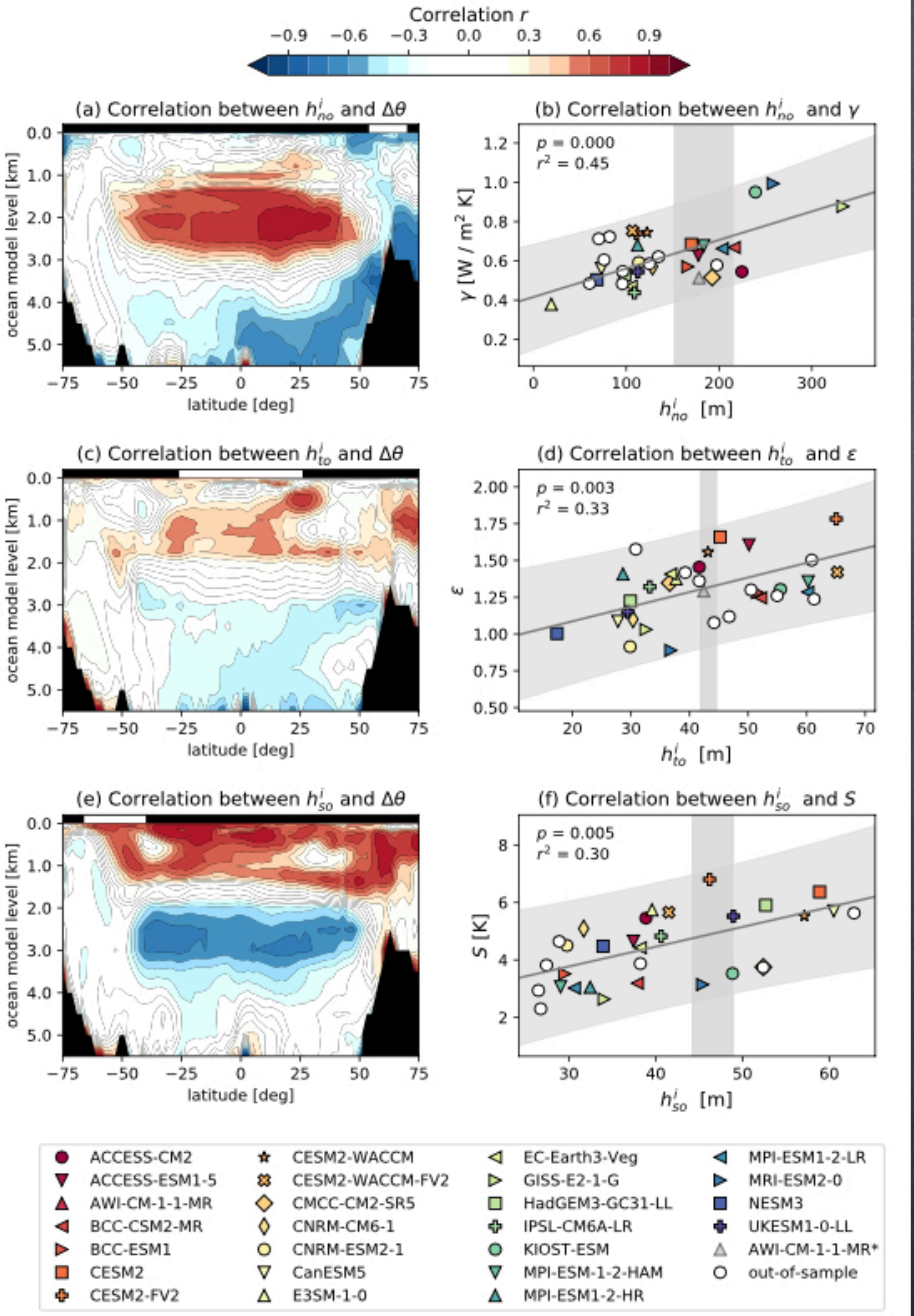


## None of the parameters are observable

$$C_S \frac{d\Delta T}{dt} = F - \lambda \Delta T - \varepsilon\gamma(\Delta T - \Delta T_D),$$

$$C_D \frac{d\Delta T_D}{dt} = \gamma(\Delta T - \Delta T_D);$$

## But MLD is, simplify into regions

- [55N, 75N] $h^i_{no}$
- [25S, 25N] $h^i_{to}$
- [65S, 45S] $h^i_{so}$

3 MLD Regions; Initial MLD

# Galen Hall: Physics Honors Thesis, May 2020

Regional mixed layer depth as a climate diagnostic and emergent constraint

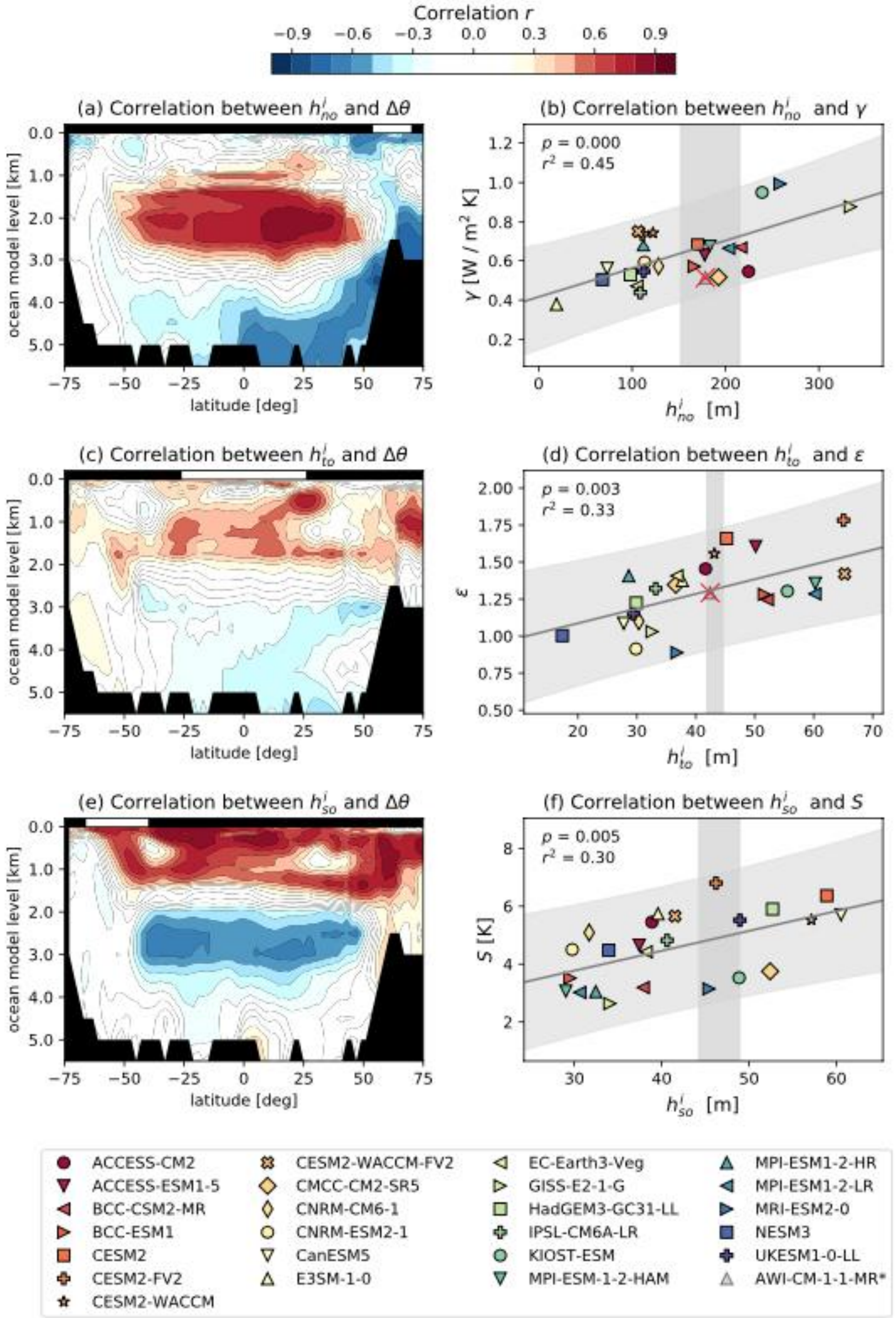


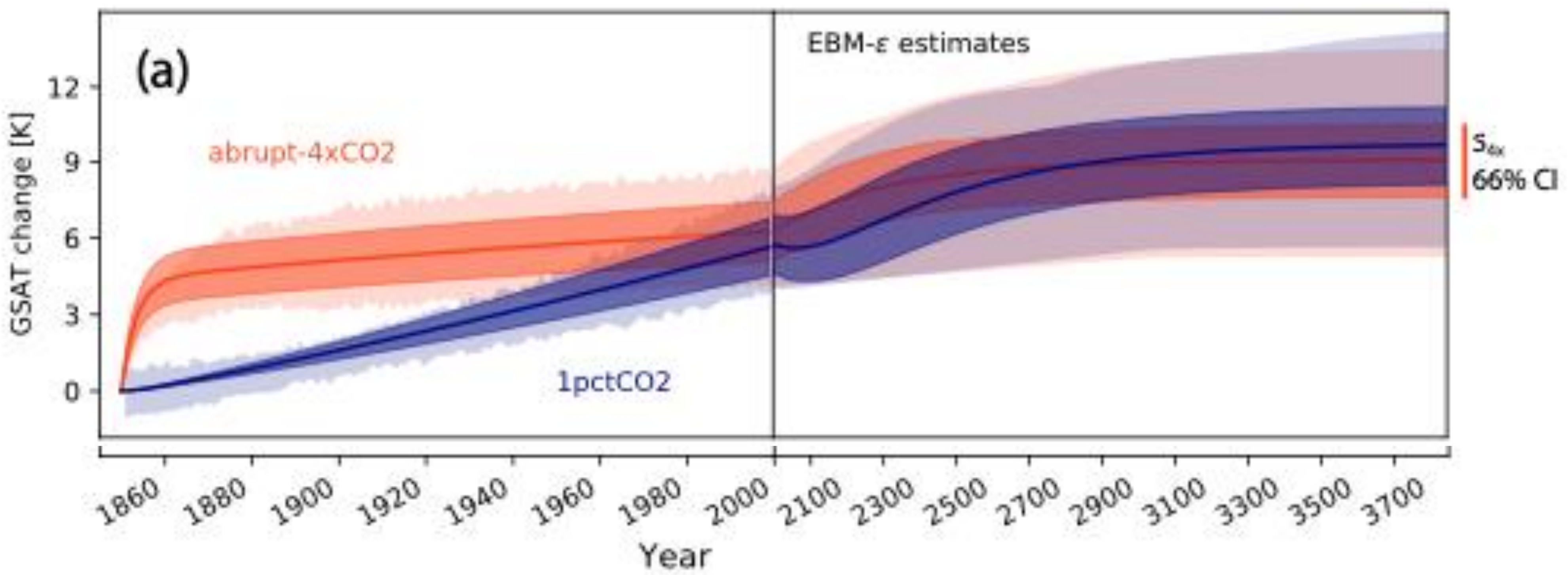


$$C_S \frac{d\Delta T}{dt} = F - \lambda \Delta T - \varepsilon\gamma(\Delta T - \Delta T_D),$$

$$C_D \frac{d\Delta T_D}{dt} = \gamma(\Delta T - \Delta T_D);$$

**Hall & Fox-Kemper, Submitted to *GRL*, 2021**

"Using these correlations and observations from the Argo float network, we revise the ensemble mean and narrow the 66% range of equilibrium climate sensitivity (ECS) for the particular CMIP6 model collection from 4.51 (3.13–5.71) °C, to 4.66 (3.88–5.43) °C, amounting to a 40% reduction in the span of the uncertainty range."

PANGEO

Emulate CMIP6 model oceans w

CMIP6 data via pangeo.io

Understand emulator parameter

Code at repository.library.brown.edu

# Galen Hall: Physics Honors Thesis, May 2020

Regional mixed layer depth as a climate diagnostic and emergent constraint

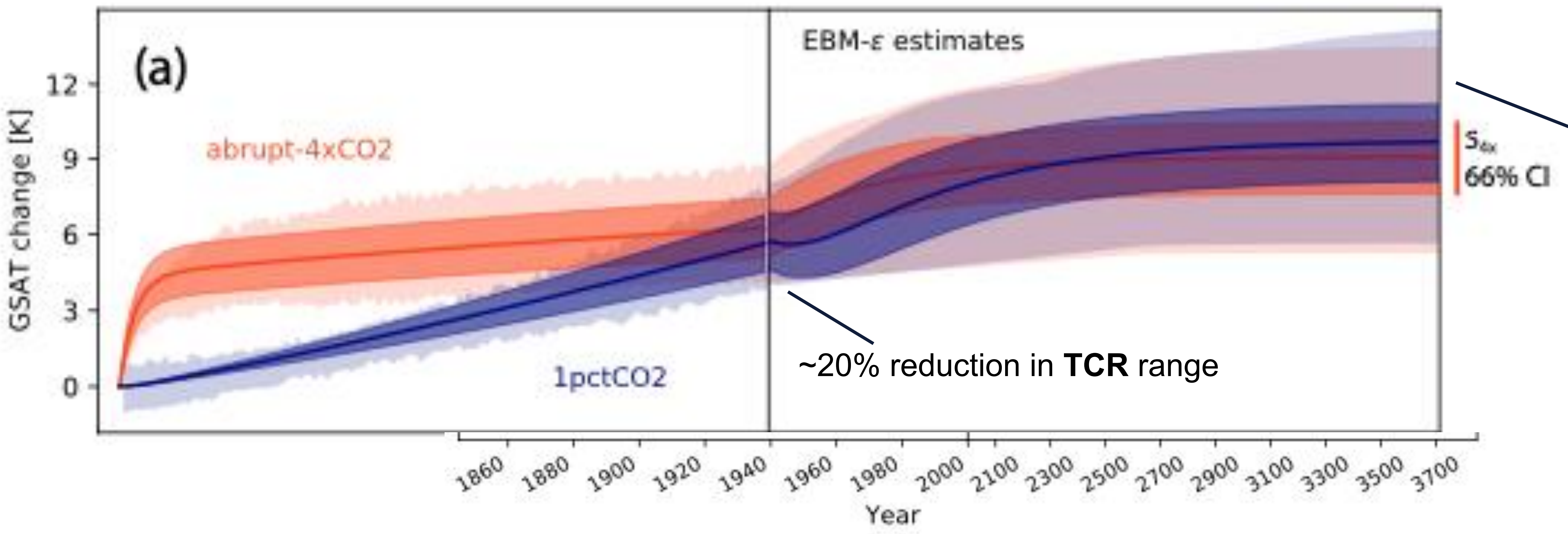


Approximately halving the uncertainty range for [transient climate response] has a net present value of about $10.3 trillion (year 2005 US$) if accomplished in time for emissions to be adjusted in 2020, falling to $9.7 trillion if accomplished by 2030.

-C. Hope, 2015, *Phil. Trans. A.*, https://doi.org/10.1098/rsta.2014.0429

PANGEO
CMIP6 data via pangeo.io
Code at repository.library.brown.edu

**Hall & Fox-Kemper, Submitted to *GRL*, 2021**

# For Today: Small-scales affect Climate

- Key Ocean Climate Questions
- Large Eddy Simulation Closures
    - Smagorinsky, Leith, QG Leith
- Effects on Global Kinetic Energy
- Submesoscale affects Mixed Layer
- Wave-Driven Turbulence affects Mixed Layer
- Regional Mixed Layer Depth affects Climate Sensitivity

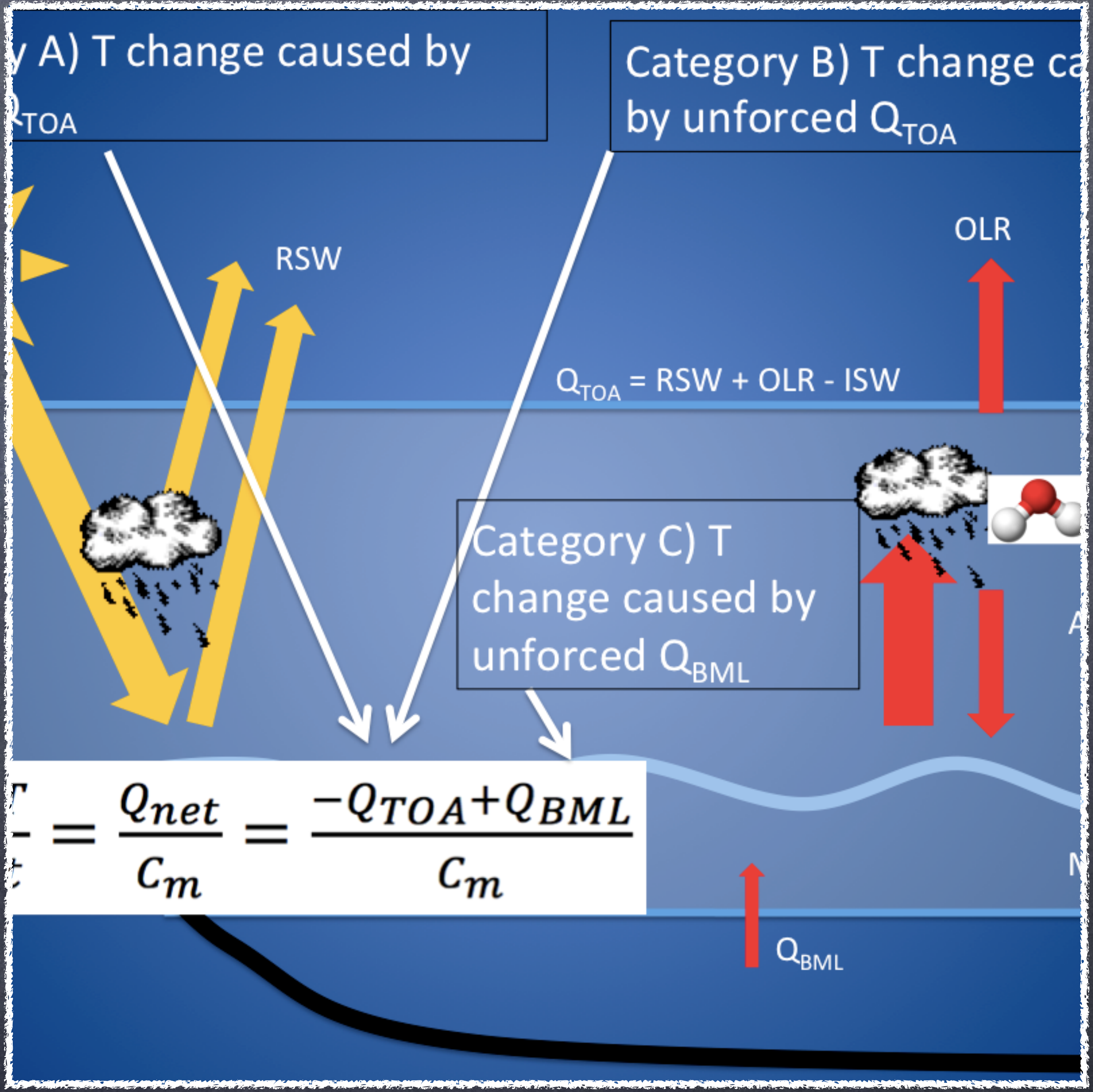

# Extras

# Surface Energy Budget

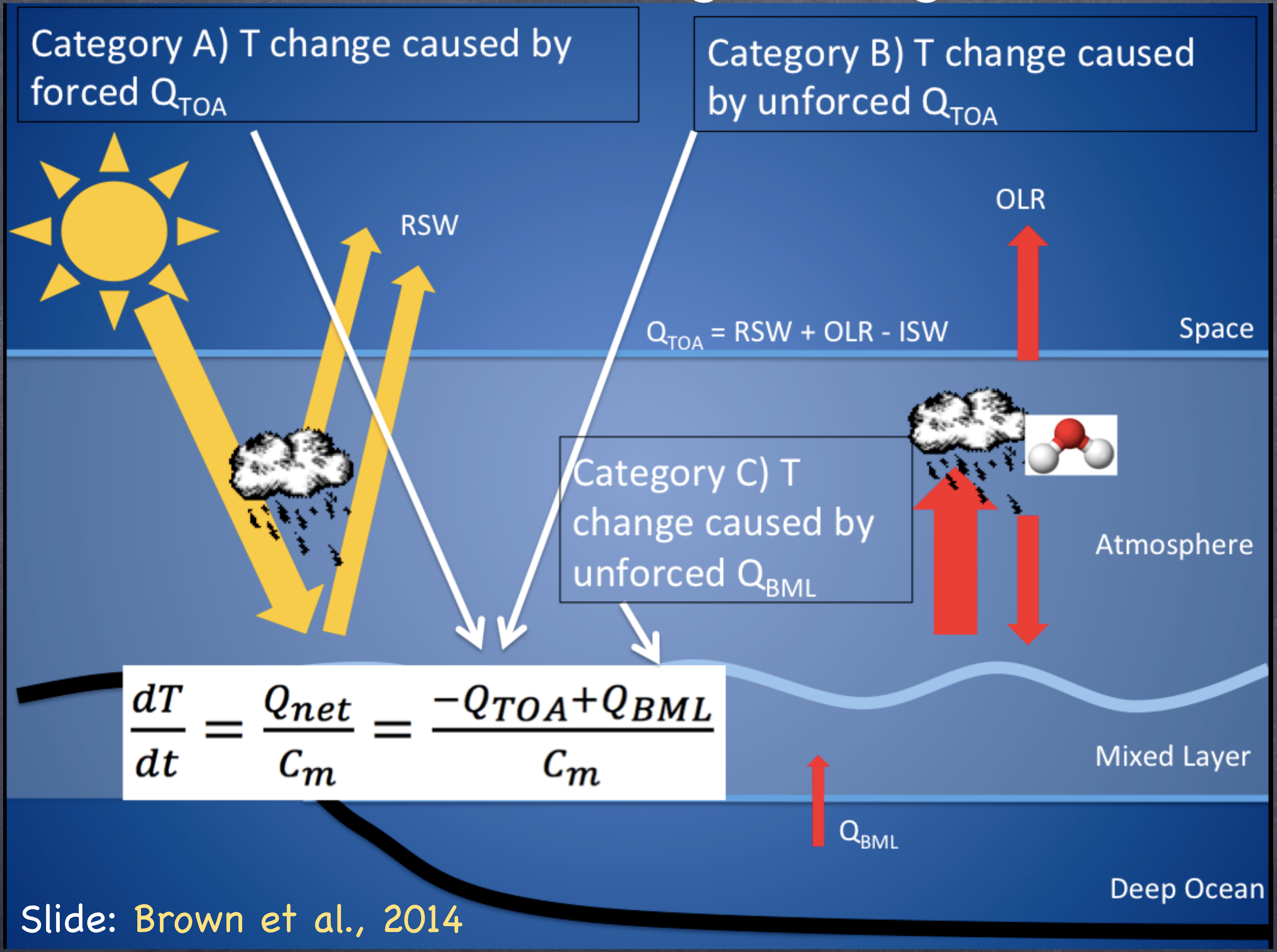


- $O(2W/m^2)$ change to $Q_{BML}$ as important as GHG
- Slight oversimplification—sensitivity + budget

# Modeling of variability

A stochastic, predictable persistence model:
Frankignoul & Hasselmann (77)

Temp Change — Random Atmosphere — Restoring — Mixed Layer

$$\frac{dT}{dt} = \frac{f_1'}{h} - \lambda T$$

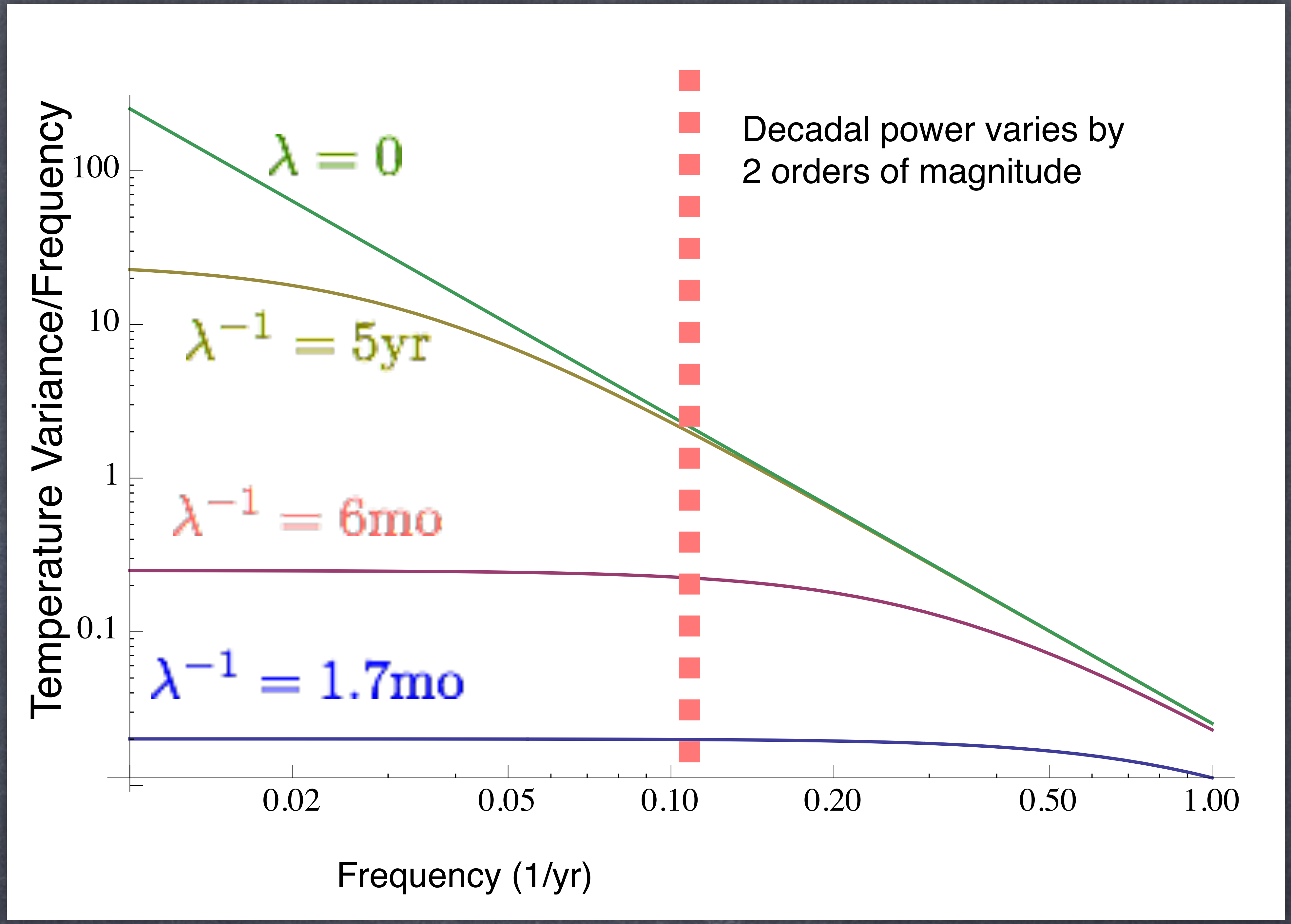


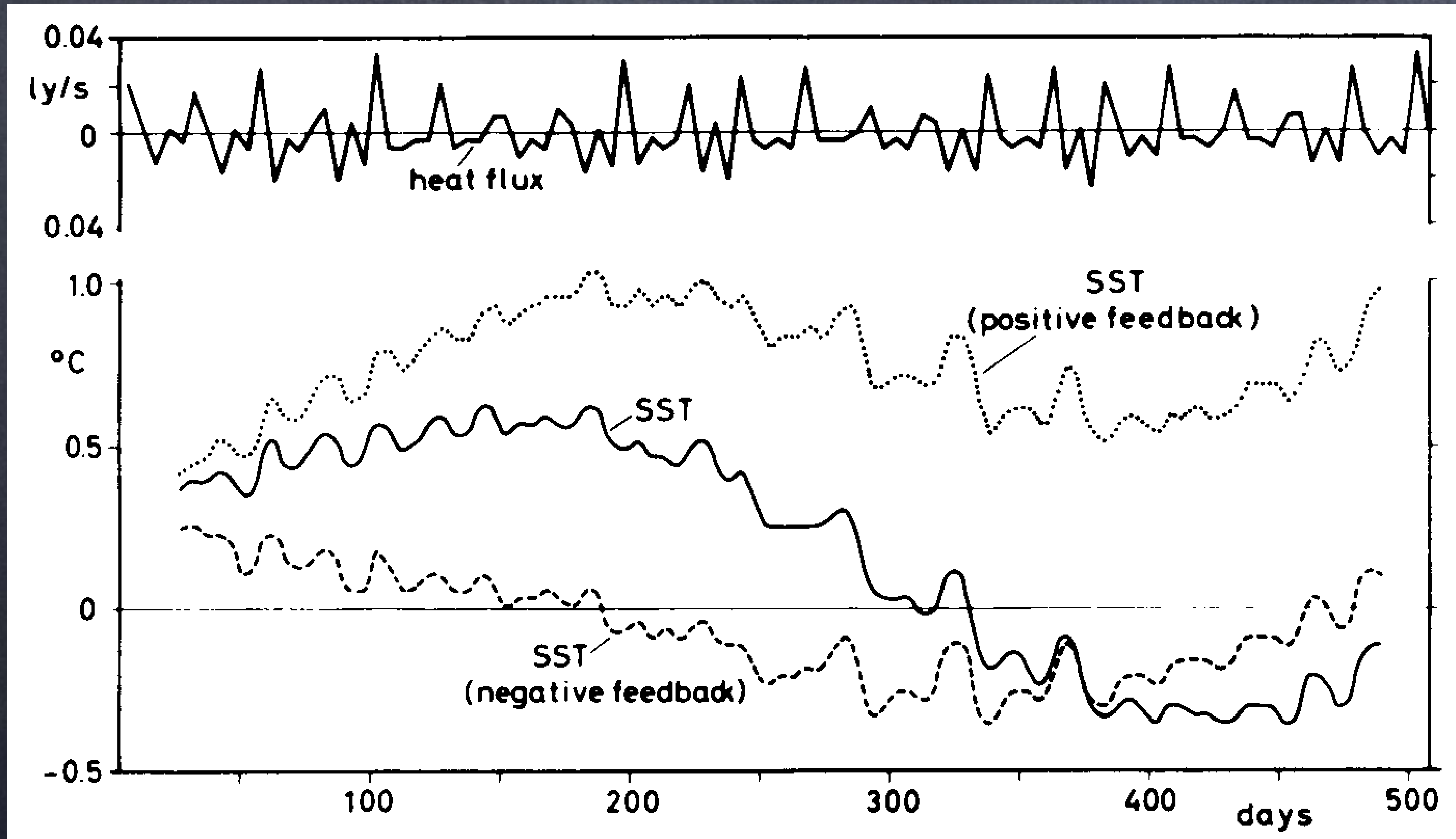


$$\lambda = \rho^a C_p^a (\rho^w C_p^w)^{-1} C_H (1 + B) \langle |U| \rangle h^{-1}$$

$$= (1.7 \text{ month})^{-1}$$

# World Ocean

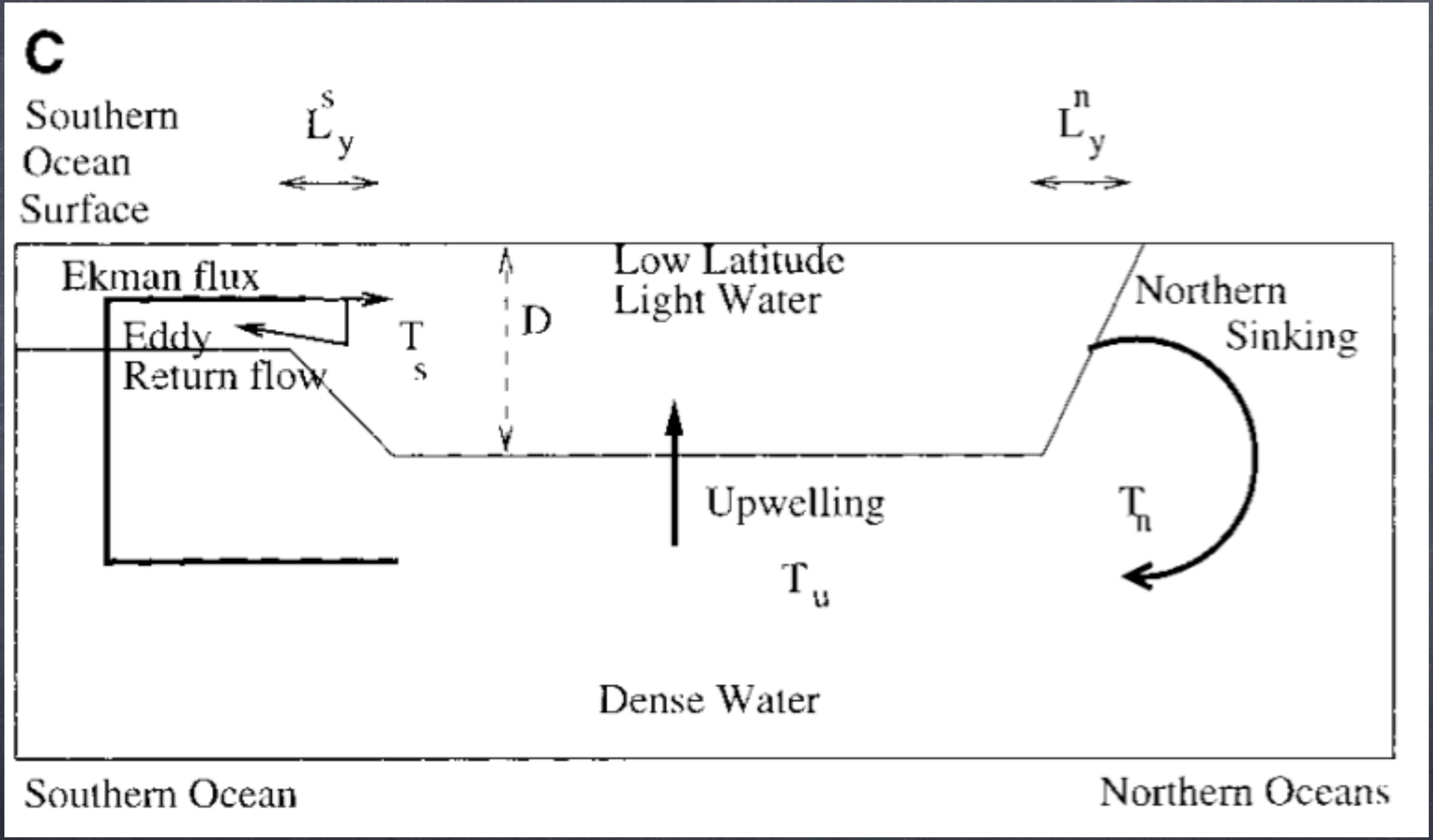


Gnanadesikan SCIENCE VOL 283 26 MARCH 1999

Even Simpler: 2-Layer Homogeneous Energy Balance Model (Gregory, 2000)

# Even Simpler: 2-Layer Homogeneous EBM (Gregory, 2000; Winton et al. 2010; Geoffroy et al. 2013)

G. Hall and BFK. Regional mixed layer depth as a climate diagnostic and emergent constraint. GRL, 2021. Submitted.

The 2-layer model parameters are estimated from 25 CMIP6 model timeseries—
None of the parameters are observable
9 further CMIP6 models are used as out-of-sample validation

$$C_S \frac{d\Delta T}{dt} = F - \lambda \Delta T - \varepsilon\gamma(\Delta T - \Delta T_D),$$
$$C_D \frac{d\Delta T_D}{dt} = \gamma(\Delta T - \Delta T_D);$$

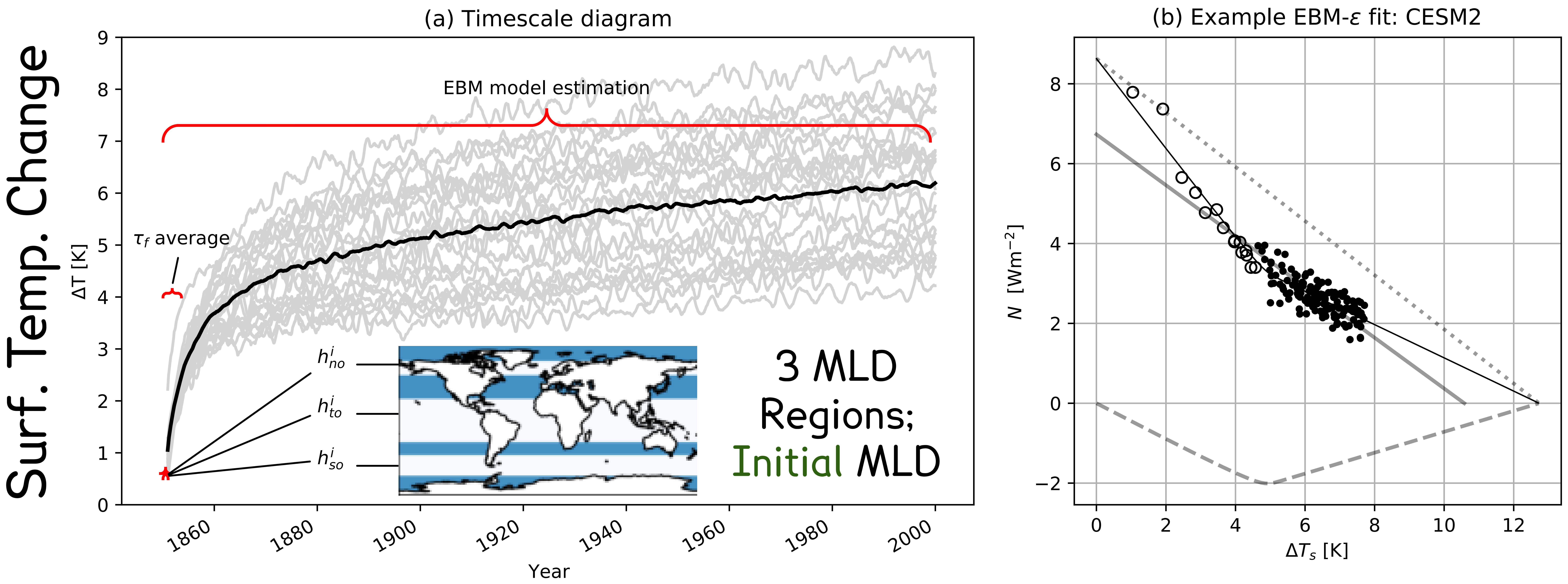

# We can use the mixed layer depth as An EMERGENT CONSTRAINT

That is, an observable that correlates or constrains the other properties useful for projections.

## CMIP6 GCMs give MLD & 2-Layer Model Properties

G. Hall and BFK. Regional mixed layer depth as a climate diagnostic and emergent constraint. GRL, 2021. Submitted.

## None of the parameters are observable

$$C_S \frac{d\Delta T}{dt} = F - \lambda \Delta T - \varepsilon\gamma(\Delta T - \Delta T_D),$$

$$C_D \frac{d\Delta T_D}{dt} = \gamma(\Delta T - \Delta T_D);$$

## But MLD is, simplify into regions

- [55N, 75N] $h^i_{no}$
- [25S, 25N] $h^i_{to}$
- [65S, 45S] $h^i_{so}$

3 MLD Regions; Initial MLD

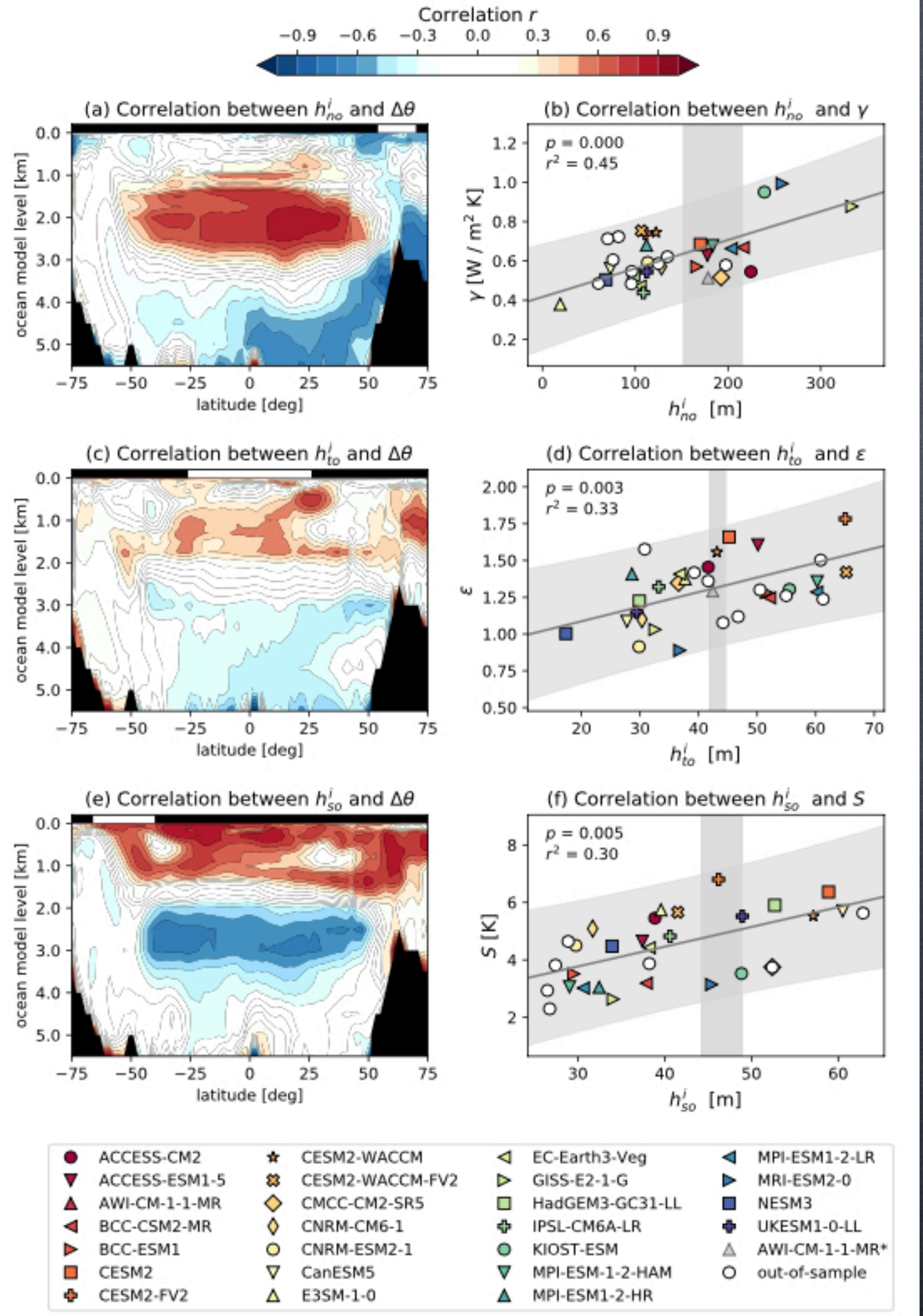

# Zoom: Submeso-Langmuir Interaction!

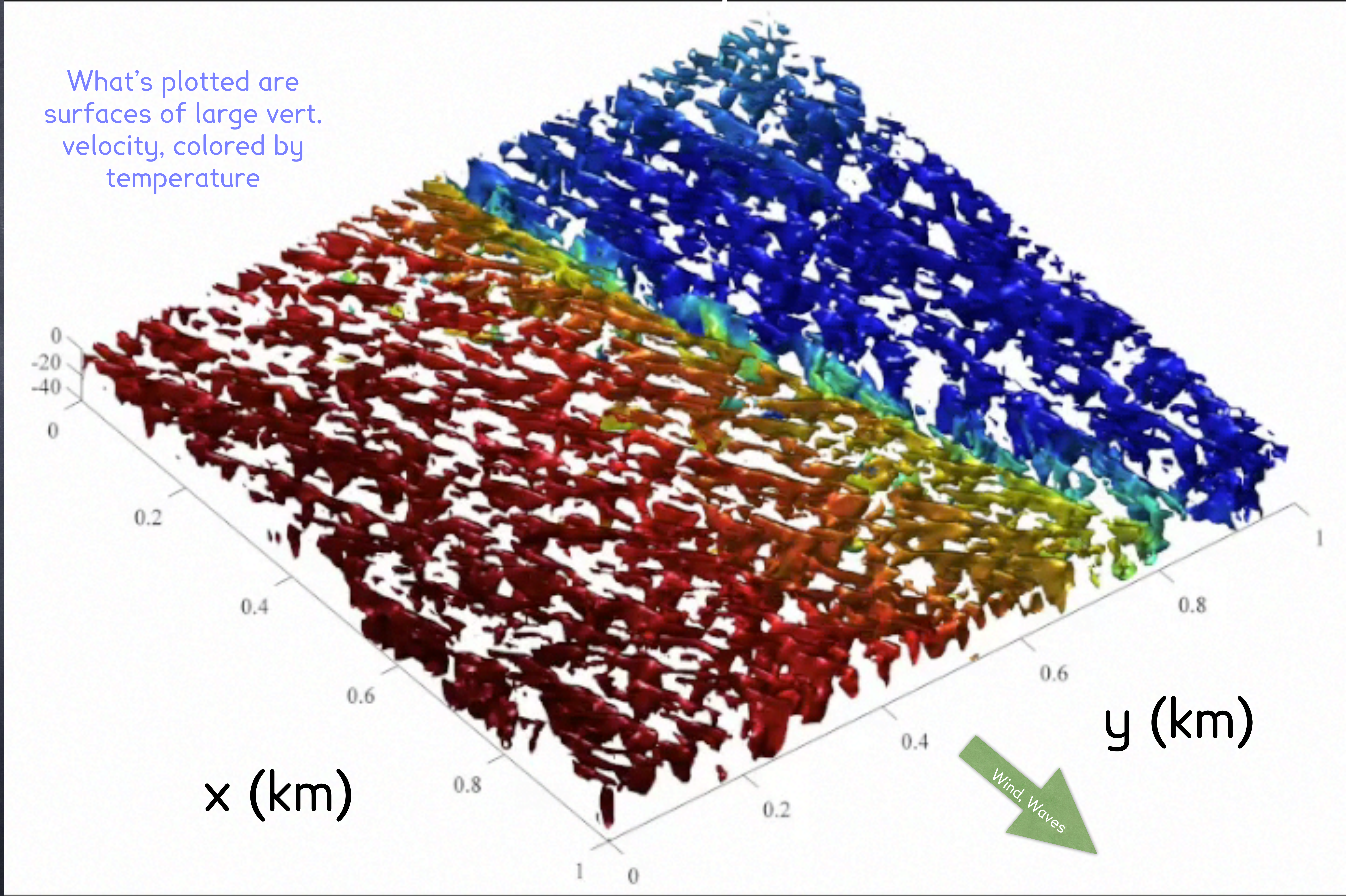


P. E. Hamlington, L. P. Van Roekel, BFK, K. Julien, and G. P. Chini. Langmuir-submesoscale interactions: Descriptive analysis of multiscale frontal spin-down simulations. JPO, 44(9):2249-2272, 2014.

# Zoom: Submeso-Langmuir Interaction!

What's plotted are surfaces of large vert. velocity, colored by temperature

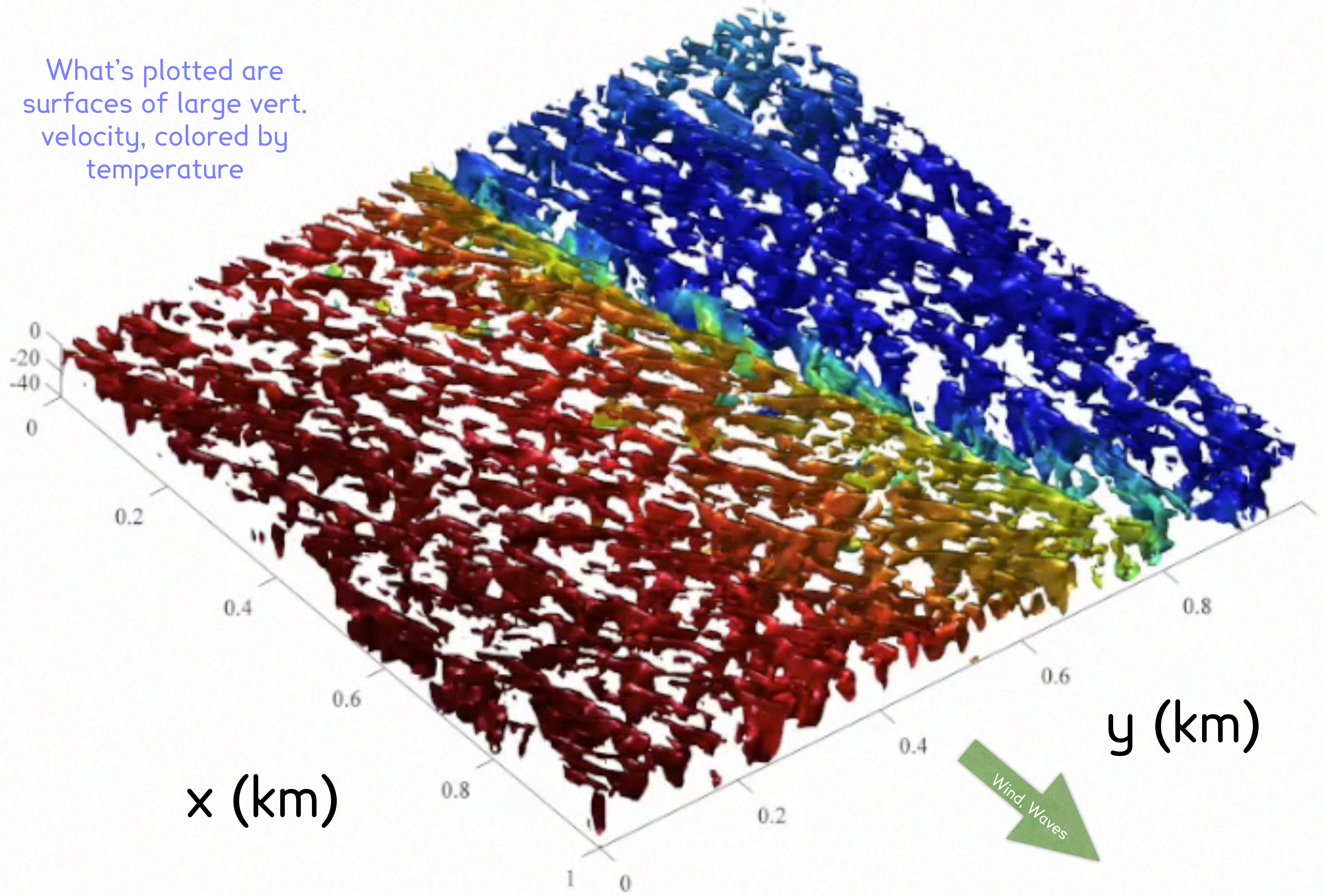


P. E. Hamlington, L. P. Van Roekel, BFK, K. Julien, and G. P. Chini. Langmuir-submesoscale interactions: Descriptive analysis of multiscale frontal spin-down simulations. JPO, 44(9):2249-2272, 2014.

image:
Thorpe, 04

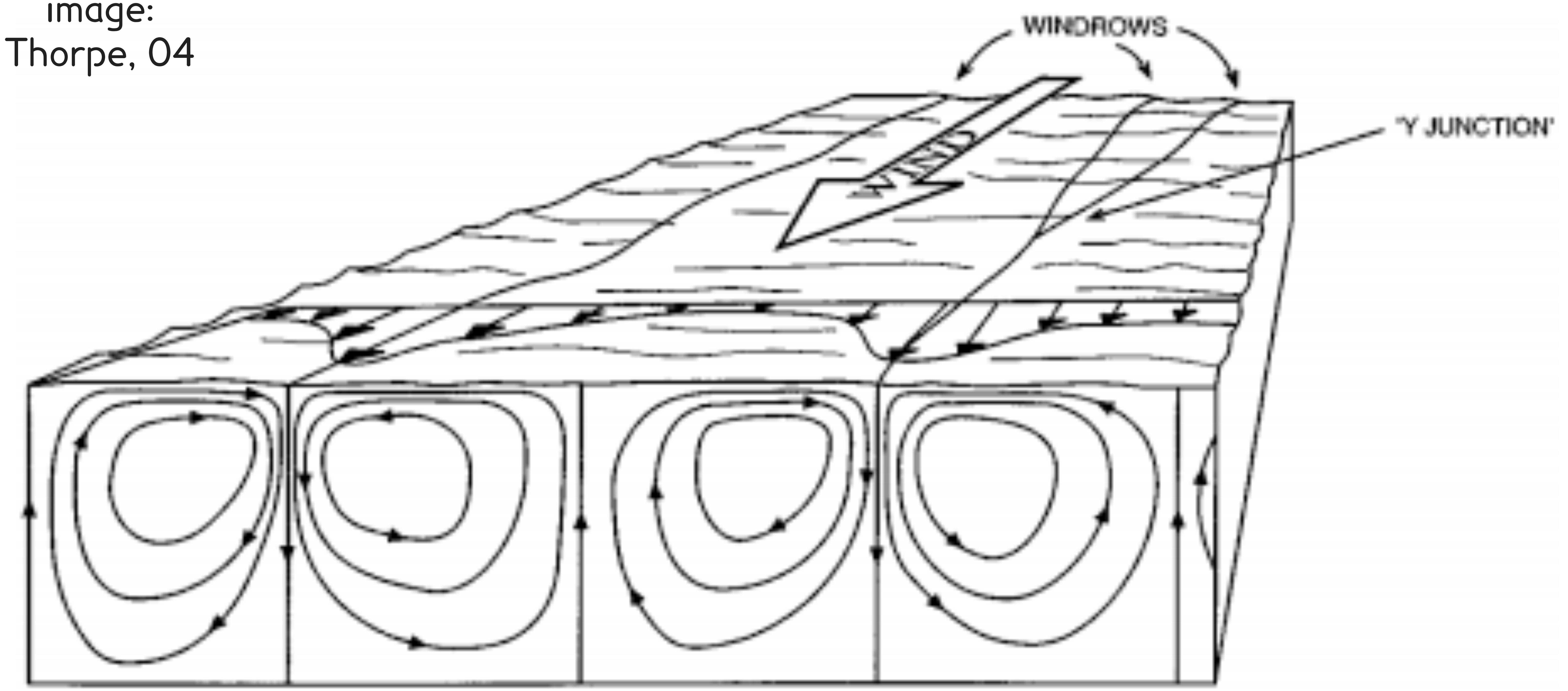


**Figure 1** Sketch showing the pattern of mean flow in idealized Langmuir circulation. The windrows may be 2 m to 300 m apart, and the cell form is roughly square (as shown). In practice the flow is turbulent, especially near the water surface, and the windrows (Figure 2) amalgamate and meander in space and time. Bands of bubbles or buoyant algae may form within the downward-going (or downwelling) flow (see Figure 3).

$$\frac{\alpha^2}{Ri}\left[w_{,t} + v_j^L w_{,j} + \frac{M_{Ro}}{RoRi} w w_{,z}\right] = -\pi_{,z} + b - \varepsilon v_j^L v^s_{j,z} + \frac{\alpha^2}{ReRi} w_{,jj}$$

N. Suzuki and BFK. Understanding Stokes forces in the wave-averaged equations. Journal of Geophysical Research-Oceans, 121:1-18, 2016.

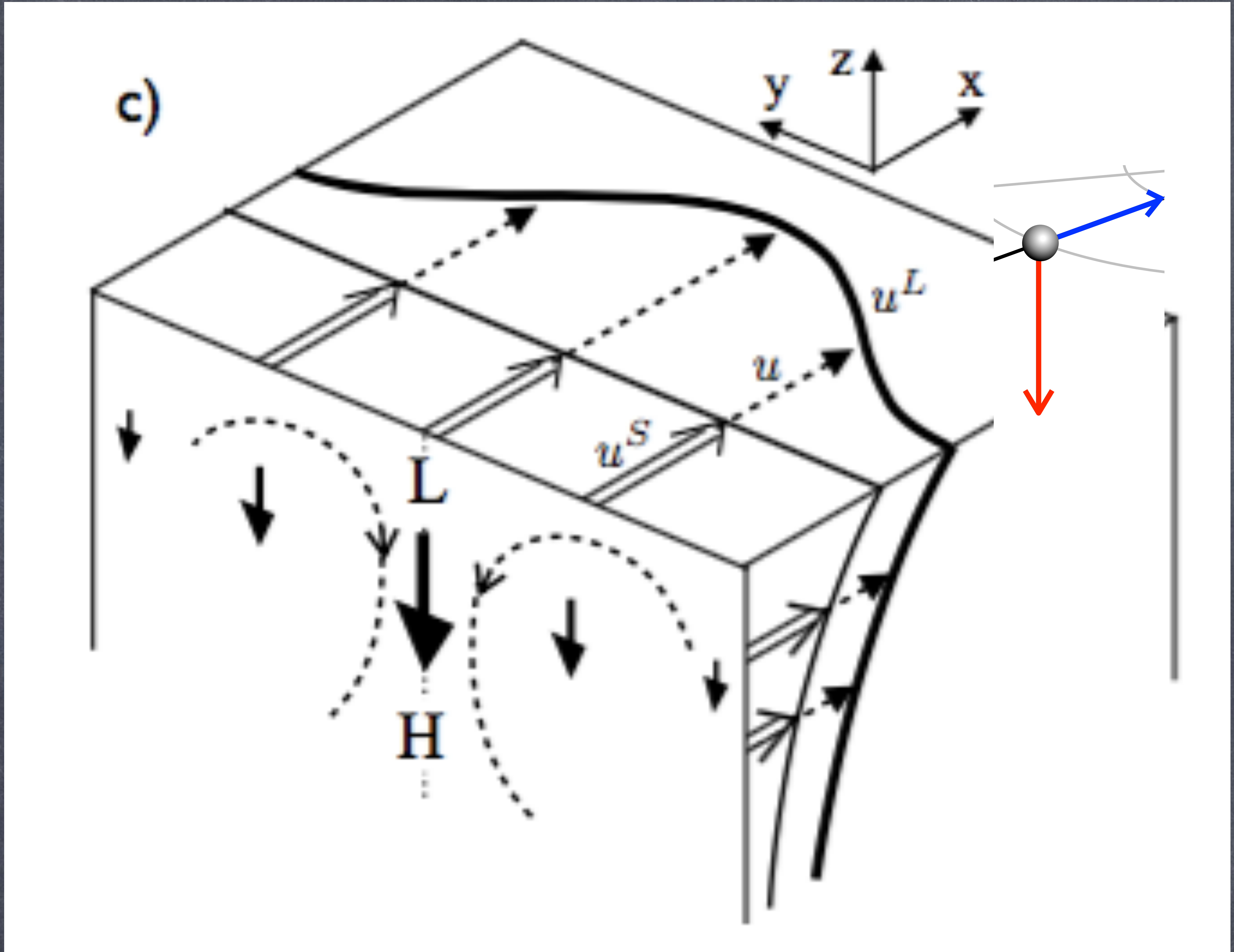


$$\frac{\alpha^2}{Ri}\left[w_{,t} + v_j^L w_{,j} + \frac{M_{Ro}}{RoRi} w w_{,z}\right] = -\pi_{,z} + b - \varepsilon v_j^L v_{j,z}^s + \frac{\alpha^2}{ReRi} w_{,jj}$$

N. Suzuki and BFK. Understanding Stokes forces in the wave-averaged equations. Journal of Geophysical Research-Oceans, 121:1-18, 2016.

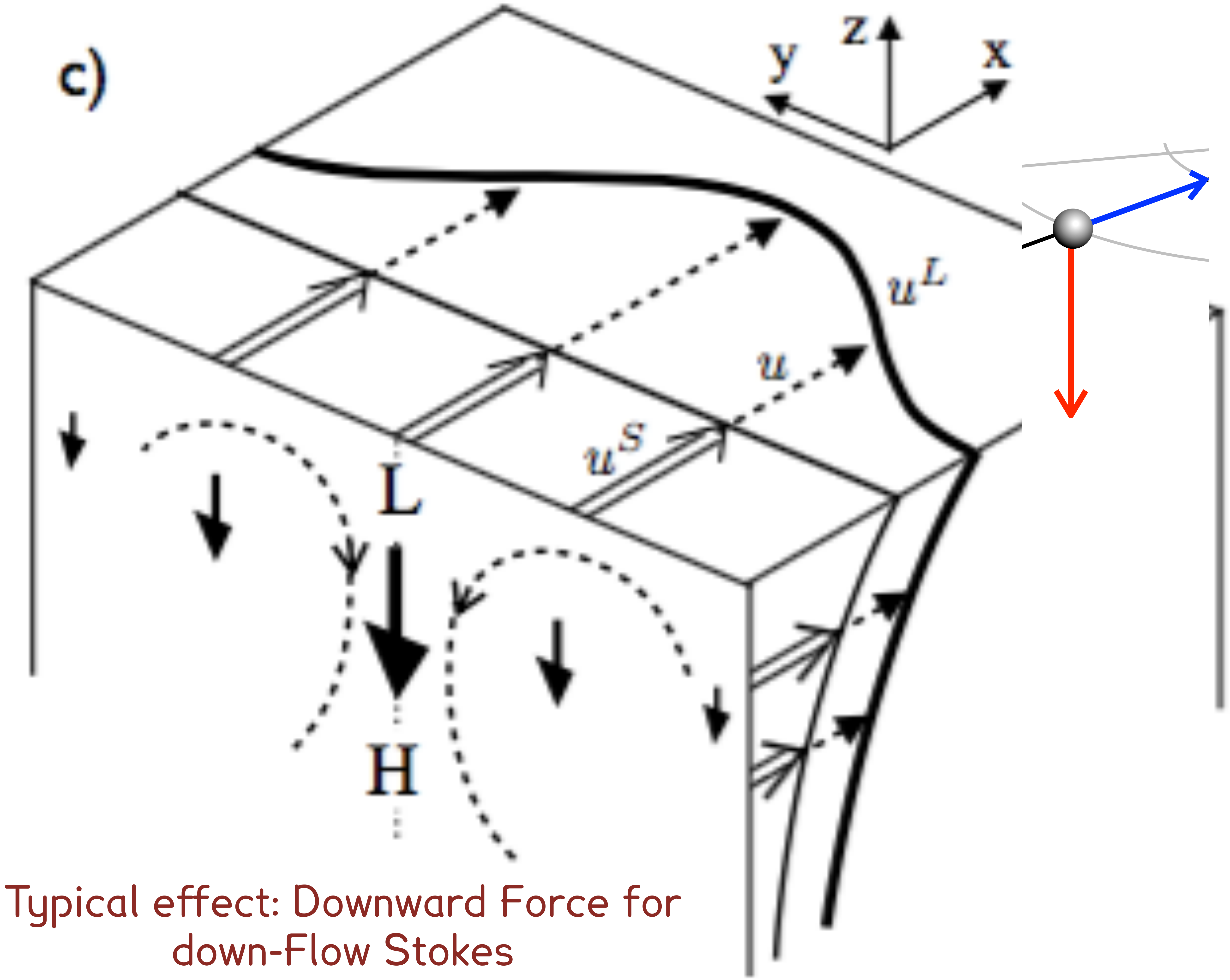

Typical effect: Downward Force for down-Flow Stokes

$$\frac{\alpha^2}{Ri}\left[w_{,t} + v_j^L w_{,j} + \frac{M_{Ro}}{RoRi} w w_{,z}\right] = -\pi_{,z} + b - \varepsilon v_j^L v_{j,z}^s + \frac{\alpha^2}{ReRi} w_{,jj}$$

N. Suzuki and BFK. Understanding Stokes forces in the wave-averaged equations. Journal of Geophysical Research-Oceans, 121:1-18, 2016.

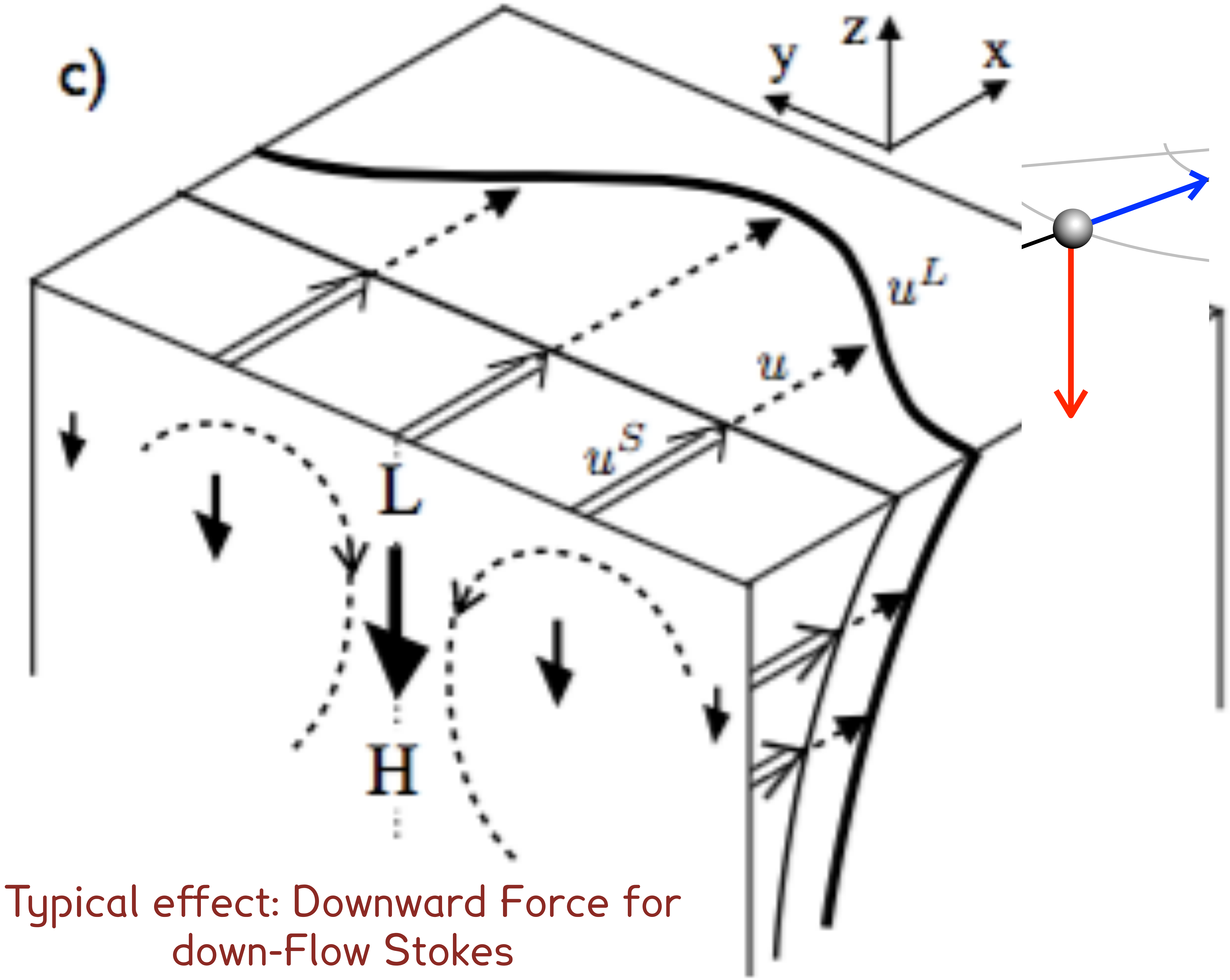


Typical effect: Downward Force for down-Flow Stokes

"wavy hydrostatic" if $\epsilon \gg 1$

$$\frac{\alpha^2}{Ri}\left[w_{,t} + v_j^L w_{,j} + \frac{M_{Ro}}{RoRi} w w_{,z}\right] = \boxed{-\pi_{,z} + b - \varepsilon v_j^L v_{j,z}^s} + \frac{\alpha^2}{ReRi} w_{,jj}$$

N. Suzuki and BFK. Understanding Stokes forces in the wave-averaged equations. Journal of Geophysical Research-Oceans, 121:1-18, 2016.

# Diverse types of interaction: Stronger Langmuir (small) Turbulence

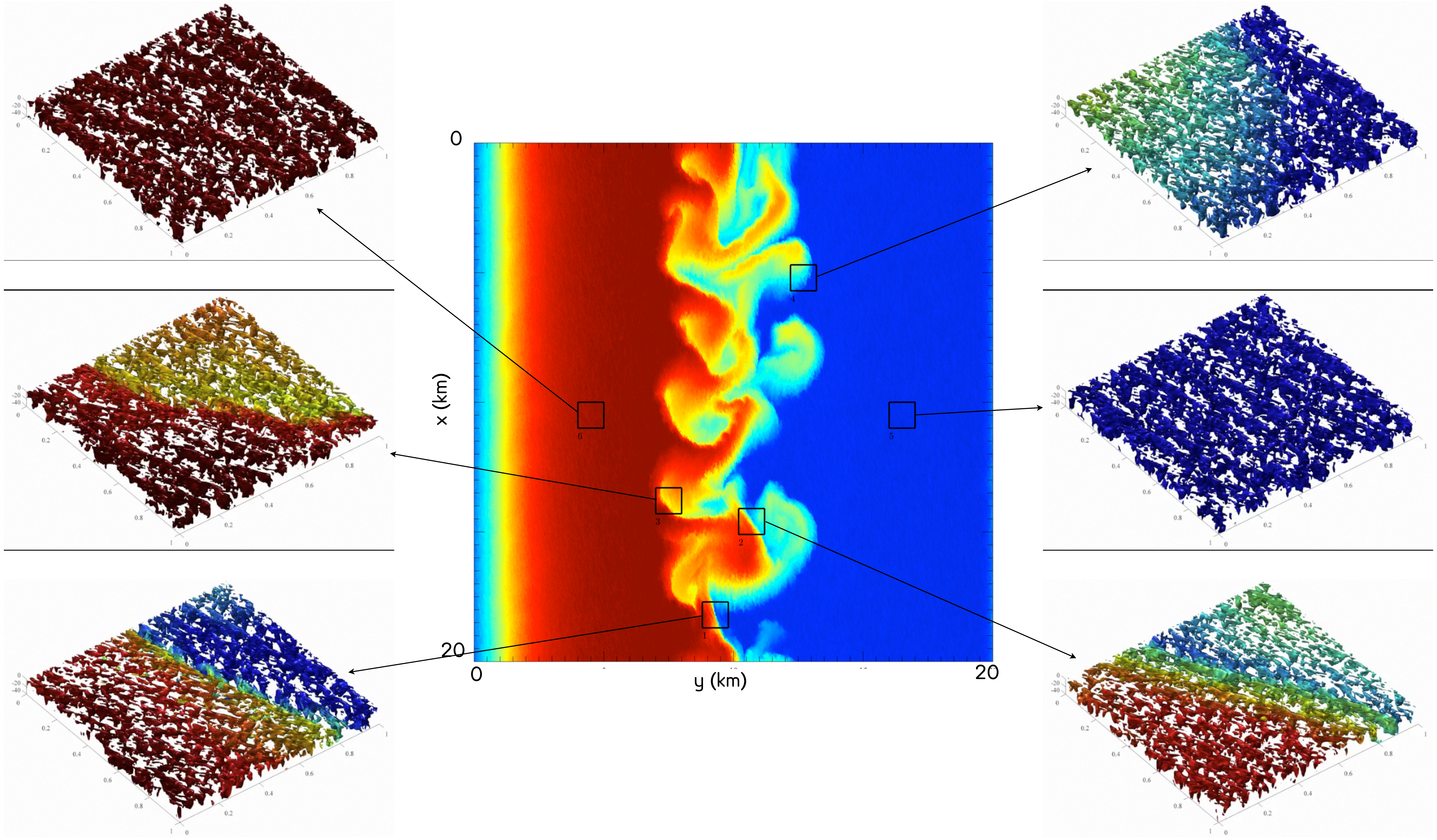


P. E. Hamlington, L. P. Van Roekel, BFK, K. Julien, and G. P. Chini. Langmuir-submesoscale interactions: Descriptive analysis of multiscale frontal spin-down simulations. Journal of Physical Oceanography, 44(9):2249-2272, September 2014.

# Diverse types of interaction: Stronger Langmuir (small) Turbulence

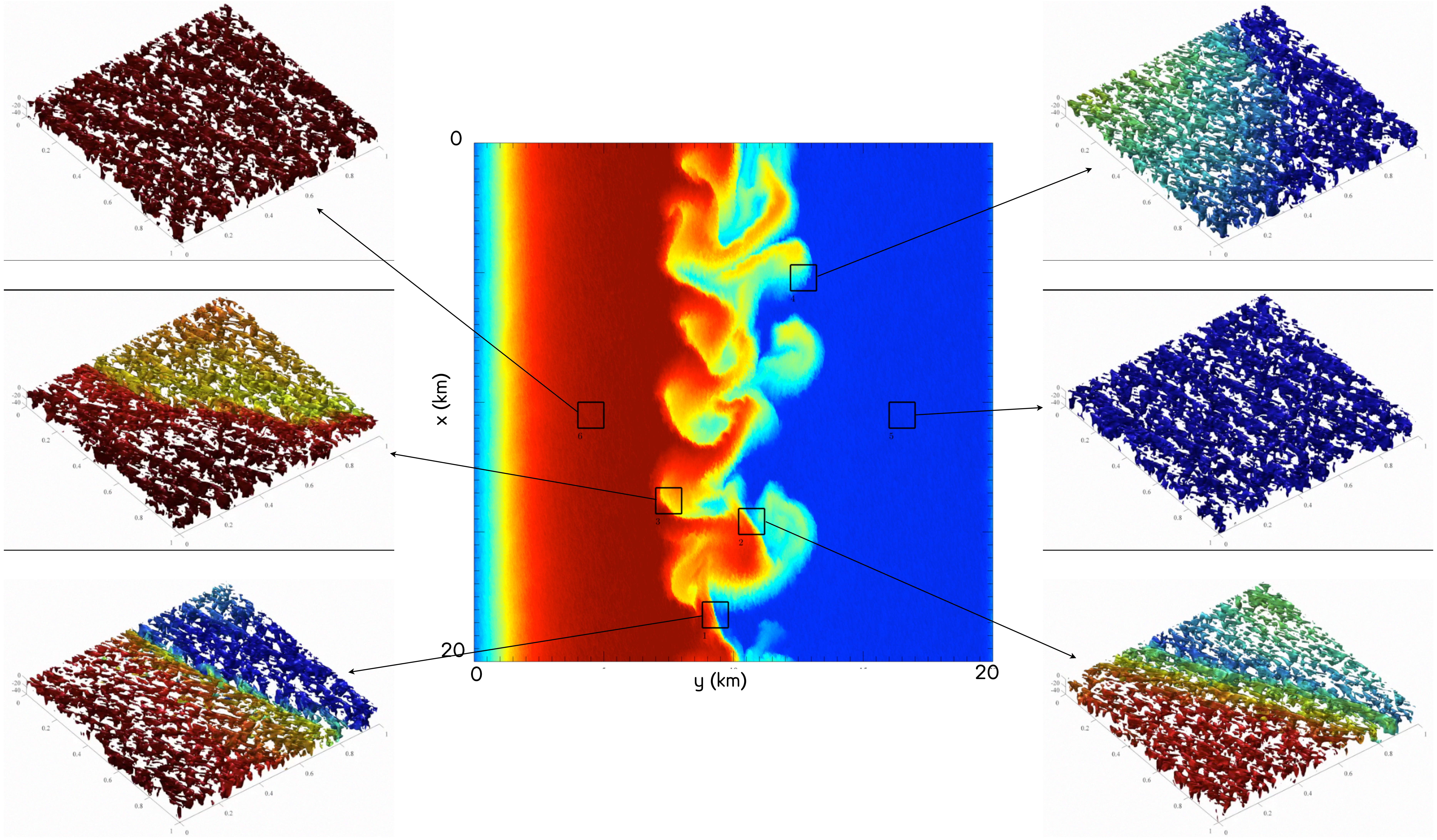


P. E. Hamlington, L. P. Van Roekel, BFK, K. Julien, and G. P. Chini. Langmuir-submesoscale interactions: Descriptive analysis of multiscale frontal spin-down simulations. Journal of Physical Oceanography, 44(9):2249-2272, September 2014.

# A front that's not aligned with winds & waves is weaker

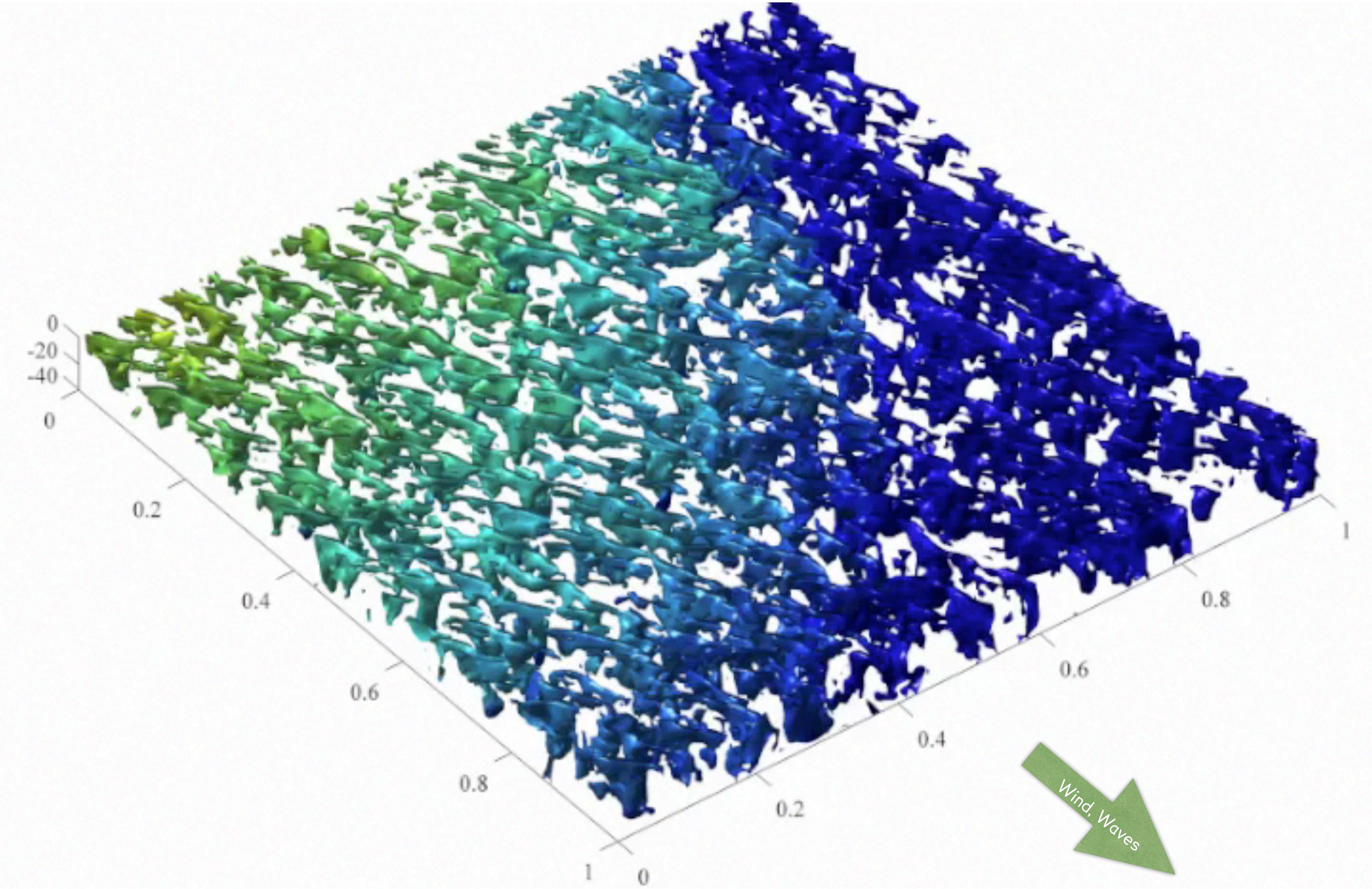


N. Suzuki, BFK, P. E. Hamlington, and L. P. Van Roekel. Surface waves affect frontogenesis. Journal of Geophysical Research-Oceans, 121:1-28, May 2016.

# A front that's not aligned with winds & waves is weaker

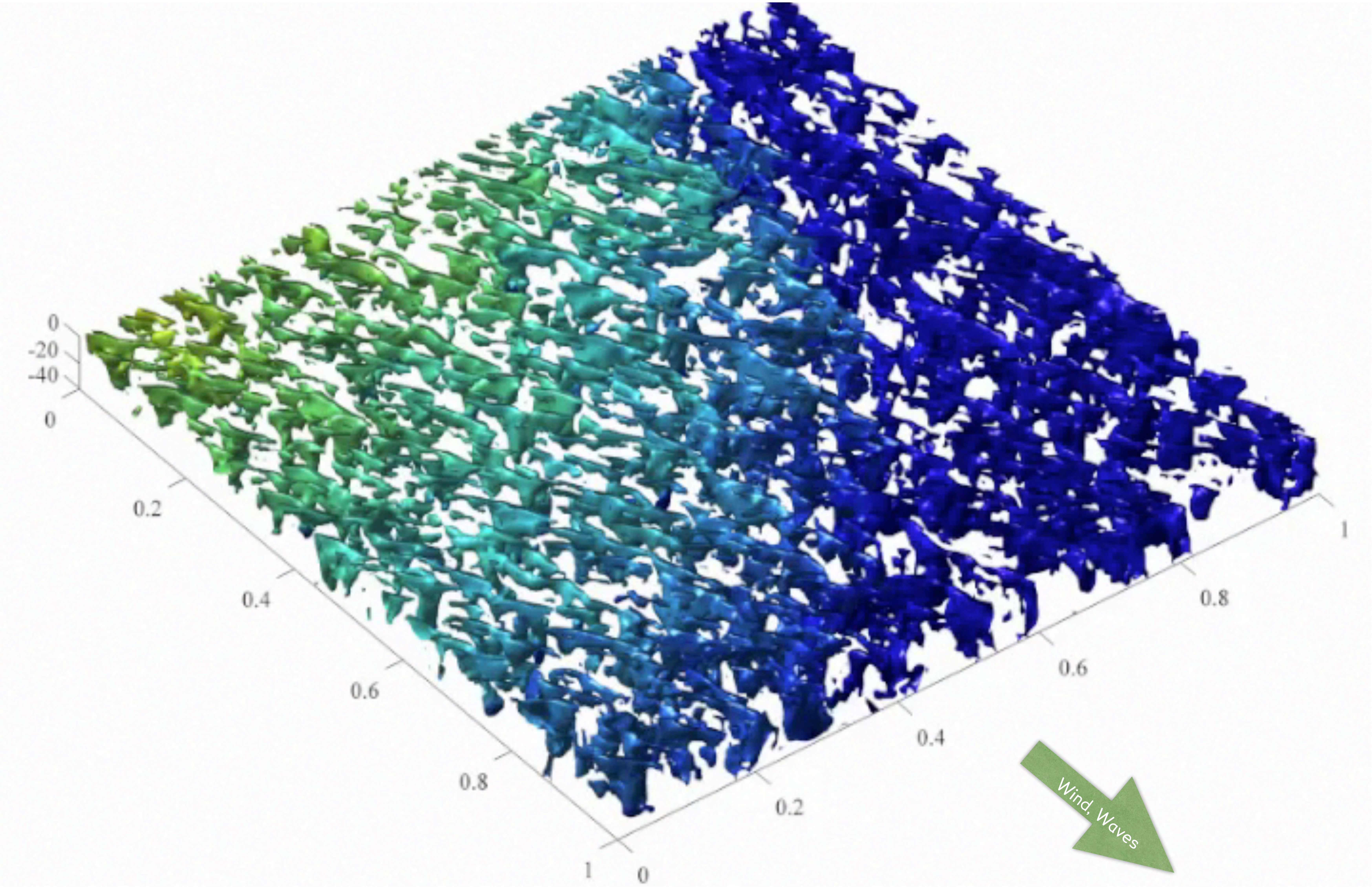


N. Suzuki, BFK, P. E. Hamlington, and L. P. Van Roekel. Surface waves affect frontogenesis. Journal of Geophysical Research-Oceans, 121:1-28, May 2016.

# Do Stokes force directly affect larger scales?

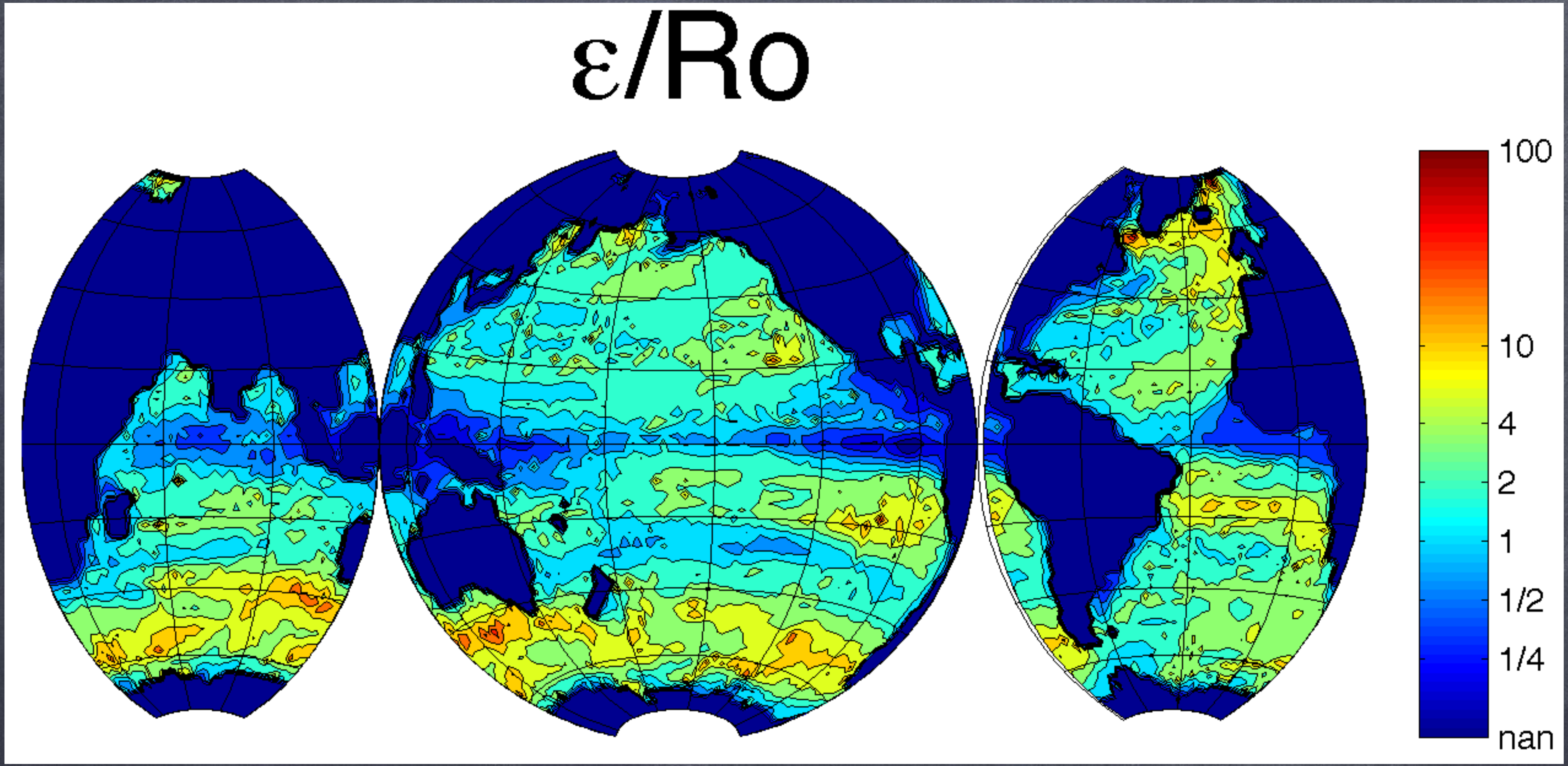


$$\varepsilon = \frac{V^s H}{f L H_s} \qquad Ro = \frac{U}{fL}$$

J. C. McWilliams and BFK. Oceanic wave-balanced surface fronts and filaments. Journal of Fluid Mechanics, 730:464-490, 2013.

# Do Stokes force directly affect larger scales?

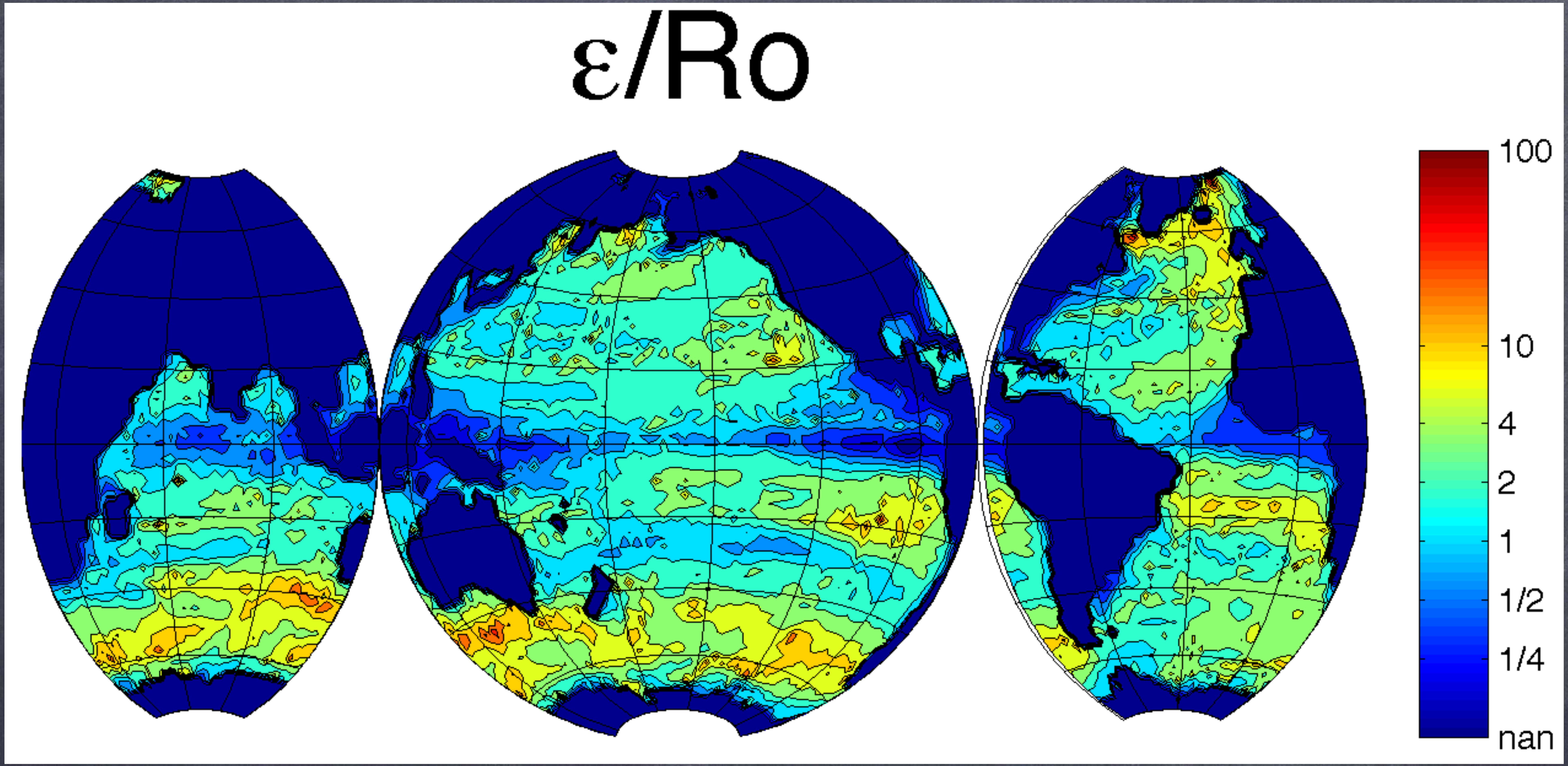


"wavy hydrostatic" if

$$\epsilon \gg 1$$

$$\varepsilon = \frac{V^s H}{f L H_s}$$

$$Ro = \frac{U}{fL}$$

J. C. McWilliams and BFK. Oceanic wave-balanced surface fronts and filaments. Journal of Fluid Mechanics, 730:464-490, 2013.

V

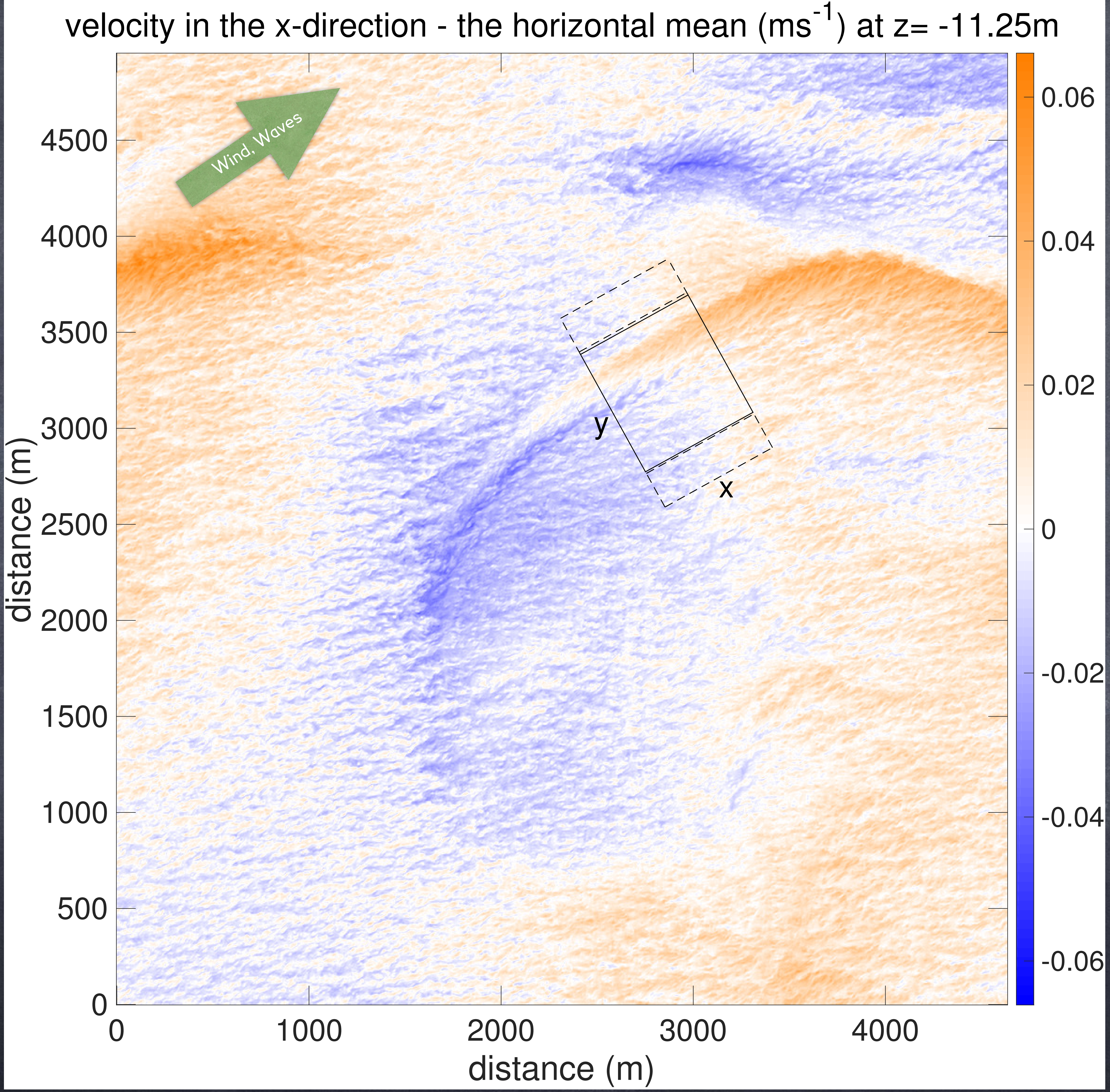


N. Suzuki, B. Fox-Kemper, P. E. Hamlington, and L. P. Van Roekel. Surface waves affect frontogenesis. Journal of Geophysical Research-Oceans, 121:1-28, May 2016.

T

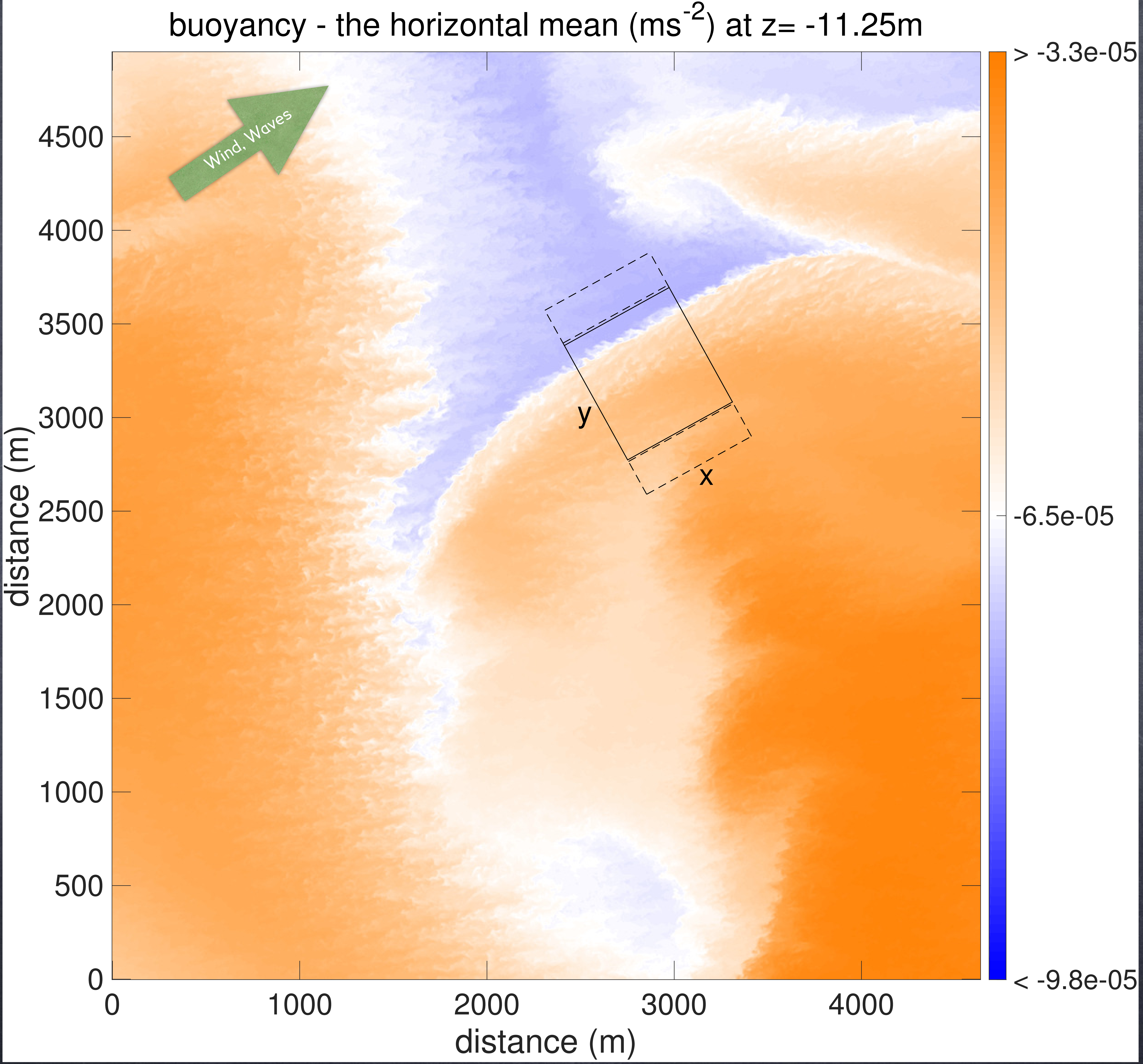


N. Suzuki, B. Fox-Kemper, P. E. Hamlington, and L. P. Van Roekel. Surface waves affect frontogenesis. Journal of Geophysical Research-Oceans, 121:1-28, May 2016.

W

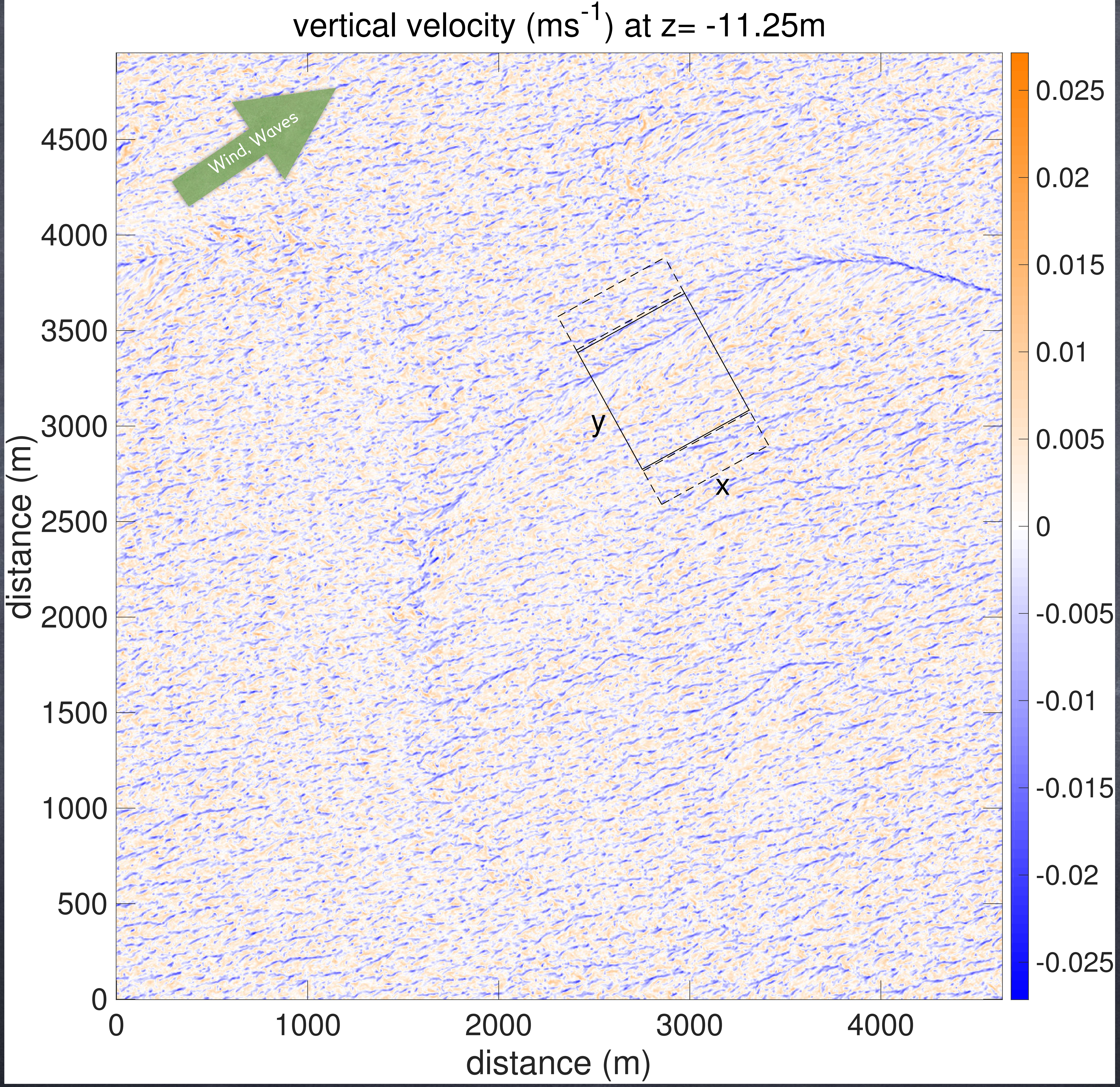


N. Suzuki, B. Fox-Kemper, P. E. Hamlington, and L. P. Van Roekel. Surface waves affect frontogenesis. Journal of Geophysical Research-Oceans, 121:1-28, May 2016.

Initially every surface node has 1 drifter,
so there are 851796 drifters in the picture

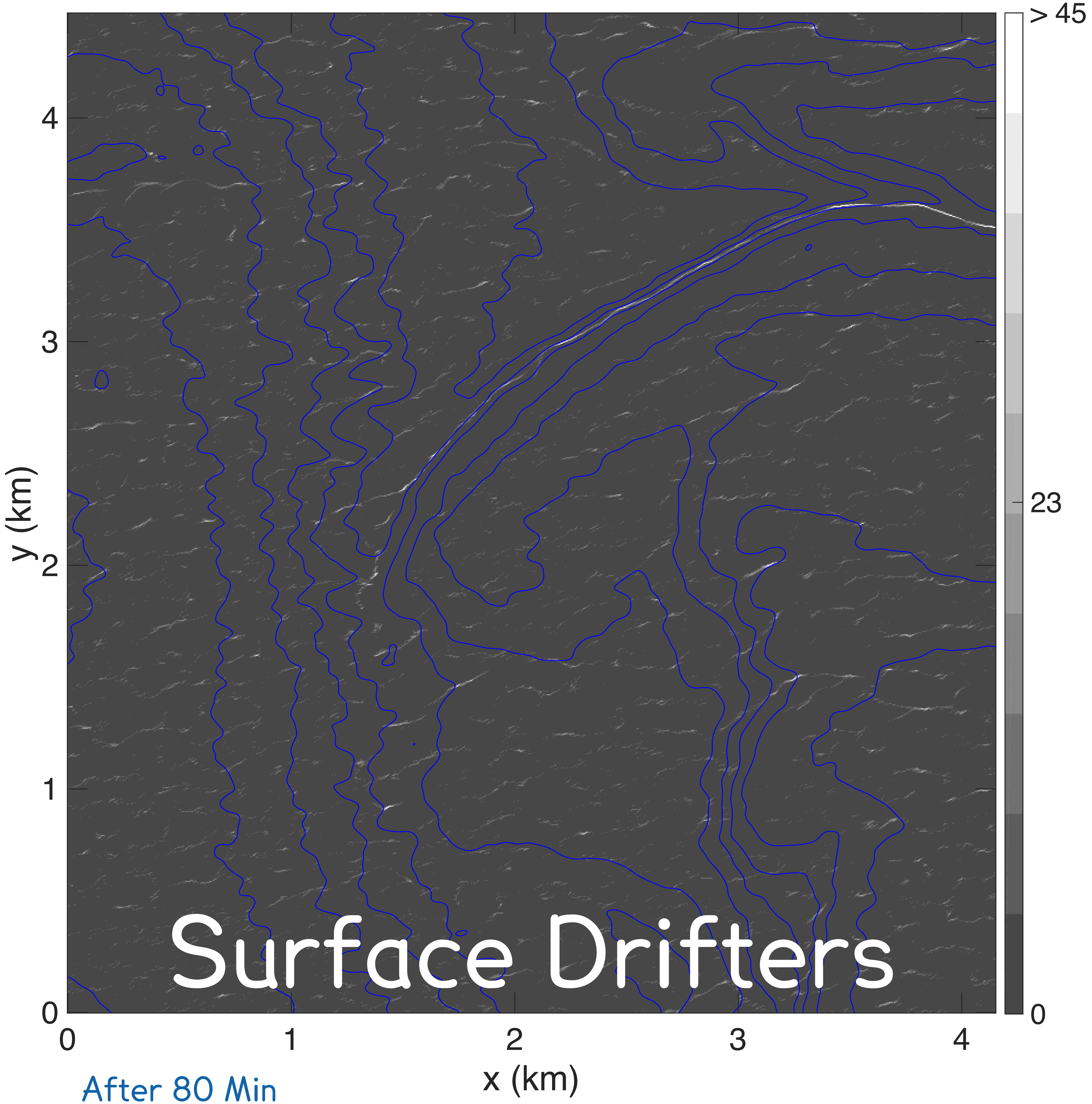


After 80 Min

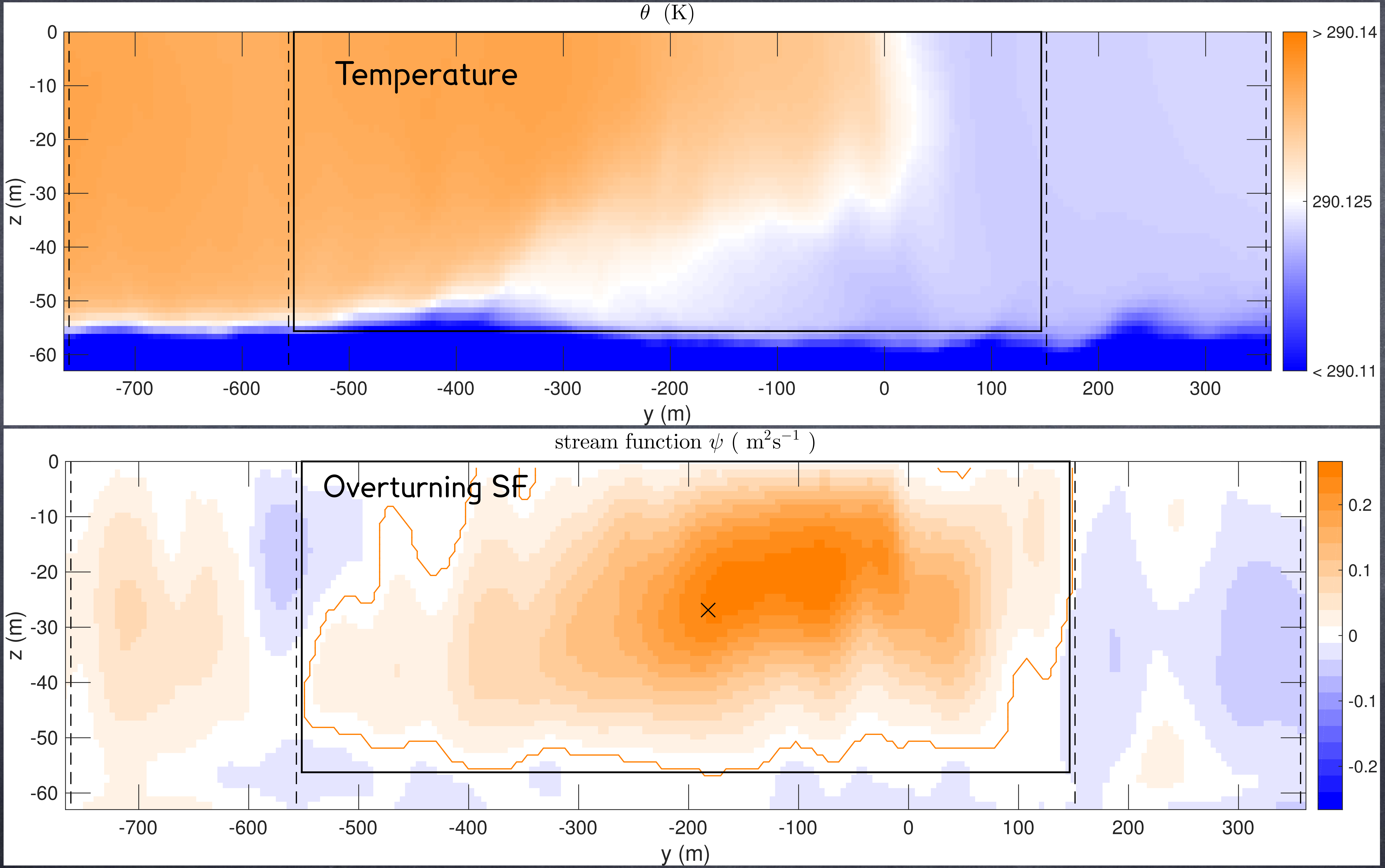


N. Suzuki, BFK, P. E. Hamlington, and L. P. Van Roekel. Surface waves affect frontogenesis. Journal of Geophysical Research-Oceans, 121:1-28, 2016.

# Do (wavy hydrostatic) Stokes Forces Matter?

## Yes! At Leading Order (in LES)

**Table 3.** Integrated Budget for Overturning Vorticity[a]

| Responsible Force | Relative Value |
|---|---|
| *Relative Tendency of Overturning Circulation along the Cell Boundary* | |
| Net tendency | $11 \pm 8\%$ |
| **Sources** | |
| Buoyancy anomaly | 100% |
| Stokes shear force anomaly | $44 \pm 4\%$ |
| Interaction with $v^H$ | $44 \pm 8\%$ |
| Frontal anomaly in pressure gradient | |
| | $6 \pm 9\%$ |
| Nonlinear interaction with $v^B$: | $2 \pm 1\%$ |
| **Sinks** | |
| Frontal turbulence anomaly | |
| (mostly, imbalance in wavy Ekman relation) | $-82 \pm 11\%$ |
| Coriolis on along-front jet | $-66 \pm 2\%$ |
| Lagrangian advection of $(v^\psi, w^\psi)$ | $-36 \pm 7\%$ |

N. Suzuki and BFK. Understanding Stokes forces in the wave-averaged equations. Journal of Geophysical Research-Oceans, 121:1-18, 2016.

N. Suzuki, BFK, P. E. Hamlington, and L. P. Van Roekel. Surface waves affect frontogenesis. Journal of Geophysical Research-Oceans, 121:1-28, 2016.

# Analytic & Numerical Wavy Submesoscale Stability: Symmetric Instabilities

- Hoskins (1974) showed that if a front in thermal wind balance is symmetrically unstable, the PV must be anticyclonic.
- Haney et al (2015) extend Hoskins' analysis to flows in Lagrangian thermal wind balance in the special case of constant Stokes shear.

Vert. Density Gradient

Horiz. Density Gradient

Anti-Stokes Shear

$$fQ = \underbrace{f^2N^2 - M^4}_{\text{geostrophic } fQ} - \underbrace{fM^2U_z^S}_{\text{Stokes-modified } fQ} < 0.$$

- In the absence of Stokes drift, this is equivalent to the familiar criteria on Richardson Number, with Stokes drift is distinct.

S. Haney, BFK, K. Julien, and A. Webb. Symmetric and geostrophic instabilities in the wave-forced ocean mixed layer. JPO 45:3033-3056, 2015.

~~$Ri < 1 \Rightarrow SI$~~

# Wavy Submesoscale Instability Different: Symmetric Instability

$fQ < 0 \Rightarrow SI$

## Ri = 0.5

## Wavy Stokes Stabilize SI

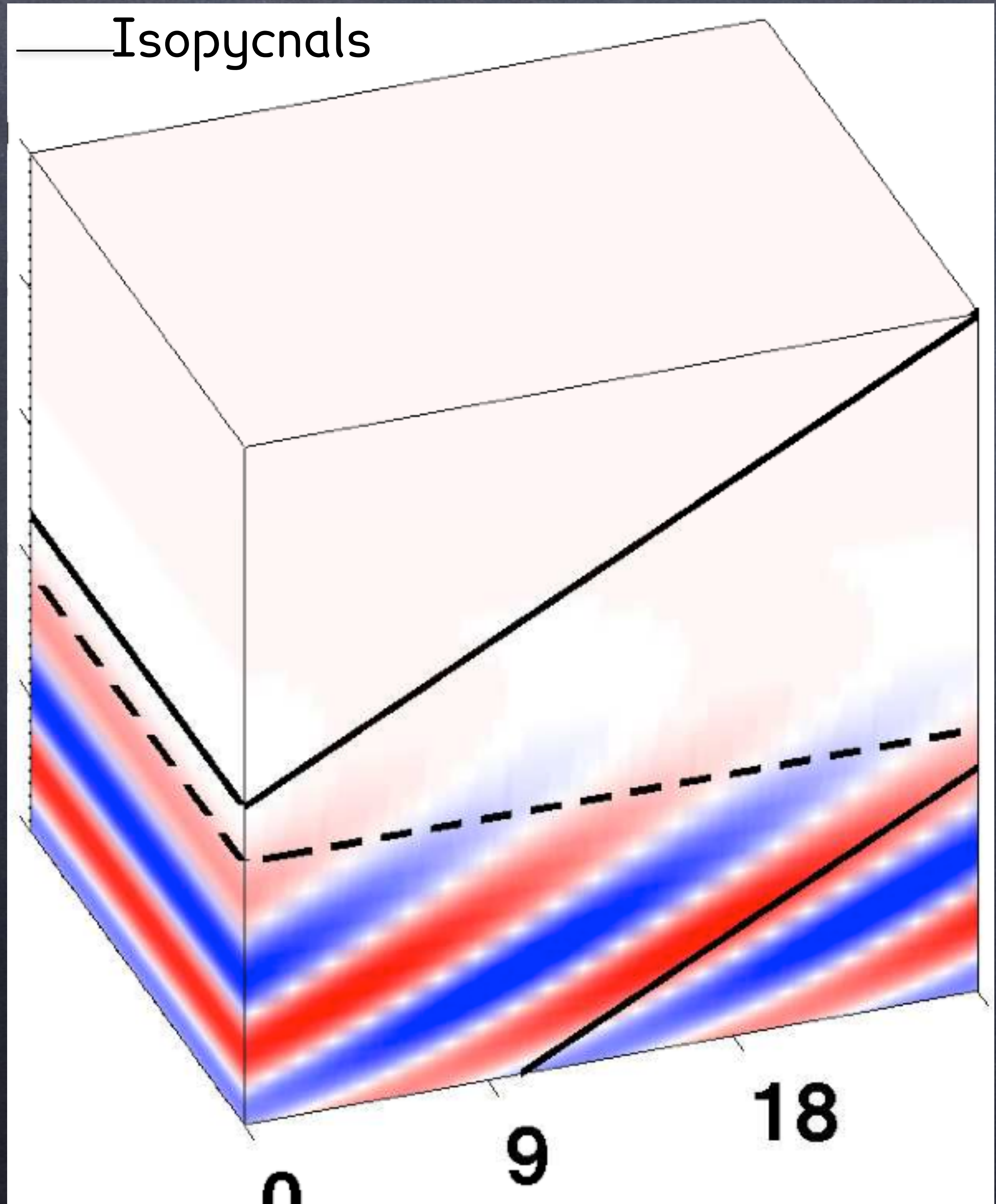


Cross front velocity for the fastest growing mode

S. Haney, BFK, K. Julien, and A. Webb. Symmetric and geostrophic instabilities in the wave-forced ocean mixed layer. JPO 45:3033-3056, 2015.

## Ri = 2

## Wavy Stokes Destabilize SI

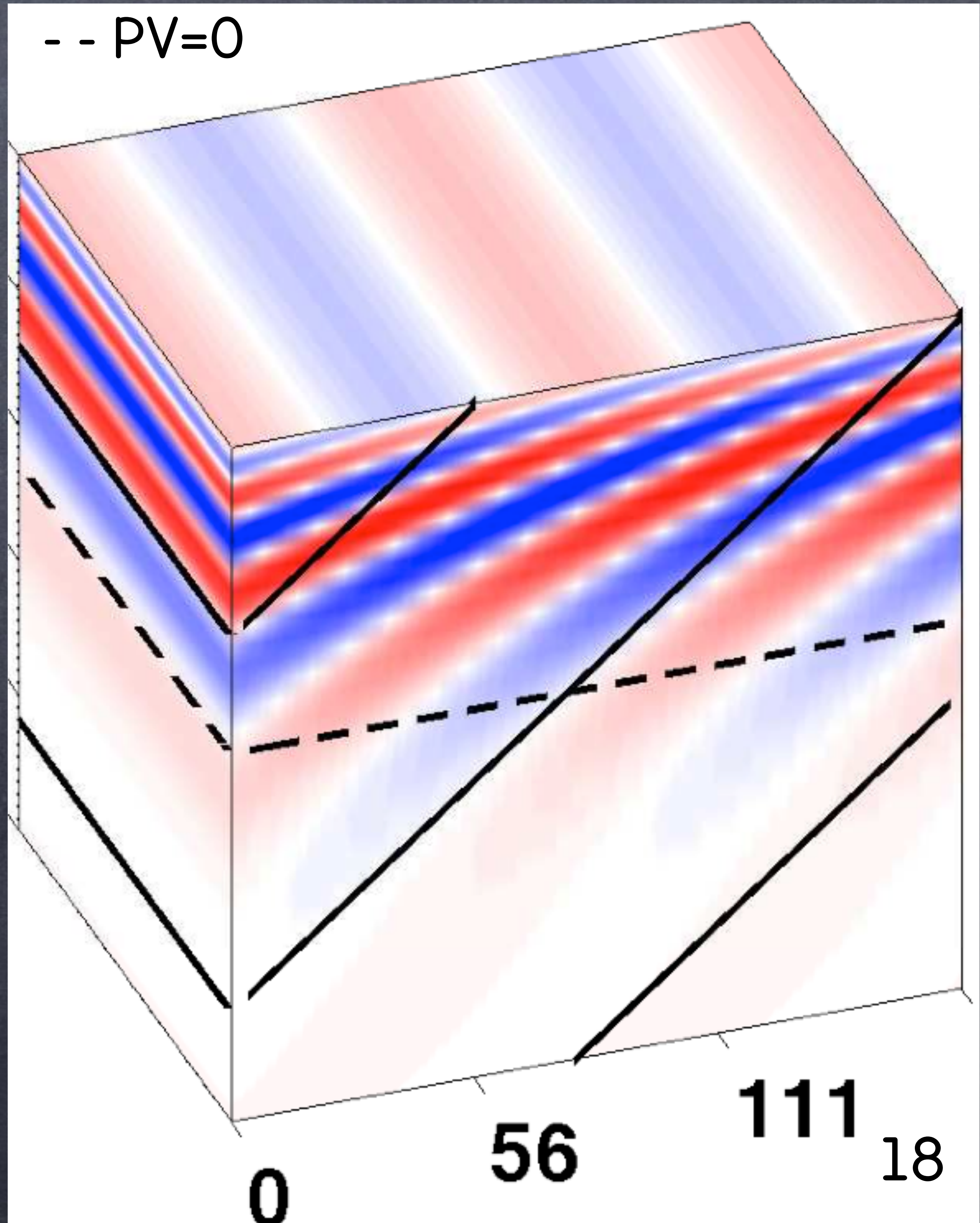

# Frontal Consequences:

## Observing Energy Flux from Global to Dissipative Scales

- Energy flows from the global winds & tides to mm-scale dissipation by viscosity
- Fronts are a key concentration effect of energy, aiding in the transfer
- However, the presence of fronts also complicates observations of the energy flow
- Observations by drifters, etc. must handle the strong heterogeneity due to the presence of fronts

N. Suzuki, BFK, P. E. Hamlington, and L. P. Van Roekel. Surface waves affect frontogenesis. Journal of Geophysical Research-Oceans, 121:1-28, 2016.
J. C. McWilliams and BFK. Oceanic wave-balanced surface fronts and filaments. Journal of Fluid Mechanics, 730:464-490, 2013.

# 'Observed' scale-sensitivity?

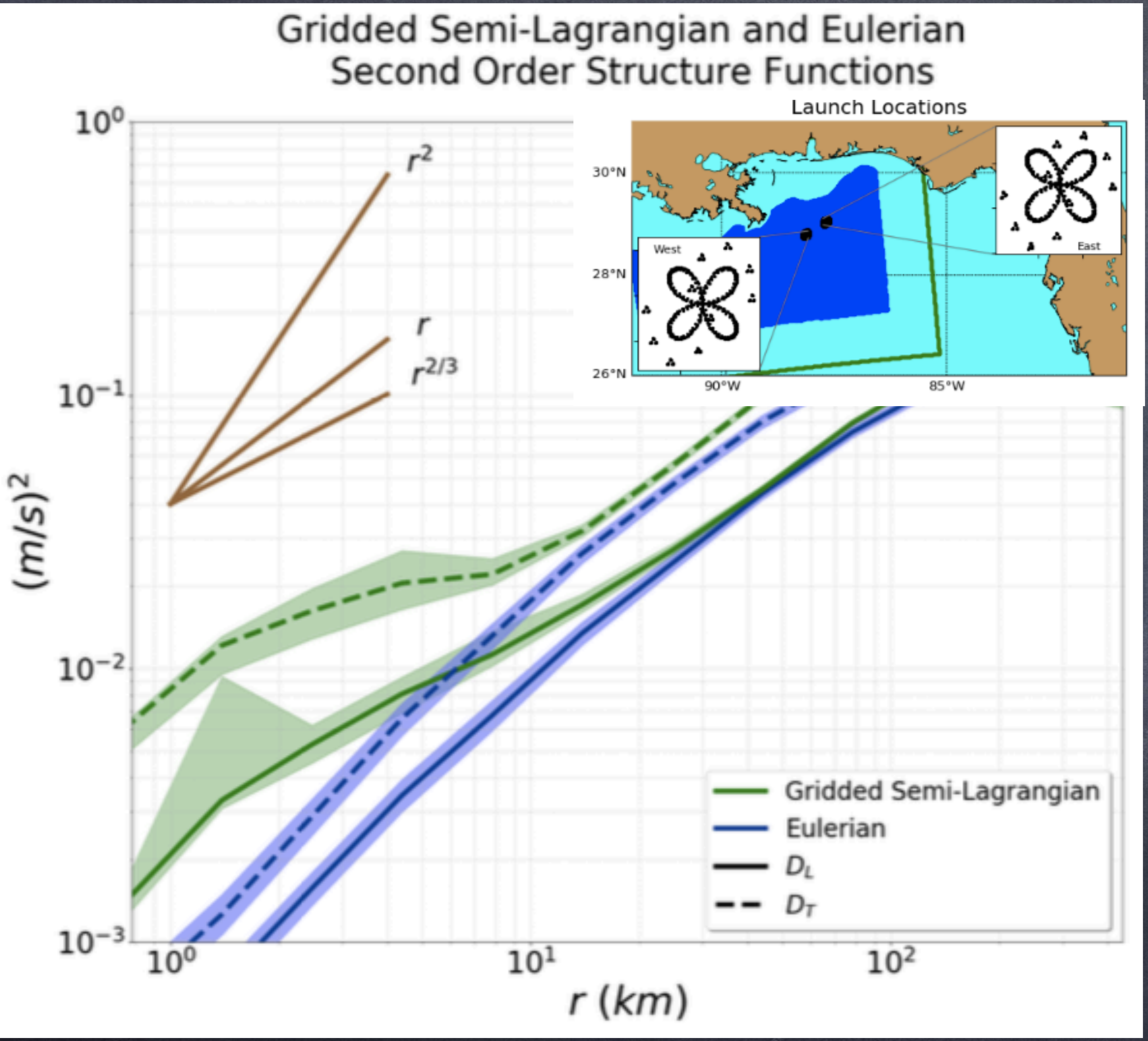


J. Pearson, B. Fox-Kemper, R. Barkan, J. Choi, A. Bracco, and J. C. McWilliams. Impacts of convergence on Lagrangian statistics in the Gulf of Mexico. Journal of Physical Oceacnography, February 2018. Submitted.

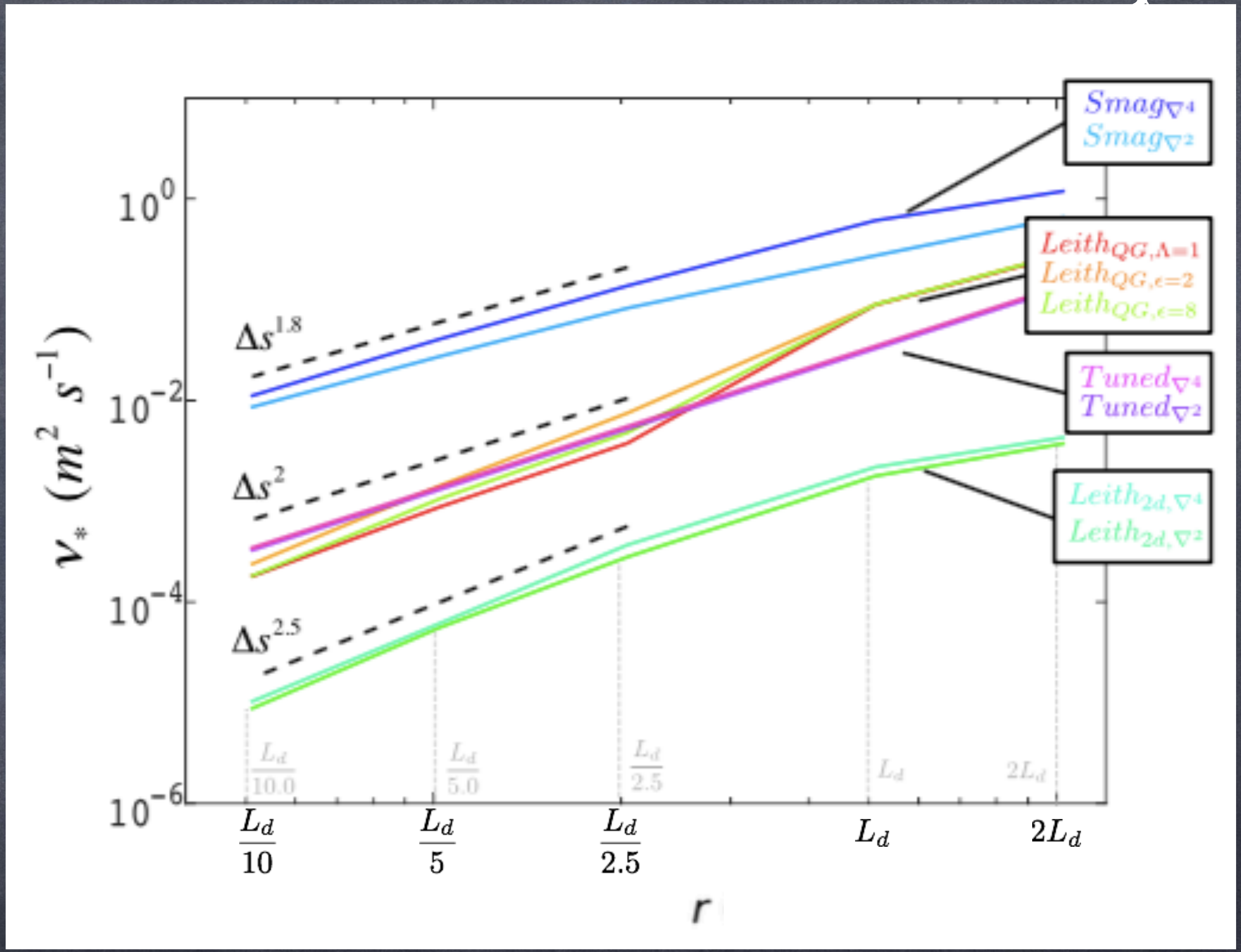


Some Theory/Model combos are inconsistent (e.g., Smagorinsky in a QG regime)

S. D. Bachman, B. Fox-Kemper, and B. Pearson, 2017: A scale-aware subgrid model for quasi-geostrophic turbulence. Journal of Geophysical Research–Oceans, 122:1529–1554.

# 'Observed' scale-sensitivity?

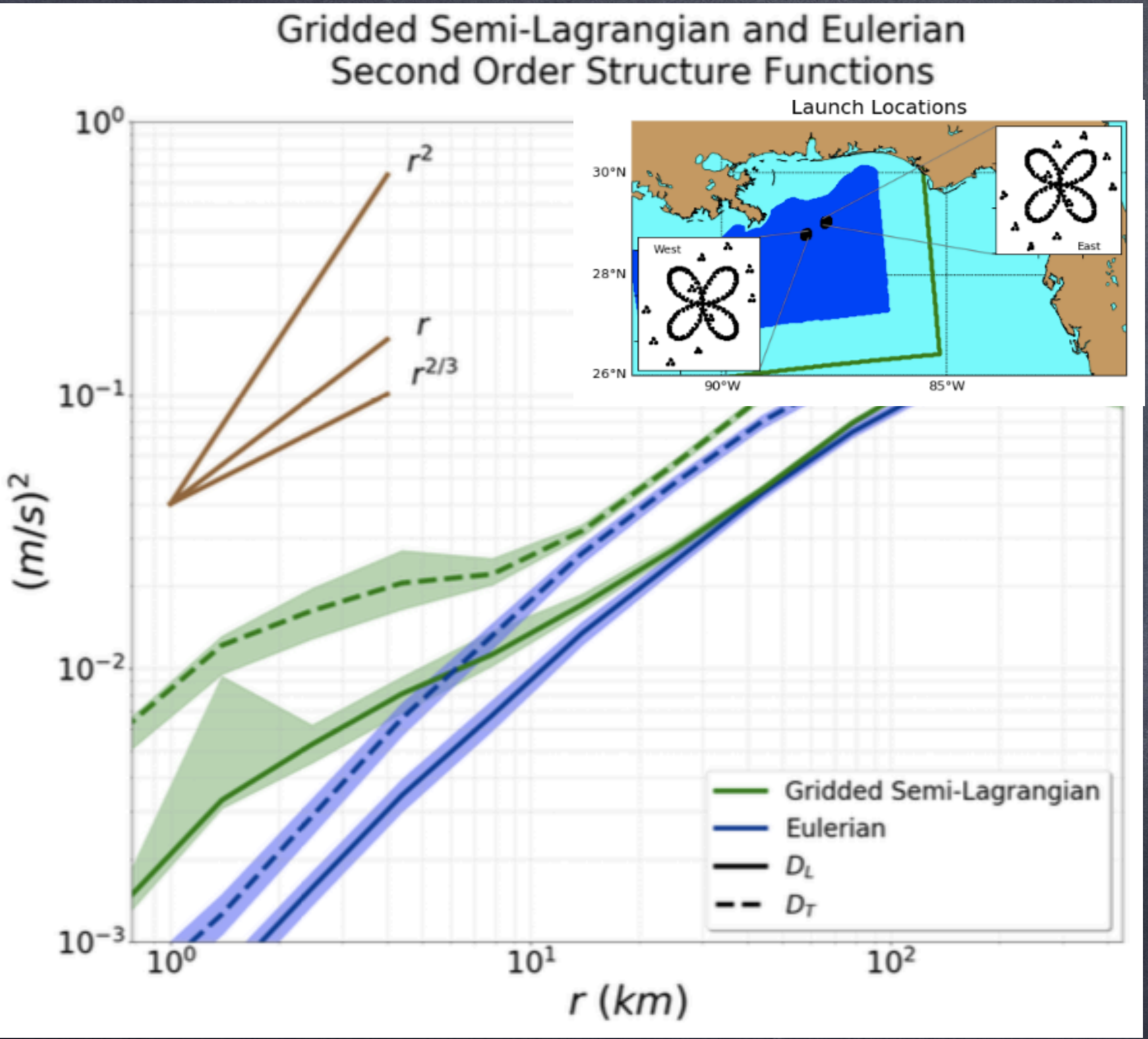


J. Pearson, B. Fox-Kemper, R. Barkan, J. Choi, A. Bracco, and J. C. McWilliams. Impacts of convergence on Lagrangian statistics in the Gulf of Mexico. Journal of Physical Oceacnography, February 2018. Submitted.

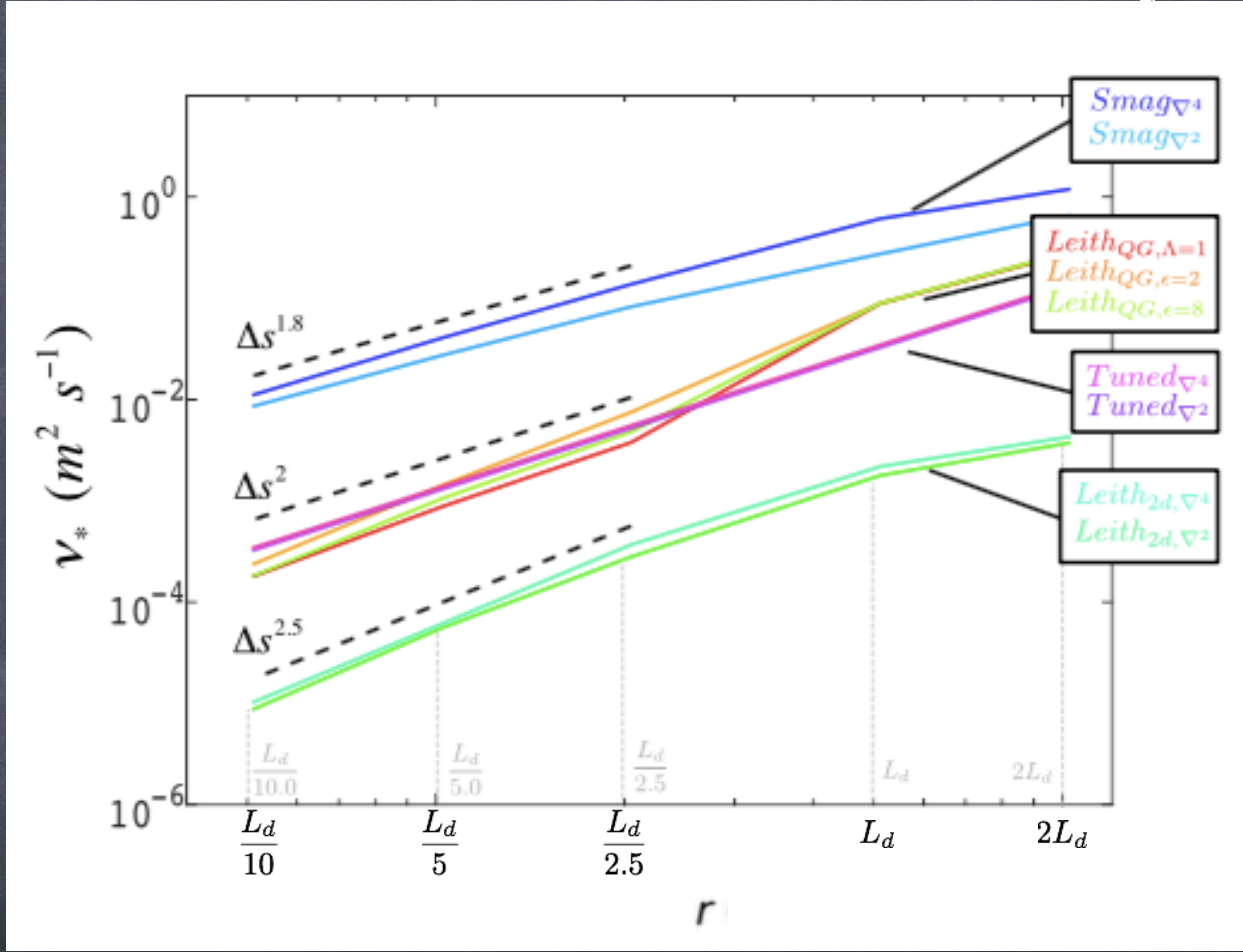


Some Theory/Model combos are inconsistent (e.g., Smagorinsky in a QG regime)

S. D. Bachman, B. Fox-Kemper, and B. Pearson, 2017: A scale-aware subgrid model for quasi-geostrophic turbulence. Journal of Geophysical Research–Oceans, 122:1529–1554.